สารออกฤทธิ์ทางชีวภาพจากราเอนโดไฟต์ที่ได้จากพืชป่าชายเลนจังหวัดสงขลาและจากชิงช้าชาลี *Tinospora baenzigeri* Forman

นางสาวสุจิตรา หาญทนง

วิทยานิพนธ์นี้เป็นส่วนหนึ่งของการศึกษาตามหลักสูตรปริญญาวิทยาศาสตรดุษฎีบัณฑิต
สาขาวิชาเทคโนโลยีชีวภาพ
คณะวิทยาศาสตร์ จุฬาลงกรณ์มหาวิทยาลัย
ปีการศึกษา 2560

BIOACTIVE COMPOUNDS FROM SONGKHLA PROVINCE MANGROVE-DERIVED ENDOPHYTIC FUNGI AND FROM HEART-LEAVED MOONSEED *Tinospora baenzigeri* Forman

Miss Sujitra Hanthanong

A Dissertation Submitted in Partial Fulfillment of the Requirements
for the Degree of Doctor of Philosophy Program in Biotechnology
Faculty of Science
Chulalongkorn University
Academic Year 2017

Thesis Title	BIOACTIVE COMPOUNDS FROM SONGKHLA PROVINCE MANGROVE-DERIVED ENDOPHYTIC FUNGI AND FROM HEART-LEAVED MOONSEED *Tinospora baenzigeri* Forman
By	Miss Sujitra Hanthanong
Field of Study	Biotechnology
Thesis Advisor	Associate ProfessorKhanitha Pudhom, Ph.D.

Accepted by the Faculty of Science, Chulalongkorn University in Partial Fulfillment of the Requirements for the Doctoral Degree

.....Dean of the Faculty of Science
(ProfessorPolkit Sangvanich, Ph.D.)

THESIS COMMITTEE

.....Chairman
(Associate ProfessorVudhichai Parasuk, Ph.D.)

.....Thesis Advisor
(Associate ProfessorKhanitha Pudhom, Ph.D.)

.....Examiner
(Associate ProfessorNattaya Ngamrojanavanich, Ph.D.)

.....Examiner
(Yupyn Chintapakorn, Ph.D.)

.....External Examiner
(Damrong Sommit, Ph.D.)

สุจิตรา หาญทนง : สารออกฤทธิ์ทางชีวภาพจากราเอนโดไฟต์ที่ได้จากพืชป่าชายเลนจังหวัดสงขลาและจากชิงช้าชาลี *Tinospora baenzigeri* Forman (BIOACTIVE COMPOUNDS FROM SONGKHLA PROVINCE MANGROVE-DERIVED ENDOPHYTIC FUNGI AND FROM HEART-LEAVED MOONSEED *Tinospora baenzigeri* Forman) อ.ที่ปรึกษาวิทยานิพนธ์หลัก: รศ. ดร.ขนิษฐา พุดหอม, 211 หน้า.

การศึกษาในครั้งนี้เพื่อประเมินสารออกฤทธิ์ทางชีวภาพจากเถาว์ของชิงช้าชาลีที่เก็บจาก 2 พื้นที่ ที่ต่างกันและจากราเอนโดไฟต์จากพืชป่าชายเลนในจังหวัดสงขลา พบสารกลุ่ม rearranged clerodane ไดเทอร์พีนใหม่ 4 ชนิด (66-69), สารไกลโคไซด์ใหม่ 1 ชนิด (70), และสารที่มีการรายงานแล้ว 6 ชนิด (61, 71-75) ถูกแยกจากชิงช้าชาลีที่ซื้อจากตลาดท้องถิ่นในกรุงเทพฯ สาร 12 ชนิด ได้แก่ สารกลุ่ม rearranged clerodane ไดเทอร์พีนใหม่ 1 ชนิด (76), สาร rearranged clerodane ไกลโคไซด์ใหม่ 1 ชนิด (77), สารที่มีการรายงานแล้ว 5 ชนิด (44, 78-81) และสาร 5 ชนิด ประกอบด้วย 61, 66, 70 และ 74-75 ได้ถูกพบที่จังหวัดบึงกาฬด้วย โครงสร้างของสารชนิดใหม่ 66-69 และ 76 ยังได้รับการตรวจสอบโดยเทคนิค single-crystal X-ray crystallography จากสารทั้งหมด 18 ชนิด สารประกอบ 13 ชนิดได้รับการประเมินฤทธิ์ทางชีวภาพต่อเซลล์มะเร็ง 4 ชนิดได้แก่ Hep-G2, KATO-3, MCF-7 และ CaSki; ฤทธิ์ต้านการอักเสบ และ ฤทธิ์ยับยั้ง α-glucosidase พบว่าสาร tinobaenzin C (68) มีความเป็นพิษที่จำเพาะต่อเซลล์ KATO-3 ด้วยค่า IC_{50} เท่ากับ 27.08 µM ในขณะที่สารอื่นไม่มีผลต่อเซลล์ที่ทดสอบ ส่วนสาร N-trans-feruloyltyramine (74) แสดงฤทธิ์ยับยั้ง α-glucosidase ได้เล็กน้อย ด้วยค่า IC_{50} 0.34 mM สำหรับเอนไซม์ sucrase และ IC50 0.36 mM สำหรับเอนไซม์ maltase อย่างไรก็ตามสารประกอบทั้งหมดไม่มีฤทธิ์ยับยั้งการอักเสบ นอกจากนี้ยังได้นำส่วนสกัดเอธิลแอซิเทตของราเอนโดไฟต์ Setosphaeria rostrata ซึ่งเพาะเลี้ยงในอาหาร SDB มาทำการแยกสารบริสุทธิ์ ได้สารอนุพันธ์ไอโซคูมารินใหม่ 5 ชนิด (84-88), สารกลุ่มแซนโทน 1 ชนิด (82) และ สารไอโซคูมารินที่มีการรายงานแล้ว 1 ชนิด (83) สาร 82 และ 83 ได้รับการทดสอบฤทธิ์ทางชีวภาพ แต่ไม่มีสารใดแสดงฤทธิ์

สาขาวิชา เทคโนโลยีชีวภาพ ลายมือชื่อนิสิต .....

ปีการศึกษา 2560 ลายมือชื่อ อ.ที่ปรึกษาหลัก .....

5672875623 : MAJOR BIOTECHNOLOGY
KEYWORDS: BIOACTIVE COMPOUND/ TINOSPORA BAENZIGERI FORMAN/ ENDOPHYTIC FUNGI

SUJITRA HANTHANONG: BIOACTIVE COMPOUNDS FROM SONGKHLA PROVINCE MANGROVE-DERIVED ENDOPHYTIC FUNGI AND FROM HEART-LEAVED MOONSEED *Tinospora baenzigeri* Forman. ADVISOR: ASSOC. PROF.KHANITHA PUDHOM, Ph.D., 211 pp.

This study has evaluated biological activities of isolated compounds from *Tinospora baenzigeri* stems collecting from two different areas, and from mangrove-derived endophytic fungi isolated from trees inhabiting in Songkhla province. Four new rearranged clerodane-type diterpenes (66-69), one new glycoside (70), and six known compounds (61, 71-75), were extracted from plant obtained from local market in Bangkok. Twelve compounds including a new rearranged clerodane-type diterpene (76), a new rearranged clerodane glycoside (77), five known compounds (44, 78-81), and five compounds counting 61, 66, 70 and 74-75 were obtained from plant collected in Bueng Kan Province. Structures of new compounds 66-69 and 76 were confirmed by single-crystal X-ray crystallography technique. Of the 18 compounds, 13 compounds were evaluated for biological activities against four cancer cell lines including Hep-G2, KATO-3, MCF-7 and CaSki ; anti-inflammatory on J774.A1; and α-glucosidase inhibitory activity. Tinobaenzin C (68) exhibited selectivity cytotoxic activity against KATO-3 cell lines with IC_{50} values of 27.08 μM, while other compounds did not affect to any of the tested cell lines. Only *N-trans*-feruloyltyramine (74) displayed the weak activity against α-glucosidase with an IC_{50} value of 0.34 mM for sucrase inhibition and 0.36 mM for maltase inhibition. However, all of the tested compounds were inactive on anti-inflammatory activities. In addition, EtOAc crude extracts from a marine-derived endophytic fungus, *Setosphaeria rostrata*, cultured in SDB medium were purified and resulted in five new isocoumarin derivatives (84-88), one xanthone (82), and one known isocoumarin (83). The compounds 83 and 85 were subjected to biological activities. Unfortunately, all of them showed to be inactive.

Field of Study: Biotechnology Student's Signature .....

Academic Year: 2017 Advisor's Signature .....

ACKNOWLEDGEMENTS

Concerning to the success of my thesis, I would like to express my deepest appreciation and gratitude to my advisor, Associate Professor Dr. Khanitha Pudhom, Department of chemistry, Faculty of Science, Chulalongkorn University, for her kindness constructions and supervision, valuable instructions and comments throughout the work in this research.

Special gratitude to the Chairperson, Associate Professor Dr. Vudhichai Parasuk, Associate Professor Dr. Nattaya Ngamrojanavanich, Department of Chemistry, Faculty of Science, Chulalongkorn University, Dr. Yupyn Chintapakorn, Department of Botany, Faculty of Science, Chulalongkorn University, and Dr. Damrong Sommit, Mahanakorn University of Technology, in devotion of their valuable time for thesis examination and useful recommendation.

I am grateful to Dr. Thapong Teerawatananond, who kindly performed Single-Crystal X-ray crystallographic analysis, and to Assistant Professor Dr. Yuwadee Insumran for identification of the fungal species. In addition, many thanks to Miss Siwattra Choodej for her assistance about NMR spectra. Moreover, special thanks to the members of the laboratory (MHMK 1532), Department of Chemistry, and Program in Biotechnology, Faculty of Science, Chulalongkorn University for their help and good friendship.

Finally, I would like to express my deepest gratitude to my mother and brothers, for their unlimited love, warmness, mental support and constant encouragement throughout my life.

This work was supported by the 90th Anniversary of Chulalongkorn University Fund (Ratchadaphiseksomphot Endowment Fund).

CONTENTS

Page

Page

Page

Page

LIST OF FIGURES

LIST OF SCHEMES

LIST OF TABLES

LIST OF ABBREVIATIONS

Å	=	Angstrom
acetone-d_6	=	Deuterated acetone
α	=	Alpha
β	=	Beta
brd	=	Broad doublet
brs	=	Broad singlet
brt	=	Broad tripet
c	=	Concentration
$^{\circ}$C	=	Degree Celsius
CC	=	Column chromatography
^{13}C NMR	=	Carbon-13 nuclear magnetic resonance
$CDCl_3$	=	Deuterated chloroform
$CHCl_3$	=	Chloroform
CH_2Cl_2	=	Dichloromethane
cm^{-1}	=	Reciprocal centimeter (unit of wave number)
δ	=	Chemical shift
d	=	Doublet (for NMR spectral data)
dd	=	Doublet of doublets (for NMR spectral data)
ddd	=	Doublet of doublets of doublets (for NMR spectral data)
dddd	=	Doublet of doublets of doublets of doublets (for NMR spectral data)
deg.	=	Degree celcius
dt	=	Double of triplet
DI water	=	Deionized water
DMSO	=	Dimethyl sulfoxide
DMSO-d_6	=	Dimethyl-d_6-sulfoxide
DNA	=	Deoxyribonucleic acid
DEPT	=	Distortionless enhancement by polarization transfer

ε	=	Molar absorptivity
EI-MS	=	Electron impact mass spectrometry
ESI-MS	=	Electrospray ionization mass spectrometry
et al	=	And other
EtOAc	=	Ethyl acetate
ESI-TOF MS	=	Electrospray Ionization Time of Flight Mass
FIC	=	Fraction Inhibitory Concentration
g	=	Gram
h	=	Hour
^{1}H-^{1}H COSY	=	Homonuclear (proton-proton) correlation spectroscopy
HMBC	=	^{1}H-detected heteronuclear multiple bond correlation
^{1}H NMR	=	Proton nuclear magnetic resonance
HPLC	=	High performance
HSQC	=	^{1}H-detected heteronuclear single quantum coherence
Hz	=	Hertz
IC_{50}	=	Inhibitory concentration required for 50% inhibition of growth
IR	=	Infrared
ITS	=	Internally transcribed spacers
J	=	Coupling constant
KBr	=	Potassium bromide
L	=	Liter
λ_{max}	=	Wavelength at maximum absorption
m	=	Multiplet (for NMR spectral data)
M	=	Molar
$[M+Na]^+$	=	Pseudomolecular ion
MEB	=	Malt extract broth
MeOH	=	Methanol
mg	=	Milligram
min	=	Minute

mL	=	Milliliter
mm	=	Millimeter
mM	=	Millimolar
MHz	=	Megahertz
MS	=	Mass spectroscopy
m/z	=	Mass to charge ratio
m.p.	=	Melting point
MW	=	Molecular weight
nm	=	Nanometer
NMR	=	Nuclear magnetic resonance
NOESY	=	Nuclear overhauser effect spectroscopy
NPDB	=	Natural Potato Dextrose Broth
NTP	=	Nucleotide triphosphate
ORTEP	=	Oak ridge thermal ellipsoid plot
PCR	=	Polymerase Chain Reaction
PDA	=	Potato Dextrose Agar
PDB	=	Potato Dextrose Broth
ppm	=	Part per million
q	=	Quartet (for NMR spectral data)
qC	=	Quaternary carbon
rDNA	=	Ribosomal deoxyribonucleic acid
rpm	=	Round per minute
rRNA	=	Ribosomal ribonucleic acid
rpm	=	Round per minute
RT	=	Room temperature
SDB	=	Sabouraud's dextrose broth
SiO_2	=	Silicon dioxide
sp.	=	Species
t	=	Triplet (for NMR spectral data)
td	=	Triplet of doublet
TLC	=	Thin layer chromatography

U	=	Unit
μL	=	Microliter
μg	=	Microgram
μM	=	Micromolar
UV	=	Ultraviolet
V	=	Volt
v	=	Volume
ν_{max}	=	Wave number at maximum absorption
w	=	Weight
w	=	Weak (for IR spectral data)
w/w	=	Weight by weight
WA	=	Water agar
YES	=	Yeast Extract Sucrose
1D NMR	=	One dimensional nuclear magnetic resonance
2D NMR	=	Two dimensional nuclear magnetic resonance
Δ	=	Delta
$[\alpha]^{20}_{D}$	=	Specific rotation at 20 ^{o}C and sodium D line (589 nm)

CHAPTER I
INTRODUCTION

1.1 Natural products remain one of the best resources for drug leads

Natural products are chemical compounds or substances produced by living organisms, such as plants, animals and microorganisms [1]. Numbers of reports have demonstrated that natural products have been used for treatments of human diseases, illnesses and also nourish [2]. The advantage of natural products has been received considerable attention due to a variety of biological activities, structure diversity and specific action on target, which may be used as templates for the development of new drugs [3]. The important advantage of natural products must be their biosynthesis, because they have involves repeated interaction with modulating enzymes to produce specific metabolites, and their actual biological function comprises binding to other proteins [4]. Besides, it has been realized that natural products possessing biologically active molecules are generally relatively small with a molecular weight below 3,000 Daltons, so they can be easily absorbed and catabolized by the human body [5, 6].

Moreover, there are some reasons indicating that why natural products are so important, as following [1]:

1. There is a strong biological and ecological rationale for plants and marine invertebrates to produce novel bioactive secondary metabolites. Plants and marine invertebrates have evolved for survival. Secondary substances are created to protect themselves and to respond to changing environmental conditions. As these compounds proved to be advantageous, they became an attribute on which natural selection. It is the unique biosynthesis of these natural products [2]. Modifications in the biosynthetic pathways may be due to natural causes (e.g., insects, viruses, diseases or environmental changes) or unnatural causes (e.g., chemical or radiation) in an effort to adapt or provide longevity for the organism [7, 8].
2. Natural products have historically provided many major new drugs such as morphine, quinine, penicillin G, vinblastine and vincristine.

3. Natural products provide drugs that would be inaccessible by other routes. Those are unlikely to be synthesized in laboratories and the chemical novelty associated with natural products is higher than that of any other source.

1.2 Types of natural products

Several drug candidates are obtained from different natural sources. These can be broadly distributed into four kinds, as described below:

1.2.1 Microorganism-derived natural products

Microorganisms have been used by human being for long time, particularly in the processes of foods, alcoholic beverages and also medicines [9]. It is well-known that microorganisms usually produce potential active substances, particularly antibiotics agents, for example, vancomycin (**1**), erythromycin (**2**), and also other valuable compounds like acarbose (**3**), an antidiabetic drug. [2, 10], as shown in **Fig. 1.1**.

Fungi, one of the most common microorganisms, can produce a variety of interesting metabolites. One kind of fungal strains called “endophytic fungi” symbiotically live in plant tissues, [11], as well as they have been currently considered to be a wellspring of novel secondary metabolites offering the potential for medicinal, agricultural, and industrial exploitation [12].

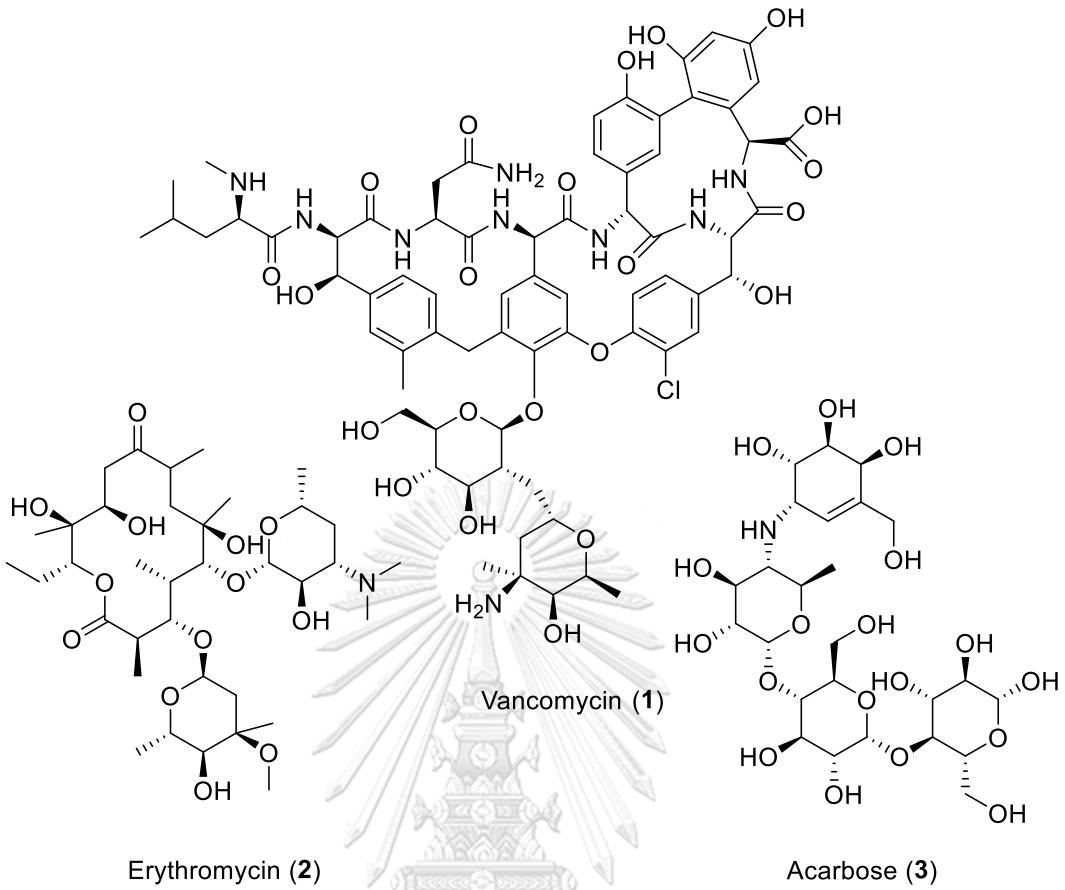

Fig. 1.1 Structures of natural products from microorganisms.

1.2.2 Marine organism-derived natural products

Marine organisms produce a diverse array of metabolites exhibiting various biological activities. In the past decade, studies on marine organism-derived metabolites have been expanded at a much faster rate owing to their potent activities, structural diversity, and complex structures. Large numbers of novel and promising metabolites have been recently discovered from marine organisms [13, 14]. Moreover, some of them have been developed as drugs. For examples, discodermolide (**4**), a potent anti-cancer agent, was one of the most potent microtubule stabilizing agents [15]. Palaulol (**5**), a sesterterpene from the sponge *Fascaplysinopsis* sp. showed great potential anti-inflammatory activity [16]. Example of cytotoxic compounds against cancer cells included plitidepsin (**6**), 4-acetoxydictylolactone (**7**), dictyolides A (**8**), B (**9**) and nordictyolide (**10**) [17, 18] (**Fig. 1.2**).

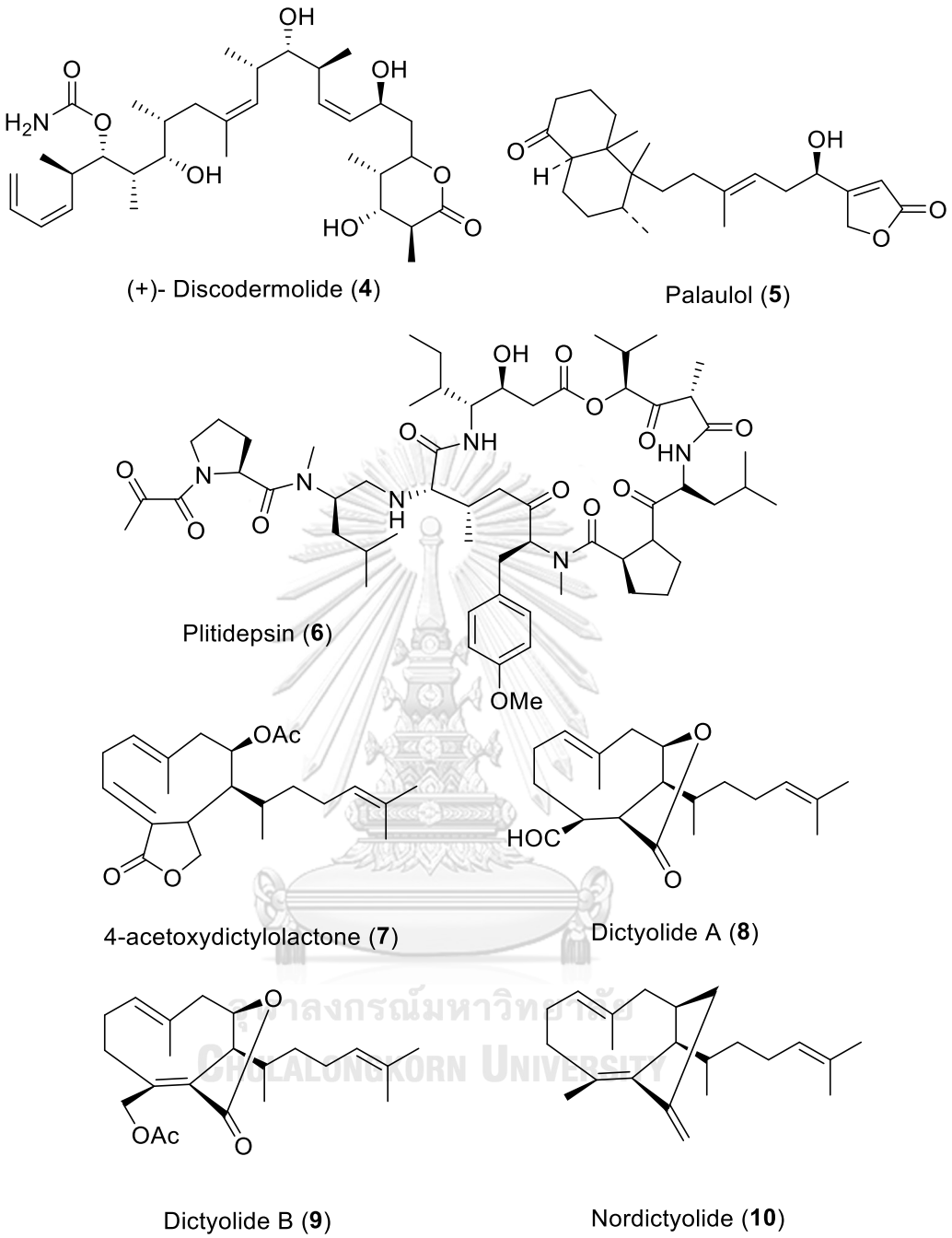

Fig. 1.2 Structures of metabolites from marine organisms.

1.2.3 Animal-derived natural products

In the past, a pharmaceutical evolution from animal products had numerous progressive. Toxins and animal secretions had been studied for its potent pharmacological activity [19], for examples, captopril (**11**) used for the treatment of hypertension [20], eptifibatide (**12**), an anti-platelet from animal venom, toxin, or

secretions [21]. Ursodiol (**13**) originated from the liver of polar bear, *Ursus maritimus*, it is used for treatment of liver disease [22]. The structures of these compounds are revealed in **Fig. 1.3**.

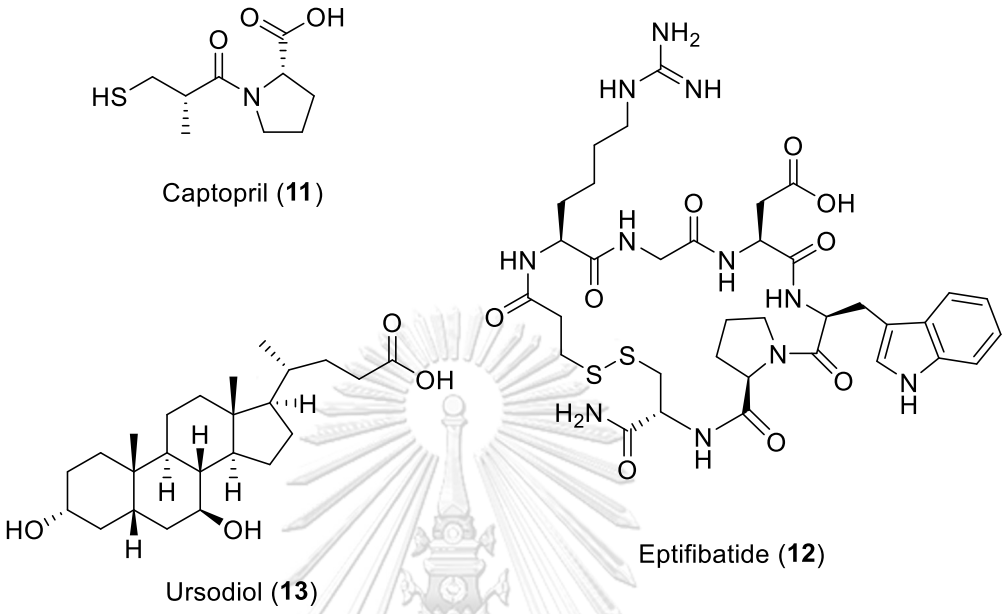

Fig. 1.3 Structures of natural products from animal sources.

1.2.4 Plant-derived natural products

The medicinal use of natural products has been historically demonstrated in the term of traditional medicines, remedies, potions and oils. The dominant knowledge source of natural product derived from medicinal plants is a result of man experimenting by trial and error for hundreds of centuries. However, many of these bioactive natural products are being unidentified [23]. Since plants have developed and modified themselves over millions of years to resist bacteria, insects, fungi, weather, and others, this evolution allows plants to construct structurally diverse secondary metabolites [24]. Thus, plant must be a potential and efficiency candidate for drug discovery. Furthermore, researchers often focus on the exploration of the plants having a history of use in traditional medicine [6, 8].

Undoubtedly, one of the most famous natural product discoveries derived from plant is taxol (paclitaxel, **14**). The discovery of taxol has indeed heightened the interest in plant-derived bioactive molecule. Many useful clinical drugs have been discovered from various plants such as quinine (**15**) used for anti-pyretic, anti-malarial, analgesic

and anti-inflammatory isolated from the bark of *Cinchona succirubra* [25]. Vincristine (16) and vinblastine (**17**) used for anti-leukemic drug and Hodgkin's disease, respectively, were isolated from *Catharanthus roseus* [1].

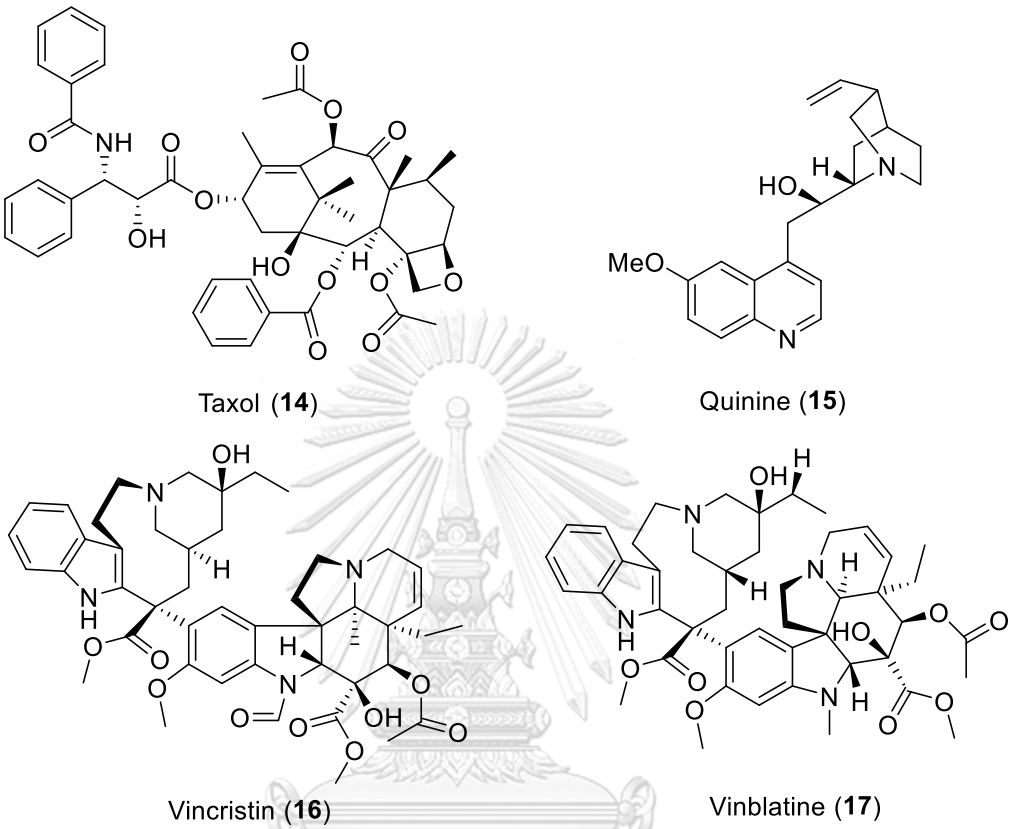

Fig. 1.4 Structures of natural products from plant sources.

1.3 Biodiversity and natural product drug discovery

Plants have provided most of the active ingredients of traditional medicinal products [6]. It might be thought that most of the plant kingdom has been thoroughly investigated and searched for biologically active molecules. However, this assumption is unlikely accurate. Indeed, only 5-15% of 250,000 flowering plants in the earth and probably about 10% of plants have as yet been evaluated for their biological activity [8, 26]. By comparing, the marine organisms have very nominal reported applications in folk medicine. Since less than 10% of the world's biodiversity has been evaluated for therapeutically relevant molecules, many more useful natural lead compounds are awaiting discovery. This is because many of the most bio-diverse regions of the earth have been relatively inaccessible to researchers. The challenge is how to investigate

this natural chemical diversity. Because of the continuing need for novel chemicals with potential drug leads against an increasing number of ever-more-challenging molecular assay targets, the chemical diversity derived from natural products will be increasingly relevant to the future of drug discovery [6]. Thailand is a relatively small country; however, it is one of the richest in biodiversity. Thailand is located on the tropical area, which encourages a diversity of tropical ecosystems. Ecosystem diversity can be indicated in the various types of forest ranging from tropical rain forest to mangrove forest. It is estimated that there are approximately 1,500 plant species in Thailand, which account for 6-10% of estimated total number of global plant species [27]. An exuberant diversity of microorganisms, fungi and slime molds, and lichens has been discovered from forests in various parts of Thailand. Among plant-derived fungi, those associated with mangrove trees have received much attention from natural product researchers due to its unique ecosystem [28]. In addition to growing in tropical areas which provide great biodiversity, mangroves have to deal with changing tides and broad ranges of salinity, temperature, and moisture as well as a number of other environment factors [29, 30]. It is reasonable to expect they must be home to a great variety of specific microorganisms including fungi [12]. Because the main sources of mangrove formations are found in Asia including Thailand [31], as well as mangroves forests cover approximately 1/3 of the coastal areas of Thailand, both Thai plants and microorganisms might thus be excellent sources for secondary metabolites and exhibit medicinal properties for drug development of various diseases.

Therefore, the objectives of this research are summarized as follow;

1. To extract and isolate compounds from the plant, *Tinospora baenzigeri* Forman collected from different areas.

2. To extract and isolate metabolites from mangrove-derived endophytic fungi isolated from trees collected from Songkhla province.

3. To evaluate biological activities of isolated compounds including anti-inflammatory and anti-cancer activities.

CHAPTER II
BIOACTIVE COMPOUNDS FROM *TINOSPORA BAENZIGERI* FORMAN

2.1 Introduction

Tinospora is the largest and most geographically widespread genera within family Menispermaceae. It consists of about 30 species distributed throughout the tropical and subtropical areas of Africa, Asia, Australia and the Pacific [32]. The Botanical Garden Organization and Thai Forest Ecological Research Network were confirmed approximately 8 species their findings in Thailand and some of them are significant medicinal plants. Similarly, plants in this genus are widely employed in traditional medicines throughout the countries in Asia and Africa. For example, *T. capillipes* has been applied in traditional Chinese medicine as a herb for the treatment of sore throat, laryngitis, gastralgia, and diarrhea [33]. *T. crispa* has been used to treat tooth and stomach aches, cough, asthma and pleurisy [34]. Previous studies revealed that chemical constituents of *Tinospora* plants consist of different types of compounds, including clerodane diterpenes, clerodane diterpene glucosides, steroids, flavonoids, lignans and alkaloids [35-37].

2.1.1 Biological activities of secondary metabolites from the genus *Tinospora*

2.1.1.1 Anti-microbial activity

In 2012, Deng and coworkers reported that two antimicrobial alkaloids, plamatin and jatrorrhizing, were isolated from tubers of traditional Chinese folk medicinal *T. capillipes.* The results indicated that palmatine (**18**) and jatrorrhizinehad (**19**) (**Fig. 2.1**) could inhibit against plant pathogens, with the EC_{50} values of 0.0348-0.8356 g/L and 0.0240-0.8649 g/L, respectively. Moreover, both compounds exhibited inhibition against animal pathogens, with the MIC values of 0.1-0.8 g/L and 0.1-0.6 g/L, respectively [38].

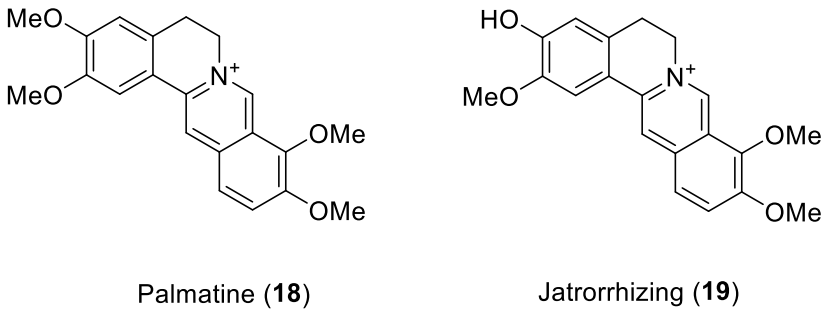

Palmatine (**18**) Jatrorrhizing (**19**)

Fig. 2.1 Structures of compounds **18** and **19**

2.1.1.2 Hypoglycemic activity

In 2013, Ruan and coworkers studied the hypoglycemic activity of borapetosides A (**20**), B (**21**) and C (**22**) (**Fig. 2.2**) which were isolated from ethanol extract of *T. crispa*. Compound **20** showed strong hypoglycemic effects than **21** and **22** [39].

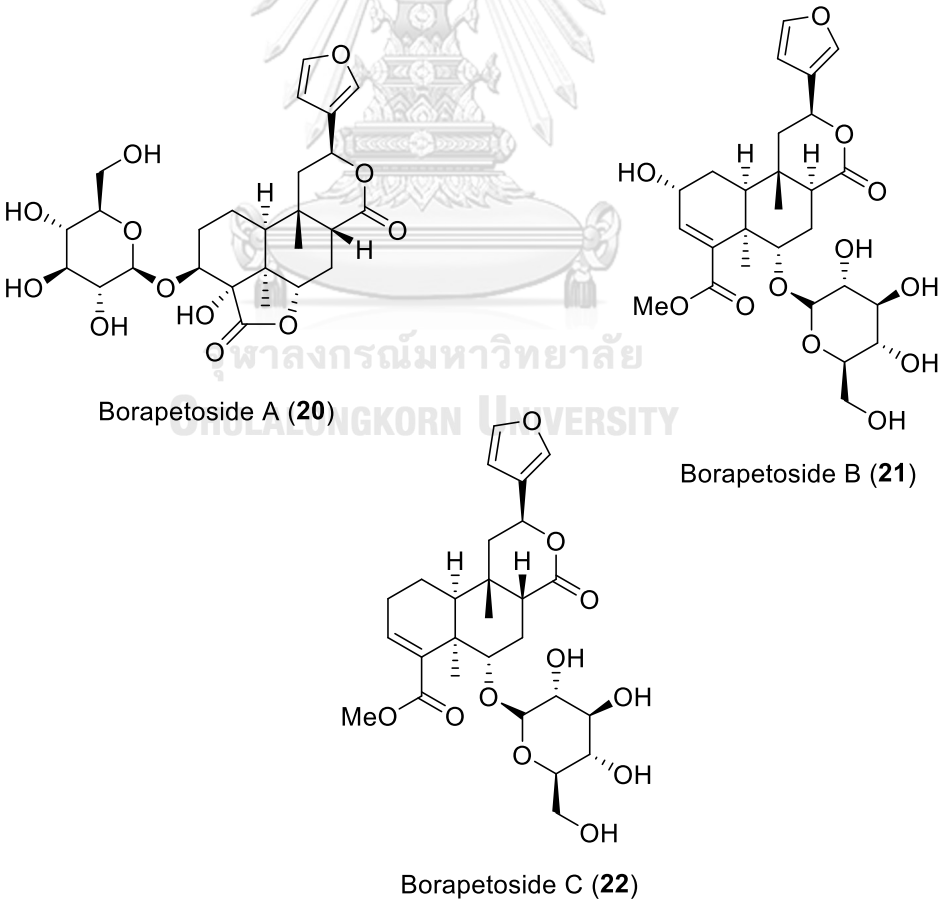

Borapetoside A (**20**)

Borapetoside B (**21**)

Borapetoside C (**22**)

Fig. 2.2 Structures of compounds **20**-**22**

2.1.1.3 Neuroprotective activity

In 2017, Yu and coworkers reported two new compounds from ethanol extracts of *T. hainanensis*, Tinosporaic acids A (**23**) and B (**24**) (**Fig. 2.3**). Both of them significantly attenuated hydrogen peroxide-induced neurotoxicity with EC_{50} values of 86.34 and 22.06 mg/mL, respectively [40].

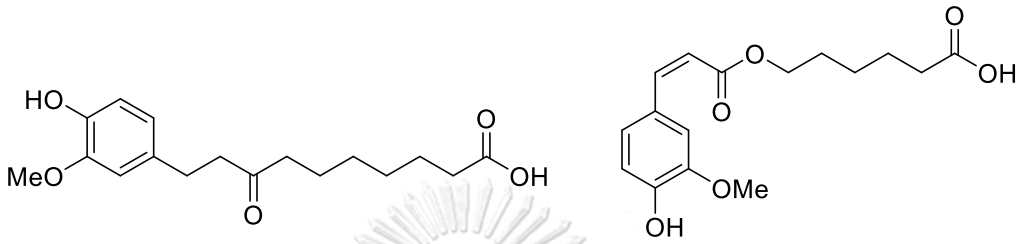

Tinosporaic acid A (**23**) Tinosporaic acid B (**24**)

Fig. 2.3 Structures of compounds **23** and **24**

2.1.1.4 Anti-cancer activity

In 2015, Bala and coworkers isolated eight compounds from the stem of *T. cordifolia* including palmatine (**18**), jatrorrhizine (**19**), *N*-formylannonain (**25**), magnoflorine (**26**), 11-hydroxymustakone (**27**), cordifolioside A (**28**), tinocordiside (**29**) and yangambin (**30**) (**Fig. 2.4**). All compounds were evaluated for anti-cancer and immunomodulatory activities. The results indicated that palmatin (**18**) was active against KB and HT-29, compound **29** was active against KB and CHOK-1, and **30** was active against KB cell lines. Furthermore, compounds **25** and **27** were found to be active on immunomodulatory activity assay [41].

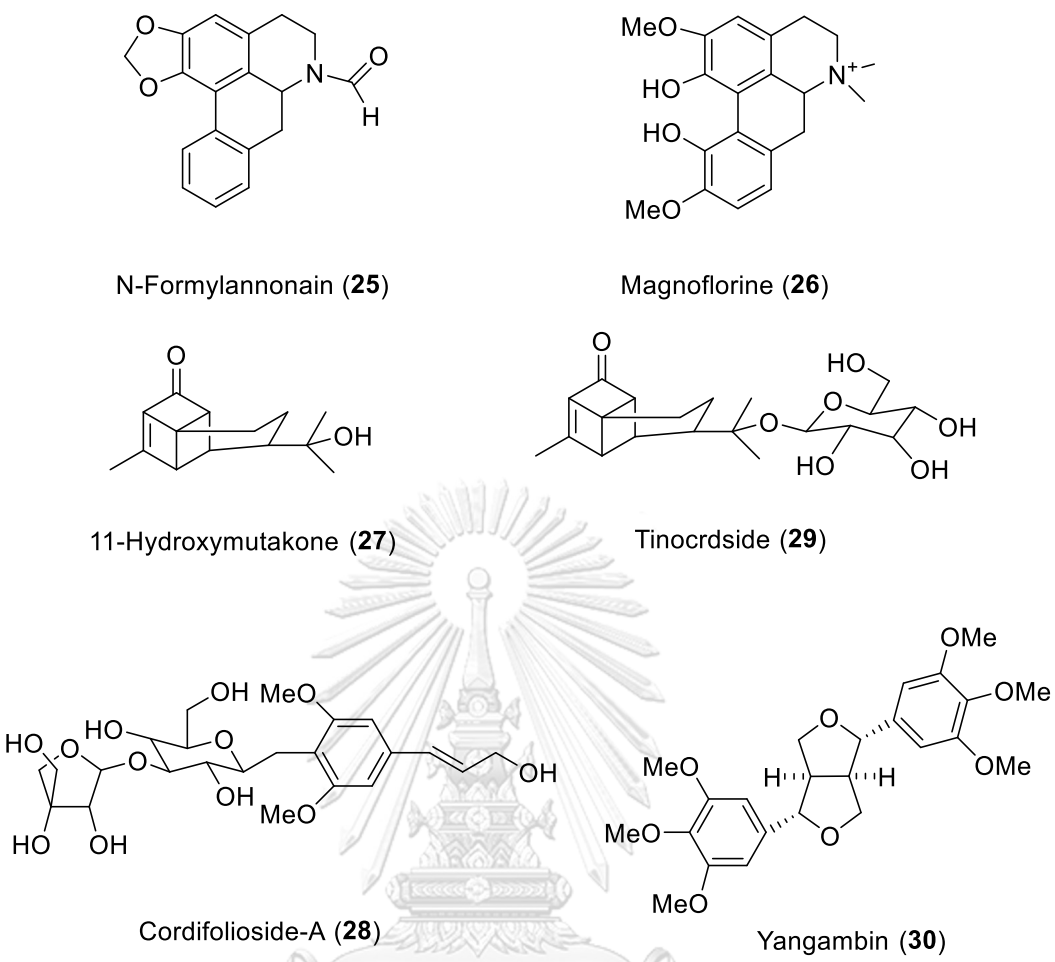

Fig. 2.4 Structures of compounds **25–30**

2.1.1.5 Cardiotonic activity

In 2002, Kongkathip and co-workers reported the isolation of two triterpenes, namely cycloeucalenol (**31**) and cycloeucalenone (**32**), from stems of *T. crispa* (**Fig. 2.5**). Both compounds displayed moderate cardiotonic effects [42].

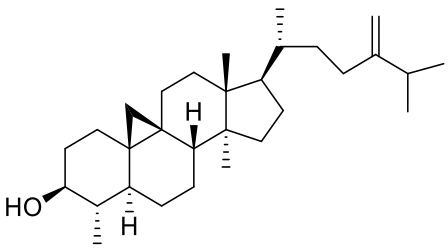

Cycloeucalenol (**31**)

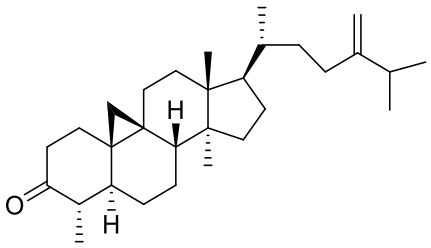

Cycloeucalenone (**32**)

Fig. 2.5 Structures of compounds **31** and **33**

2.1.1.6 α-Glucosidase inhibitory activity

In 2015, Chang and coworkers disclosured four new acylatedglycosyl flavonoids from *T. crispa* leaves: isoorientin 2″-*O*-(*E*)-sinapate (**38**), isovitexin 2″-(*E*)-*p*-coumarate (**40**), cosmosiin 6′-(*E*)-ferulate (**41**) and cosmosiin 6′-(*E*)-cinnamate (**47**), together with thirteen known flavonoids: isoorientin (33), orientin (34), isovitexin (35), luteolin-7-*O*-b-glucoside (36), apigenin 7-*O*-b-glucoside (37), isoorientin 2′-(*E*)-*p*-coumarate (39), cosmosiin 6′-(*E*)-*p*-coumarate (42), cosmosiin 6″-(*Z*)-*p*-coumarate (43), apigenin (44), 7-*O*-*β*-glucosyl-6″-(*E*)-*p*-cinnamate (45), 3′-*O*-methylluteolin (46), 4′-*O*-b-glucoside (48) and luteolin (49) (**Fig. 2.6**). Compound 40 exhibited the most potent activity against **α**-glucosidase with an IC_{50} value of 4.3 μM, while 39 is much less activity at the IC_{50} value of 35.7 μM [43].

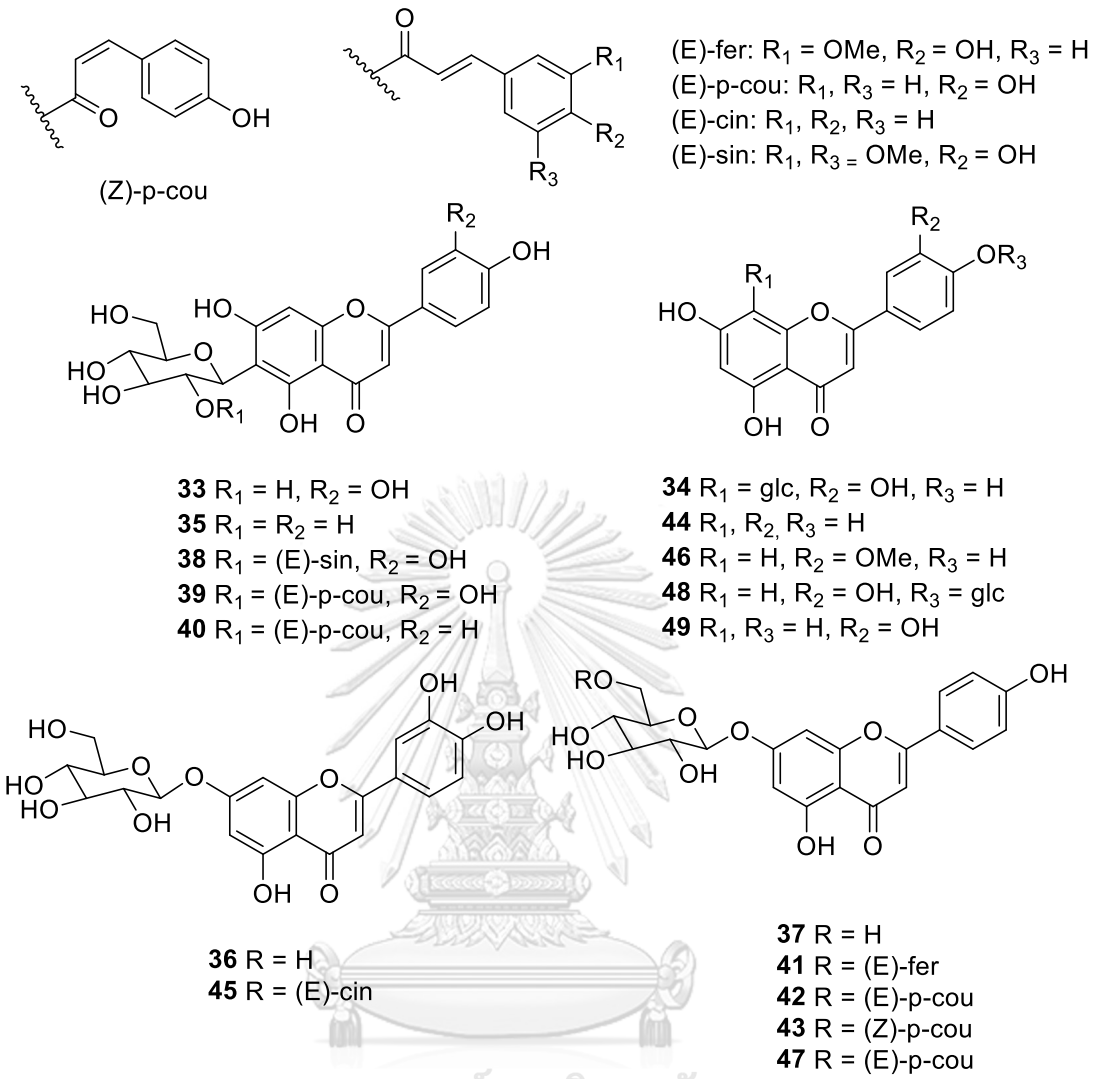

Fig. 2.6 Structures of compounds **33–49**

2.1.1.7 Cytotoxic activity

In 2015, Wang and coworkers investigated chemical constituent of *T. capillipes*, a local Chinese medicinal plant and three new diterpenoids, namely tinocapillins A-C (**50**-**52**), together with three known compounds (**53**-**55**) were isolated (**Fig. 2.7**). Compounds **50**, **51**, and **54** showed inhibitory activity against proliferation of A549, Hep-G2, Hela, and OS-RC-2 cancer cell lines [33].

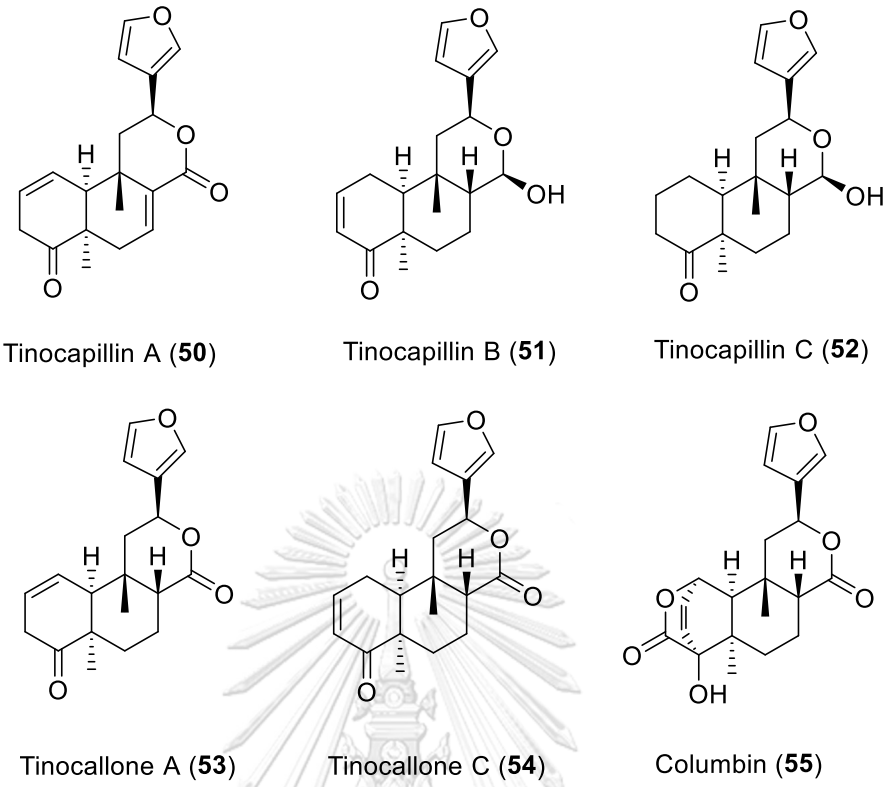

Fig. 2.7 Structures of compounds **50–55**

In the same year, Qin and coworkers reported tinosporins A (**56**) and B (**57**), along with two known compounds columbin (**58**) and fibaruretin B (**59**) (**Fig. 2.8**), a clerodane-type furanoditerpenoids from root of *T. sagittata*. Compound **56** showed moderate cytotoxicity against HL-60 and MCF-7 cell lines, with IC_{50} values of 18.63 and 23.58 μM, respectively [44].

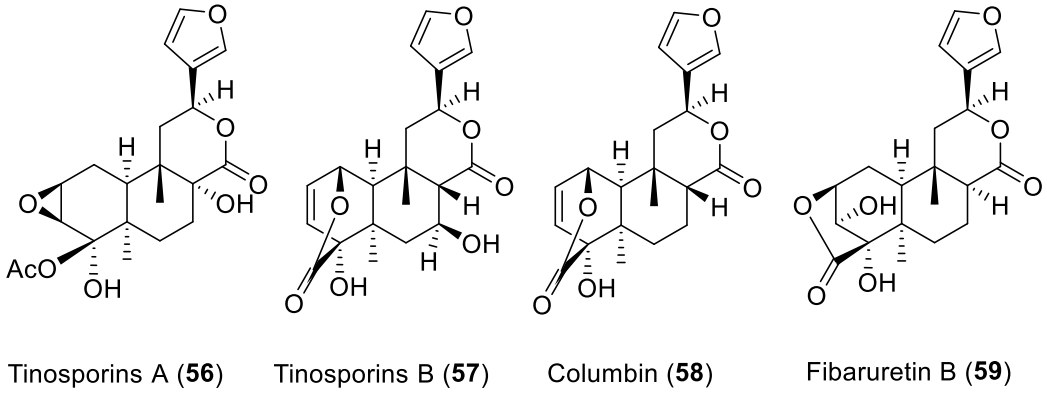

Fig. 2.8 Structures of compounds **56–59**

2.1.3 Plant *Tinospora baenzigeri* Forman

2.1.3.1 Taxonomical Characteristic of *Tinospora baenzigeri* Forman

Taxonomy of *Tinospora baenzigeri* Forman is classified as

Kingdom: Plantae

Division: Magnoliphyta

Class: Magnoliops

Order: Ranunculales

Family: Menispermaceae

Genus: Tinospora

Species: *T. baenzigeri* Forman [45]

2.1.3.2 Botanical Characteristic of *Tinospora baenzigeri* Forman

The species of *T. baenzigeri* is deciduous woody climber and the majority of the species can be found in countries with a tropical climate. The morphological characteristics of *T. baenzigeri* are described in **Table 2.1** and **Fig. 2.9**

Table 2.1 Morphological characteristics of *T. baenzigeri* [45]

Part of plant	*T. baenzigeri*
Stem	Climber and less prominently tuberculate
Leaf	Cordate or reniform, caudate apex, alternate, entire margin, cordate base, 5-7 cm. long petiole and two nodes appearing at leaf base
Flower	Inflorescence spike, 3 petals and greenish-yellow color
Fruit	Ellipsoidal, smooth, 1-1.5 cm. long with dark yellow color
Seed	Moon seed, rough, 0.5-1 cm. long with black color

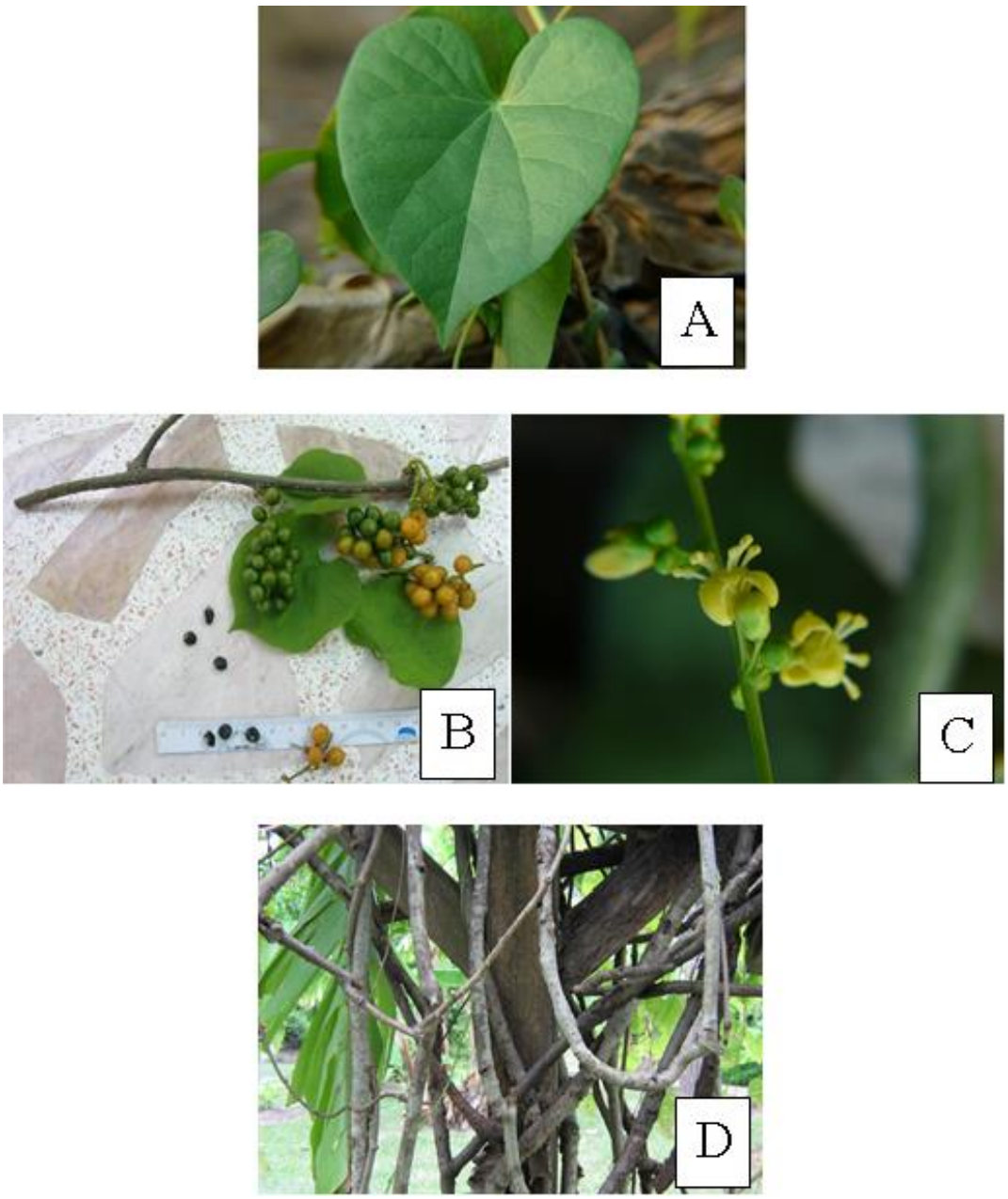

Fig. 2.9 *Tinospora baenzigeri* Forman

A = Leaf, B = Fruit, C = Flower and D = Stem

(Image from: http:// medthai.com/ชิงช้าชาลี/)

2.1.3.3 Chemical constituents and bioactivities of *Tinospora baenzigeri*

In Thailand, stems of *T. baenzigeri* are generally used for malaria treatment and anti-pyretic. Moreover, a number of reports that the extracts of its roots, leaves and stems showed good anti-malarial activity [46]. Additionally, only two publications of the studies on its chemical constituents have been found, there is less information on their biological activities. A perusal of literature reveals that bioactive compounds from *T. baenzigeri* are likely to be sources of new drug. In 1999 and 2001, Tuntiwachwuttikul and co-workers described the isolation and characterization of two new rearranged clerodane diterpene glucosides, baenzigeride A (**60**) and baenzigeroside B (**61**), from *T. baenzigeri* stems, together with their acetate derivatives (**62**-**63**), baenzigeroside A (**64**) and baenzigeride B (**65**). Compounds **60**, **61** and **64** (**Fig. 2.10**) was also obtained from the leaves of the same plant [47, 48]. However, they did not show any significant antimalarial activity as expected.

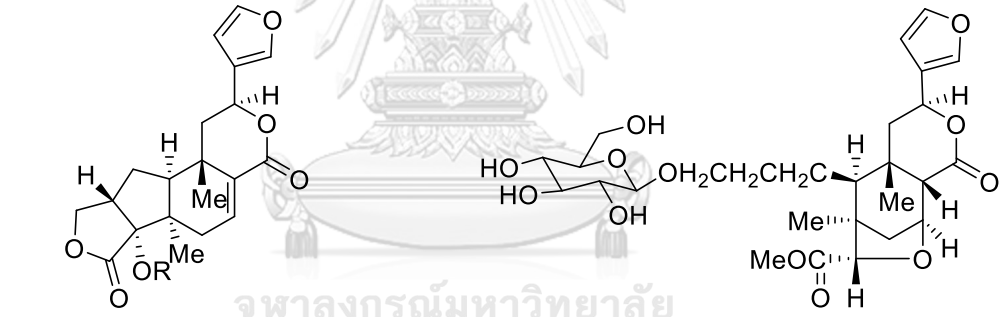

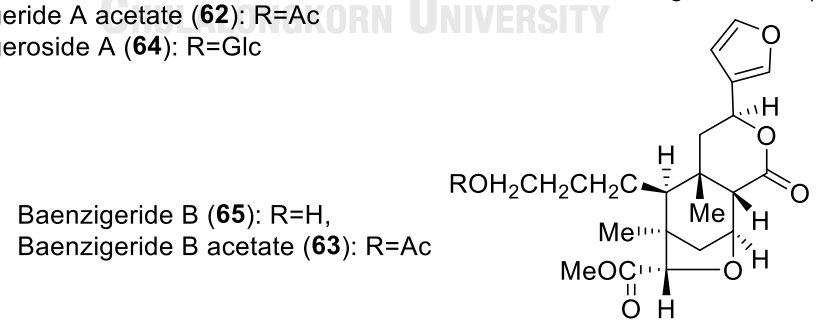

Fig. 2.10 Structures of compounds **60**–**65**

2.2 Materials

2.2.1 Plant samples

The fresh stems of *T. baenzigeri* were bought from Chaokrompoe, a local market in Bangkok, in April 2013 and collected from Phu Wua Wildlife Sanctuary, Nong Doen, Bueng Kan Province, Thailand, in April 2016. Voucher specimens were designated with the code CUCHEM2013-003 and CUCHEM2016-002, respectively, and are deposited at Department of Chemistry, Faculty of Science, Chulalongkorn University.

2.2.2 Equipments

2.2.2.1 Column chromatography

Merck's silica gel 60H (No. 7734 and No. 9385) and ODS (Wakogel® 100C18, 63-212 μM) were normally used as the adsorbents for open column chromatography. Sephadex LH-20 (Amersham Pharmacia Biotech AB) was used to separate substances by molecular sizing.

2.2.2.2 Thin-layer chromatography (TLC)

Merck's TLC alumina sheets, silica gel^{60} GF_{254} precoated 25 sheets, 20x20 cm, layer thickness 0.2 mm were used for TLC analysis.

2.2.2.3 High performance liquid chromatography (HPLC)

High performance liquid chromatography (HPLC) was performed using a Thermo Scientific Spectra System (Thermo Scientific P200 pump and Thermo Scientific UV6000LP detector). Column VertiSep^{TM} UPD C_{18} (4.6x150 mm, 5 µM) was used for analysis and Column GL Sciences (20x250 mm, 5 µM) was used for separation.

2.2.3 General Experimental Procedures

2.2.3.1 Nuclear magnetic resonance spectroscopy (NMR)

The NMR data were performed on Bruker AV400 and Varian Mercury 400 plus spectrometer at 400 MHz for ^{1}H NMR and 100 MHz for ^{13}C NMR by using TMS (tetramethylsilane) as an internal standard. Deuterated solvents, chloroform-*d* ($CDCl_3$), dimethysulfoxide-d_6 (DMSO-d_6) and acetone-d_6, were used for NMR

experiments and chemical shifts (δ) were referenced by the signals of residual solvents at 7.26 (s) ppm (^{1}H NMR) and 77.00 (t) ppm (^{13}C NMR) for $CDCl_3$, at 2.50 (t) ppm (^{1}H NMR) and 39.5 (sept) ppm (^{13}C NMR) for DMSO-d_6 and at 2.09 ppm (^{1}H NMR) and 29.9 and 206.7 ppm (^{13}C NMR) for acetone-d_6.

2.2.3.2 Mass spectrometry (MS)

ESI-TOF mass spectra and HRESIMS were examined with a Bruker microOTOF mass spectrometer.

2.2.3.3 Ultraviolet-visible measurements (UV-vis)

Spekol 1200 (Analytic JENA) and GBC Cintra 404 UV-Visible spectrophotometers were used to recorde UV spectral data.

2.2.3.4 Fourier transforms infrared spectroscopy (FT-IR)

The FT-IR spectra were measured with a Perkin-Elmer Model 1760X Fourier Transform Infrared Spectrophotometer.

2.2.3.5 Melting point

Melting points were measured by a Fisher-Johns melting point apparatus.

2.2.3.6 Optical rotation

Optical rotations were measured on a JASCO P-1010 polarimeter.

2.2.3.7 X-ray crystallography

The crystal structure was solved by direct methods and using the SHELXS97 program. Crystallographic data, excluding structure factors, have been deposited at the Cambridge Crystallographic Data Centre.

2.2.4 Chemicals

All commercial grade solvents used in this investigation including hexane, dichloromethane (CH_2Cl_2) ethyl acetate (EtOAc), acetone, ethanol (EtOH) and methanol (MeOH) were distillated prior to use. In addition, HPLC grade solvents, MeOH and Milli-Q water, were used for HPLC purification.

The deuterated solvents for NMR measurement, $CDCl_3$, DMSO-d_6 and acetone-d_6, were purchased from Merck Millipore.

2.3 Methods

2.3.1 Extraction and purification of crude extract

2.3.1.1 *Tinospora baenzigeri* extract from local market

The powdered air-dried stem of *T. baenzigeri* (5 kg) bought from a local market in Bangkok was extracted three times with MeOH (10 L x 3, each 2 days) at room temperature. After filtration, the filtrate was evaporated *in vacuo* to give the combined MeOH crude extract. The MeOH extract was suspended in water and the solution was successively partitioned against hexane and then EtOAc. The EtOAc fraction was concentrated under reduced pressure to yield a dark green thick oil (108 g). Fractionation of the EtOAc extract was performed on a silica gel column using a gradient of EtOAc/hexane (10%-100%) and MeOH/EtOAc (10%-20%) to yield twenty fractions (Q1-Q20). Each fraction was analyzed by TLC and ^{1}H NMR spectrum. Crystallization of fraction Q11 (7.69 g) in acetone gave compound **66** (1.72 g). Purification of fraction Q12 (4.35 g) was performed by gel filtration chromatography using Sephadex LH-20, eluted with 100%MeOH to give 6 fractions, Q12P1-Q12P6. Subfraction Q12P3 (2.91 g) was rechromatographed on silica gel and eluted with acetone/hexane (10%-50%) to yield compound **68** (8.0 mg). Fraction Q13 (8.51 g) was purified by Sephadex LH-20 and eluted with 100%MeOH to afford 4 fractions, Q13P1-Q13P4. Subfraction Q13P1 (4.64 g) was separated on silica gel and eluted with EtOAc/hexane (60%-100%) to obtain compounds **66** (30.2 mg), **67** (110.5 mg), **71** (4.2 mg), while fraction Q13P1S7 (170.0 mg) gave compound **72** (5.1 mg) when 15% mixture of acetone/CH_2Cl_2 was used as eluent. Fraction Q16 (6.14 g) was fractionated by column chromatography using silica gel. Elution systems were MeOH/CH_2Cl_2 gradients (2%-50%) to provide 7 fractions, Q16S1-Q16S7. Subfraction Q16S4 (1.19

g) was rechromatographed on silica gel and eluted with MeOH/CH_2Cl_2 (2%-6%) to obtain compound **74** (6.4 mg) and **75** (2.6 mg), and Q16S4.4 (119.4 mg) gave compound **69** (6.4 mg) when 2% mixture of MeOH/CH_2Cl_2 was used as eluent. While subfraction Q16S5 (2.32 g) was purified by Sephadex LH-20 (100%MeOH), followed by silica gel using MeOH/CH_2Cl_2 (2%-10%) to afford compound **73** (6.8 mg). Finally, fraction Q19 (22.85 g) was separated on a silica gel column eluting with MeOH/CH_2Cl_2 (5%-50%) to afford 3 fractions, Q19S1-Q19S3. Q19S3 (11.73 g) was purified by Sephadex LH-20 (100%MeOH) and applied to ODS column chromatography using MeOH/H_2O (50%-100%) to furnish compounds **61** (34.0 mg). Fraction Q19S3P2 was subjected to silica gel column eluting with MeOH/CH_2Cl_2 (4%-20%), followed by ODS column chromatography (2%-6%, MeOH/CH_2Cl_2) to yield compound **70** (53.4 mg). The isolation and purification procedures were briefly summarized in **Scheme 2.1**

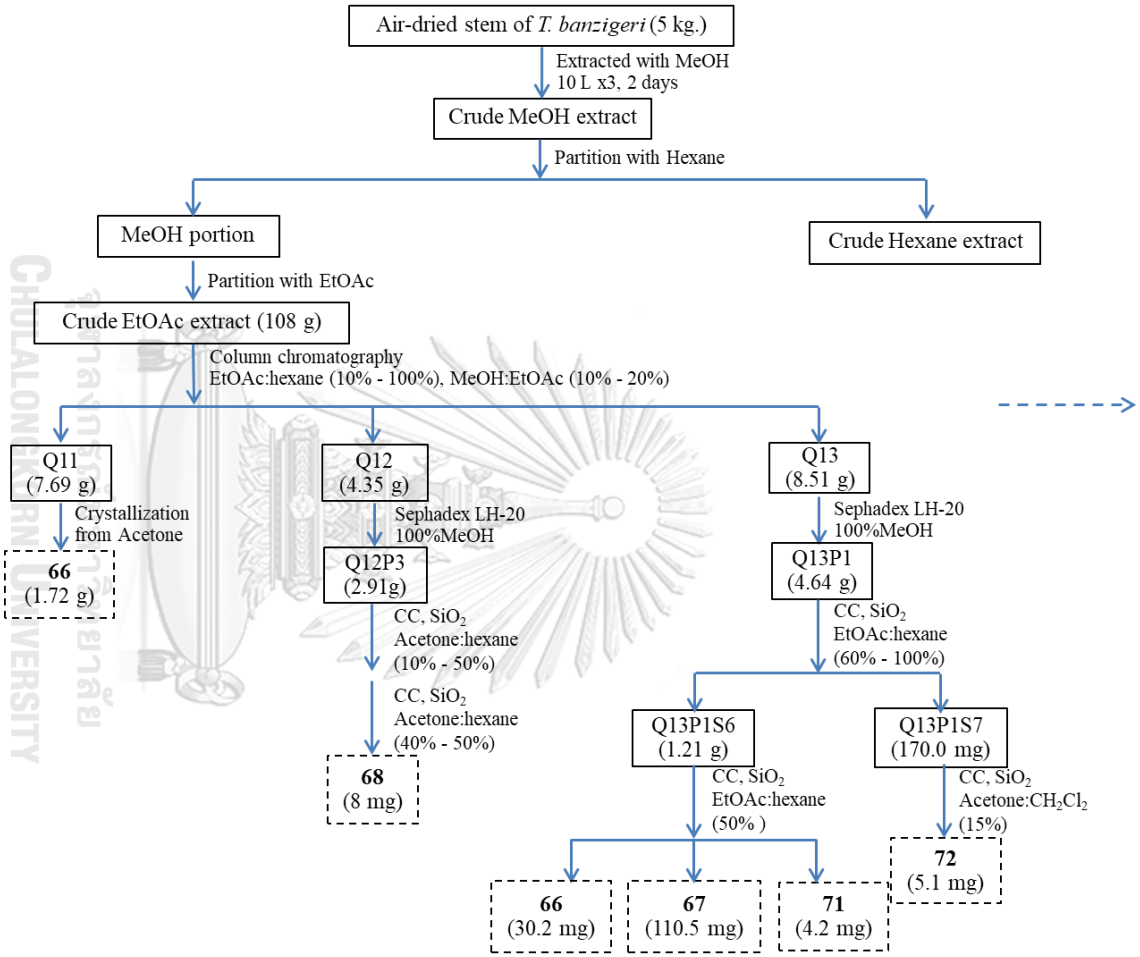

Scheme 2.1 The isolation of *T. baenzigeri* bought from a local market in Bangkok

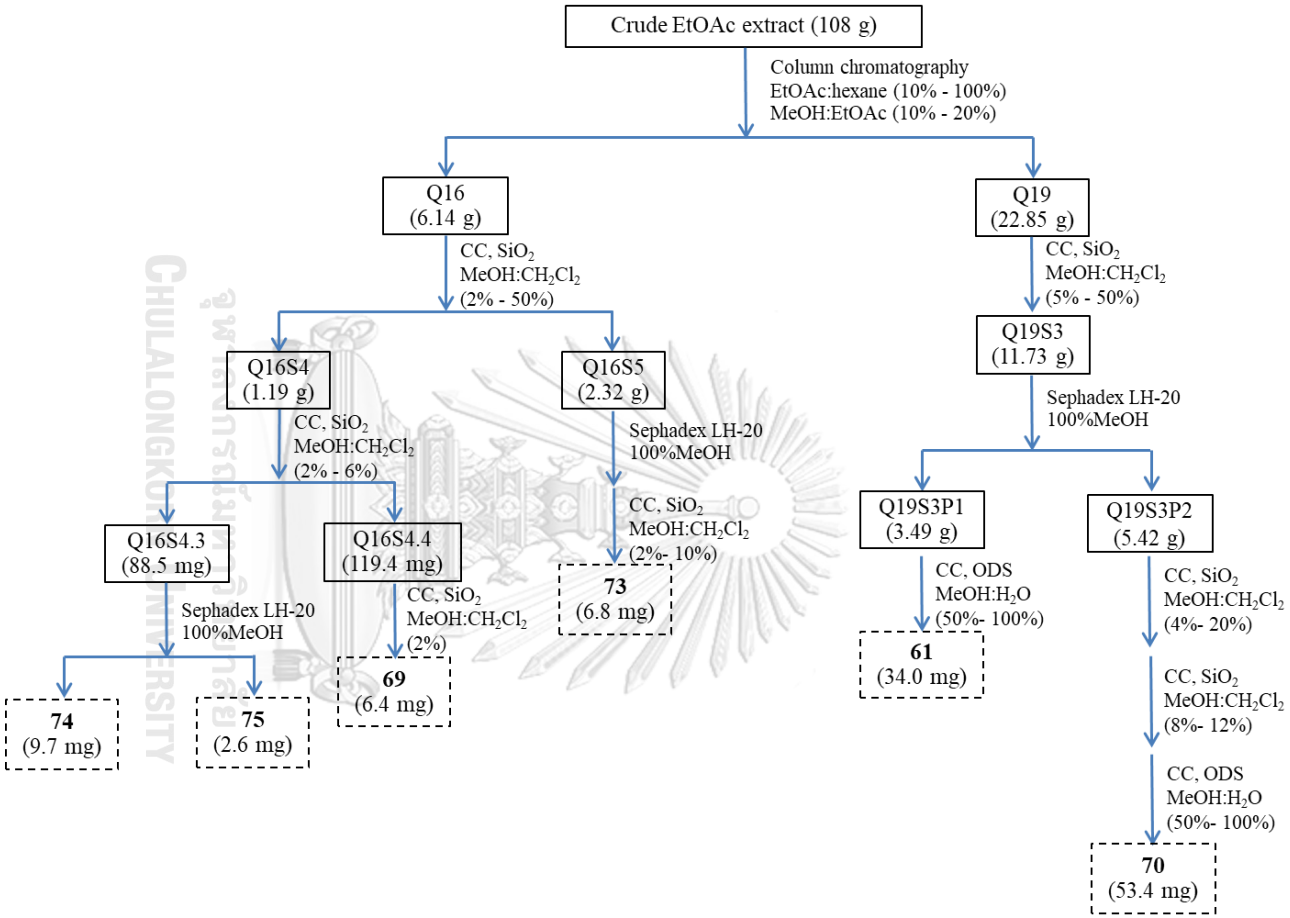

Scheme 2.1 The isolation of *T. baenzigeri* bought from a local market in Bangkok (continue)

2.3.1.2 *Tinospora baenzigeri* extract from Bueng Kan Province

The powdered air-dried stem of *T. baenzigeri* (5 kg) from Bueng Kan Province was prepared as mentioned provisory. Fractionation of the EtOAc extract (111 g) was separated by flash silica gel column using a gradient of EtOAc/hexane (20%-100%) and of MeOH/EtOAc (20%, 50%). According to TLC analysis, ten fractions (F1-F10) were collected, then were analyzed by ^{1}H NMR spectrum. Fraction F4 (12.08 g) was rechromatographed on silica gel, eluted with 5%-50% EtOAc/hexane. Subfraction F4S8 (791.2 mg) was separated on silica gel, eluted with EtOAc/hexane (10%-60%), and further purified by preparative HPLC (C18) silica gel using a mixture of ACN/H_2O (40%) to obtain compound **81** (13.0 mg). Whereas F4S10 was fractionated on silica gel and eluted with EtOAc/hexane (40%-100%) to give compound **78** (24.7 mg) While subfraction F4S10A (934.6 mg) was further recrystallized in acetone to afford compound **66** (713.7 mg), next subfraction F4S10A1 was separated on silica gel column eluted with a gradient mixture of EtOAc/hexane (60%) to obtain compound **76** (3.6 mg). F4S11 (3.17 g) was subjected to column chromatography over silica gel eluting with acetone/CH_2Cl_2 (5%-100%) to furnish compound **44** (8.3 mg). Subfraction F4S11A (119.5 mg) was rechromatographed on silica gel flash column and eluted with acetone/CH_2Cl_2 (10%-50%) to afford compounds **79** (5.3 mg) and **80** (6.7 mg). Fraction F5 (16.34 g) was subjected to silica gel column chromatography eluting with acetone/CH_2Cl_2 (10%-100%), gave three interesting fractions (F5S5, F5S6 and F5S9). F5S9 (5.08 g) was selected for separation by using a gradient of EtOAc/hexane (40%-60%). The obtained F5S9A (2.75 mg) was rechromatographed on silica gel and eluted with EtOAc/hexane (50%-100%) to afford compound **66** (220.0 mg). Furthermore, fraction F8 (5.31 g) was fractionated over a silica gel column using a gradient of EtOAc/hexane (50%-100%), followed with a gradient mixture of MeOH/EtOAc (10%-20%), and next subfraction F8S6 (432.0 mg) was separated on silica gel and eluted with MeOH/CH_2Cl_2(2%-10%), respectively. F8S6A (67.0 mg) was purified on silica gel flash column and eluted with 2%-8% MeOH/CH_2Cl_2 to yield compounds **74** (16.6 mg) and **75** (3.6 mg). Finally, F9 (52.95 g) was fractionated on silica gel, eluted with MeOH/CH_2Cl_2(2%-10%) resulted subfraction F9.5A (115.5 mg) that was applied to ODS column chromatography using MeOH/H_2O (40%-100%) to furnish compounds **61** (25.7 mg) and **70** (44.5 mg). On the other hand, subfraction

F9.5B (452.9 mg) was subjected to pass column chromatography with MeOH/CH_2Cl_2 (7%) to afford compound **70** (74.2 mg). The obtained subfraction F9.5B1 was further purified by preparative HPLC to yield **77** (8.6 mg). The isolation and purification procedures were briefly summarized in **Scheme 2.2**

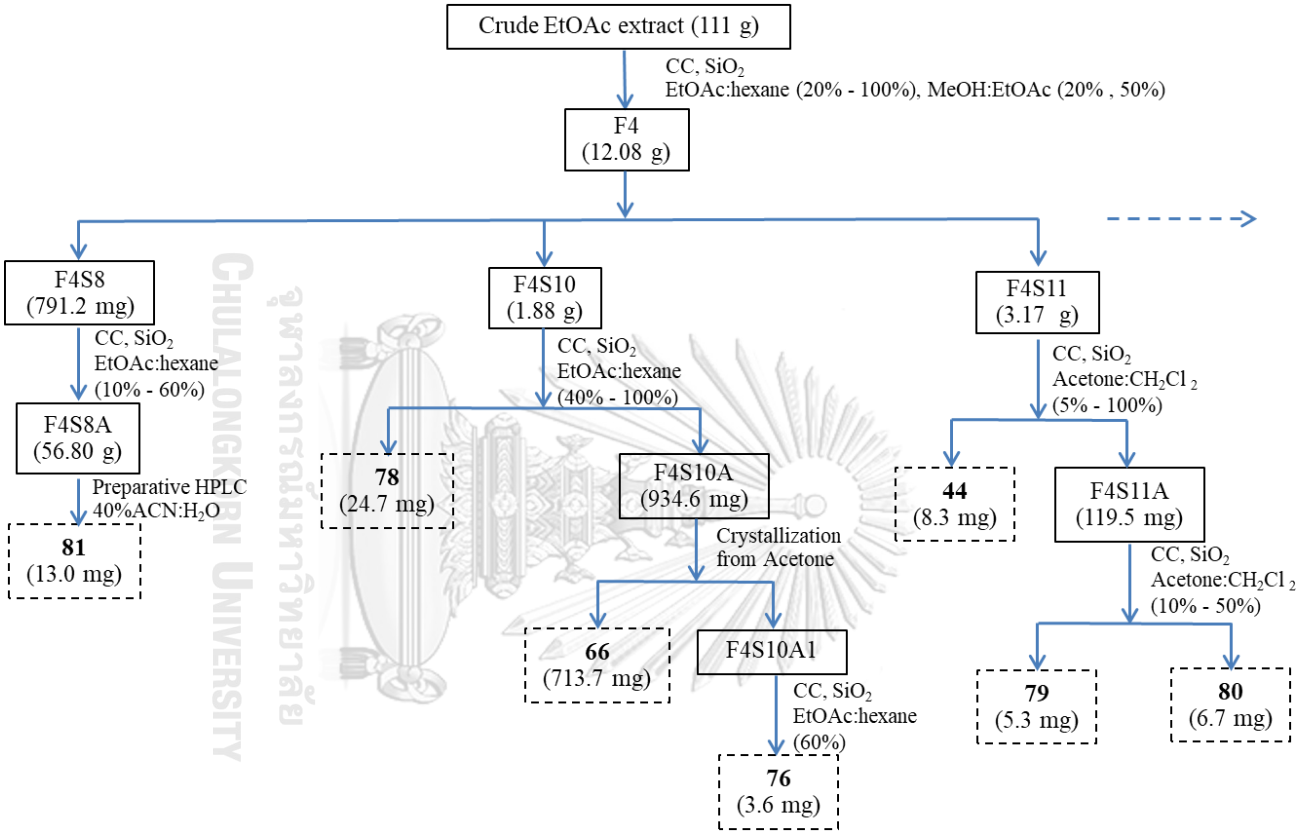

Scheme 2.2 The isolation of *T. baenzigeri* from Bueng Kan Province

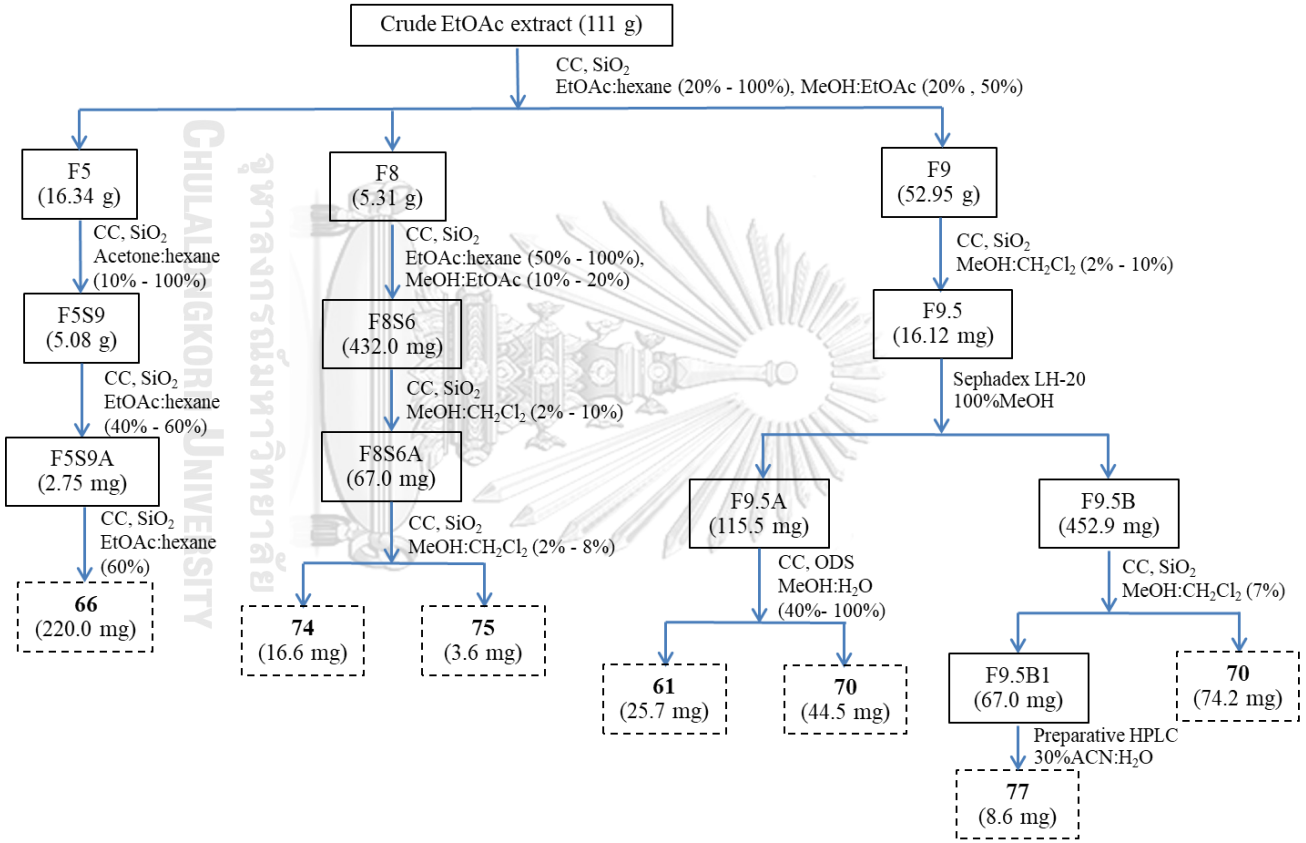

Scheme 2.2 The isolation of *T. baenzigeri* from Bueng Kan Province (continue)

2.4 Bioactivity assay

2.4.1 Cytotoxicity assay

Cytotoxicity assay of isolated compounds against hepato carcinoma (Hep-G2), gastric carcinoma (KATO-3), breast carcinoma (MCF-7) and cervix carcinoma (CaSki) was performed in vitro by MTT (3-(4,5-dimethylthiazol-2-yl)-2,5-diphynyltrazolium bromide) calorimetric method [49-51]. In principle, the viable cell number/well was directly proportional to the production of formazan, followed by solubilization, and could be measured by spectrophotometrically.

The human cancer cell line was seed in a 96-well culture plate ($1x10^4$ cell/ml) in 100 μL of Roswell Park Memorial Institute (RPMI) medium with 10% fetal bovine serum (FBS) and incubated in 5% CO_2 at 37 °C, 100% relative humidity for 24 h. Culture medium containing the pure compound was dispensed into the appropriate wells (n=3) and doxorubicin was used as a positive control. Culture plates were then incubated for 3 days. Then, MTT solution (5 mg/mL; 10 μL) was added and cells were further incubated at 37 °C for additional 4 h under the same condition. At the end of the incubation, DMSO (100 μL) was added to dissolve formazan and the absorbance was measured at 540 nm. Percentage of cell viability (%) was calculated using the following formula:

$$\% \text{ cell viability} = \frac{\text{OD test - OD blank x 100}}{\text{OD control -OD blank}}$$

2.4.2 Anti-inflammatory assay

The anti-inflammatory activity and toxicity of the isolated compounds on macrophage cell line were determined by suppressing nitric oxide (NO) production in activated macrophages and by using MTT assay, respectively.

Griess reaction [52] was used to measure amount of nitrite production. Murine macrophage cell line J774.A1 was cultured in 96-well plate ($5x10^4$ cells) containing Dulbecco's modified Eagle's medium (DMEM) with 10% FBS. It was incubated at 37 °C in a humidified atmosphere with 5% CO_2 for all experiments. The 24 hr. incubated cells were treated by various concentrations of the test compounds and vehicle (DMSO) for 2 h, subsequently, the cells were inflamed by adding lipopolysaccharide (LPS, 1 μg/mL) for 18 h and indromethacin was used as a positive control. After an additional 18 h of incubation, the culture supernatant was harvested for NO assay by Griess reaction and the absorbance was measured at 540 nm. Activated J774.A1 cell line was treated MTT as described in 2.3.1.

2.4.3 α-Glucosidase inhibitory activity

α-Glucosidase is a crude enzyme generated from rat intestine that consistence maltase and sucrase. The analysis of intestinal α-glucosidase inhibitory activity was based on the previously described [53]. Briefly, 1 g of rat intestinal acetone powder was homogenized with 30 ml of 0.9% NaCl solution. Subsequently, the solution was centrifuged at 12,000 g for 30 min then subjected to assay. The crude enzyme solution (20 μL) was incubated with substrate (maltose:10 mM or sucrose 100 mM) 20 μL, 10 μL of the test sample at various concentrations, followed by the addition of 0.1 M phosphate buffer, pH 6.9, and 80 μL of glucose Kit to give a final volume of 160 μL, acrabose was used as a positive control. The mixtures were incubated at 37°C for 10 min (maltase assay) or 40 min (sucrase assay). The concentration of glucose released from the reaction mixtures were determined by glucose oxidase method with absorbance at a wavelength of 520 nm. The percentage inhibition was calculated using the following formula:

$$\% \text{ Inhibition} = (Abs_{blank} - Abs_{Sample}) / Abs_{blank} \times 100$$

Abs_{blank} are the absorbance without sample

2.5 Results and Discussion

2.5.1 Isolation of compounds of *T. baenzigeri* from a local market in Bangkok.

The ethyl acetate crude extract from the stems of *T. baenzigeri* bought from a local market in Bangkok was purified by chromatographic techniques to provide 11 compounds including five new rearranged clerodane diterpenes, namely tinobaenzins A-D (**66**-**69**) and tinobaenzin A glucoside (**70**), together with six known compounds, baenzigeroside B (**61**), caruilignan D (**71**), lariciresinol (**72**), aglycone of breyniaionoside D (**73**), *N*-*trans*-feruloyltyramine (**74**) and *N*-*trans*-coumaroyltyramine (**75**). The structures of isolated compounds are shown in **Fig 2.11**.

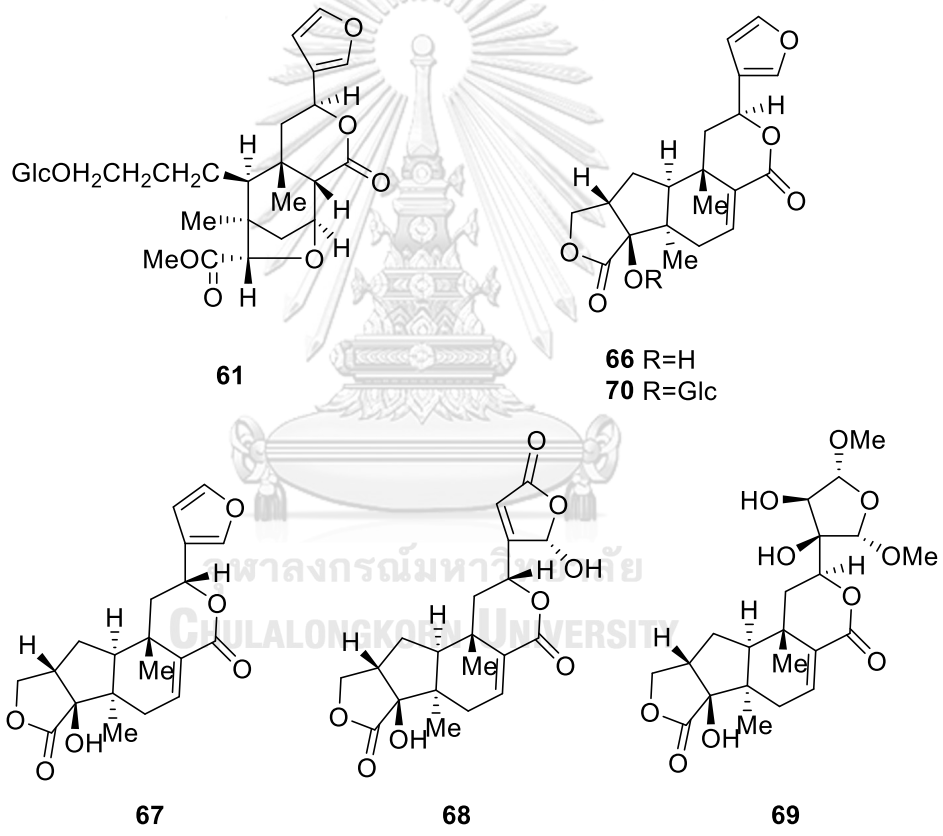

Fig. 2.11 Chemical structures of compounds from *T. baenzigeri* from a local market in Bangkok

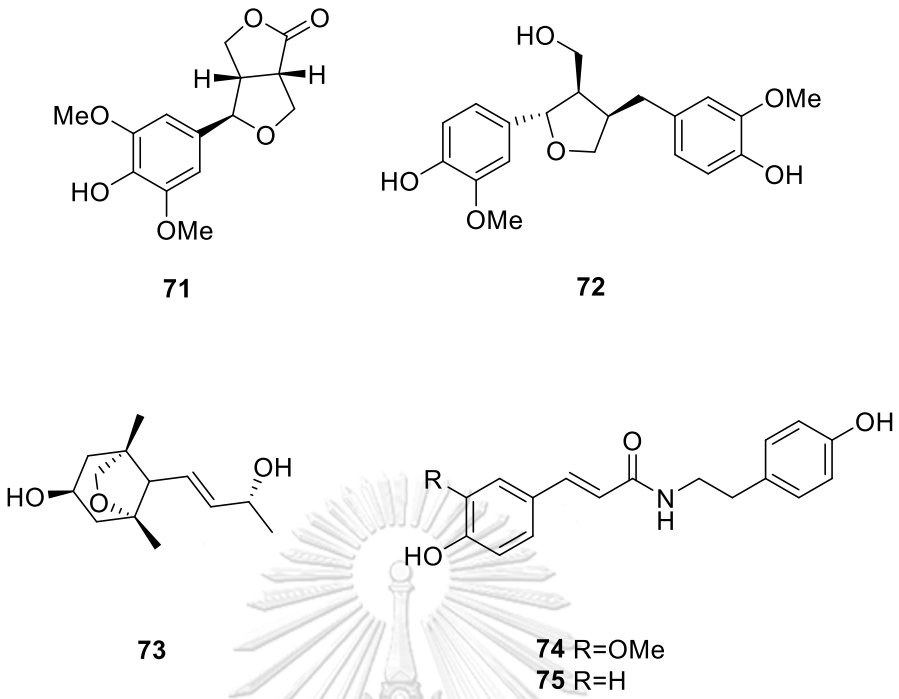

Fig. 2.11 Chemical structures of compounds from *T. baenzigeri* from a local market in Bangkok (continued)

2.5.1.1 Structural elucidation of isolated compounds

2.5.1.1.1 Structural elucidation of compound 61

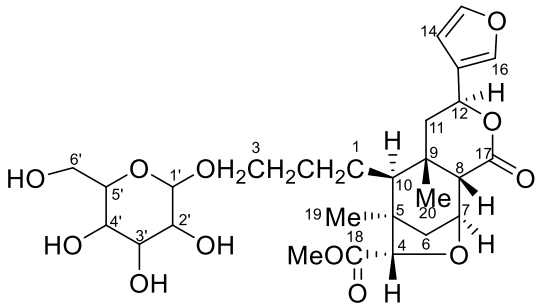

Fig. 2.12 Compound **61** (baezigeroside B)

Compound **61** obtained as a colorless powder, was assigned a molecular formula of $C_{27}H_{38}O_{12}$. The ^{1}H NMR data (**Table 2.2)** showed typical signals of *β*-substituted furan ring at δ_H 7.67 (t, *J* = 1.4 Hz), 7.75 (s) and 6.59 (d, *J*=0.8 Hz), which were assigned to α-H-15 and α-H-16 and *β*-proton (H-14), respectively. The ABX systems presented by ^{1}H NMR at δ_H 5.70 (d, *J* = 11.6 Hz), 1.45 (d, *J* = 12.0 Hz) and 1.95 (m) were given to H-12 and H_2-11. The spectra also displayed a signal of an anomaric proton [δ_H 4.09 (d, *J* = 7.6 Hz)] with an anomaric carbon at δ_C 102.6 of the glucopyranosyl group. Additionally, ^{13}C NMR (**Table 2.3)** showed two carbonyl groups (δ_C 170.1; C-17 and 172.1; C-18) and two quaternary carbons (δ_C 47.5; C-5 and 35.6; C-9). It also indicated the presence of six methylene carbons (δ_C 23.4; C-1, 31.2; C-2, 60.9; C-3, 41.1; C-6, 41.0; C11 and 76.7; C-6′). Moreover, it presented ten methine groups (δ_C 79.5; C-4, 78.4; C-7, 53.2; C-8, 47.4; C-10, 69.4; C-12, 102.6; C-1′, 73.3; C-2′, 68.4; C-3′/C-4′ and 69.9; C5′), two methyl carbons (δ_C 20.0; C-19 and 26.6; C-20), together with a methoxyl group (δ_C 51.4). The HMBC experiment was used for establishing the connectivity among the ^{1}H-^{1}H COSY derived fragments with the remainder of the molecule (**Fig. 2.13**). The COSY experiments were useful in the assignment between H_2-2/H_2-3, H_2-6/H-7/H-8, H-10/H_2-1, H_2-11/H-12 and H-1′/H-2′/H-3′/H-4′ H-5′/H_2-6′. Comparison of the NMR data with those reported by Tuntiwachwuttikul and Taylor (2001) indicated that compound **61** was baezigeroside B [48].

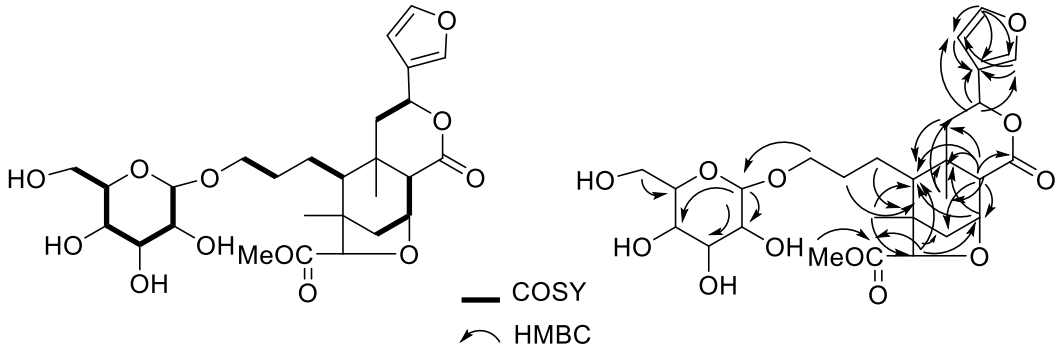

Fig. 2.13 Key COSY and HMBC correlations of compound **61**

2.5.1.1.2 Structural elucidation of compound 66

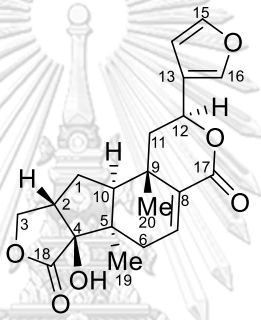

Fig. 2.14 Compound **66** (tinobaenzin A)

Compound **66,** obtained as colorless crystals, UV (MeOH) λ_{max}(log ε) 209 (3.91) nm, $[\alpha]^{20}_D$ +27.06 (c 0.1, MeOH), was assigned a molecular formula of $C_{20}H_{22}O_6$ by the HRESIMS peak at *m*/z 381.1316 $[M + Na]^+$. Its IR spectrum showed characteristic absorptions for hydroxyl (3497 cm^{-1}), carbonyl (1740 cm^{-1}) and olefinic 55groups (1663 cm^{-1}). The ^1H NMR spectrum (**Table 2.2)** displayed typical signals for two tertiary methyls [δ_H 1.17 (s), 1.23 (s)], one olefinic proton [δ_H 6.69 (dd, *J* = 2.0, 6.8 Hz)], and three aromatic protons of *β*-substituted furan ring at δ_H 7.42 (t, *J* = 1.6 Hz), 7.45 (s) and 6.41 (d, *J* = 1.6 Hz), which similar to those of **61**. Combined analysis of ^{13}C NMR (**Table 2.3**) and HSQC data revealed the presence of two tertiary methyls, four methylenes (one oxygenated at δ_C 73.3; C-3), three methines (one oxygenated at δ_C 71.2; C-12), three quaternary carbons (one oxygenated at δ_C 86.4; C-4), a trisubstituted double bond, a *β*- furanyl ring and two ester carbonyl groups (δ_C 169.7; C-17 and 177.4; C-18). These functionalities accounted for six degrees of unsaturation, and thus the structure must contain four additional rings. Indeed, its NMR spectroscopic data were similar to those of baenzigeride A [47]. Moreover, analysis of

^{1}H-^{1}H COSY and HMBC correlations (**Fig. 2.15**) indicated the planar structure of **66** was the same as that of baenzigeride A. Partial structures of H_2-1/H-2/H_2-3, H_2-6/H-7, H_2-11/H-12, and H-14/H-15 were deduced by analysis of the ^{1}H-^{1}H COSY spectrum, and the complete structure was further established by the following HMBC correlations: H-3 to C-4 and C-18; H-7 to C-8 and C-17; H-12 to C-13, C-14, C-16 and C-17; H-15 to C-16; H_3-19 to C-4, C-5, C-6 and C-10; H_3-20 to C-8, C-9, C-10 and C-11. However, the ^{1}H NMR signal of H-2 for **66** was slightly different from that for baenzigeride A, as well as there was a big different in their melting point, suggesting that its H-2 orientation of **66** was different from that of baenzigeride A. The NOESY (**Fig. 2.16**) of **66** showed correlation between H-10 and H_3-19, but none between H-10 and H_3-20, indicating ring A/B and B/C to be *cis*- and *trans*-fused, respectively, as usually found in the clerodane diterpene of *Tinospora* spp. The obvious NOESY correlation of H-10/H-12 and H_3-19/H-12, but lack of correlation between H-10/H-2, supported that compound **66** was a C-2 epimer of baenzigeride A. Moreover, the structure and the relative configuration of **66** were further confirmed by single-crystal X-ray diffraction analysis with MoKα radiation (**Table 2.4**), and its ORTEP drawing is depicted in **Fig. 2.17.** Thus, compound **66** was assigned to be tinobaenzin A.

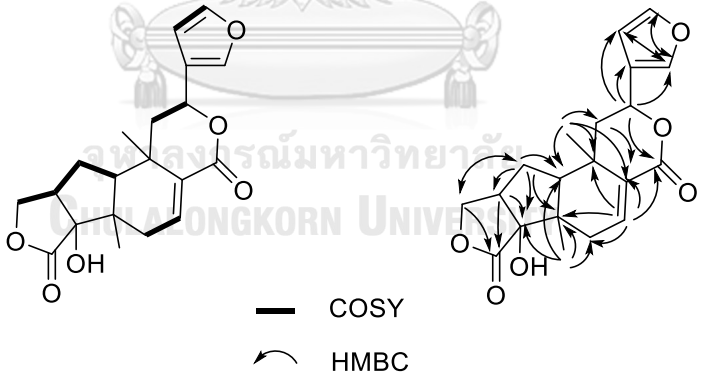

Fig. 2.15 Key COSY and HMBC correlations of compound **66**

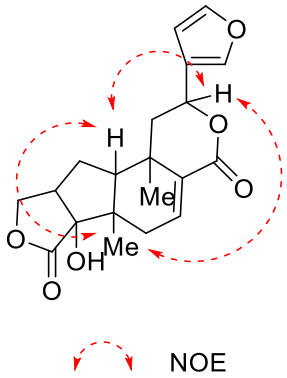

Fig. 2.16 NOESY correlations of compound **66**

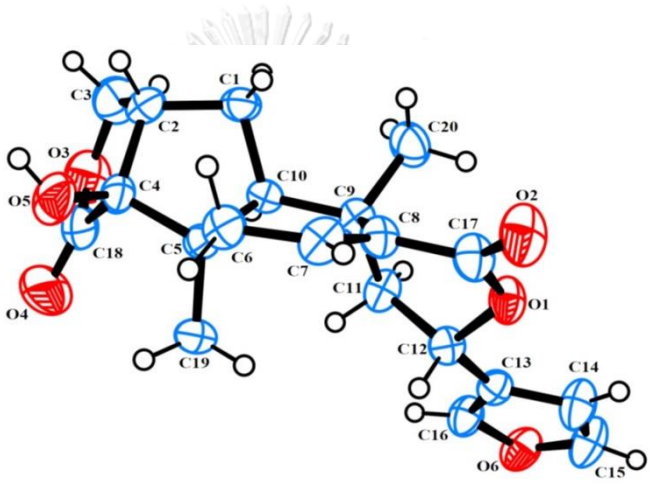

Fig. 2.17 ORTEP of compound **66**

2.5.1.1.3 Structural elucidation of compound 67

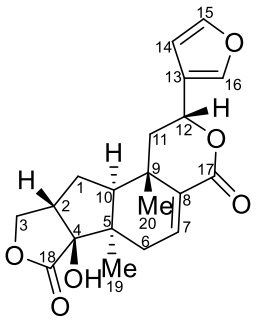

Fig. 2.18 Compound **67** (tinobaenzin B)

Compound **67** was obtained as colorless crystals, UV (MeOH) λ_{max} (log ε) 212 (3.92) nm, $[\alpha]^{20}_{D}$ -58.44 (c 0.1, MeOH) and its molecular formula deduced from the HRESIMS peak was at *m*/z 381.1316 $[M + Na]^+$, which was identical to the compound **66**. The IR spectrum of **67** indicated the presence of hydroxyl (3492 cm^{-1}), lactone (1769 cm^{-1}) and olefinic groups (1680 cm^{-1}). Interestingly, analysis of 1D (**Tables 2.2** and **2.3**) and 2D NMR spectroscopic data revealed both **66** and **67** had an identical overall structure. However, the ^{1}H NMR signal of H-12 for **67** was obviously different from that for **66**, indicating that its H-12 orientation of **67** was different from that of **66**. The proposed structure of **67** was further confirmed by NOESY correlations between H-12 and H_3-19 (**Fig. 2.19**), as well as its relative configuration were established by single-crystal X-ray diffraction analysis using MoKα radiation (**Table 2.4**), and perspective ORTEP plot is depicted in **Fig. 2.20.** Therefore compound **67** was a C-12 epimer of tinobaenzin A (**66**), namely tinobaenzin B as shown.

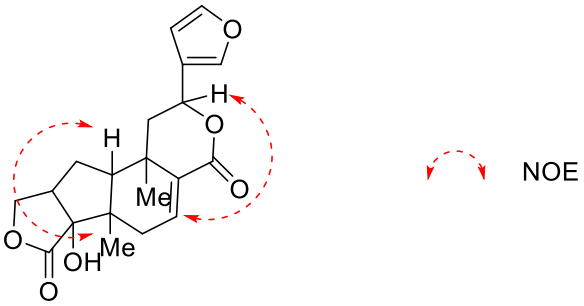

Fig. 2.19 Key NOESY correlations of compound **67**

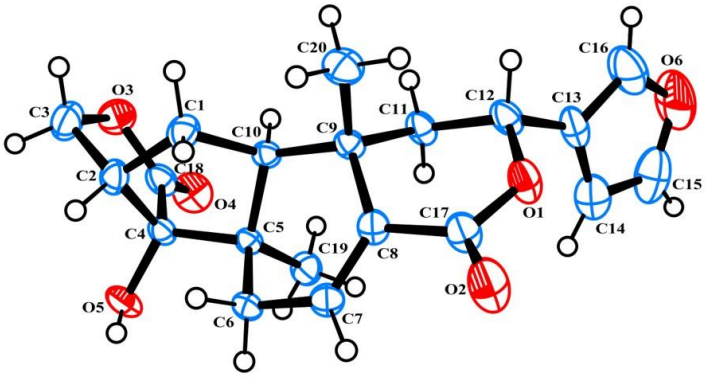

Fig. 2.20 ORTEP of compound **67**

Table 2.2 ^{1}H NMR data of compounds **61**, **66** and **67**

position	δ_H mult, (*J* in Hz)		
	61 (DMSO-d_6)	**66** ($CDCl_3$)	**67** ($CDCl_3$)
1	1.40 m	1.73 ddd, (1.2, 7.2, 13.2)	1.74 m
	1.59 m	2.03 m	2.20 m
2	1.58 m	2.90 m	2.90 m
	1.71 m		
3	3.43 m	4.02 dd, (3.2, 9.2)	4.00 dd, (4.0, 9.6)
	3.64 m	4.58 t, (9.2)	4.59 t, (9.2)
4	4.37 s	-	-
5	-	-	-
6	1.74 d, (14.4)	2.13 d, (6.4)	2.13 m
	2.02 d, (14.0)	2.40 d, (18.4)	2.43 d, (18.4)
7	4.77 t, (5.6)	6.69 dd, (2.0, 6.8)	7.03 dd, (2.4, 7.6)
8	2.83 d, (4.0)	-	-
9	-	-	-
10	1.90 m	1.91 m	1.78 m
11	1.45 d, (12.0)	1.96 m	1.95 dd, (4.8, 13.6)
	1.95 m	2.26 dd, (5.2, 14.0)	2.17 m
12	5.70 d, (11.6)	5.09 dd, (5.2, 11.2)	5.59 dd, (4.4, 11.6)
13	-	-	-
14	6.59 d, (0.8)	6.41 d, (1.6)	6.37 s
15	7.67 t, (1.4)	7.42 t, (1.6)	7.40 t, (1.6)
16	7.75 s	7.45 s	7.44 brd
17	-	-	-
18	-	-	-
19-Me	1.03 s	1.23 s	1.17 s
20-Me	1.16 s	1.17 s	1.27 s
18-OMe	3.65 s	-	-
1′	4.09 d, (7.6)	-	-
2′	2.91 m	-	-
3′	3.44 m	-	-
4′	4.73 m	-	-
5′	3.04 m	-	-
6′	3.05 m	-	-
	3.11 m		

Table 2.3 ^{13}C NMR data of compounds **61**, **66** and **67**

position	δ_c ppm		
	61 (DMSO-d_6)	**66** ($CDCl_3$)	**67** ($CDCl_3$)
1	23.4	33.3	33.5
2	31.2	42.9	43.1
3	60.9	73.3	73.1
4	79.5	86.4	86.5
5	47.5	47.2	47.9
6	41.1	30.3	30.5
7	78.4	133.5	137.6
8	53.2	134.5	133.2
9	35.6	34.6	35.3
10	47.4	51.5	52.4
11	41.0	43.7	42.6
12	69.4	71.2	71.3
13	124.9	123.9	125.2
14	108.9	108.6	108.4
15	143.8	143.7	143.8
16	140.1	139.7	139.5
17	170.1	169.7	165.8
18	172.1	177.7	177.8
19-Me	20.5	21.8	21.5
20-Me	26.6	27.7	23.1
18-OMe	51.4	-	-
1′	102.6	-	-
2′	73.3	-	-
3′	68.4	-	-
4′	68.4	-	-
5′	69.9	-	-
6′	76.7	-	-

Table 2.4 Crystal data and structure refinement for compounds **66** and **67**

Identification code	tinobaenzin A (**66**)	tinobaenzin B (**67**)
Empirical formula	$C_{20}H_{22}O_6$	$C_{20}H_{22}O_6$
Formula weight	358.38	358.38
Temperature	293(2) K	293(2) K
Wavelength	0.71073 Å	0.71073 Å
Crystal system, space group	Monoclinic, $P2_1$	Orthorhombic, $P2_12_12_1$
Unit cell dimensions	a = 8.2790(5) Å	a = 8.8330(3) Å
	b = 7.3433(4) Å	b = 13.3504(5) Å
	c = 14.0699(9) Å	c = 19.1573(9) Å
Volume	853.47(9) $Å^3$	1747.59(13) $Å^3$
Z, Calculated density	2	4
Absorption coefficient	0.10 mm^{-1}	0.10 mm^{-1}
F(000)	380	760
Crystal size	0.42 x 0.18 x 0.16 mm	0.52 x 0.48 x 0.42 mm
Reflections collected/unique	3069 [R_{int} = 0.0220]	4821 [R_{int} = 0.0210]
Final R indices [I>2sigma(I)]	R_1 = 0.0360, wR2 = 0.138	R_1 = 0.0420, wR2 = 0.107

2.5.1.1.4 Structural elucidation of compound 68

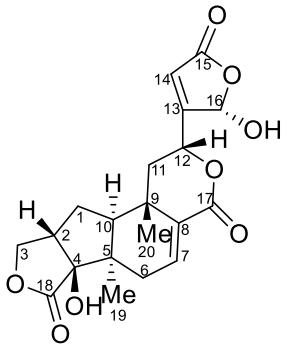

Fig. 2.21 Compound **68** (tinobaenzin C)

Compound **68** was obtained as colorless crystals, UV (MeOH) λ_{max} (log ε) 205 (4.08) nm, $[\alpha]^{20}_{D}$ -23.42 (c 0.1, MeOH) and its molecular formula of $C_{20}H_{22}O_8$ was determined from the HRESIMS peak at *m*/z 413.3778 $[M + Na]^+$, indicating 11 degrees of unsaturation. On comparing its NMR spectroscopic data (**Tables 2.5** and **2.6**) of **66** and **67**, the differences in their ^{1}H NMR spectra were the presence of signals for one olefinic proton of a trisubstituted alkene at δ_H 7.24 and one oxymethine proton at δ_H 6.15 in **68** instead of the signals for aromatic protons of the furan ring (H-14, H-15 and H-16) in **61**, **66** and **67**, while the ^{13}C NMR spectrum of **68** showed signals for an additional ester carbonyl at δ_C 170.7; C-15, one hemiketal carbon at δ_C 99.5; C-16, and one double bone at δ_C 137.7; C-13 and 148.6; C-14 instead of the carbon resonances of the furan ring in **61**, **66** and **67**. This finding suggested that the furan ring in **61**, **66** and **67** was replaced by a γ-hydroxybutenolide moiety for **68** as supported by the HMBC correlations from H-12 to C-13, C-14 and C-16, from H-14 to C-13 and C-15, and from H-16 to C-13 and C-15 (**Fig. 2.22**). Thus, the structure of **68** was established as shown. The proposed structure of **68** was further confirmed, along with the establishment of its relative configuration by single-crystal X-ray diffraction analysis using MoKα radiation (**Table 2.7**), and perspective ORTEP plot is depicted in **Fig. 2.23**. This indicated its relative configuration at H-12 was the same as in compound **67**. Therefore, the structure of **68**, named tinobaenzin C, was established as shown in **Fig. 2.21**.

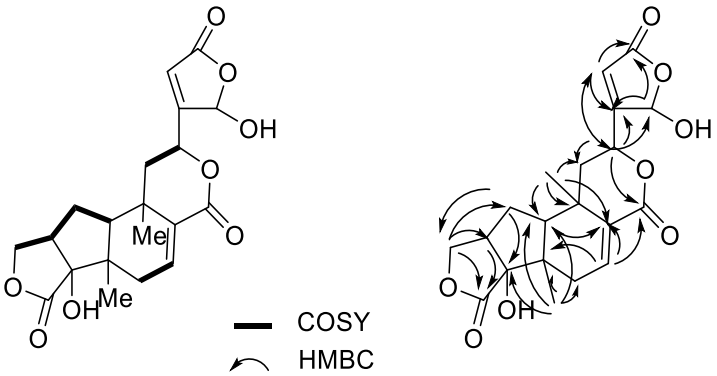

Fig. 2.22 Key COSY and HMBC correlations of compound **68**

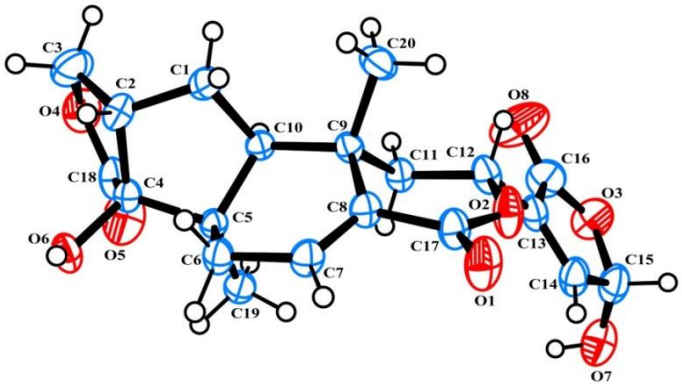

Fig. 2.23 ORTEP of compound **68**

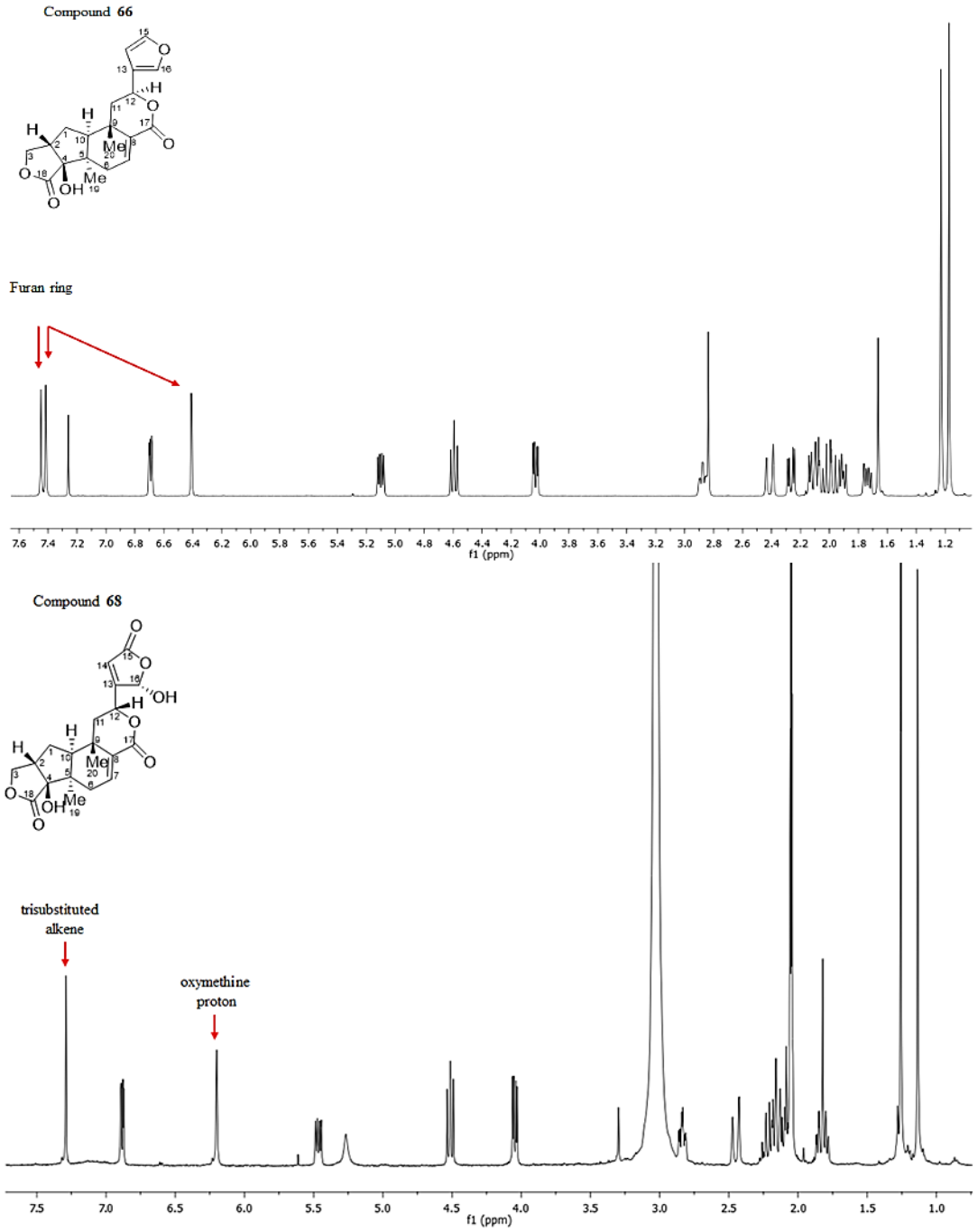

Fig. 2.24 Comparison of ^{1}H NMR spectra of compound **66** in $CDCl_3$ and compound **68** in acetone-d_6

2.5.1.1.5 Structural elucidation of compound 69

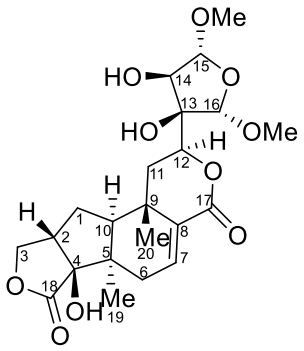

Fig. 2.25 Compound **69** (tinobaenzin D)

Compound **69,** obtained as colorless crystal, UV (MeOH) λ_{max} (log ε) 207 (3.91) nm, $[\alpha]^{20}_{D}$ -152.6 (c 0.1, MeOH), was determined to have a molecular formula of $C_{22}H_{30}O_{10}$ based on the HRESIMS peak at *m*/z 477.4718 $[M + Na]^+$. The 1D NMR spectroscopic data (**Tables 2.5** and **2.4**) of **69** were also comparable to those of **66** and **67**, except for the existence of two methoxyl groups [δ_H 3.32 (s), 3.37 (s); δ_C 56.2 and 57.1], two hemiketal groups [δ_H 4.83 (s), 4.87 (d, *J* = 4.0 Hz); δ_C 110.3, 113.3], one oxygenated methine [δ_H 3.92 (d, *J* = 4.0 Hz); δ_C 78.6; C-12], and one oxygenated quaternary carbon (δ_C 81.5; C-13), and the concomitant absence of signals for a furan ring in **61**, **66** and **67**. This indicated that the furan ring in **61**, **66** and **67** was replaced by a tetrahydrofuran ring for **69**. The presence of the tetrahydrofuran on C-12 was supported by the ^1H-^1H COSY correlation between H-14 and H-15, and HMBC correlations from H-13 to C-12, from H-14 to C-12, and from H-15 to C-13 and C-16, while two methoxyl groups were located on C-15 and C-16 of the tetrahydrofuran ring based on HMBC correlations from those methoxyl protons to C-15 and C-16 (**Fig. 2.26**). The structure of **69** was thus established as show. Single-crystal X-ray analysis using MoK*α* radiation (**Table 2.7**) confirmed the structure of **69**, as well as defined its relative configuration and the relative configuration of H-12 was the same as in compound **66** as ORTEP plot in **Fig. 2.27**. To the best of our knowledge, the compound with fully oxygenated tetrahydrofuran moiety seems to be rare, and the only precedents included rhumphiol E from *T. crispa* [54], and rhumphiosides C and C-1 from *T. rumphii* [55]. Therefore, the structure of **69** was identified as tinobaenzin D.

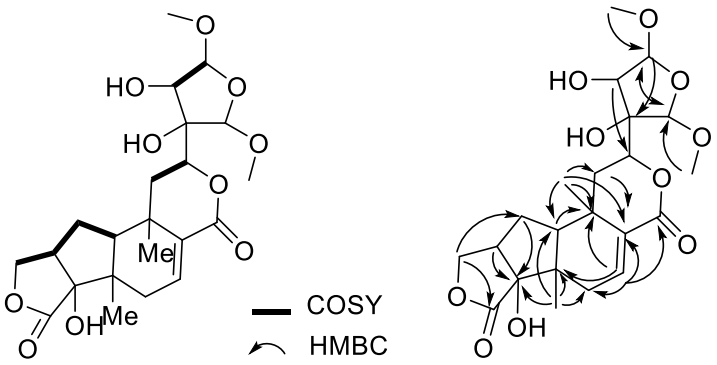

Fig. 2.26 Key COSY and HMBC correlations of compound **69**

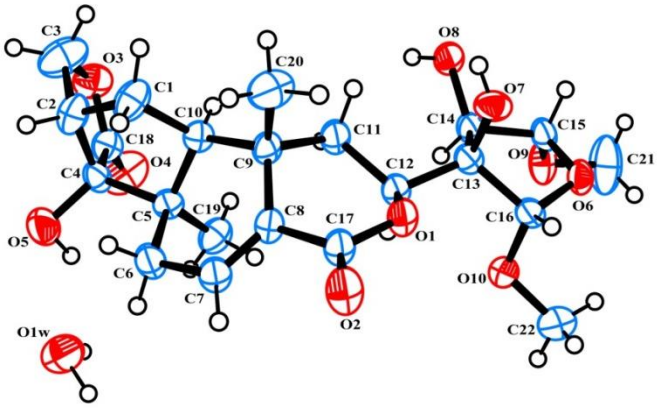

Fig. 2.27 ORTEP of compound **69**

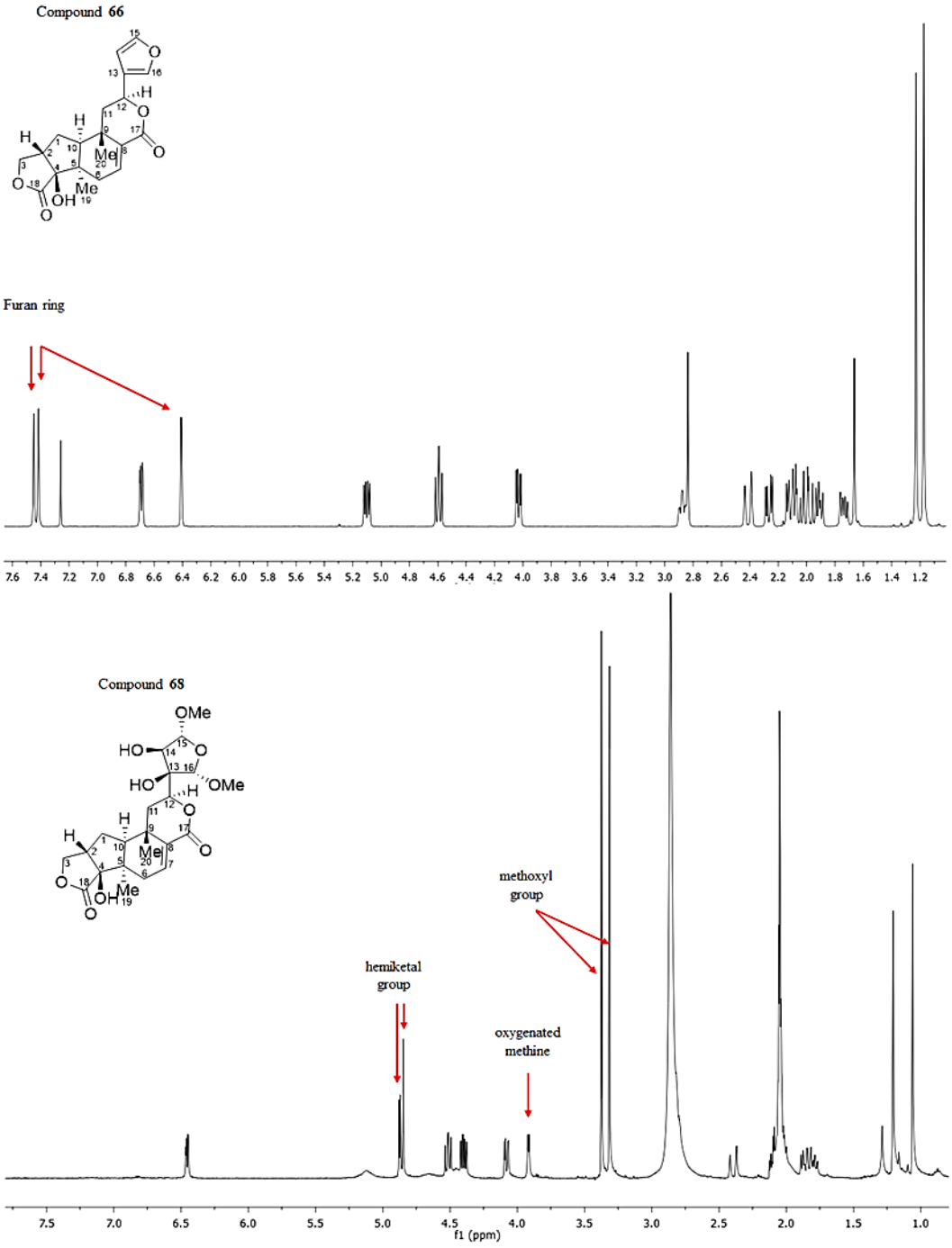

Fig. 2.28 Comparison of ^{1}H NMR spectra of compound **66** in $CDCl_3$ and compound **69** in acetone-d_6

2.5.1.1.6 Structural elucidation of compound 70

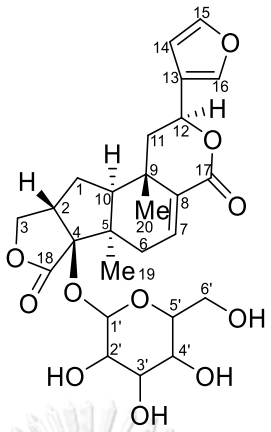

Fig. 2.29 Compound **70** (tinobaenzin A glucoside)

Compound **70,** obtained as white powder, UV (MeOH) λ_{max} (log ε) 208 (3.91) nm, $[\alpha]^{20}_{D}$ -37.0 (c 0.1, MeOH), was assigned a molecular formula of $C_{26}H_{32}O_{11}$. The 1D NMR data of **70** (**Tables 2.5** and **2.6**) were identical to those of **66** and **67**, but a hydroxyl group was substituted by a glucopyranosyl moiety. The NMR spectral data showed signal of an anomeric proton [δ_H 4.57 (t, J = 5.6 Hz)] with an anomeric carbon at δ_C 99.9; C-1′, together with five oxygenated carbon signals at δ_C 73.5;C-2′, 77.2: C-3′, 69.9; C-4′, 76.4; C-5′ and 60.9; C-6′, which was further confirmed by ^{1}H-^{1}H COSY (**Fig. 2.30**) correlations from H_2-1′ to H_2-6′. The HMBC correlation between an anomeric proton to C-4 supported the position of the glucopyranosyl group at C-4. Consequently, compound **70** was described to tinobaenzin A glucoside.

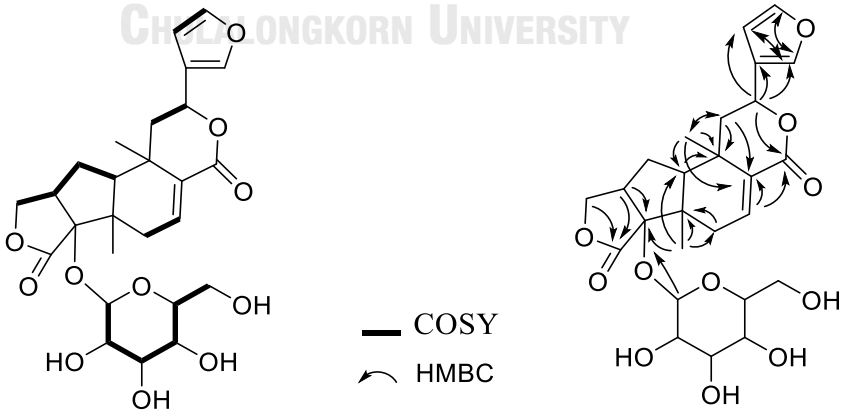

Fig. 2.30 Key COSY and HMBC correlations of compound **70**

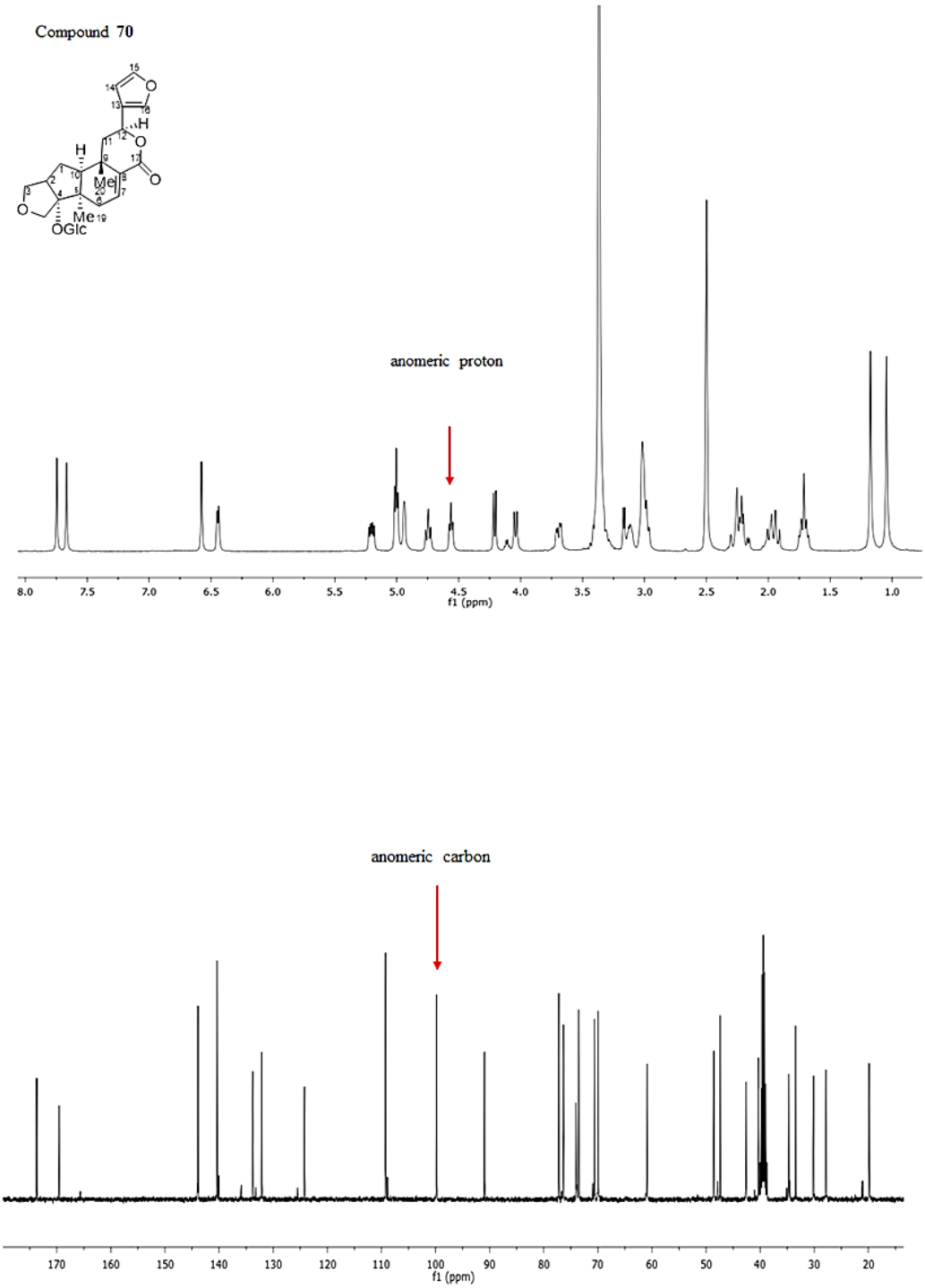

Fig. 2.31 Elucidation of ^{1}H and ^{13}C NMR spectra of compound **70** in DMSO- d_6

Table 2.5 ^{1}H NMR data of compounds **68**, **69** and **70**

position	δ_H mult, (*J* in Hz)		
	68 (acetone-d_6)	**69** (acetone-d_6)	**70** (DMSO-d_6)
1	1.70 m	1.79 m	1.71 m
	2.10 m	2.08 m	2.16 d, (6.0)
2	2.75 ddd, (3.6, 8.4, 13.6)	2.86 m	3.01 m
3	3.93 dd, (3.2, 9.2)	4.08 dd, (2.8, 9.6)	4.03 d, (8.8)
	4.39 t, (9.2)	4.51 dd, (8.0, 9.2)	4.74 t, (8.4)
4	-	-	-
5	-	-	-
6	2.03 m	2.10 m	2.21 t, (4.4)
	2.34 d, (18.4)	2.39 d, (18.8)	2.49 t, (1.6)
7	6.76 dd, (2.4, 7.2)	6.45 dd, (2.0, 6.4)	6.57 d, (5.2)
8	-	-	-
9	-	-	-
10	1.69 m	1.87 m	1.93 d, (1.2)
11	1.99 m	2.05 m	1.99 d, (12.4)
	2.00 m	2.09 m	2.24 m
12	5.34 dd, (5.6, 11.6)	4.39 dd, (6.0, 11.2)	5.19 dd, (6.0, 11.2)
13	-	-	-
14	7.24 s	3.92 d, (4.0)	6.43 dd, (1.6, 5.6)
15	-	4.83 s	7.66 t, (1.6)
16	6.15 brs	4.87 d, (4.0)	7.74 s
17	-	-	-
18	-	-	-
19-Me	1.02 s	1.02 s	1.17 s
20-Me	1.14 s	1.14 s	1.04 s
15-	-	3.32 s	-
OMe	-	3.37 s	-
16-	-	-	4.57 t, (5.6)
OMe	-	-	3.16 d, (4.8)
1′	-	-	3.42 s
2′	-	-	3.42 s
3′	-	-	3.10 m
4′	-	-	3.67 d, (4.4)
5′			3.70 d, (4.8)
6′			

Table 2.6 ^{13}C NMR data of compounds **68**, **69** and **70**

position	δ_c ppm		
	68 (acetone-d_6)	**69** (acetone-d_6)	**70** (DMSO-d_6)
1	35.3	35.2	34.7
2	45.2	45.1	40.4
3	73.1	74.4	74.0
4	86.8	87.8	90.9
5	48.3	48.7	47.4
6	31.2	32.1	30.2
7	139.0	133.6	132.1
8	134.4	137.0	133.8
9	35.9	35.6	33.5
10	52.2	52.8	48.6
11	41.5	37.9	42.6
12	72.8	78.6	70.6
13	137.7	81.5	124.2
14	148.6	78.6	109.2
15	170.7	110.3	143.8
16	99.4	113.3	140.4
17	166.6	171.1	169.6
18	177.8	178.8	173.7
19-Me	22.8	22.4	19.8
20-Me	21.5	28.8	27.9
15-OMe	-	56.2	-
16-OMe	-	57.1	-
1′	-	-	99.9
2′	-	-	73.5
3′	-	-	77.2
4′	-	-	69.9
5′	-	-	76.4
6′	-	-	60.9

Table 2.7 Crystal data and structure refinement for compounds **68** and **69**

Identification code	tinobaenzin C (**68**)	tinobaenzin D (**69**)
Empirical formula	$C_{20}H_{22}O_8$	$C_{22}H_{30}O_{10} \cdot H_2O$
Formula weight	390.38	472.48
Temperature	293(2) K	293(2) K
Wavelength	0.71073 Å	0.71073 Å
Crystal system, space group	Monoclinic, $P2_1$	Monoclinic, $P2_1$
Unit cell dimensions	a = 6.4985(3) Å	a = 7.4637(2) Å
	b = 12.2997(6) Å	b = 11.9636(2) Å
	c = 11.3759(6) Å	c = 12.9831(3) Å
Volume	876.59(7) $Å^3$	1143.3(1) $Å^3$
Z, Calculated density	2	2
Absorption coefficient	0.12 mm^{-1}	0.10 mm^{-1}
F(000)	760	760
Crystal size	0.50 x 0.20 x 0.20 mm	0.52 x 0.48 x 0.42 mm
Reflections collected/unique	3683 [R_{int} = 0.0157]	4073 [R_{int} = 0.0401]
Final R indices [I>2sigma(I)]	R_1 = 0.0418, wR2 = 0.1267	R_1 = 0.0447, wR2 = 0.1063

2.5.1.1.7 Structural elucidation of compound 71

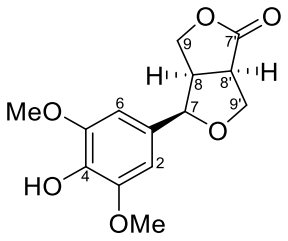

Fig. 2.32 Compound **71** (caruilignan D)

Compound **71,** was obtained as amorphous powder and establishment of molecular formula $C_{14}H_{16}O_6$ was based on its NMR spectral data. The ^{1}H NMR spectrum (**Table 2.8)** showed a singlet aromatic proton δ_H 6.50 (s) and the one signal integrated for two methoxyl groups at δ_H 3.84 (s). The ^{13}C NMR spectrum (**Table 2.9)** indicated the presence of six aromatic carbons (δ_C 129.0; C-1, 102.9; C-2 and C-6, 147.4; C-3, 135.0; C-4, 147.4; C-5), and one ester carbonyl group (δ_C 177.9; C-7′). Since aromatic protons were observed as only one singlet signal in the ^{1}H-NMR spectrum, the compound should contain a symmetrically substituted phenyl ring. Therefore, the hydroxy group was located at C-4. The ^{1}H-^{1}H COSY spectrum indicated the connection of the methylenes and methines, together with HMBC correlations were observed between H-9 to C-7′ and C-8′, as well as H-7 to C-9′ which led to the partial structure in the aliphatic part of **71**. Moreover, HMBC correlations observed between H-7 to C-1, H-7 to C-6, enabled the connection of C-7 to C-1 and thus the planar structure of **71** was established as shown in **Fig. 2.33** The ^{1}H NMR and 2D NMR data of this compound were similar to that previously published, confirmed that compound **71** is caruilignan D [56].

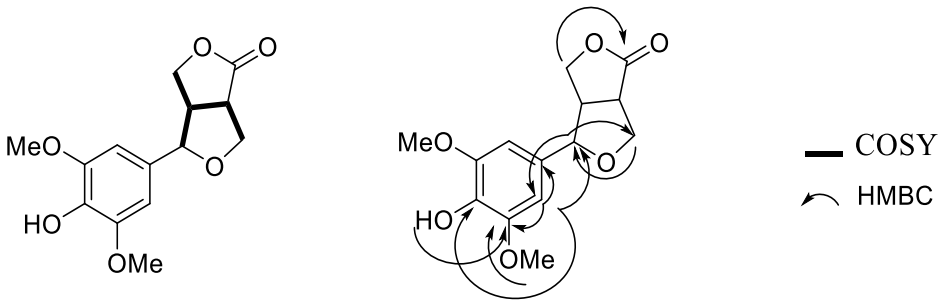

Fig. 2.33 Key COSY and HMBC correlations of compound **71**

2.5.1.1.8 Structural elucidation of compound 72

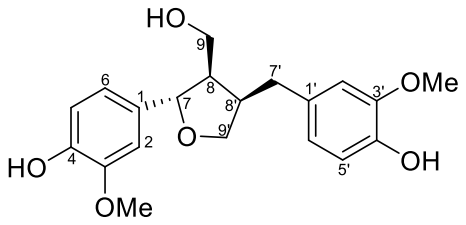

Fig. 2.34 Compound **72** (lariciresinol)

Compound **72** obtained as brownish amorphous powder its molecular formula was determined as $C_{20}H_{24}O_6$ on the basis of NMR data. The ^{1}H NMR spectrum of **72** (**Table 2.8**) demonstrated signals attributable to two pairs of 1,3,4-trisubstituted benzene ring signals at δ_H 6.89 (d, *J* = 2.4 Hz), 6.88 (s), 6.84 (dd, *J* = 1.6, 8.4 Hz), 6.71 (d, *J* = 2.0 Hz), 6.85 (brd) and 6.72 (d, *J* = 1.6 Hz), which were assigned to H-2, H-5, H-6, H-2′, H-5′ and H-6′, and two aromatic methoxyl proton at δ_H 3.91 (s) and 3.93 (s). Furthermore, in the ^{1}H NMR spectrum, an *O*-bearing methine proton signals at δ_H 4.81, an aliphatic methylene proton signals at δ_H 2.58 and 2.94, two oxygenated methylene protons (δ_H 3.81, 3.95 and 3.77, 4.08), together with two aliphatic methine protons (δ_H 2.43 and 2.76) were indicated. Besides the carbon resonances corresponding to the above units, the ^{13}C NMR spectrum (**Table 2.9**) suggested the presence of twelve aromatic carbons (δ_C 134.8; C-1, 108.4; C-2, 146.5; C-3, 144.1; C-4, 114.2; C-5, 118.8; C-6, 132.3; C-1′, 111.2; C-2′, 146.5; C-3′, 145.1; C-4′, 114.4; C-5′ and 121.2; C-6′), together with a hydroxymethyl carbon signal at δ_C 72.9; C-9′. In addition, the ^{13}C NMR spectrum signals at δ_C 82.9, 52.6, 42.4 and 72.9 combined with ^{1}H NMR of spectrum signals at δ_H 4.81(d, *J* = 6.8 Hz), 2.43 (m), 2.76 (m), 3.77 (dd, *J* = 6.2, 8.4 Hz) and 4.08 (dd, *J* = 6.6, 8.4 Hz) displayed the presence of a furan ring. The structure of this compound further established by analysis of ^{1}H-^{1}H COSY and HMBC spectrum (**Fig. 2.35**). Partial structures of H-7/H-8/H$_2$-9, H-8/H-8′ and H$_2$-7′/H-8′/H$_2$-9′ were deduced by analysis of the ^{1}H-^{1}H COSY spectrum, and the complete structure was further established by the following HMBC correlations: H-7 to C-1 and C-9; H-8 to C-9; H$_2$-7′ to C-1′ and C-9′; H$_3$-3 to C-2 and C-3; H$_3$-3′ to C-2′ and C-3′. On the basis of these findings, and comparison of its NMR data with previous study, it suggested that compound **72** is lariciresinol [57].

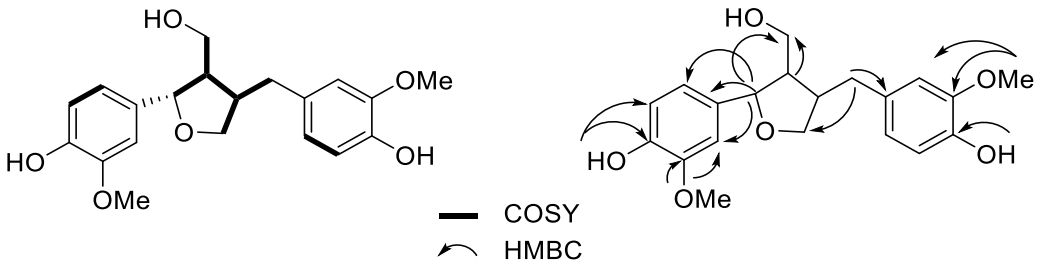

Fig. 2.35 Key COSY and HMBC correlations of compound **72**

2.5.1.1.9 Structural elucidation of compound 73

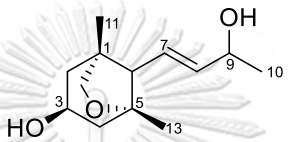

Fig. 2.36 Compound **73** (aglycone of breyniaionoside D)

Compound **73** was obtained as amorphous powder and its molecular formular was determined to be $C_{13}H_{22}O_3$ based on it NMR spectral data (**Tables 2.8** and **2.9**). The ^{13}C-NMR spectra showed signals attributable to 13 carbon signals including three methyl groups (δ_C 23.3; C-10, 20.0; C-11 and 24.2; C-13), three methylenes (δ_C 47.7; C-2, 48.5; C-4 and 75.4; C-12) and two quaternary carbons (δ_C 43.7; C-1, 82.9; C-5). It also indicated the presence of two methines with an oxygen atom (δ_C 64.5; C-3, 66.3; C-9), and a trans double bond (δ_C 125.1; C-7, 138.5; C-8). The linkages of the structure were determined using a combination of ^{1}H-^{1}H COSY and HMBC (**Fig. 2.37**). The COSY spectrum exhibited two series of spin–spin couplings: from H-6 to H-10 and H_2-2 to H_2-4. Due to long-range coupling *via* a w-letter interaction in 2 Hz, H_2-2ax [δ_H 1.28 (dd, J = 1.6, 12.4 Hz)] was coupled with H_2-12a [δ_H 3.44 (d, J = 2.0 Hz)]. The HMBC spectrum showeds a cross peak between δ_H 3.54 (d, J = 7.6), H_2-12b) and δ_C 82.9 (C-5). Thus, the structure of **73** was assumed to have an epoxy ring between C-12 and C-5. The results showed that the NMR spectroscopic data of the compound **73** closely related to those of breyniaionoside D, except for the disappearance of the signals for glucose moiety. Consequently, compound **73** was assigned to be aglycone of breyniaionoside D [58].

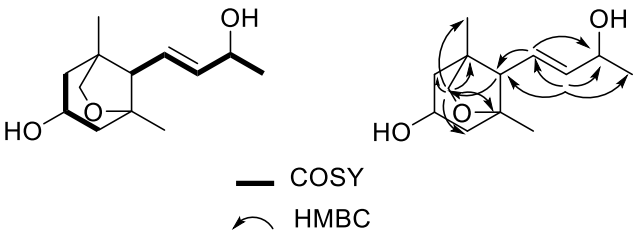

Fig. 2.37 Key COSY and HMBC correlations of compound **73**

Table 2.8 ^{1}H NMR data of compounds **71**, **72** and **73**

position	δ_H mult, (*J* in Hz)		
	71 ($CDCl_3$)	**72** ($CDCl_3$)	**73** (DMSO-d_6)
1	-	-	-
2	6.50 s	6.89 d, (2.4)	1.28 dd, (1.6, 12.4)
3	-	-	3.86 m
4	-	-	1.32 dd, (2.0, 10.4) 1.90 dd, (6.4, 12.4)
5	-	6.88 s	-
6	6.50 s	6.84 dd, (1.6, 8.4)	1.98 d, (10.4)
7	4.52 d, (7.4)	4.81 d, (6.8)	5.35 dd, (10.4, 16.0)
8	3.04 dddd, (2.0, 7.4, 7.4, 8.5)	2.43 m	5.51 dd, (5.2, 15.6)
9	4.13 dd, (3.8, 9.4) 4.32 dd, (9.0, 9.1)	3.81 m 3.95 m	4.13 m
10	-	-	1.11 dd, (6.4)
11	-	-	0.81 s
12	-	-	3.44 d, (2.0) 3.54 d, (7.6)
13	-	-	1.01 s
1′	-	-	-
2′	-	6.71 d, (2.0)	-
3′	-	-	-
4′	-	-	-
5′	-	6.85 brd	-
6′	-	6.72 d, (1.6)	-
7′	-	2.58 dd, (10.8, 13.6)	-
8′	3.38 ddd, (3.7, 8.5, 9.0)	2.94 dd, (4.8, 13.6) 2.76 m	-
9′	4.27 dd, (2.0, 10.0) 4.44 dd, (7.4, 10.0)	3.77 dd, (6.2, 8.4) 4.08 dd, (6.6, 8.4)	-
3-OMe	3.84 s	-	-
5-OMe	3.84 s	3.93 s	-
6-OMe	-	-	-
3′-OMe	-	3.91 s	-

Table 2.9 ^{13}C NMR data of compounds **71**, **72** and **73**

position	δ_c ppm		
	71 ($CDCl_3$)	**72** ($CDCl_3$)	**73** (DMSO-d_6)
1	129.0	134.8	43.7
2	102.9	108.4	47.7
3	147.4	146.5	64.5
4	135.0	144.1	48.5
5	147.4	114.2	82.9
6	102.9	118.8	59.8
7	86.3	82.9	125.1
8	48.5	52.6	138.5
9	70.1	61.0	66.3
10	-	-	24.2
11	-	-	20.0
12	-	-	75.4
13	-	-	23.3
1′	-	132.3	-
2′	-	111.2	-
3′	-	146.5	-
4′	-	145.1	-
5′	-	114.4	-
6′	-	121.2	-
7′	177.9	33.4	-
8′	46.0	42.4	-
9′	69.8	72.9	-
3-OMe	56.4	-	-
5-OMe	56.4	55.9	-
6-OMe	-	-	-
3′-OMe	-	55.9	-

2.5.1.1.10 Structural elucidation of compound 74

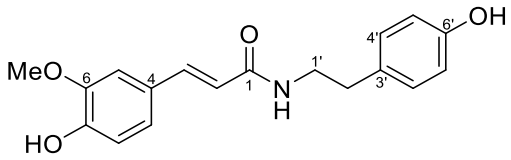

Fig. 2.38 Compound **74** (*N-trans*-feruloyltyramine)

Compound **74** was obtained as amorphous solid and its molecular formula was assigned to be $C_{18}H_{19}NO_4$ based on the HRESIMS peak at *m*/z 336.12 $[M + Na]^+$. The ^1H NMR spectrum of **74** (**Table 2.10**) indicated seven aromatic protons [δ_H 7.11 (d, *J* = 2.0 Hz), 6.79 (d, *J* = 8.4 Hz), 7.00 (d, *J* = 1.2 Hz), 7.02 (d, *J* = 8.4 Hz) x2, and 6.68 (d, *J* = 8.4 Hz) x2], which were assigned to H-5, H-8, H-9, H-4′/H-8′ and H-7′/H-9′, respectively. The correctness of this structure was confirmed by the ^{13}C NMR spectrum (**Table 2.11**) of twelve aromatic carbons at δ_C 126.5; C-4, 110.9; C-5, 147.9; C-6, 148.3; C-7, 115.7; C-8, 121.6; C-9, 129.5; C-4′, 115.2; C-5′, 115.2; C-7′ and 129.5; C-8′. These NMR spectrums revealed the presence of a 1, 3, 4-trisubstituted aromatic ring and 1, 4-disubstituted aromatic ring. Additionally, ^1H NMR data also indicated a signal of methoxy group at δ_H 3.79 (s) and a carbonyl group (δ_C 165.6; C-1) signal was demonstrated by ^{13}C NMR. Partial structures H-2/H-3, H-8/H-9, H_2-1′/H_2-2′, H-4′/H-5′, H-7′/H-8′ and NH/ H-1/H-1′ were deduced by analysis of the ^1H-^1H COSY (**Fig. 2.39**) spectrum. In addition, correlations observed by HMBC experiments also assisted to determine the carbon skeleton. The linkage of the methoxyl group to C-6 was established based on the observation of a correlation between this carbon and the methoxyl protons by HSQC experiments. The results were comparable to the previous research [59], the structure of this compound was elucidated as *N-trans*-feruloyltyramine.

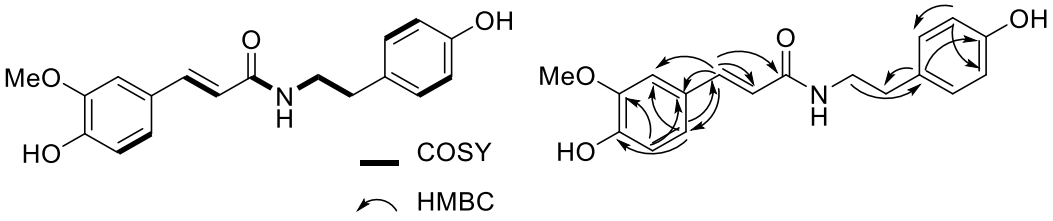

Fig. 2.39 Key COSY and HMBC correlations of compound **74**

2.5.1.1.11 Structural elucidation of compound 75

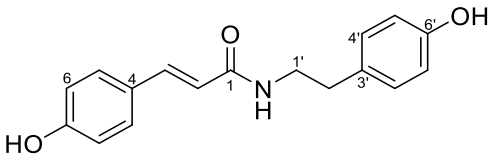

Fig. 2.40 Compound **75** (*N-trans*-coumaroyltyramine)

Compound **75** was isolated as faint white powder and its molecular formula, $C_{17}H_{17}NO_3$, was determined by ^{1}H NMR and ^{13}C NMR experiments (**Tables 2.10** and **2.11**). The NMR data of **75** were similar to those of **74,** except for the absence of aromatic methoxyl proton signal at C-6, and the appearance of the signal for aromatic proton at δ_H 6.77 (d, J = 8.4 Hz) in **75**. It suggested that the methoxyl group of **74** was replaced by H-proton in **75**. By comparing its data with literatures, **75** turned out to be *N-trans*-coumaroyltyramine [60].

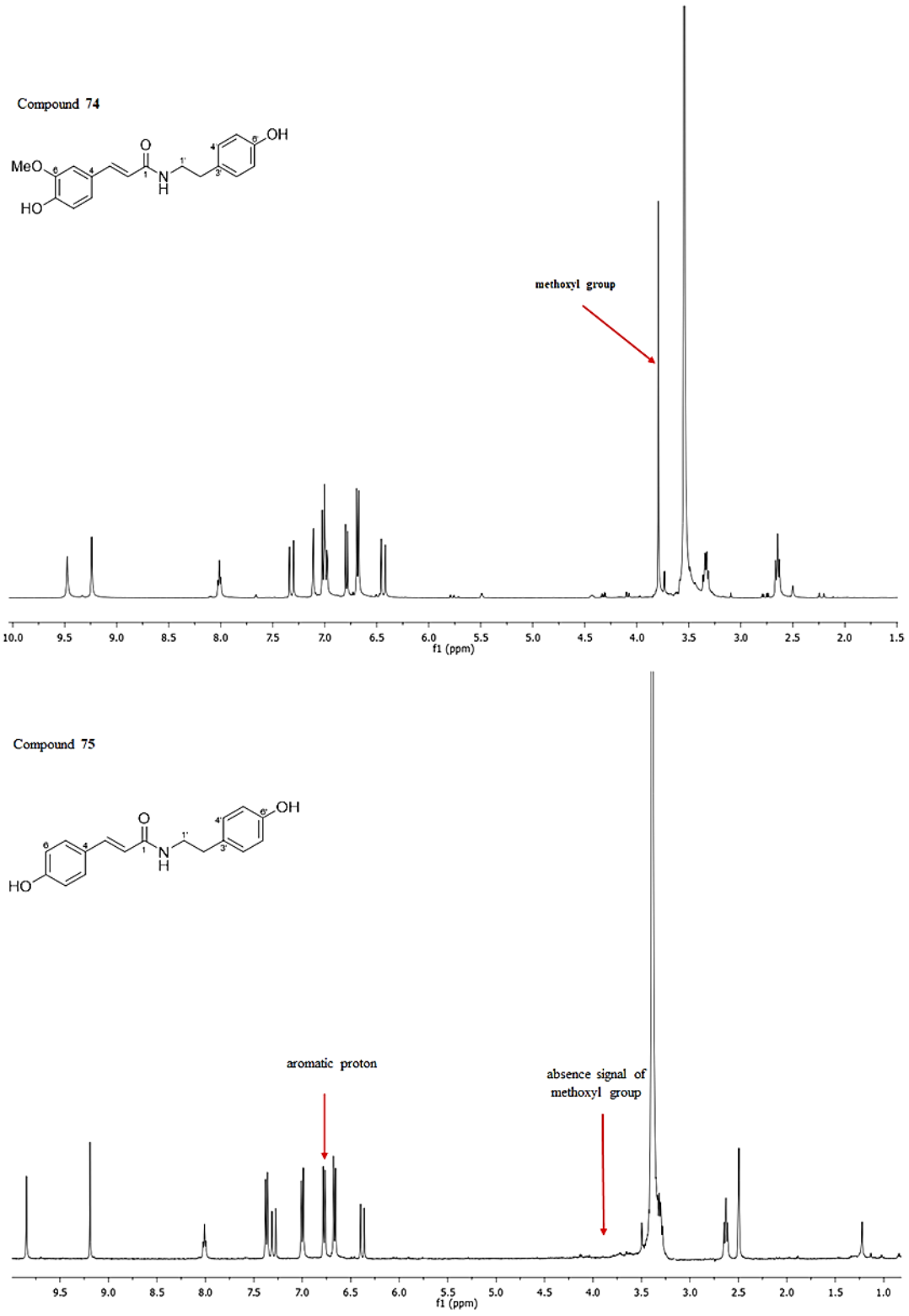

Fig. 2.41 Comparison of ^{1}H NMR spectra of compound **74** and **75** in DMSO-d_6

Table 2.10 ^{1}H NMR data of compounds **74** and **75**

position	δ_H mult, (*J* in Hz)	
	74 (DMSO-d_6)	**75** (DMSO-d_6)
1	-	-
2	6.44 d, (15.6)	6.38 d, (15.6)
3	7.32 d, (15.6)	7.29 d, (16.0)
4	-	-
5	7.11 d, (2.0)	7.37 d, (8.4)
6	-	6.77 d, (8.4)
7	-	-
8	6.79 d, (8.4)	6.77 d, (8.4)
9	7.00 d, (1.2)	7.37 d, (8.4)
1′	3.33 dd, (6.8, 14.0)	3.32 t, (6.4)
2′	2.64 t, (7.6)	2.63 t, (7.6)
3′	-	-
4′	7.02 d, (8.4)	6.99 d, (8.4)
5′	6.68 d, (8.4)	6.67 d, (8.4)
6′	-	-
7′	6.68 d, (8.4)	6.67 d, (8.4)
8′	7.02 d, (8.4)	6.99 d, (8.4)
6-OMe	3.79 s	-
NH	8.01 t, (5.6)	8.01 t, (5.6)

Table 2.11 ^{13}C NMR data of compounds **74** and **75**

position	δ_c ppm	
	74 (DMSO-d_6)	**75** (DMSO-d_6)
1	165.6	165.3
2	119.0	118.7
3	139.0	138.5
4	126.5	125.9
5	110.9	129.1
6	147.9	115.7
7	148.3	158.7
8	115.7	115.7
9	121.6	129.1
1′	40.7	40.6
2′	34.4	34.3
3′	129.4	129.4
4′	129.5	129.5
5′	115.2	115.0
6′	155.6	155.5
7′	115.2	115.0
8′	129.5	129.5
6-OMe	55.6	-

2.5.2 Isolation of compounds of *T. baenzigeri* from Bueng Kan Province

The EtOAc crude extract of the stems of *T. baenzigeri* from Bueng Kan Province was purified by chromatographic techniques to afford 12 compounds including two new rearranged clerodane diterpenes, tinobaenzigerides A (**76**) and B (**77**), together with apigenin (**44**), baenzigeroside B (**61**), tinobaenzine A (**66**), tinobaenzine A glucoside (**70**), *N-trans*-feruloyltyramine (**74**), *N-trans*-coumaroyltyramine (**75**), naringenin (**78**), eriodictyol (**79**), tyrosol (**80**) and lariciresinol acetate (**81**). The structures of isolated compounds are shown in **Fig. 2.42**.

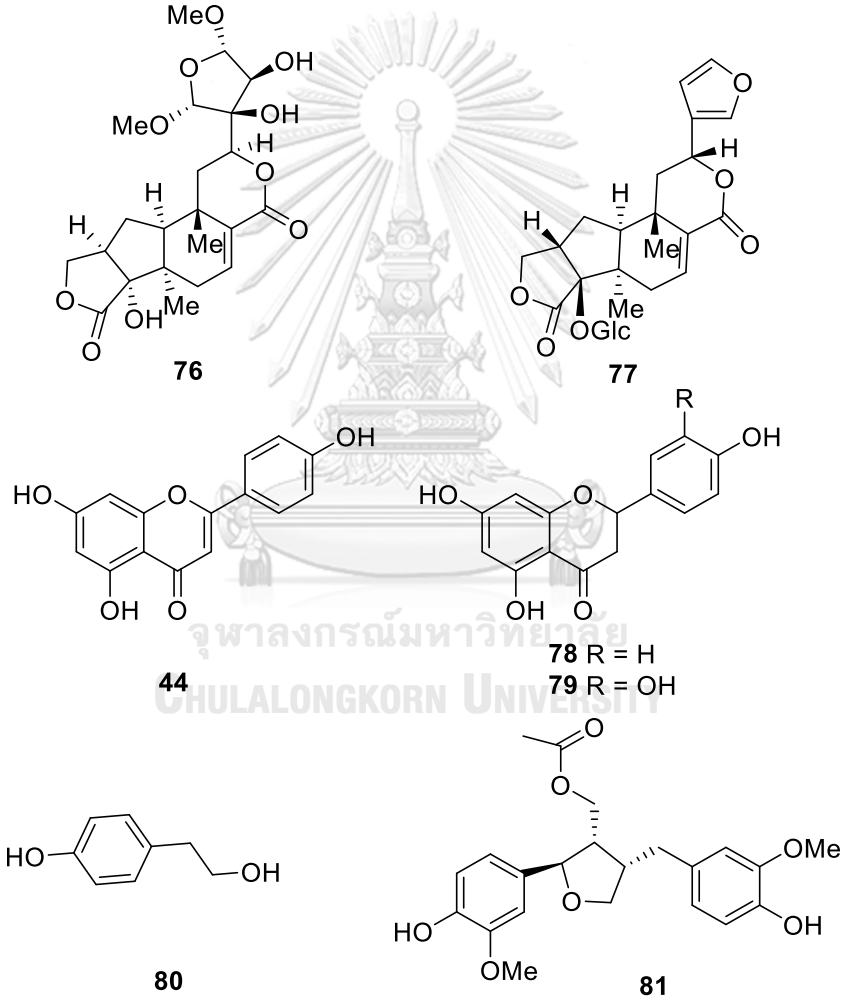

Fig. 2.42 Chemical structures of compounds from *T. baenzigeri* from Bueng Kan Province

2.5.2.1 Structural elucidation of isolated compounds

2.5.2.1.1 Structural elucidation of compound 44

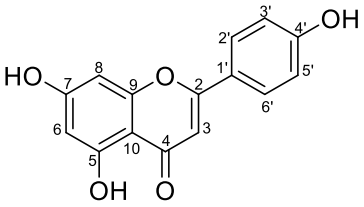

Fig. 2.43 Compound **44** (apigenin)

Compound **44** was obtained as yellow powder and its molecular formula was established as $C_{15}H_{10}O_5$ by analysis of ^{1}H NMR and ^{13}C NMR data. Examination of NMR data analysis (**Tables 2.14** and **2.15**) suggested that **44** was a flavanone. Its ^{1}H NMR spectrum of **44** showed the presence of two meta couple aromatic doublets at δ_H 6.19 (d, J = 2.0 Hz) and 6.48 (d, J = 1.6 Hz) corresponding to H-6 and H-8 protons. Four proton signals of ring B appearing as two doublets at δ_H 7.92 (d, J = 8.8 Hz) and 6.92 (d, J = 8.4 Hz) for H-2'/H-6' and H-3'/H-5' protons, respectively, revealed characteristic resonances of aromatic protons. The presence of the quilted signal consisting of 5-OH at δ_H 12.95 (s), 7-OH at 10.71 (s) and 4′-OH at 10.43(s) was the characteristic of a 5,7,4'-trisubstituted flavone. Simultaneously, the signals of ^{13}C NMR at δ_C 181.6 (carbonyl carbon), seven quaternary carbons (δ_C 163.7; C-2, 161.4; C-5, 164.0; C-7, 157.2; C-9, 103.6; C-10, 121.1; C-1′ and 161.1; C-4′) showed the flavonone skeleton. It also presented seven methane carbons (δ_C 102.8; C-3, 95.7; C-6, 94.9; C-8, 128.1; C-2′/6′ and 115.1; C-3′/5′). Moreover, the complete structure of **44** was confirmed by ^{1}H-^{1}H COSY and HMBC correlations (**Fig. 2.44**). Comparison of the NMR data with those previously reported, **44** was a common dietary flavonoid namely apigenin [61].

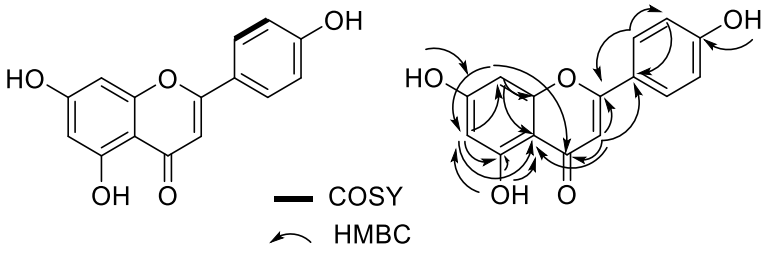

Fig. 2.44 Key COSY and HMBC correlations of compound **44**

2.5.2.1.2 Structural elucidation of compound 76

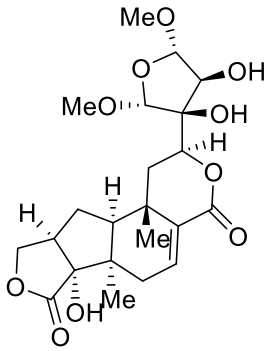

Fig. 2.45 Compound **76** (tinobaenzigerides A)

Compound **76** was obtained as colorless crystal, $[\alpha]^{20}_{D}$ -37.8 (c 0.1, MeOH) with molecular formula that is identical to **69**, due to their HRESIMS peak at *m*/z 477.1126 $[M + Na]^{+}$. Based on the analysis of 1D and 2D NMR spectroscopic data (**Tables 2.12** and **2.13**), both **69** and **76** had an equivalent structure. The relative configuration of **76** was further confirmed by single-crystal X-ray diffraction analysis using MoKα radiation, and a perspective ORTEP plot was depicted in **Fig. 2.46.** Compound **76** was assigned to be tinobaenzigerides A.

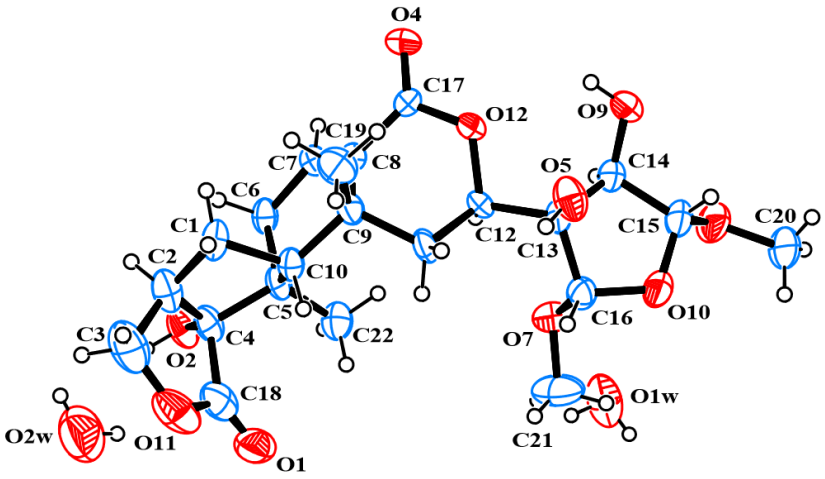

Fig. 2.46 ORTEP of compound **76**

2.5.2.1.3 Structural elucidation of compound 77

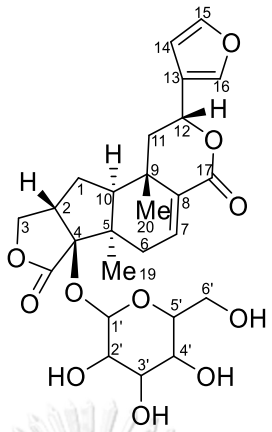

Fig. 2.47 Compound **77** (tinobaenzigerides B)

Compound **77**, obtained as white powder, $[\alpha]^{20}_{D}$ -37.4 (c 0.1, MeOH), its molecular formula, $C_{26}H_{32}O_{11}$, was deduced from the HRESIMS peak at *m*/z 512.2124 $[M + Na]^{+}$. The 1D (**Tables 2.12** and **2.13**) and 2D NMR data of **77** were identical to rearranged clerodane diterpenes glucoside **70.** Comparison of the ^{1}H NMR, the H-12 orientation of **77** was distinctive from that of **70**. Further, the acid hydrolysis of the compound resulted aglycone **67**, indicated that compound **77** was tinobaenzigerides B, a tinobaenzin B's glycoside.

Table 2.12 ^{1}H NMR data of compounds **76** and **77**

position	δ_H mult, (*J* in Hz)	
	76 ($CDCl_3$)	**77** (DMSO-d_6)
1	2.04 m	1.74 dd, (7.2, 12.8)
		2.08 m
2	2.83 t, (8.4)	3.01 m
3	4.03 dd, (2.0, 9.6)	4.03 d, (8.8)
		4.74 t, (8.0)
4	-	-
5	-	-
6	2.11 m	2.24 m
	2.33 m	2.27 m
7	6.57 d, (5.6)	6.69 dd, (1.6, 6.4)
8	-	-
9	-	-
10	1.83 m	1.60 dd, (6.8, 12.0)
11	1.93 m	2.02 m
	2.17 m	2.11 m
12	4.39 dd, (5.2, 11.2)	5.67 dd, (5.2, 11.6)
13	-	-
14	4.32 d, (3.2)	6.50 brs
15	4.95 d, (3.2)	7.65 s
16	4.68 s	7.73 s
17	-	-
18	-	-
19-Me	1.18 s	1.10 s
20-Me	1.09 s	1.15 s
15-OMe	3.46 s	-
16-OMe	3.32 s	-
1′	-	4.20 d, (7.6)
2′	-	3.01 m
3′	-	3.01 m
4′	-	3.01 m
5′	-	3.11 d, (6.4)
6′	-	3.38 s
		3.69 dd, (3.6, 11.6)

Table 2.13 ^{13}C NMR data of compounds **76** and **77**

position	δ_c ppm	
	76 ($CDCl_3$)	**77** (DMSO-d_6)
1	33.8	35.1
2	42.1	40.9
3	73.6	73.9
4	86.4	90.9
5	46.9	47.8
6	30.3	30.2
7	132.9	135.8
8	134.1	133.2
9	33.9	34.5
10	50.7	48.5
11	35.6	41.0
12	79.7	70.9
13	79.3	125.5
14	80.0	108.9
15	110.8	143.9
16	108.1	140.1
17	171.2	165.6
18	177.7	173.7
19-Me	20.4	21.2
20-Me	27.8	21.0
5-OMe	56.5	-
3′-OMe	55.2	-
1′	-	99.8
2′	-	73.5
3′	-	77.2
4′	-	69.9
5′	-	76.3
6′	-	60.7

2.5.2.1.4 Structural elucidation of compound 78

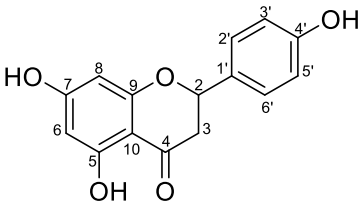

Fig. 2.48 Compound **78** (naringenin)

Compound **78** was obtained as amorphous powder and its elemental composition was determined to be $C_{15}H_{12}O_5$. The NMR data of **78** (**Tables 2.14** and **2.15**) were similar to those of the compound **44**, with the difference of the existing signals for C-2 and C-3 double bond in **44** were replaced by C-2 and C-3 single bond in **78.** The downfield shift of the carbonyl carbon at δ_C 196.2 (C-4) supported the presence of the single bond at this position shown in **Fig. 2.51**. This conclusion was reinforced by the correlation of peak signals at δ_H 2.68 and 3.26 ppm with the signal at δ_H 5.43 observed in the ^1H-^1H COSY spectrum. Other heteronuclear correlations were deduced from the HMBC spectrum (**Fig. 2.49)**. According to its NMR data and the literature [61], the structure of **78** was identified as naringenin.

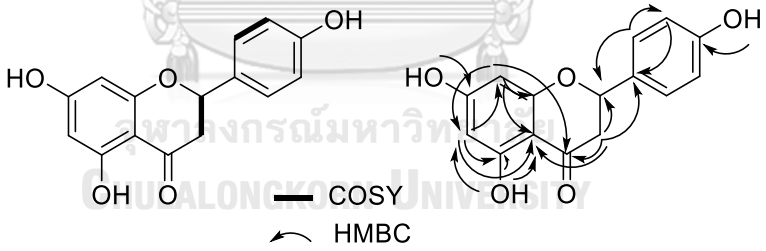

Fig. 2.49 Key COSY and HMBC correlations of compound **78**

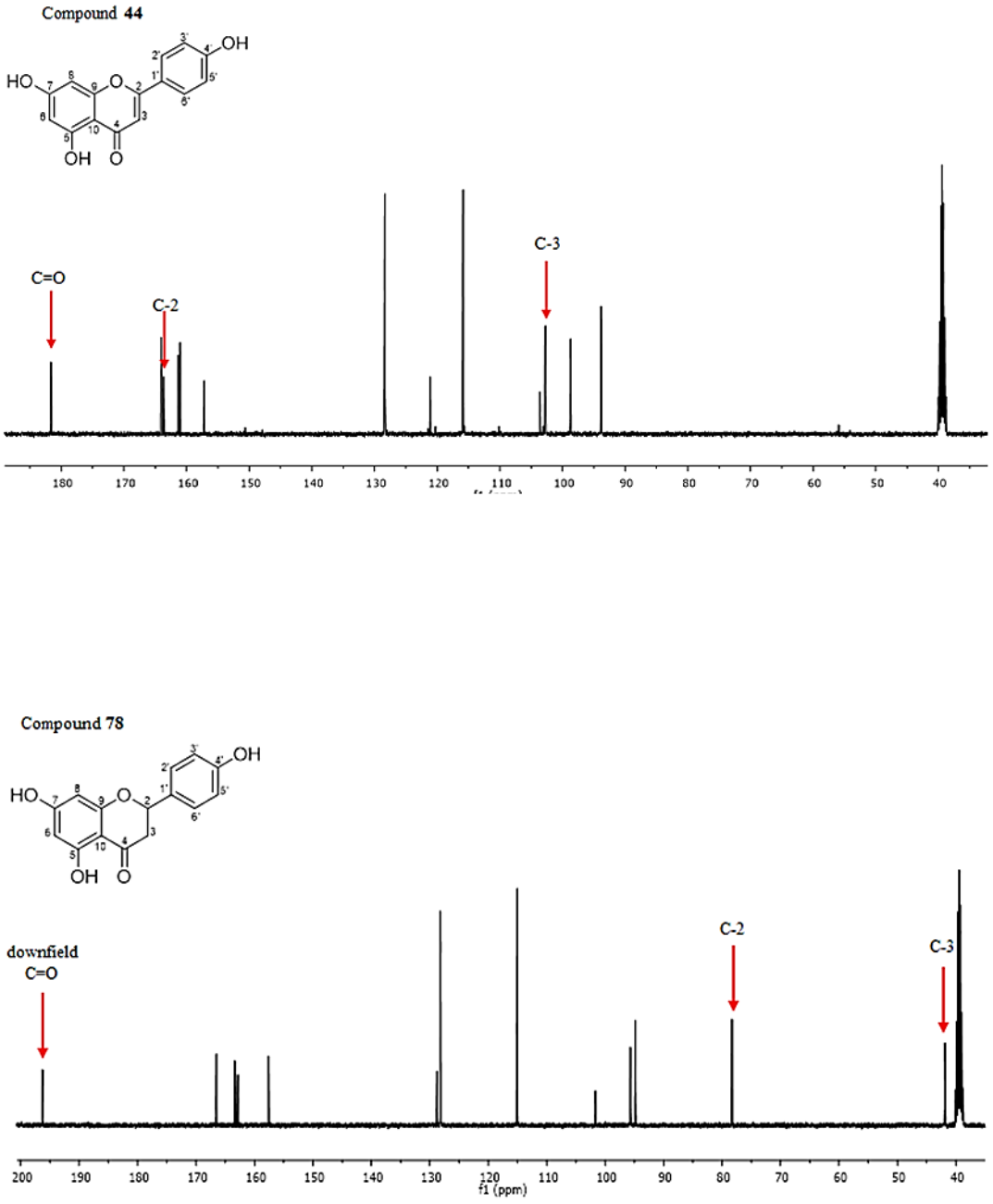

Fig. 2.50 Comparison of ^{13}C NMR spectra of compound **44** and **78** in DMSO-d_6

2.5.2.1.5 Structural elucidation of compound 79

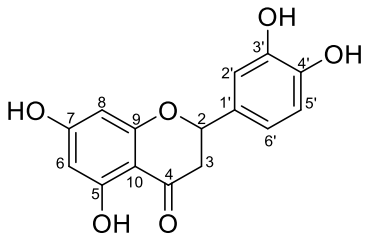

Fig. 2.51 Compound **79** (eriodictyol)

Compound **79** was obtained as yellow powder and its molecular formula was assigned as $C_{15}H_{12}O_6$, based on its ^{1}H NMR and ^{13}C NMR data. The NMR spectra of **79** (**Tables 2.14** and **2.15**) were very similar to those of the compound **78**. The major difference between the two compounds was the disappearance of an aromatic proton at H-3' of **79,** as well as the substitution of qC-OH in **79** for CH-3' of **78** (**Fig. 2.52**). This was further confirmed by ^{13}C NMR spectral data showing C-3' aromatic carbon signal of **78** was at δ_H 6.79 (d, J = 8.4 Hz), whereas C-3' signal of **79** arose as qC. Thus compound **79** was identified as eriodictyol, which was further confirmed by comparing its NMR data to those in the literature [62].

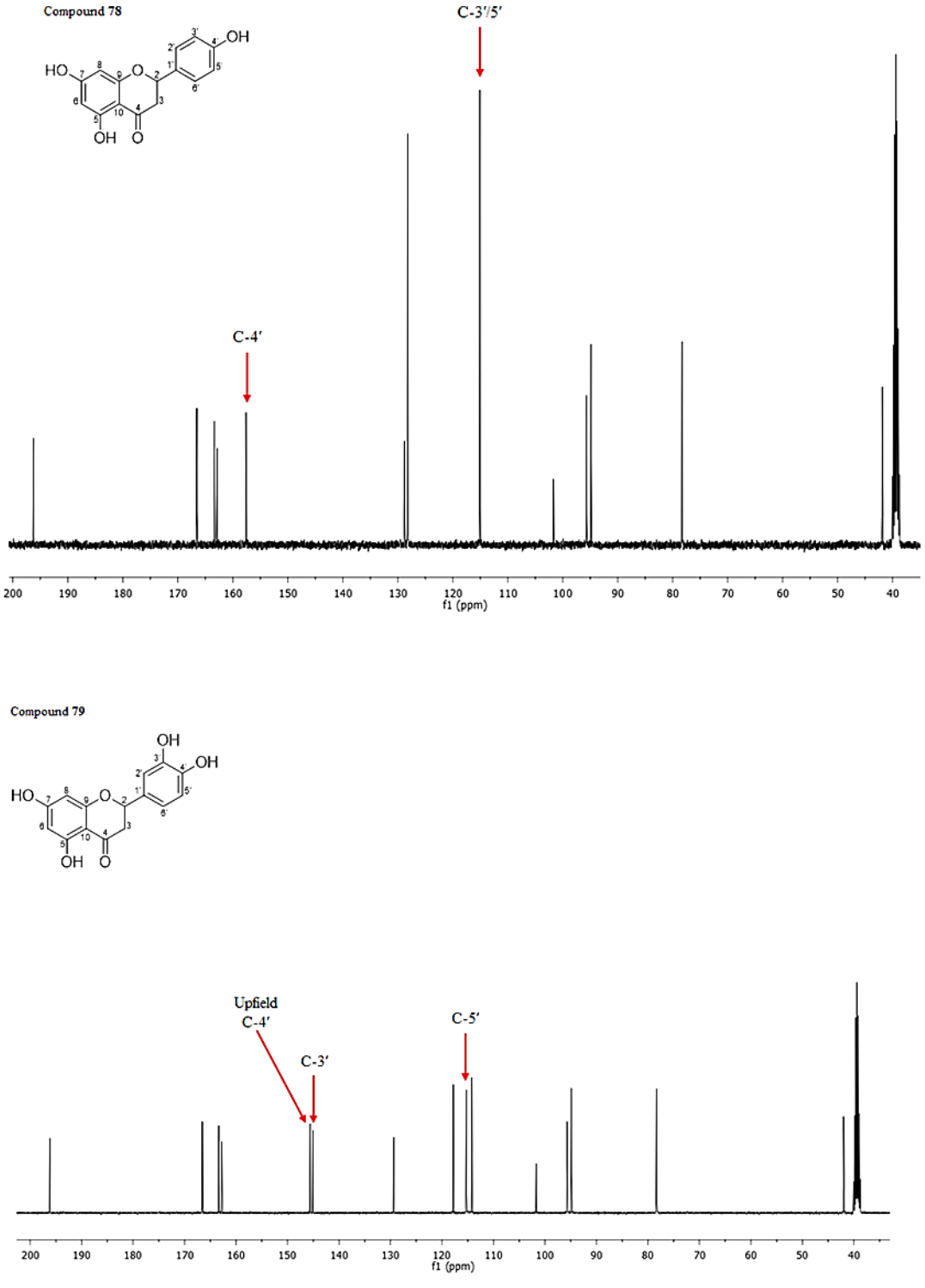

Fig. 2.52 Comparison of ^{13}C NMR spectra of compound **78** and **79** in DMSO-d_6

Table 2.14 ^{1}H NMR data of compounds **44**, **78** and **79**

position	δ_H mult, (*J* in Hz)		
	44 (DMSO-d_6)	**78** (DMSO-d_6)	**79** ($CDCl_3$)
1	-	-	-
2	-	5.43 dd, (2.8, 12.8)	5.37 dd, (2.8, 12.4)
3	6.77 s	2.68 dd, (4.0, 16.0)	2.68 dd, (2.8, 17.2)
		3.26 dd, (12.8, 17.2)	3.18 dd, (12.4, 17.2)
4	-	-	-
5	-	-	-
6	6.19 d, (2.0)	5.89 s	5.88 s
7	-	-	-
8	6.48 d, (1.6)	5.89 s	5.88 s
9	-	-	-
10	-	-	-
1′	-	-	-
2′	7.92 d, (8.8)	7.31 d, (8.4)	6.88 s
3′	6.92 d, (8.8)	6.79 d, (8.4)	-
4′	-	-	-
5′	6.92 d, (8.8)	6.79 d, (8.4)	6.74 s
6′	7.92 d, (8.8)	7.31 d, (8.4)	6.74 s
5-OH	12.95 s	12.15 s	12.26 s
7-OH	10.71 brd	10.79 s	10.68 brd
3′-OH	-	-	*
4′-OH	10.43 brd	9.59 s	9.06 brs

* No signal

Table 2.15 ^{13}C NMR data of compounds **44**, **78** and **79**

position	δ_C (ppm)		
	44 (DMSO-d_6)	**78** (DMSO-d_6)	**79** ($CDCl_3$)
1	-	-	-
2	163.7	78.3	78.4
3	102.8	41.9	42.0
4	181.6	196.2	196.2
5	161.4	163.4	163.4
6	98.7	95.7	95.7
7	164.0	166.5	166.6
8	93.9	94.9	94.9
9	157.2	162.8	162.3
10	103.6	101.7	101.7
1′	121.1	128.8	129.4
2′	128.4	128.1	114.3
3′	115.9	115.1	145.1
4′	161.1	157.6	145.6
5′	115.9	115.1	115.3
6′	128.4	128.1	117.9

2.5.2.1.6 Structural elucidation of compound 80

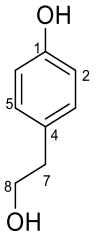

Fig. 2.53 Compound **80** (tyrosol)

Compound **80** was obtained as colorless powder and its assigned molecular formula was $C_8H_{10}O_2$. The ^{1}H NMR spectrum of compound **80 (Table 2.16)** indicated a pair of doublets at δ_H 6.65 (d, J = 8.0 Hz) and 6.98 (d, J = 8.0 Hz), which were assigned to H-2/H-6 and H-3/H-5, respectively. These were corresponded to the A_2-B_2 system characteristic of an aromatic ring di-substituted in a *para* position. The presence of doublets of doublets at δ_H 3.52 (dd, J = 7.2, 12.0 Hz) appeared integrating two protons and corresponded to the two geminal protons of the hydroxyl aliphatic group presenting in the molecule. It also indicated the presence of two protons at δ_H 2.95 (t, J = 7.2, Hz) that corresponded to the methylene that links to the aromatic ring. It was consistent with the ^{13}C NMR data (**Table 2.17)** that possess of two quaternary carbons of the aromatic ring at δ_C 155.3 (C-1) and δ_C 129.3 (C-4). According to the molecule symmetry, it presented two methane carbons (δ_C 114.8; C-2/6, 129.5; C-3/5). Finally, higher signals of C-1 (δ_C 155.3) and C-8 (δ_C 62.4) were assigned to the two side chain carbons that correspond to the carbon linking to the hydroxyl group and to the carbon binding to the aromatic ring. Compound **80** was identified as tyrosol, due to the comparison of NMR spectroscopic data with those in the literature [63].

2.5.2.1.7 Structural elucidation of compound 81

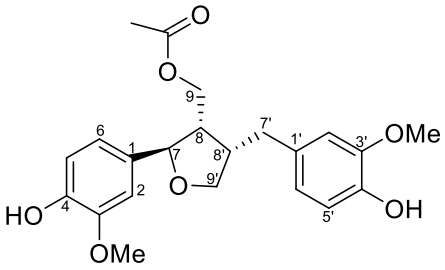

Fig. 2.54 Compound **81** (lariciresinal acetate)

Compound **81** was obtained as brownish amorphous powder and its molecular formula was assigned to be $C_{22}H_{26}NO_4$ established by 1D and 2D NMR. In consideration of ^{1}H NMR and ^{13}C NMR data (**Tables 2.6** and **2.17**), compound **81** was very similar to the compound **72**. The major difference between these two compounds was presence of acetoxy group, carbonyl carbon at δ_C 170.9, together with a methyl group (δ_C 20.8) of compound **81** (**Fig. 2.57**). The position of acetoxy group was corroborated by ^{1}H-^{1}H COSY and HMBC correlations from H-9 to C=O and C-7 (**Fig. 2.56**). From these results, the structure of **81** was identified as lariciresinal acetate [57].

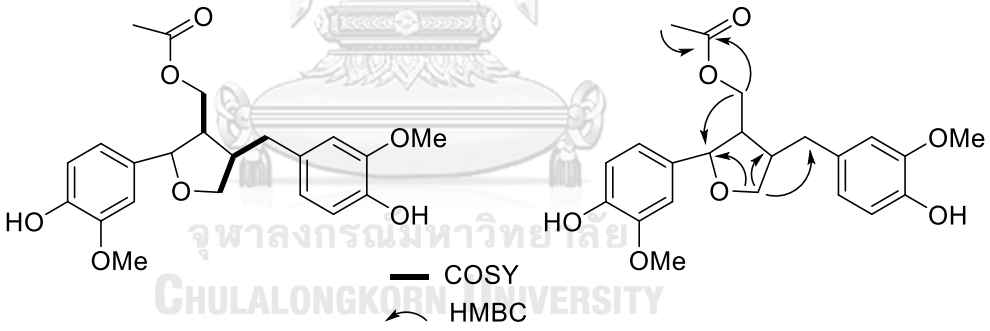

Fig. 2.55 Key COSY and HMBC correlations of compound **81**

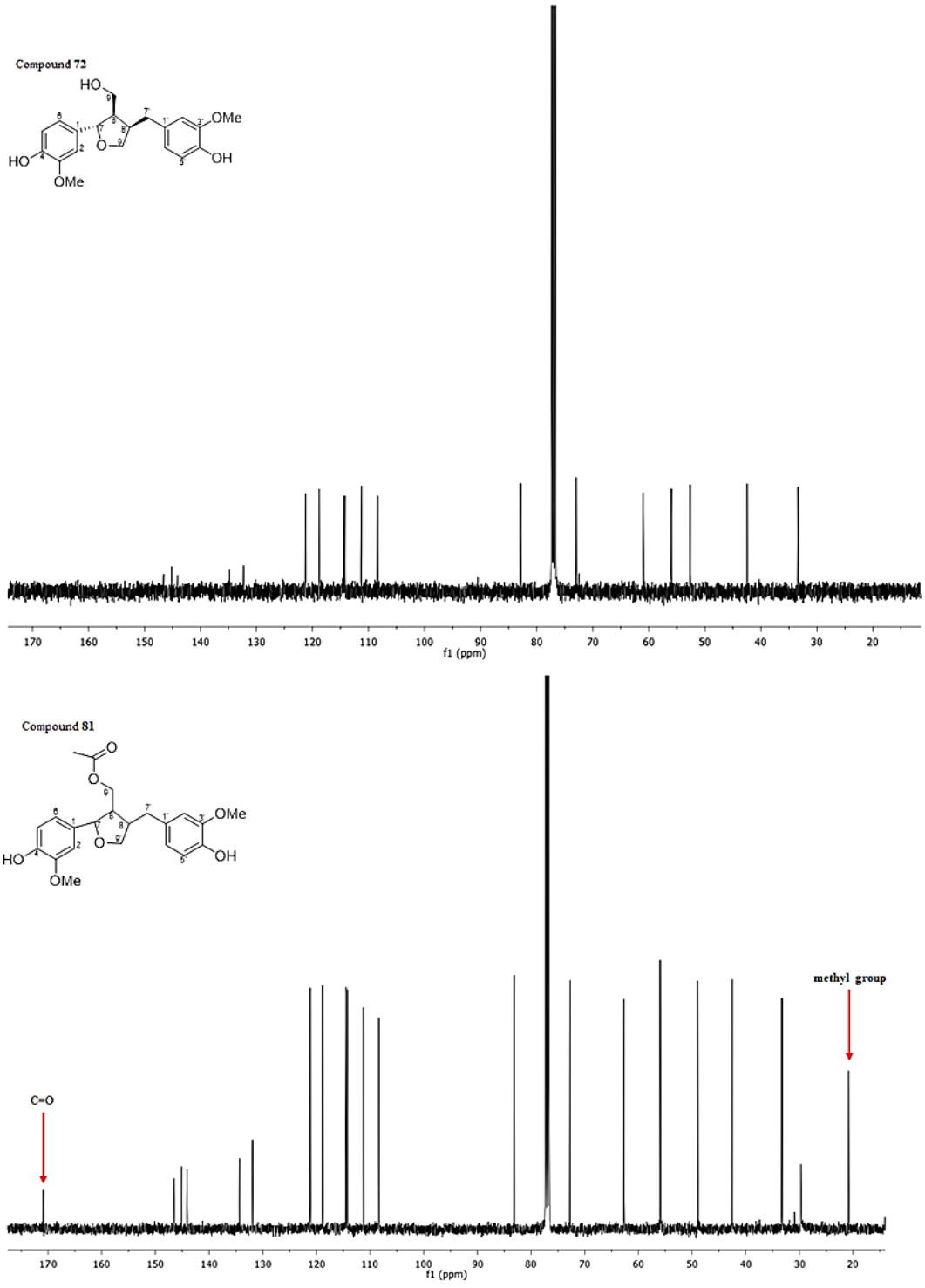

Fig. 2.56 Comparison of ^{13}C NMR spectra of compound **72** and **81** in $CDCl_3$

Table 2.16 ^{1}H NMR data of compounds **80** and **81**

position	δ_H mult, (*J* in Hz)	
	80 (DMSO-d_6)	**81** ($CDCl_3$)
1	-	-
2	6.65 d, (8.0)	6.85 m
3	6.98 d, (8.0)	-
4	-	-
5	6.98 d, (8.0)	6.87 m
6	6.65 d, (8.0)	6.81 m
7	2.59 t, (7.2)	4.76 d, (8.0)
8	3.52 dd, (7.2, 12.0)	2.55 m
9	-	4.17 m
		4.35 m
1′	-	-
2′	-	6.68 d, (6.4)
3′	-	-
4′	-	-
5′	-	6.83 m
6′	-	6.68 d, (6.4)
7′	-	2.53 m
		2.83 m
8′	-	2.72 m
9′	-	3.73 m
		4.06 m
3′-OMe	-	3.87s
5-OMe	-	3.89 s
$OCOCH_3$	-	-

Table 2.17 ^{13}C NMR data of compounds **80** and **81**

position	δ_C (ppm)	
	80 (DMSO-d_6)	**81** ($CDCl_3$)
1	155.3	134.3
2	114.8	108.4
3	129.5	145.5
4	129.3	145.1
5	129.5	114.2
6	114.8	118.8
7	38.1	83.1
8	62.4	49.0
9	-	62.7
1′	-	131.9
2′	-	111.2
3′	-	146.5
4′	-	144.1
5′	-	114.5
6′	-	121.2
7′	-	33.3
8′	-	42.5
9′	-	72.7
3′-OMe	-	55.9
5-OMe	-	56.0
$O\underline{C}OCH_3$	-	170.9

2.5.3 Biological activities of isolated compounds

2.5.3.1 Cytotoxic activities

Cytotoxic effect of the isolated compounds on hepato carcinoma (Hep-G2), gastric carcinoma (KATO-3), breast carcinoma (MCF-7) and cervix carcinoma (CaSki) were evaluated by using MTT colorimetric method. Results are presented in **Table 2.18**, tinobaenzin C (**68**) showed selectively cytotoxic activity against KATO-3 cell lines with IC_{50} values of 27.08 μM, while other compounds did not affect to any of the tested cell lines.

Table 2.18 Cytotoxic activity of pure compounds on Hep-G2, KATO-3, MCF-7 and CaSKi cell lines

Compound	IC_{50} (μM)			
Cell line	Hep-G2	KATO-3	MCF-7	CaSKi
apigenin (**44**)	I	I	I	I
baenzigeroside B (**61**)	I	I	I	I
tinobaenzin A (**66**)	I	I	I	I
tinobaenzin B (**67**)	I	I	I	I
tinobaenzin C (**68**)	I	27.08	I	I
tinobaenzin D (**69**)	I	I	I	I
tinobaenzin A glucoside (**70**)	I	I	I	I
caruilignan D **(71)**	I	I	I	I
lariciresinol (**72**)	I	I	I	I
aglycone of breyniaionoside D (**73**)	I	I	I	I
N-trans-feruloyltyramine (**74**)	I	I	I	I
N-trans-coumaroyltyramine (**75**)	I	I	I	I
tinobaenzigeride A (**76**)	ND	ND	ND	ND
tinobaenzigeride B **(77)**	ND	ND	ND	ND
naringenin (**78**)	ND	ND	ND	ND
eriodictyol (**79**)	ND	ND	ND	ND
tyrosol (**80**)	I	I	I	I
lariciresinol acetate (**81**)	ND	ND	ND	ND
Doxorubicin (positive)	0.91	0.98	0.06	0.20

I = Inactive

ND=not determined

2.5.3.2 Anti-inflammatory activities

Anti-inflammatory of thirteen isolated compounds were assessed by suppressing nitric oxide (NO) production in activated macrophages (J774.A1). Results showed all of the compounds were inactive.

Table 2.19 anti-inflammatory activity of pure compounds on J774.A1 cell line

Compound	IC_{50} (μM)
apigenin (**44**)	I
baenzigeroside B (**61**)	I
tinobaenzin A (**66**)	I
tinobaenzin B (**67**)	I
tinobaenzin C (**68**)	I
tinobaenzin D (**69**)	I
tinobaenzin A glucoside (**70**)	I
caruilignan D **(71)**	I
lariciresinol (**72**)	I
aglycone of breyniaionoside D (**73**)	I
N-trans-feruloyltyramine (**74**)	I
N-trans-coumaroyltyramine (**75**)	I
tinobaenzigeride A (**76**)	ND
tinobaenzigeride B **(77)**	ND
naringenin (**78**)	ND
eriodictyol (**79**)	ND
tyrosol (**80**)	I
lariciresinol acetate (**81**)	ND
Indomethacin (positive)	28.4

I = Inactive

ND=not determined

2.5.3.3 α-Glucosidase inhibitory activities

All selected compounds were investigated for their α-glucosidase inhibition by using the enzymes from rat intestine. *N-trans*-feruloyltyramine displayed the weak activity against **α**-glucosidase with an IC_{50} value of 0.34 mM for sucrase inhibition and 0.36 mM for maltase inhibition.

Table 2.20 α-Glucosidase inhibitory activity of pure compounds

Compound	IC_{50} (μM)	
Enzyme	Sucrase	Maltase
apigenin (**44**)	I	I
baenzigeroside B (**61**)	I	I
tinobaenzin A (**66**)	I	I
tinobaenzin B (**67**)	I	I
tinobaenzin C (**68**)	I	I
tinobaenzin D (**69**)	I	I
tinobaenzin A glucoside (**70**)	I	I
caruilignan D **(71)**	I	I
lariciresinol (**72**)	I	I
aglycone of breyniaionoside D (**73**)	I	I
N-trans-feruloyltyramine (**74**)	340	360
N-trans-coumaroyltyramine (**75**)	I	I
tinobaenzigeride A (**76**)	ND	ND
tinobaenzigeride B **(77)**	ND	ND
naringenin (**78**)	ND	ND
eriodictyol (**79**)	ND	ND
tyrosol (**80**)	I	I
lariciresinol acetate (**81**)	ND	ND
Acarbose (positive)	2.3	1.5

I = Inactive

ND=not determined

CHAPTER III
BIOACTIVE COMPOUNDS FROM ENDOPHYTIC FUNGI

3.1 Introduction

3.1.1 Important roles of fungi

Fungi are one of important organisms to human, as they play impact roles in medicine, food, agriculture and industry. Particularly, they produce a diverse group of bioactive compounds that inhibit antimicrobial, anticancer, anticholesterol, immunosuppressive, antioxidant properties. Besides penicillin, the first fungal derived drug found in 1928, some commercial medicines originated from fungi have been released to the market; for example, the discovery of cyclosporine originally derived from *Tolypocladium inflatum,* was an important step in immunopharmacology because this substance prevents rejection after organ or tissue transplantations [64, 65]. Subsequently, mycophenolate, an autoimmne suppressive agent was derived from the fungi *Penicillium stoloniferum*, *P. brevicompactum* and *P. echinulatum* [66, 67]. Lovastatin, a member of statin drugs which exhibit anticholesteremic agent, was extracted from *Aspergillus terreus* and *Pleurotus ostreatus.* While a depsipeptide called beauvericin with antibiotic and insecticidal effects was first isolated from *Beaveria bassiana*, is also produced by several other fungi [68]. Additionally, exploring of the new potential drug has been investigated, *Ganoderma lucidum*, a fungus used in traditional Chinese medicine, produces polysaccharides and oxygenated triterpenoids as a dietary supplement recommended in many countries as a cancer therapeutic [69]. Interestingly, the most important, Paclitaxel (taxol), the first billion-dollar anticancer drug in the world, was produced by an endophytic fungus *Taxomyces andreanae* growing on one particular specimen of yew tree (*T. brevifolia*) [70], the original plant species of taxol isolation [71]. Afterwards, there have been a few reports on the explorarion of taxol-producing endophytic fungi such as *Monocheetia* sp., *Alternaria* sp., *Pestalotiopsis* sp., *Pithomyces* sp., *Fusarium lateritium*. For this reason, natural products chemists and pharmacologists has turned to investigat bioactive compounds from endophytic fungi.

3.1.2 Endophytic fungi

Endophytic fungi are microbes residing in internal tissues of plants hosts for all or part of their life cycle. They colonize the internal plant tissues beneath the epidermal cell layers without causing any disease symptomatic to their host (**Fig. 3.1**). Strobel and Daisy (2003) reported that nearly 300,000 plant species are being on earth and each plant is the host of "Endophytes". The relationship between the host plant and its endophyte shows symbiotic characteristics as the endophytic occupant usually obtains nutrients and protection from the host plant and in return profoundly enhances the fitness of the host by producing certain functional metabolites. Endophytes are currently considered to be a wellspring of novel secondary metabolites offering the potential for medical, agricultural and industrial exploitation [72]. These fungi appear to a capacity to produce an array of secondary metabolites exhibiting a variety of biological activity. Its produced various useful bioactive molecules which some compounds show the powerful of antimalarial, antimicrobial, antiviral, antioxidant and anticancer [73]. Moreover, endophytes consist of a various group of compounds, including alkaloids, steroids, terpenoids, flavonoids, glycosides, xanthones, isocoumarins, quinones, phenyl propanoids, lignans, aliphatic metabolites, lactones etc. [74, 75].

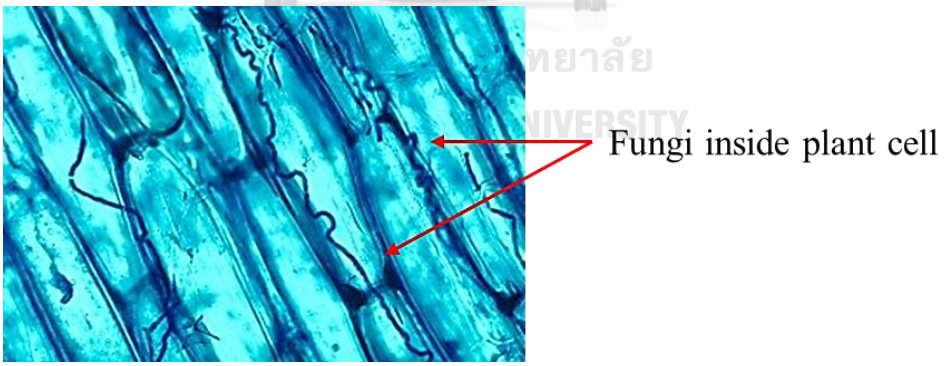

Fig. 3.1 Endophytic fungal hyphae in plant cells
(http://www.hmwf.org/2015/10/hidden-diversity-fungal-endophytes/**)**

3.1.3 Selection of promising sources for the isolation of endophytic fungi

It is the most important to comprehend the methods and rationale used to give the best opportunity to isolate novel endophytic fungi, since the number of species in

the world is so great. In addition, each individual plant is also the host to numerous endophytes. Generative strategies must be used to quickly narrow the search for the host plants for isolation and target endophytes displaying bioactivity.

The collection of each plant for endophytic isolation and natural compound discovery should be seriously considered following some strategies [76, 77]: Plants from a unique ecological environmental setting and growing in special residences, for instance, rainforest, swamp forest ancient forest, desert, hot spring, crater mouth, pole, Dead sea should be selected firstly because it have to cope with extreme living conditions. However, young plant tissue is appropriate for endophytic isolation more than older tissues which often contain many additional fungi that make isolation of slow growing fungi difficult to isolate. Plants that have long been used for traditional medicines would be also the proper sources for inhabiting endophytes [78]. The pathogen infected plants without symptoms are of interest to lodge endophytes possessing antimicrobial activity than other plant. Moreover, plants growing in areas which provide great biodiversity also have the potential for housing endophytes with great diversity.

3.1.4 Mangrove endophytic fungi

Mangroves are salt-tolerant trees or shrubs that grow at the interface between land and sea within the intertidal zone in tropical and subtropical regions which provide great biodiversity. Mangrove forests are considered an open interface ecosystem connecting upland terrestrial and coastal estuarine ecosystems. They have special adaptations to survive in conditions of high salinity, extreme tides, strong winds, high temperatures and muddy, anaerobic soils as well as a number of other environment factors [29, 30]. It is reasonable to expect mangrove as habitats to a great variety of specific microorganisms including fungi [12]. Furthermore, their unique living conditions are thought to predestine mangroves as promising sources for the isolation of endophytic fungi, that constitute a consortium of soil, marine and freshwater fungi [29, 79].

Endophytic fungi are microbes that inhabit such biotopes, namely, higher plants, which is why they are currently considered to be a wellspring of novel secondary metabolites offering the potential for medicinal, agricultural, and industrial exploitation[12]. Among plant-derived fungi, those associated with mangrove trees

have received much attention from natural product researchers due to its unique ecosystem [28]. Examples of recent publications of bioactive compounds from mangrove-derived fungi are listed as follows:

In 2009, Dai and co-workers revealed that the endophyte *Nodulisporium* sp. (Xylariaceae), isolated from *Erica arborea* (Ericaceae), yielded six novel metabolites including nodulisporins D-F (**82-84**), (3*S*,4*S*,5*R*)-2,4,6-trimethyloct-6-ene-3,5-diol (**85**), 5-hydroxy-2-hydroxy-methyl-4*H*-chromen-4-one (**86**) and 3-(2,3-dihydroxyphenoxy)-butanoic acid (**87**), together with seven known compounds (**88**-**94**) (**Fig. 3.2**). All of them showed anti-fungal and anti-algal activities, while compounds **82**-**84** also exhibited antibacterial activity [80].

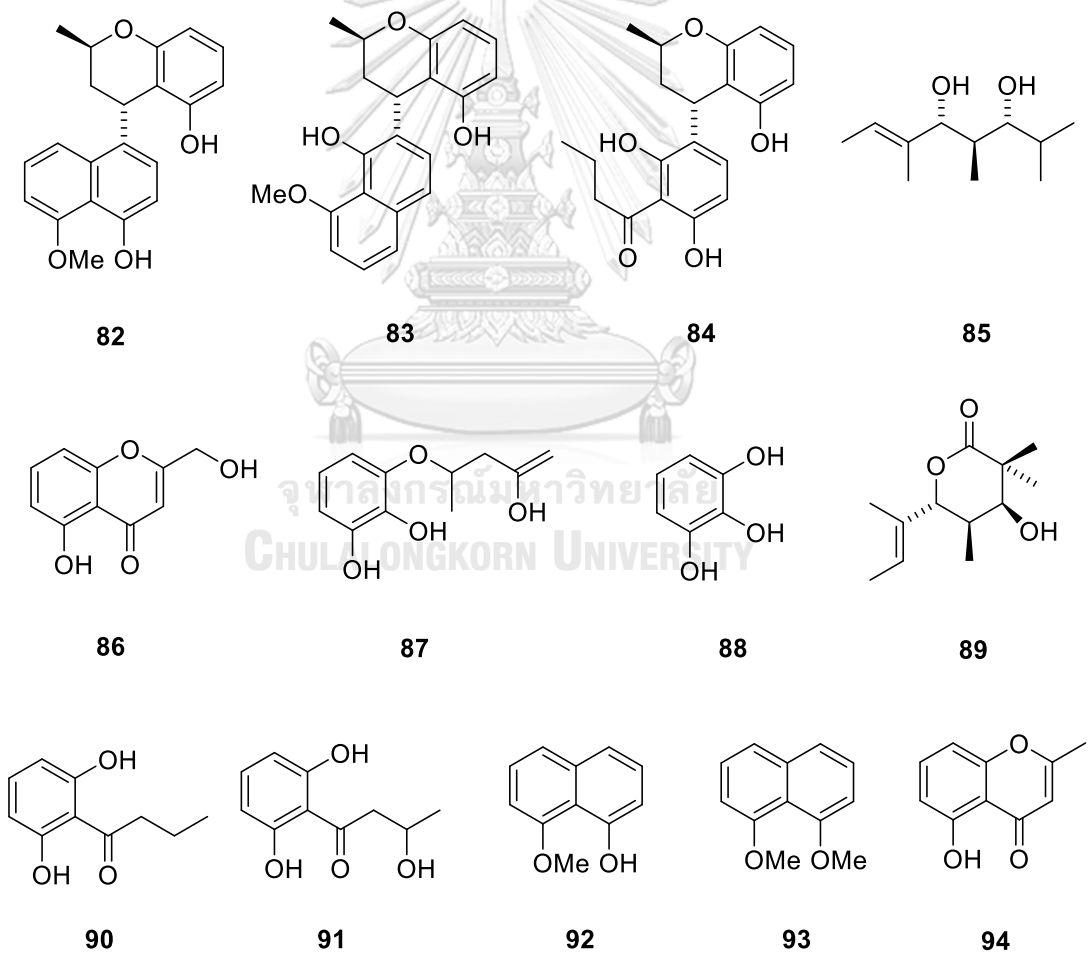

Fig. 3.2 Structures of compounds from *Nodulisporium sp.*

In 2014, Li and co-workers disclosed three new metabolites (**95-96** and **100**), one azaphilone, and two meroterpenes, together with eleven known compounds (**97-99** and **101-108**) (**Fig. 3.3**). These compounds have been isolated from a mangrove endophytic fungus, Penicillium 303#. Cytotoxic activity of the compounds **95-96** and **100-101** were evaluated in vitro against human cancer lines MDA-MB-435, HepG2, HCT-116 and A549. The compounds showed weak to moderate cytotoxic activities [81].

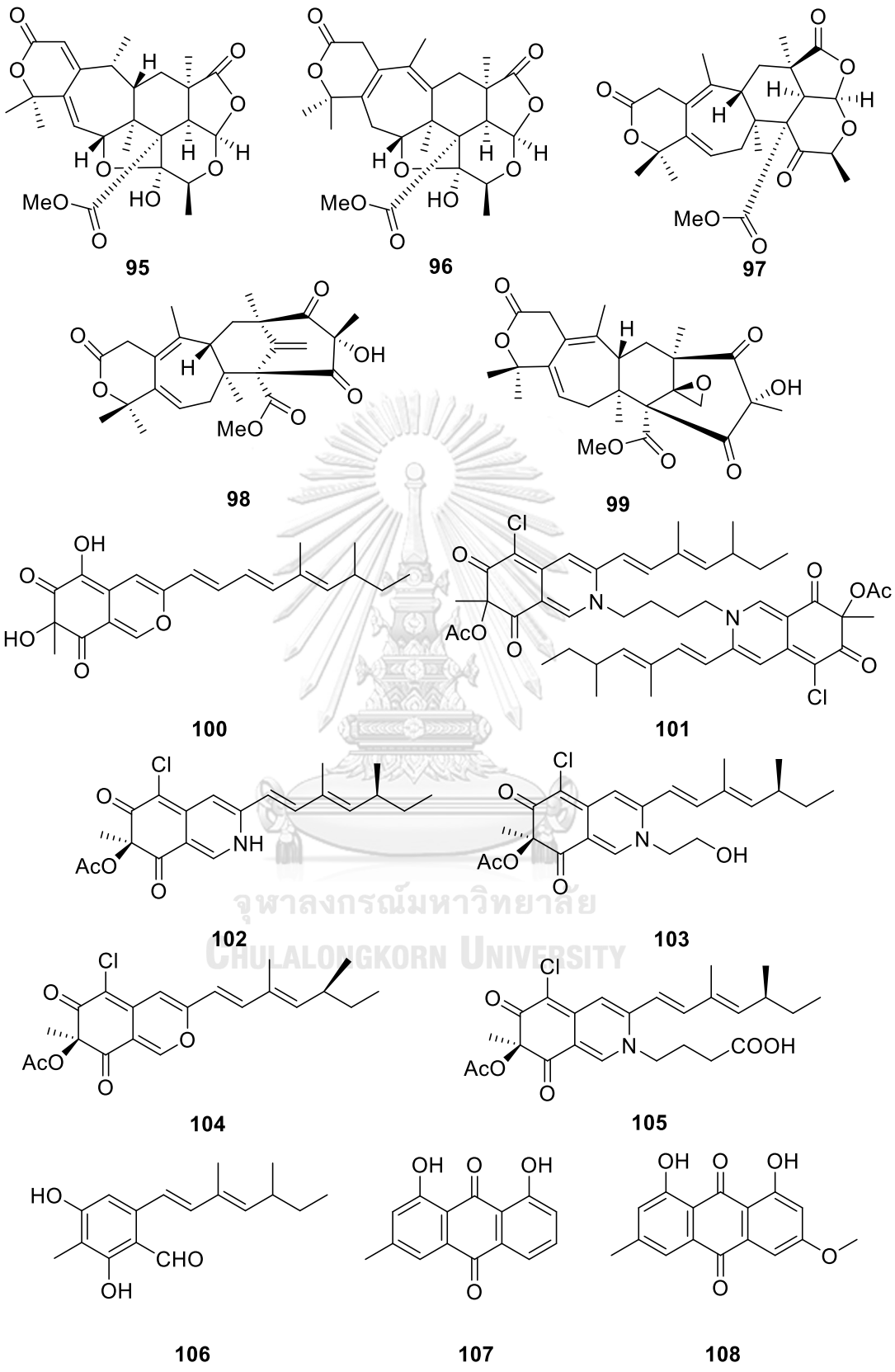

Fig. 3.3 Structures of compounds from *Penicillium* 303#.

In 2015, Bai and co-workers reported four new meroterpenoids (**110-113**), along with three known analogues (**109** and **114-115**) (**Fig. 3.4**), isolated from endophytic fungus *Aspergillus flavipes*, which was obtained from a mangrove plant *Acanthus ilicifolius*. All compounds were evaluated for antibacterial activity and cytotoxic activities; however, they were found to be inactive [82].

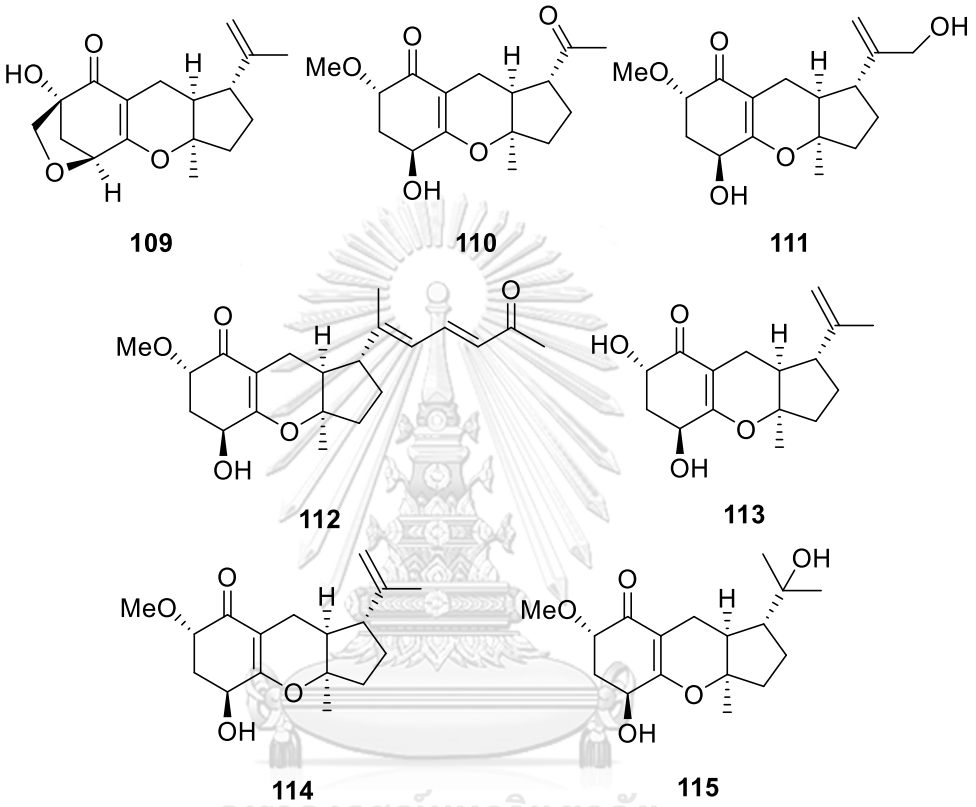

Fig. 3.4 Structures of compounds from *Aspergillus flavipes*

3.1.6 Constituents of media

Since fungi are differ in their nutritional requirements, media selection is very significant when fungi are grown. Difference in media composition can produce very diverse growth and behavioral responses. A wide range of media have been used to grow endophytic fungi for studying of bioactive compounds. Media universally comprise of a source of carbon, nitrogen and vitamins.

A. Carbon is one of the elements that are necessary for growth which made up half of the dry weight of the fungal cells. It is required in greater quantities than any

other essential elements by the fungus, and this nutrition is of important to the fungus [83, 84].

B. Nitrogen is required by all organisms for the synthesis of amino acids and are required for building protoplasm. Accordingly, without protein, growth cannot originate. Fungi may use inorganic nitrogen in the form of nitrate, nitrite, ammonia, or organic nitrogen in the form of amino acid [84]. Many fungi can apply nitrate as a nitrogen source. Although, basidiomycetes are not able to utilize nitrate for expansion [85]. Nitrite is the least utilizable source of nitrogen and is commonly toxic to most species of fungi, especially if it accumulates in the medium. Nitrite exert it toxic effect by delaminating used in fungal media [84]. Numerous fungi use ammonium ion, or in the form of organic nitrogen, such as an ammonium salt, which has the same oxidation level as the ammonium ion.

C. Vitamins are organic compounds that play a role as coenzymes or composition of coenzymes, which catalyze specific interaction. These compounds are required in very small dosage, normally in the range 10^{-5}-10^{-6} M. Some fungi are able to synthesize vitamins, but some species acquire them from the environment or medium [84-86].

Dextrose (glucose) is the most widely utilizable carbon source and hence is the most usually used in culture media. Whilst sucrose was used in some media. Nitrogen sources consist peptone, yeast extract, malt extract, amino acids, ammonium and nitrate compounds. Fungi have natural deficiencies for vitamins that are satisfied at μM to nM concentrations. Other organic nutrients for example glucose are frequently contaminated with vitamins sufficient to supply the growth requirements of fungi [87].

We will use “Semi-synthetic” media, containing both natural ingredients and defined components include fresh potatoes, potato extract, yeast extract and peptone.

3.2 Materials

3.2.1 Plant samples

Healthy mature leaves and barks of 21 mangrove plants including Avicennia alba, Callerya atropurpurea, Xylocarpus granatum, Rhizophora apiculate, Bruguiera cylindrica, Ceriops decandra, Syzygium gratum, Sonneratia alba, Xylocarpus moluccensis, Cerbera manghas, Aegiceras corniculatum, Ceriops tagal, Azima sarmentosa, Sonneratia ovata, Rhizophora mucronate, Bruguiera gymnorrhiza, Xylocarpus rumphii, Ipomoea pes-caprae, Excoecaria agallocha, Unknow A and Unknow B were carefully collected from Ko Yo, Muang Songkhla, Songkhla province, Thailand. Fresh specimens were kept in a plastic bag, then immediately brought to the laboratory and processed within 24 h after collection.

3.2.2 Culture media for endophytic fungi cultivation

Water Agar (WA) was culture medium for isolation of endophytic fungi. Potato dextrose agar (PDA) was used for morphological observation of isolated endophytic fungi. In addition, potato dextrose broth (PDB), natural potato dextrose broth (NPDB), yeast extract sucrose broth (YEB) and sabouraud's dextrose broth (SDB) were also used for growing isolated endophytic fungi.

The culture media formulae were shown in Appendix A.

3.2.3 Equipments

3.2.3.1 Column chromatography

Merck's silica gel 60H (No. 7734 and No. 9385) and ODS (Wakogel® 100C18, 63-212 μM) were normally used as the adsorbents for open column chromatography. Sephadex LH-20 (Amersham Pharmacia Biotech AB) was used to separate substances by molecular sizing.

3.2.3.2 Thin-layer chromatography (TLC)

Thin-layer chromatography (TLC) was carried out on a silica gel^{60} GF_{254} coated on aluminum sheet (Merck). Detection was visualized under ultraviolet light at wavelengths of 254 and 356 nm and dipped with $(NH_4)_6Mo_7O_{24}$ solution in 5% H_2SO_4: EtOH.

3.2.4 General Experimental Procedures

3.2.4.1 Nuclear magnetic resonance spectroscopy (NMR)

NMR spectra were acquired on a Bruker AV400 and Varian Mercury 400 plus NMR spectrometer at 400 MHz for ^{1}H NMR and 100 MHz for ^{13}C NMR. The chemical shifts were expressed δ values with TMS (tetramethyl silane) as the internal standard. Deuterated solvents, chloroform-*d* ($CDCl_3$), dimethysulfoxide-d_6 (DMSO-d_6) and acetone-d_6, were used for NMR experiments and chemical shifts (δ) were referenced by the signals of residual solvents at 7.26 (s) ppm (^{1}H NMR) and 77.00 (t) ppm (^{13}C NMR) for $CDCl_3$, at 2.50 (t) ppm (^{1}H NMR) and 39.5 (sept) ppm (^{13}C NMR) for DMSO-d_6 and at 2.09 ppm (^{1}H NMR) and 29.9 and 206.7 ppm (^{13}C NMR) for acetone-d_6.

3.2.4.2 Mass spectrometry (MS)

ESI-TOF mass spectra and HRESIMS were obtained with a Bruker microOTOF mass spectrometer.

3.2.4.3 Ultraviolet-visible measurements (UV-vis)

UV-VIS spectra were measured in MeOH and recorded on Spekol 1200 (Analytic JENA) and GBC Cintra 404 UV-Visible spectrophotometers

3.2.4.4 Fourier transforms infrared spectroscopy (FT-IR)

The FT-IR spectra were recorded on a Perkin-Elmer Model 1760X Fourier Transform Infrared Spectrophotometer.

3.2.4.5 Melting point

Melting points were determined by a fisher-Johns melting point apparatus.

3.2.4.6 Optical rotation

Optical rotations were measured on a JASCO P-1010 polarimeter.

3.2.5 Chemicals used in the experiments

3.2.5.1 Solvent

All commercial grade solvents used in used in the present study including hexane, dichloromethane (CH_2Cl_2) ethyl acetate (EtOAc), acetone, ethanol

(EtOH) and methanol (MeOH) were purified by distillation prior to use. The deuterated solvents for NMR measurement, $CDCl_3$, DMSO-d_6 and acetone-d_6, were purchased from Merck Millipore.

3.2.5.2 Other chemicals

- Clorox® (6% NaOCl) was used as a detergent for surface sterilization.
- Glycerol and liquid paraffin were used to storage of pure fungal strains.

3.3 Methods

3.3.1 Isolation of Fungal endophyte

Endophytic fungi of the selected plants were isolated using the surface sterilization method which modified by Petrini (1991). The plant samples were washed in tap water and dried before using Healthy plant materials were cut into small pieces and immersed in 70% ethanol (EtOH) for 1-3 min, followed with a solution of 6% NaOCl for 2-5 min and rinsed twice with sterile distilled water. The surface sterilized samples were dried on sterilized filter papers and cut into smaller size, and then put on WA for culturing at room. After several days of incubation, the first fungal growth was observed under a stereomicroscope. The fungal hyphal tips were transferred to the potato dextrose agar (PDA) plate and cultured in the same conditions for 7-14 days. The purity of isolated endophytic fungi was determined by colony morphology.

3.3.2 Preservation of Endophytic Fungi

For short-term storage, pieces of pure fungal strains were transferred to microtubes containing sterilized water or 15% glycerol, then kept at 4 ^{o}C. While the long-term storage (6-12 month), pure fungal strains were grown on PDA slant at room temperature. Approximately 7-10 days, the mature cultures (depending on the fungal strain) were covered up 10 mm height with sterilized liquid paraffin, and then kept at room temperature for further experiments.

3.3.3 Cultivation for screening and isolation

The stock of endophytic fungal isolates were grown on PDA plates, the duration of individual culture depends on the growth rate. Five pieces (5x5 mm^2) of each cultured isolate were inoculated into 250 mL flask containing 100 mL of culture media; PDB, NPDB, YEB, SDB, and incubated under static condition at room temperature for

21 days. After fermentation, cultured broth of each endophyte isolate was filtered through filter paper (Whatman No. 1). The filtrates were extracted with EtOAc for 3 times, the EtOAc layer was concentrated in vacuum to yield a crude extract. The crude extract was dissolved in EtOAc, transferred into a vial, dried and kept at 4 ^{o}C. White mycelia were dried, crush and extracted by soaking in a mixture of CH_2Cl_2 and MeOH 1:1 (v/v) for 2 days, 3 times. The solvent was evaporated under reduced pressure, dissolved in a mixture of MeOH and water (1:1) (v/v) and then extracted 3 times with hexane to afford hexane layer and residue. The hexane layer was evaporated to give a crude extract, whereas the residue was repeatly extracted with EtOAc 3 times, the EtOAc layer was concentrated in vacuum to furnish a crude extract, dried and stored at 4 ^{o}C.

The procedure of the extraction was summarized in **Scheme 3.1**. For preliminarily screening of interesting compounds, all dried crude extracts of each fungal isolate were examined by ^{1}H-NMR analysis.

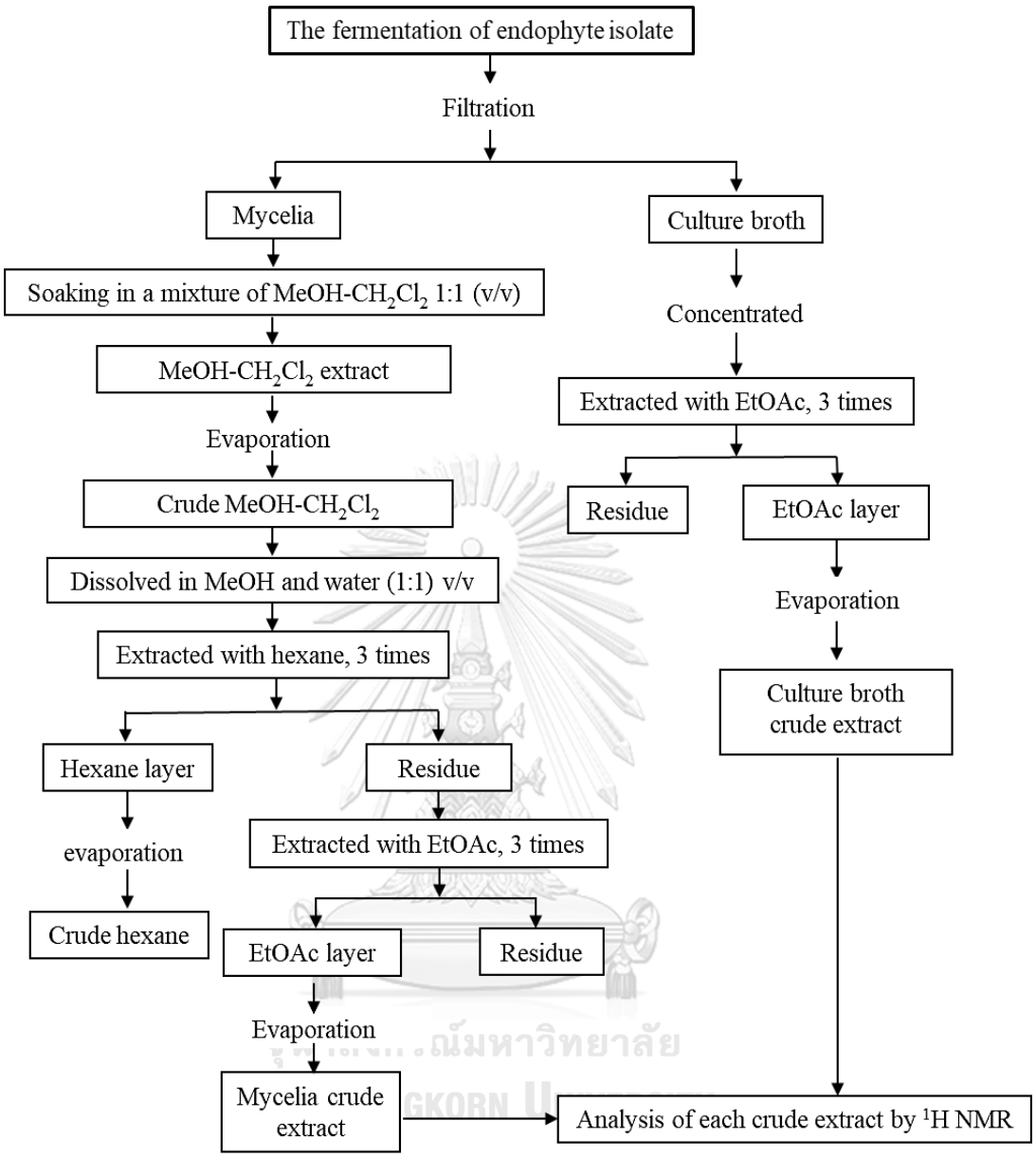

Scheme 3.1 Experimental steps used to get crude extract

3.3.4 Isolation and purification of selected fungus

Based on ^{1}H NMR data analysis, endophytic fungus strain SH8-8, obtained from *Ipomoea pes-caprae*, was selected to culture in SDB (10.0 L) for 21 days at room temperature. According to the procedure in **3.3.3**, the EtOAc crude extracts of cultured broth of the fungus SH8-8 were obtained in amounts of 5.14 g.

The EtOAc crude extract (5.14 mg) of culture broth of endophytic fungal isolate SH8-8 was fractionated by gel filtration chromatography column (CC), eluted by a gradient mixture of EtOAc/hexane (10%-100%) and of MeOH/EtOAc (20%-50%) to give 15 fractions (F1-F15). Fraction F5 (203.0 mg) was rechromatographed on SiO_2 flash column, eluted with acetone/CH_2Cl_2 (2%-4%), then subfraction F5S1 (40.9 mg) was subjected to a silica gel CC (CH_2Cl_2/hexane, 50%) to give compound **82** (5.4 mg). Fraction F6 (1.67 g) was performed on a silica gel CC, eluted with EtOAc/hexane (40%) to yield compound **83** (327.6 mg). Fraction F7 (50.4 mg) was further purified by a silica gel CC (EtOAc/CH_2Cl_2, 2%-6%) to give compound **83** (69.2 mg), while fraction F7S1 (28.0 mg) gave compound **84** (9.3 mg) when a gradient mixture of EtOAc/CH_2Cl_2 (2%-4%) was used as eluent. Fraction F12 (227.5 mg) was subjected to silica gel CC, eluted with a gradient mixture of (EtOAc/CH_2Cl_2, 30%-60%) to give 3 fractions (F12S1-F12S3), then F12S2 (92.9 mg) was separated by silica gel CC (acetone/ CH_2Cl_2, 10%-20%), then F12S2.2 (31.6 mg) was purified on Sephadex LH-20 and eluted with 100%MeOH to afford compound **85** (7.4 mg). Whilst subfraction F12S2.2.2 (12.7 mg) was applied to ODS column chromatography using MeOH/H_2O (60%-100%) to furnish compounds **85** (4.8 mg) and **86** (5.1 mg). Finally, fraction F14 (646.9 mg) was further separated on a Sephadex LH-20 column (MeOH) to yield 4 subfractions, F14P1-F14P4, then F14P1 (222.3 mg) was subjected by a silica gel CC (MeOH/CH_2Cl_2, 1%-4%), followed by ODS CC with a gradient mixture of MeOH/H_2O (50%-100%) to give compound **87** (4.2 mg) and **88** (7.1 mg) The isolation and purification procedures were briefly summarized in **Scheme 3.2**.

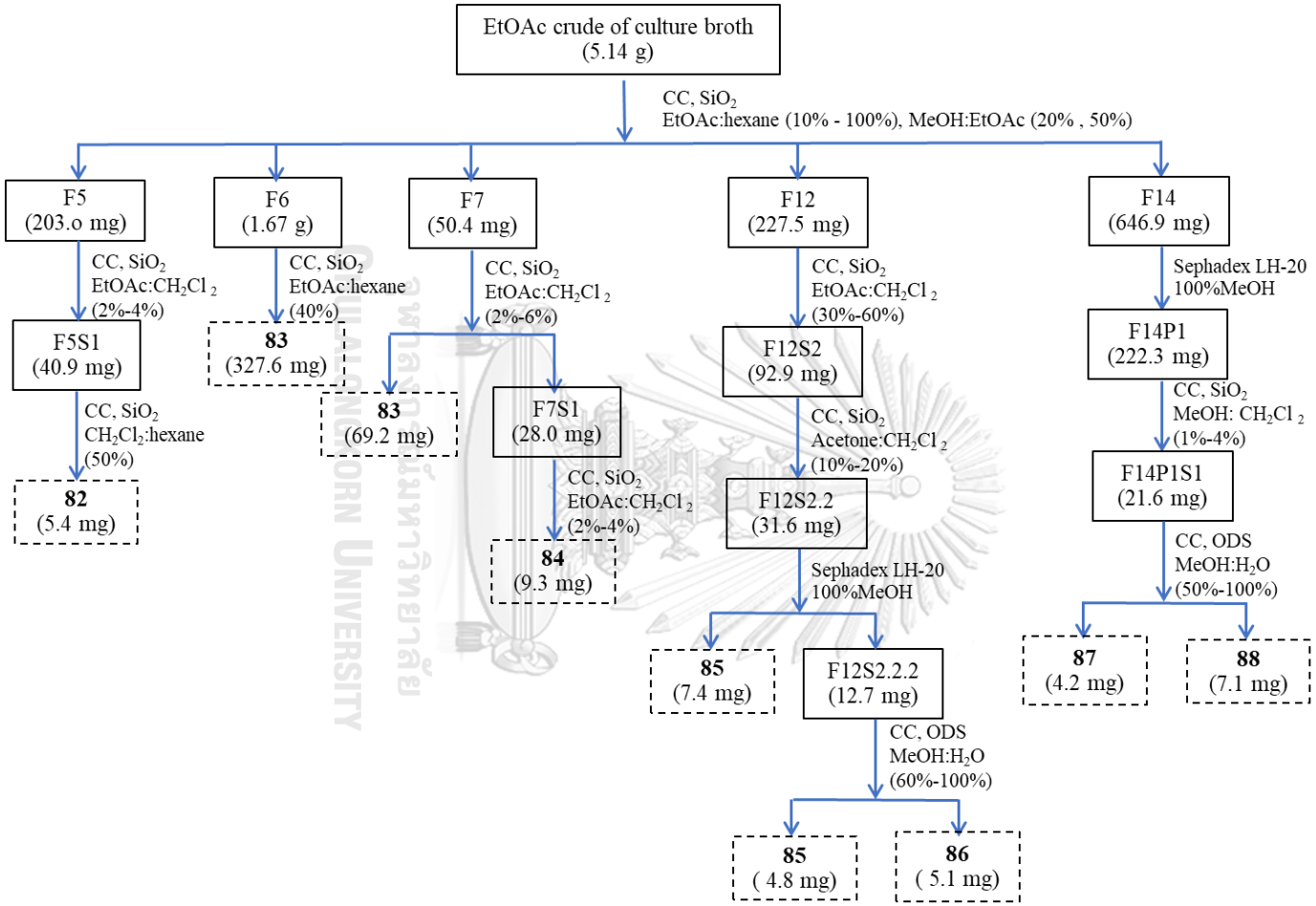

Scheme 3.2 The isolation and procedure of culture broth of the fungus isolate SH8-8

3.3.5 Identification and classification of the endophytic fungi isolate

3.3.5.1 Conventional method

The selected fungus isolate was grown on PDA for 7-14 day at room temperature and photographed, then colony characteristics was observed on the basis of morphological identification, for example, spores, mycelia, shape, size, color, margin, pigment and others.

3.3.5.2 Molecular method

The selected fungus isolate was grown PDA, the 7 days mycelia were harvested and homogenated into powder in liquid nitrogen, and then the genomic DNA was extracted by using Plant Genomic DNA Extraction Kit (RBC Bioscience Corp, Taiwan) following the manufacturer's protocol. A fragment of the ITS region was amplified using the primers ITS1 and ITS4 [88]. The PCR reaction was performed in a total volume of 50 μL containing 1x reaction buffer, 1.5 mM $MgCl_2$, 0.2 mM of each dNTP, 2.5 μM of each primer, 0.4 units of Taq DNA polymerase and 2 μl of DNA sample (diluted 1:20 in ddH_2O). The temperature profile was 94°C for 2 min; followed by 36 cycles of denaturing at 94°C for 45 s, annealing at 50°C for 45 s and extension at 72°C for 1.30 min; and a final extension at 72 °C for 5 min. PCR products were checked on a 1% agarose gel containing 0.125 mg/L ethidium bromide. The PCR products were cleaned using the PCR purification kit (RBC Bioscience, Taiwan) and were sequenced using the same primers as in the PCR by the Macrogen DNA Sequencing Service (Seoul, Korea).

3.4 Bioactivity assay

The pure compounds were evaluated for anti-cancer, anti- inflammatory and α-glucosidase inhibition following the procedures as mentioned in Chapter 2.

3.5 Results and Discussion

3.5.1 Pure isolates of endophytic fungi

Based on different morphology of fungi, a total of 52 pure isolates of endophytic fungi were obtained (**Table 3.1**). All pure strains were cultured on potato dextrose agar (PDA) until grown fully on petri dish, to observe their morphological characteristics including colony, color, produced pigment and sporulation. The characteristics of each strain are shown in **Fig. 3.5** to **3.25**.

Table 3. 1 Isolation of fungal endophytesophytes

Plant	Fungal Code		Numbers of isolates
	Leave	Bark	
Avicennia alba	Avi L	Avi B	3
Callerya atropurpurea	Call L	Ball B	4
Xylocarpus granatum	Xg L	Xg B	1
Rhizophora apiculate	Rhia L	Rhia B	1
Bruguiera cylindrica	Bruc L	Bruc B	2
Ceriops decandra	Cerd L	Cerd B	2
Syzygium gratum	Syz L	Syz B	1
Sonneratia alba	Son L	Son B	2
Xylocarpus moluccensis	Xm L	Xm B	4
Cerbera manghas	Cerb L	Cerb B	2
Aegiceras corniculatum	Aeg L	Aeg B	1
Ceriops tagal	Cert L	Cert B	1
Azima sarmentosa	Azi L	Azi B	1
Sonneratia ovata	Sonn L	Sonn B	1
Rhizophora mucronate	Rhim L	-	3
Bruguiera gymnorrhiza	Brug L	Blug B	8
Xylocarpus rumphii	Xr L	Xr B	4
Ipomoea pes-caprae	SH8	-	3
Excoecaria agallocha	SH9	-	4
Unknow A	SH10	-	3
Unknow B	SH11	-	1

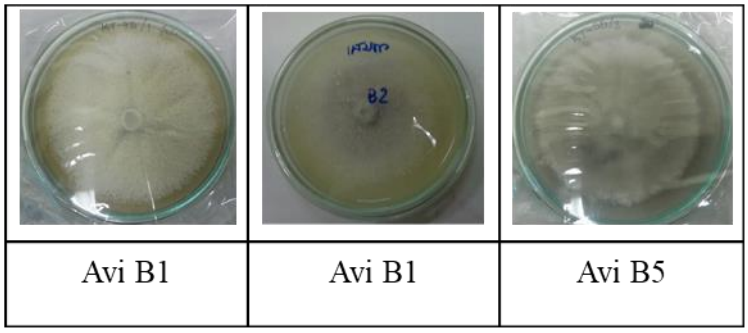

Fig. 3.5 Isolated endophytic fungi from *Avicennia alba*

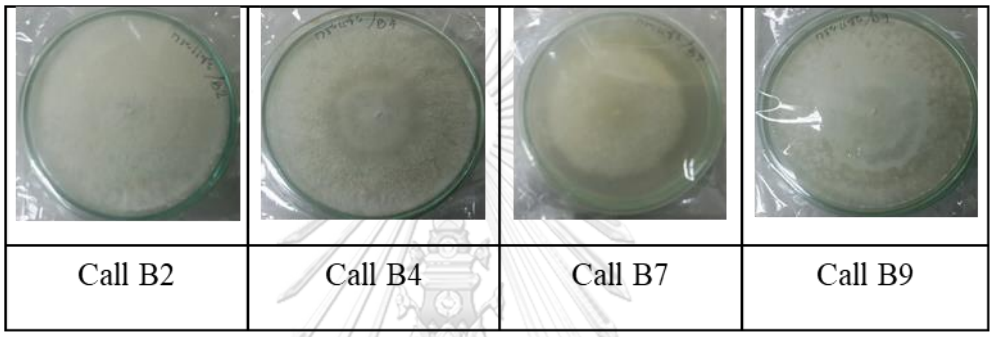

Fig. 3.6 Isolated endophytic fungi from *Callerya atropurpurea*

Fig. 3.7 Isolated endophytic fungi from *Xylocarpus granatum*

Fig. 3.8 Isolated endophytic fungi from *Rhizophora apiculate*

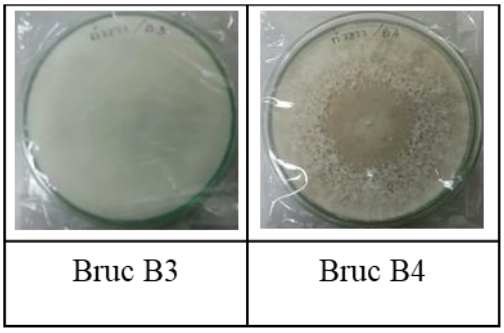

Fig. 3.9 Isolated endophytic fungi from *Bruguiera cylindrical*

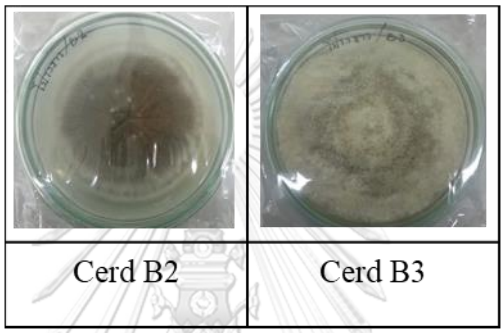

Fig. 3.10 Isolated endophytic fungi from *Ceriops decandra*

Fig. 3.11 Isolated endophytic fungi from *Syzygium gratum*

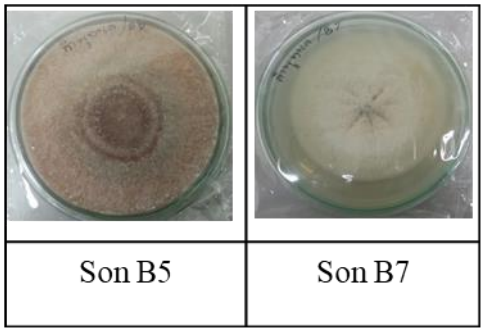

Fig. 3.12 Isolated endophytic fungi from *Sonneratia alba*

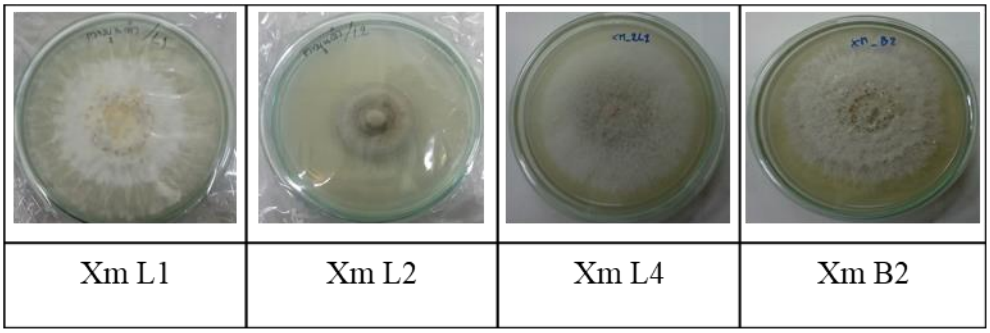

Fig. 3.13 Isolated endophytic fungi from *Xylocarpus moluccensis*

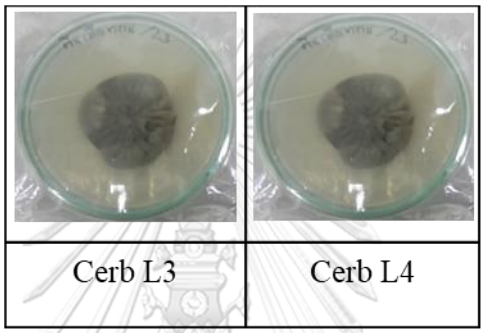

Fig. 3.14 Isolated endophytic fungi from *Cerbera manghas*

Fig. 3.15 Isolated endophytic fungi from *Aegiceras corniculatum*

Fig. 3.16 Isolated endophytic fungi from *Ceriops tagal*

Fig. 3.17 Isolated endophytic fungi from *Azima sarmentosa*

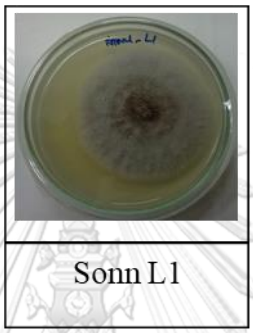

Fig. 3.18 Isolated endophytic fungi from *Sonneratia ovata*

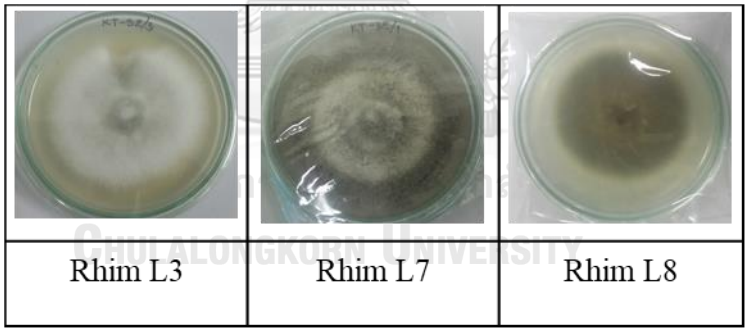

Fig. 3.19 Isolated endophytic fungi from *Rhizophora mucronate*

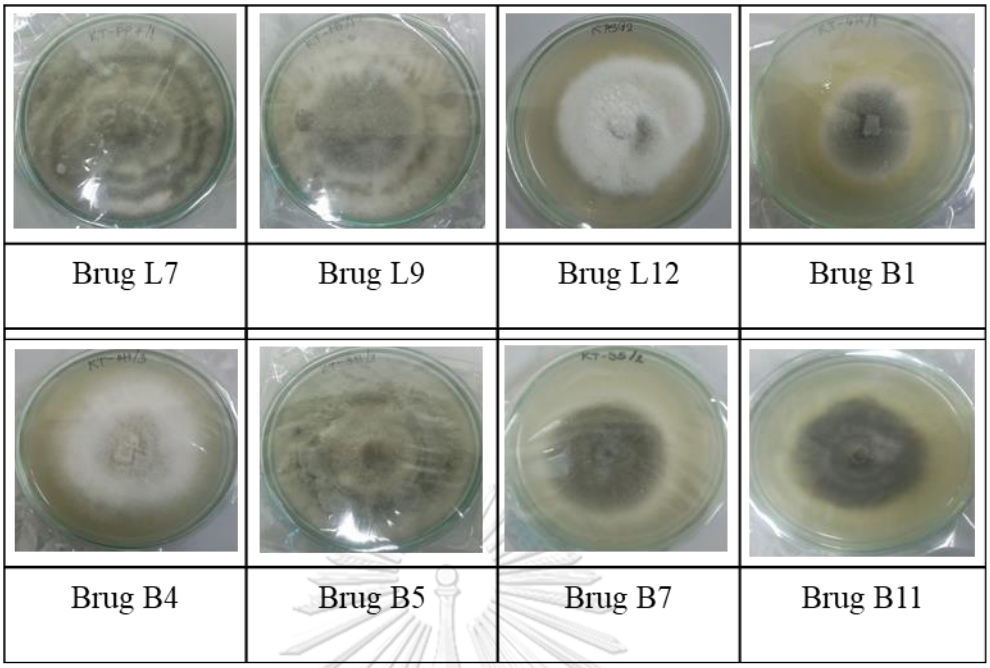

Fig. 3.20 Isolated endophytic fungi from *Bruguiera gymnorrhiza*

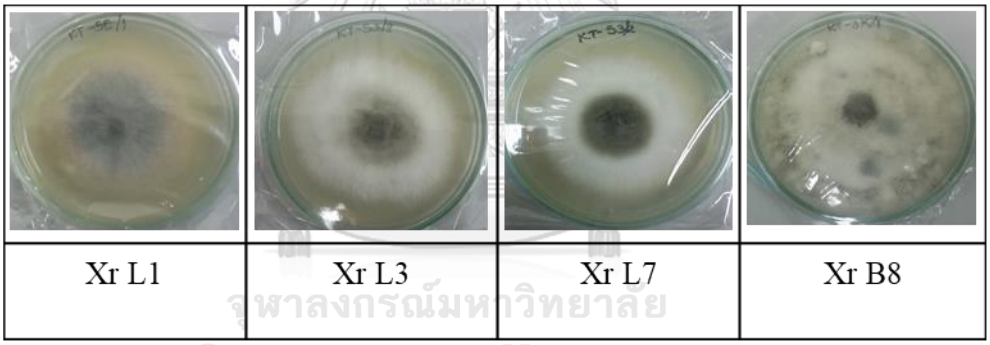

Fig. 3.21 Isolated endophytic fungi from *Xylocarpus rumphii*

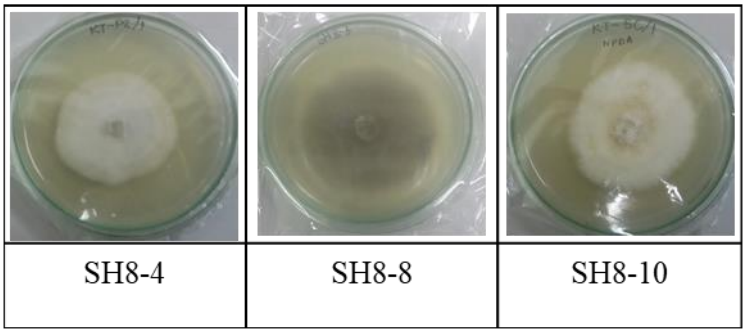

Fig. 3.22 Isolated endophytic fungi from *Ipomoea pes-caprae*

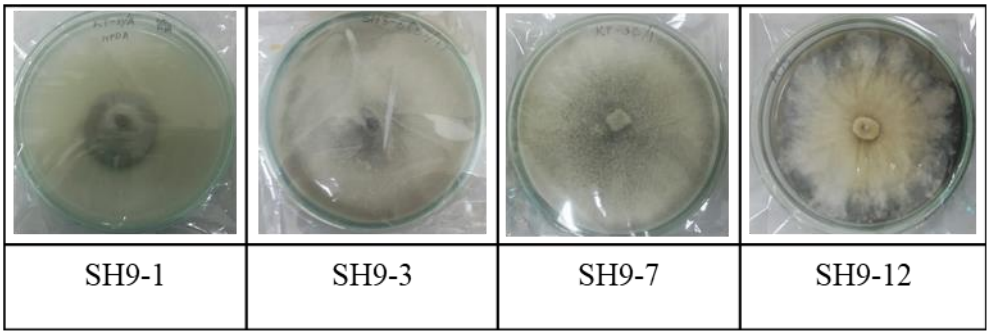

Fig. 3.23 Isolated endophytic fungi from *Excoecaria agallocha*

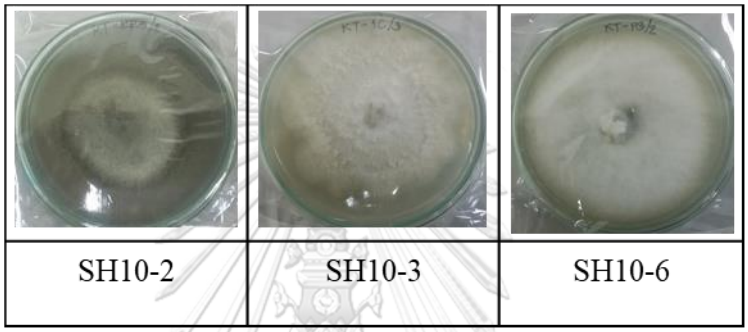

Fig. 3.24 Isolated endophytic fungi from Unknow A

Fig. 3.25 Isolated endophytic fungi from Unknow B

3.5.2 Selected mangrove-derived endophytic fungus

Generally, type of culture media affects metabolite production of each fungus [84]. This present investigation, cultivation of each isolated endophyte on four types of media, including potato dextrose broth (PDB), natural potato dextrose broth (NPDB), yeast extract sucrose broth (YEB) and sabouraud's dextrose broth (SDB) were carried out. After 21 days fermentation, followed by extraction according to **Scheme 3.1**, the EtOAc crude extract (broth) of each fungal strain cultured on each medium was

subjected to the analysis by ^{1}H NMR spectroscopy. Consequently, fungal strain SH8-8 grown on SDB, was selected to cultivate in large scale (10 L) for isolating bioactive metabolites in the further step, due to the signals of various functionalities including aromatic (6-8 ppm), olefinic (5-6 ppm) and oxygenated (3-4 ppm) protons as shown in **Fig. 3.26**.

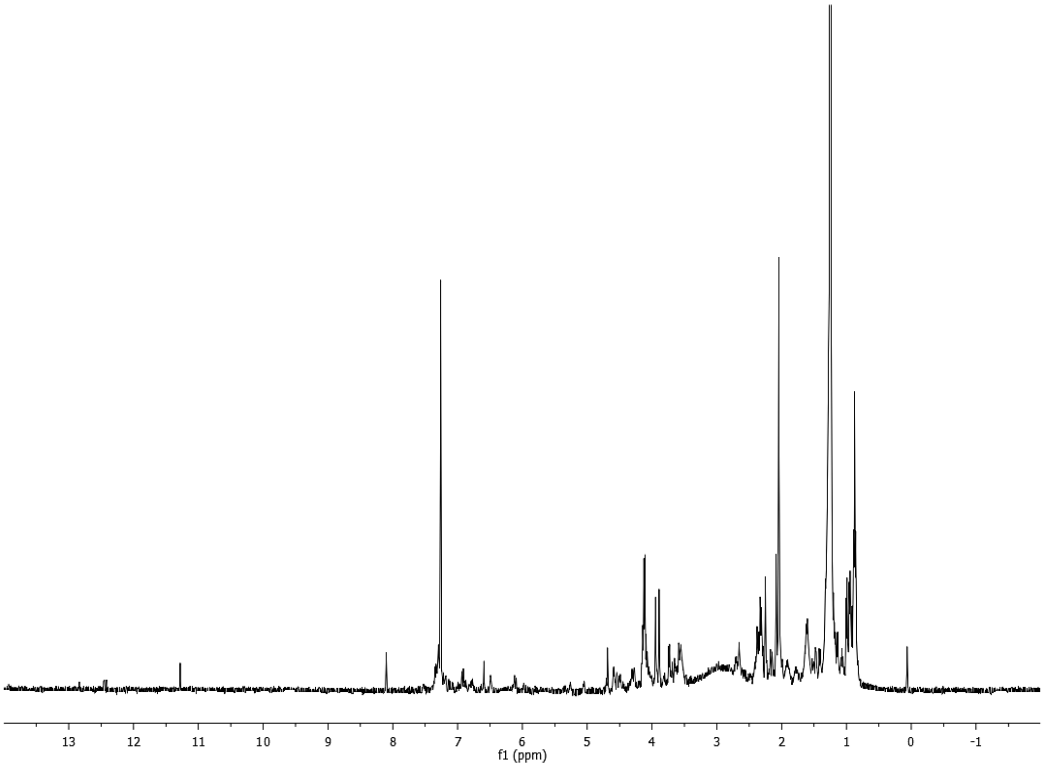

Fig. 3.26 ^{1}H NMR spectrum of EtOAc extract (broth) of fungus SH8-8 grown on PDA

3.5.3 Classification of the endophytic fungal isolate SH8-8

3.5.3.1 Conventional method

The endophyte fungal isolate SH8-8 grew on PDA as dark gray filamentous colonies, as shown **Fig. 3.27**. SH8-8 produced mature conidia with a distinct protruding hilum. The conidia are either straight, curved or bent and the septum above the hilum is thickened and dark. The walls are typically roughened and brown to olive in colour and there are typically 7-9 septa, however, some have 4-14. These are the characteristic of *Setosphaeria rostrata* [89].

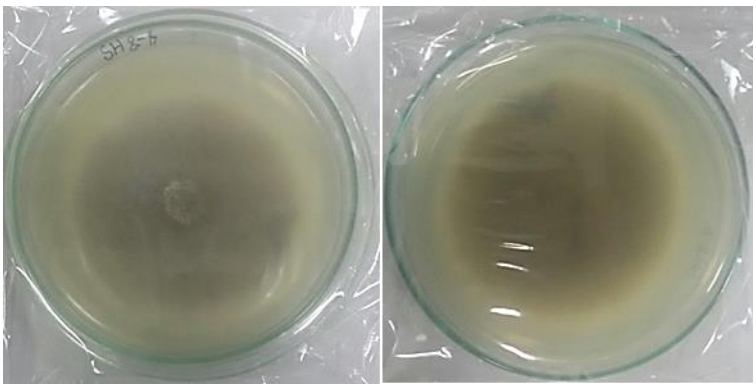

Fig. 3.27 Colony morphology of endophytic fungus isolate SH8-8 on PDA.

Obverse Reverse

3.5.3.2 Molecular method

The isolate was identified by using molecular analyses based on the partial sequence; the ribosomal internal transcribed spacer region (ITS1-5.8S-ITS2) using universal fungal primers ITS1-ITS4 [88]. Based on on-line BLAST alignment in GenBank database (http://www.ncbi.nlm.nih.gov/), it's ITS sequences (519 base pairs) (**Fig. 3.28**) matched 100% identity with six strains of *Setosphaeria rostrata*, which are MH302508, MH290745, MH201155, MH201151, MH107245 and KT933712. Thus, the fungus SH8-8 was then identified as *Setosphaeria rostrata*, as a fungal member in Family Pleosporaceae.

```
            ....|....| ....|....| ....|....| ....|....| ....|....| ....|....|
                5         15         25         35         45         55
P-01_ITS1   AGACAAAACA CATGTATTTT TGCGCACTTA TTTGTTTTCC TGGGCGAGTT ACGCTCGCCA

            ....|....| ....|....| ....|....| ....|....| ....|....| ....|....|
               65         75         85         95        105        115
P-01_ITS1   CCAGGACCCA ACCATAAACC TTTTTTTTAT GCAGTTGCAA TCAGCGTCAG TATAATAATT

            ....|....| ....|....| ....|....| ....|....| ....|....| ....|....|
              125        135        145        155        165        175
P-01_ITS1   CAATTTATTA AAACTTTCAA CAACGGATCT CTTGGTTCTG GCATCGATGA AGAACGCAGC

            ....|....| ....|....| ....|....| ....|....| ....|....| ....|....|
              185        195        205        215        225        235
P-01_ITS1   GAAATGCGAT ACGTAGTGTG AATTGCAGAA TTCAGTGAAT CATCGAATCT TTGAACGCAC

            ....|....| ....|....| ....|....| ....|....| ....|....| ....|....|
              245        255        265        275        285        295
P-01_ITS1   ATTGCGCCCT TTGGTATTCC AAAGGGCATG CCTGTTCGAG CGTCATTTGT ACCCCTCAAG

            ....|....| ....|....| ....|....| ....|....| ....|....| ....|....|
              305        315        325        335        345        355
P-01_ITS1   CTTTGCTTGG GTGTTGGGCG TCCTTTTTGT CTCTCCCCTT GTTGGGGGAG ACTCGCCTTA

            ....|....| ....|....| ....|....| ....|....| ....|....| ....|....|
              365        375        385        395        405        415
P-01_ITS1   AAACGATTGG CAGCCGACCT ACTGGTTTTC GGAGCGCAGC ACAAATTTGC GCCTTCCAAT

            ....|....| ....|....| ....|....| ....|....| ....|....| ....|....|
              425        435        445        455        465        475
P-01_ITS1   CCACGGGGCG GCATCCAGCA AGCCTTTGTT TTCTATAACA AATCCACATT TTGACCTCGG

            ....|....| ....|....| ....|....| ....|....
              485        495        505        515
P-01_ITS1   ATCAGGTAGG GATACCCGCT GAACTTAAGC ATATCATAA
```


Fig. 3.28 Nucleotide sequences of 18S (partial), ITS1-5.8S-ITS2 (complete) and 28S (partial) ribosomal RNA genes of endophytic fungi isolate SH8-8

```
Alignment: C:\Users\Desktop\Setosphaeria rostrata.txt

             ....|....| ....|....| ....|....| ....|....| ....|....| ....|....|
                 5         15         25         35         45         55
P-01_ITS1    AGACAAAACA CATGTATTTT TGCGCACTTA TTTGTTTTCC TGGGCGAGTT ACGCTCGCCA

             ....|....| ....|....| ....|....| ....|....| ....|....| ....|....|
                65         75         85         95        105        115
P-01_ITS1    CCAGGACCCA ACCATAAACC TTTTTTTTAT GCAGTTGCAA TCAGCGTCAG TATAATAATT

             ....|....| ....|....| ....|....| ....|....| ....|....| ....|....|
               125        135        145        155        165        175
P-01_ITS1    CAATTTATTA AAACTTTCAA CAACGGATCT CTTGGTTCTG GCATCGATGA AGAACGCAGC

             ....|....| ....|....| ....|....| ....|....| ....|....| ....|....|
               185        195        205        215        225        235
P-01_ITS1    GAAATGCGAT ACGTAGTGTG AATTGCAGAA TTCAGTGAAT CATCGAATCT TTGAACGCAC

             ....|....| ....|....| ....|....| ....|....| ....|....| ....|....|
               245        255        265        275        285        295
P-01_ITS1    ATTGCGCCCT TTGGTATTCC AAAGGGCATG CCTGTTCGAG CGTCATTTGT ACCCCTCAAG

             ....|....| ....|....| ....|....| ....|....| ....|....| ....|....|
               305        315        325        335        345        355
P-01_ITS1    CTTTGCTTGG GTGTTGGGCG TCCTTTTTGT CTCTCCCCTT GTTGGGGGAG ACTCGCCTTA

             ....|....| ....|....| ....|....| ....|....| ....|....| ....|....|
               365        375        385        395        405        415
P-01_ITS1    AAACGATTGG CAGCCGACCT ACTGGTTTTC GGAGCGCAGC ACAAATTTGC GCCTTCCAAT

             ....|....| ....|....| ....|....| ....|....| ....|....| ....|....|
               425        435        445        455        465        475
P-01_ITS1    CCACGGGGCG GCATCCAGCA AGCCTTTGTT TTCTATAACA AATCCACATT TTGACCTCGG

             ....|....| ....|....| ....|....| ....|....
               485        495        505        515
P-01_ITS1    ATCAGGTAGG GATACCCGCT GAACTTAAGC ATATCATAA
```

Fig. 3.29 Nucleotide sequences of 18S (partial), ITS1-5.8S-ITS2 (complete) and 28S (partial) ribosomal RNA genes of *Setosphaeria rostrata*

3.5.4 Structural elucidation of pure compounds

An endophytic fungus, *Setosphaeria rostrata* isolated from the mangrove plant, *Ipomoea pes-caprae* was cultured in liquid medium. The obtained EtAOc crude extract yielded five new isocoumarins, rostrarin A-E (**84-88**), together with two known fungal metabolites, ravenelin (**82**) and 1*H*-2-Benzopyran-1-one,3,4-dihydro-4,8-dihydroxy-3-[(2*R*)-2-hydroxypentyl]-6,7-dimethoxy-,(3*R*,4*R*)- (**83**). The structures of isolated compounds are shown in **Fig. 3.30**.

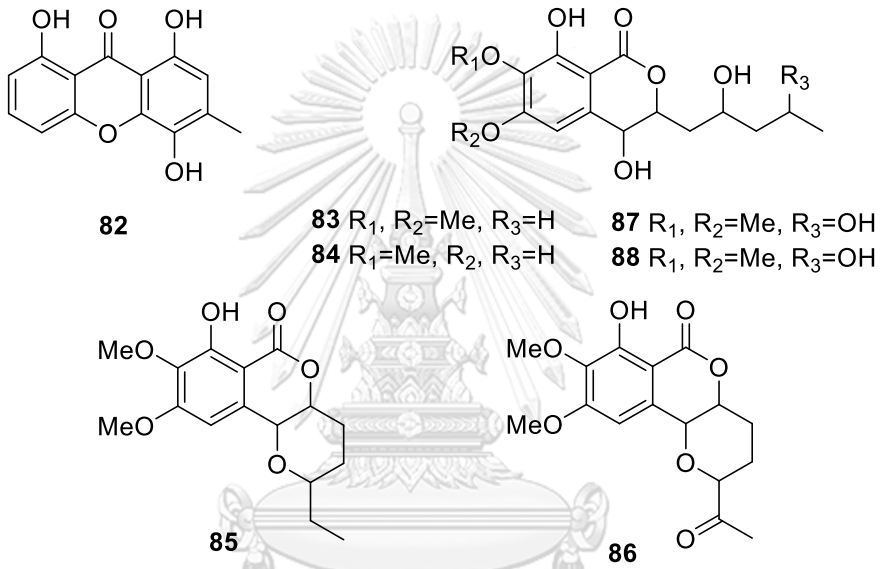

Fig. 3.30 Structures of compounds from the fungus isolate SH8-8

3.5.4.1 Structural elucidation of compound 82

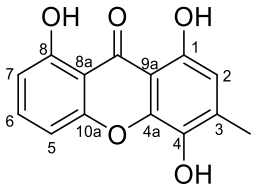

Fig. 3.31 Compound **82** (ravenelin)

Compound **82,** obtained as yellow powder, was assigned a molecular formula of $C_{14}H_{10}O_5$ was determined from the NMR spectral data, indicating 10 degrees of unsaturation. The ^{1}H NMR data (**Table 3.2)** showed two signals at δ_H 10.95 (s) and 11.82 (s) indicated the presence of chelated hydroxyl proton. Besides, four aromatic proton signals and a methyl group. The ^{13}C NMR spectrum of **82** revealed a resonance

at δ_C 185.1; C-9, which was assigned to carbonyl carbon. Additionally, the presence of seven carbon signals were assigned to quaternary carbons (five oxygenated at δ_C 151.6; C-1, 136.9; C-4, 143.6; C-4a, 160.3; C-8 and 155.6; C-10a), together with four aromatic carbons (111.1; C-2, 107.3; C-5, 137.7; C-6 and 110.3; C-7) and a methyl carbon (δ_C 16.9). Both the ^{1}H NMR and^{13}C NMR spectral data were in agreement with the proposed structure ravenelin [90].

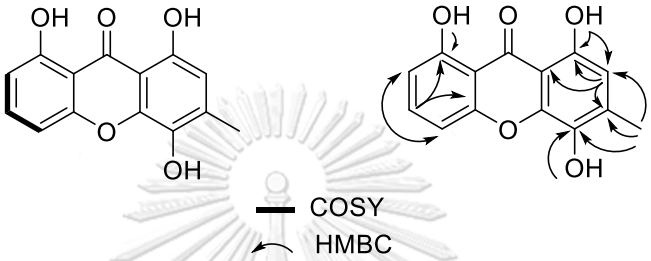

Fig. 3.32 Key COSY and HMBC correlations of compound **82**

3.5.4.2 Structural elucidation of compound 83

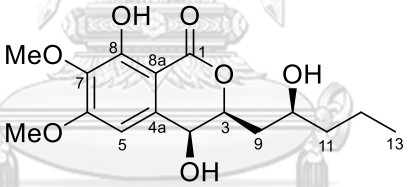

Fig. 3.33 Compound **83**

Compound **83,** obtained as a colorless oil, $[\alpha]^{20}_D$ +26.8 (c 0.1, MeOH), was assigned a molecular formula of $C_{16}H_{22}O_7$ on the basis of NMR data. The ^{1}H NMR data (**Table 3.2)** showed typical signals of chelated hydroxy at δ_H 11.28 (s); OH-8, an aromatic ring hydrogen at δ_H 6.59 (s), three oxygenated methines proton [δ_H 5.05 (dd, J = 2.8, 5.6 Hz), 4.54 (d, J = 2.8 Hz), 4.11 (m)], together with two methoxyl groups [δ_H 3.95 (s), 3.89 (s); δ_C 56.6, 60.9]. Combined analysis of ^{13}C NMR (**Table 3.3)** and HSQC signal revealed the presence of one carbonyl ester conjugate (δ_C 167.9; C-1) chelated by hydrogen bond with hydroxyl and six aromatic carbons (three oxygenated at δ_C 158.9; C-6, 137.5; C-7 and 156.3; C-8, one unreplaced at δ_C 104.6; C-5), three oxygenated methines carbon (δ_C 81.3; C-3, 74.6; C-4, 78.8; C-10) , three methylene (δ_C 39.2; C-9, 38.2; C-11 and 19.3; C-12) and one methyl (δ_C 14.0; C-13). The structure was further confirmed by the ^{1}H-^{1}H COSY correlations from H-4 to H_3-13, and by the

HMBC correlations of H-3 to C-4; H-4 to C-8a; H-5 to C-4, C-6, C-7 and C-8a; H-9 to C3, C-4 and C-10; H-11 to C-10; H-13 to C-11 and C12. Two methoxyl groups were located on C-6 and C-7 based on HMBC correlations from those methoxyl protons to C-6 and C-7 (**Fig. 3.33**). Comparison of the optical rotation and its NMR spectroscopic data with those in the literature indicated that compound **83** is isocoumarin derivative [91] namely 1*H*-2-Benzopyran-1-one,3,4-dihydro-4,8-dihydroxy-3-[(2*R*)-2-hydroxypentyl]-6,7-dimethoxy-,(3*R*, 4*R*)-.

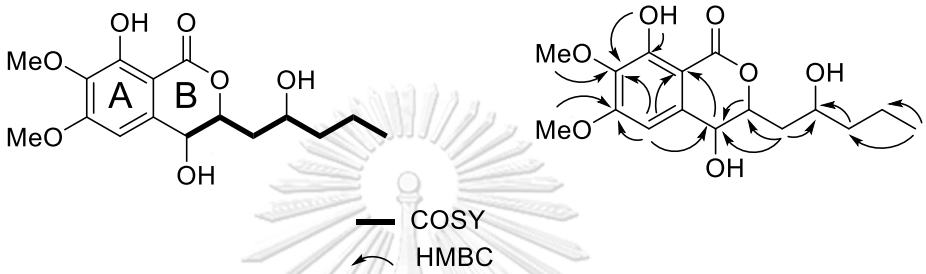

Fig. 3.34 Key COSY and HMBC correlations of compound **83**

3.5.4.3 Structural elucidation of compound 84

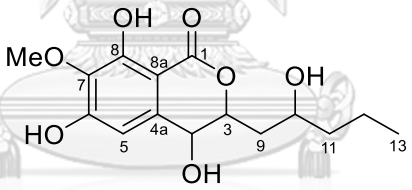

Fig. 3.35 Compound **84** (rostrarin A)

Compound **84**, obtained as a colorless oil, $[\alpha]^{20}_{D}$ +64.40 (c 0.1, MeOH), was assigned a molecular formula of $C_{15}H_{20}O_7$. Based on the analysis of 1D (**Tables 3.2** and **3.3**) and 2D NMR spectroscopic data, compound **84** were very similar to those of compound **83**. The ^{1}H NMR spectra differences between **83** and **84** were the absence of methoxyl group signal at δ_H 3.95 (s) in compound **83**, and the appearance of a hydroxyl group signal at δ_H 6.47 (brs) in compound **84** as shown in **Fig. 3.36**. It suggested that a methoxyl group of **83** was replaced by a hydroxyl group in **84**, which was further confirmed by HMBC correlations from a methoxyl proton to C-6. Therefore, the structure of **84** was identified as shown ad a new compound, namely rostrarin A.

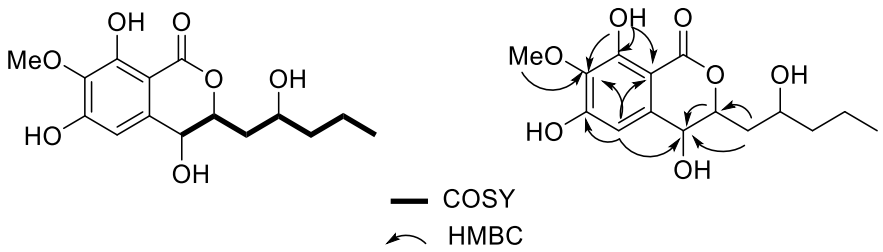

Fig. 3.36 Key COSY and HMBC correlations of compound **84**

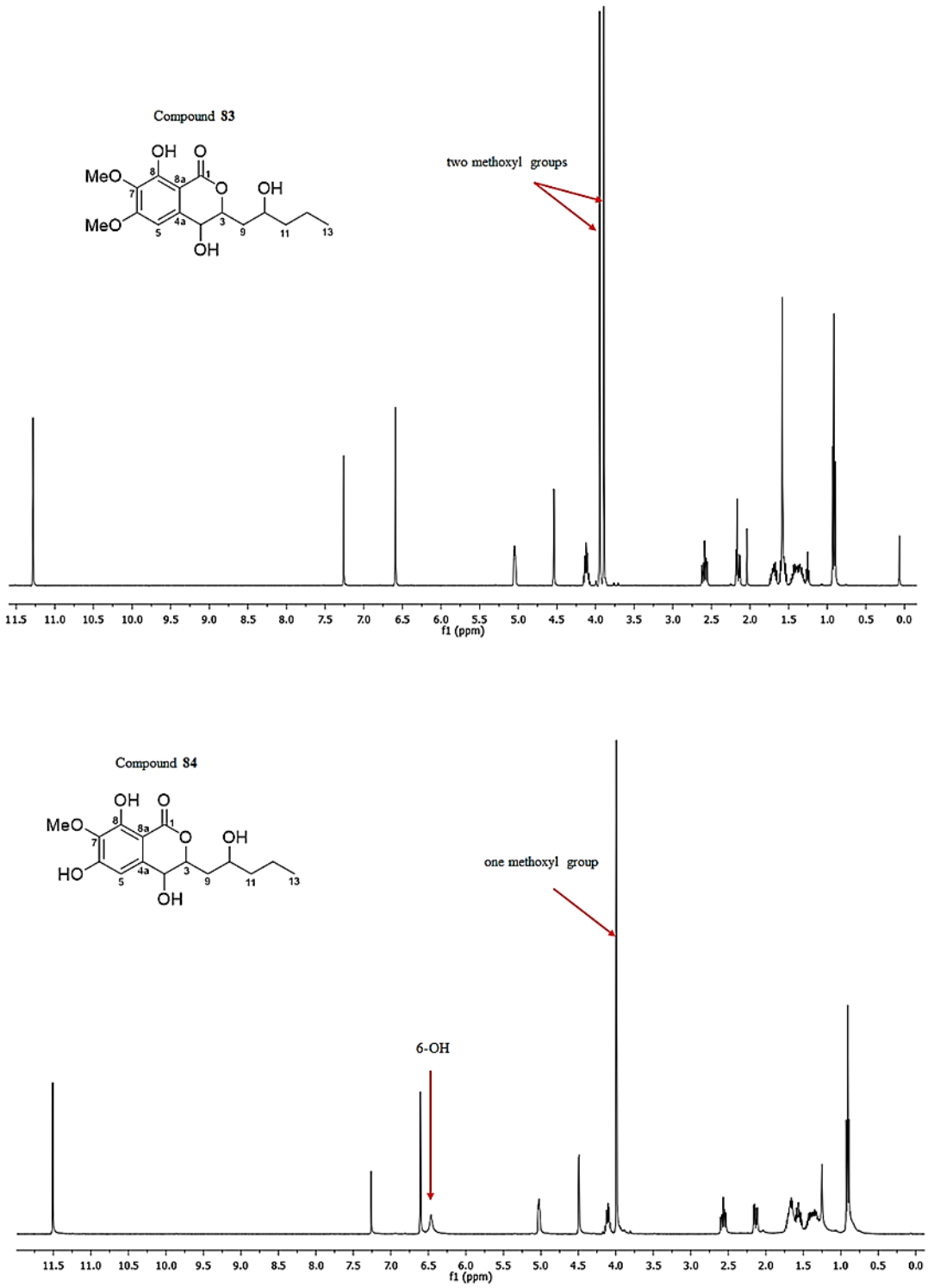

Fig. 3.37 Comparison of ^{1}H NMR spectra of compound **83** and **84** in $CDCl_3$

Table 3.2 ^{1}H NMR data of compounds **82**, **83** and **84**

position	δ_H mult, (*J* in Hz)		
	82 (DMSO-d_6)	**83** ($CDCl_3$)	**84** ($CDCl_3$)
1	-	-	-
2	6.65 s	-	-
3	-	5.05 dd, (2.8, 5.6)	5.01 dd, (2.8, 5.6)
4	-	4.54 d, (2.8)	4.48 d, (2.8)
4a	-	-	-
5	7.06 d, (8.4)	6.59 s	6.59 s
6	7.74 t, (8.0)	-	-
7	6.81 d, (8.0)	-	-
8	-	-	-
8a	-	-	-
9	-	2.10 m	2.11 dd, (8.4, 15.2)
		2.50 m	2.55 m
9a	-	-	-
10	-	4.11 m	4.09 m
10a	-	-	-
11	-	1.54 m	1.55 m
		1.57 m	1.65 m
12	-	1.40 m	1.33 m
		1.47 m	1.35 m
13	-	0.92 t, (7.2)	0.89 t, (7.6)
3-Me	2.30 s	-	-
6-OMe	-	3.95 s	-
7-OMe	-	3.89 s	3.98 s
1-OH	10.95 s	-	-
4-OH	9.15 s	4.53 s	4.51 dd, (4.0)
6-OH	-	-	6.47 brs
8-OH	11.82 s	11.30 s	11.49 s
10-OH	-	4.12 m	4.13 m

Table 3.3 ^{13}C NMR data of compounds **82**, **83** and **84**

position	δ_c ppm		
	82 (DMSO-d_6)	**83**($CDCl_3$)	**84** ($CDCl_3$)
1	151.6	167.9	168.2
2	111.1	-	-
3	134.9	81.3	81.3
4	136.9	74.6	74.2
4a	143.6	131.2	131.4
5	107.3	104.6	107.9
6	137.7	158.9	155.2
7	110.3	137.5	134.8
8	160.3	156.5	155.4
8a	107.1	102.1	101.3
9	185.1	39.2	39.1
9a	105.8	-	-
10	-	78.8	78.6
10a	155.6	-	-
11	-	38.2	38.1
12	-	19.3	19.1
13	-	14.0	14.1
3-Me	16.9	-	-
6-OMe	-	56.6	-
7-OMe	-	60.9	60.8

3.5.4.4 Structural elucidation of compound 85

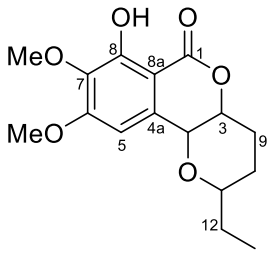

Fig. 3.38 Compound **85** (rostrarin B)

Compound **85,** obtained as white powder, $[\alpha]^{20}_{D}$ -10.32 (c 0.1, MeOH), was assigned a molecular formula of $C_{16}H_{20}O_6$ (seven degrees of unsaturation) on the basis of NMR data. The IR spectrum of compound **85** indicated the presence of hydroxyl (3494 cm^{-1}) and ester carbonyl (1736 cm^{-1}). The ^{1}H NMR (**Table 3.4**) spectral data of **85** showing a chelated proton, three oxygenated methine protons and two methoxyl groups, were similar to **83**, indicated that rings A and B of the two compounds were identical. This was confirmed by the ^{13}C NMR (**Table 3.5**) signals of **85** relating to rings A and B, agreed with the corresponding values for **83**. Unsaturation requirement of **85**, however, C-4 and C-11 attached to the remaining oxygen atom to be the fused pyran ring (ring C). In addition to the mentioned fragment, the ^{1}H-^{1}H COSY data of **85** showed correlation from H-4 to H_3-13, while two methoxyl proton groups of this compound were located on C-6 and C-7 according to HMBC correlations (**Fig. 3.38**). As a result, compound **85** was assigned to be rostrarin B.

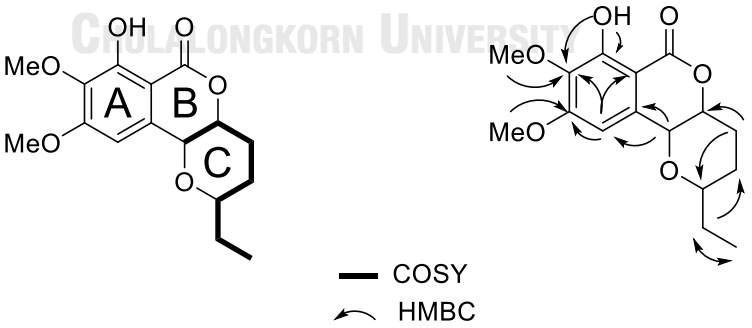

Fig. 3.39 Key COSY and HMBC correlations of compound **85**

3.5.4.5 Structural elucidation of compound 86

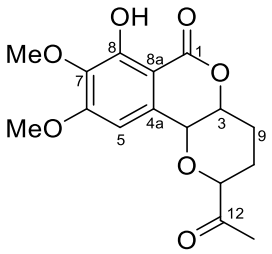

Fig. 3.40 Compound **86** (rostrarin C)

Compound **86** obtained as amorphous, $[\alpha]^{20}_{D}$ +44.4 (c 0.1, MeOH), and its molecular formula of $C_{14}H_{14}O_7$ was determined from the NMR spectral data, indicating 8 degrees of unsaturation. Comparison of ^{13}C NMR spectroscopic data (**Tables 3.4** and **3.5**) between C-12 of **85** and **86**, methylene carbon (δ_C 18.6) of **85** was substituted by carbonyl carbon (δ_C 206.2). This was confirmed by HMBC (**Fig. 3.40**) correlations of H_2-10 to C-12 and H_3-13 to C-12. Moreover, the complete structure of compound **86** was confirmed by ^1H-^1H COSY correlation between H-3/H_2-9 and H_2-10/H-11. Thus, compound **86** was assigned to be rostrarin C.

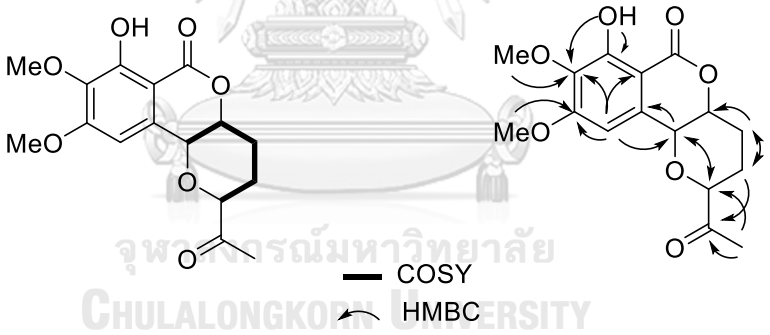

Fig. 3.41 Key COSY and HMBC correlations of compound **86**

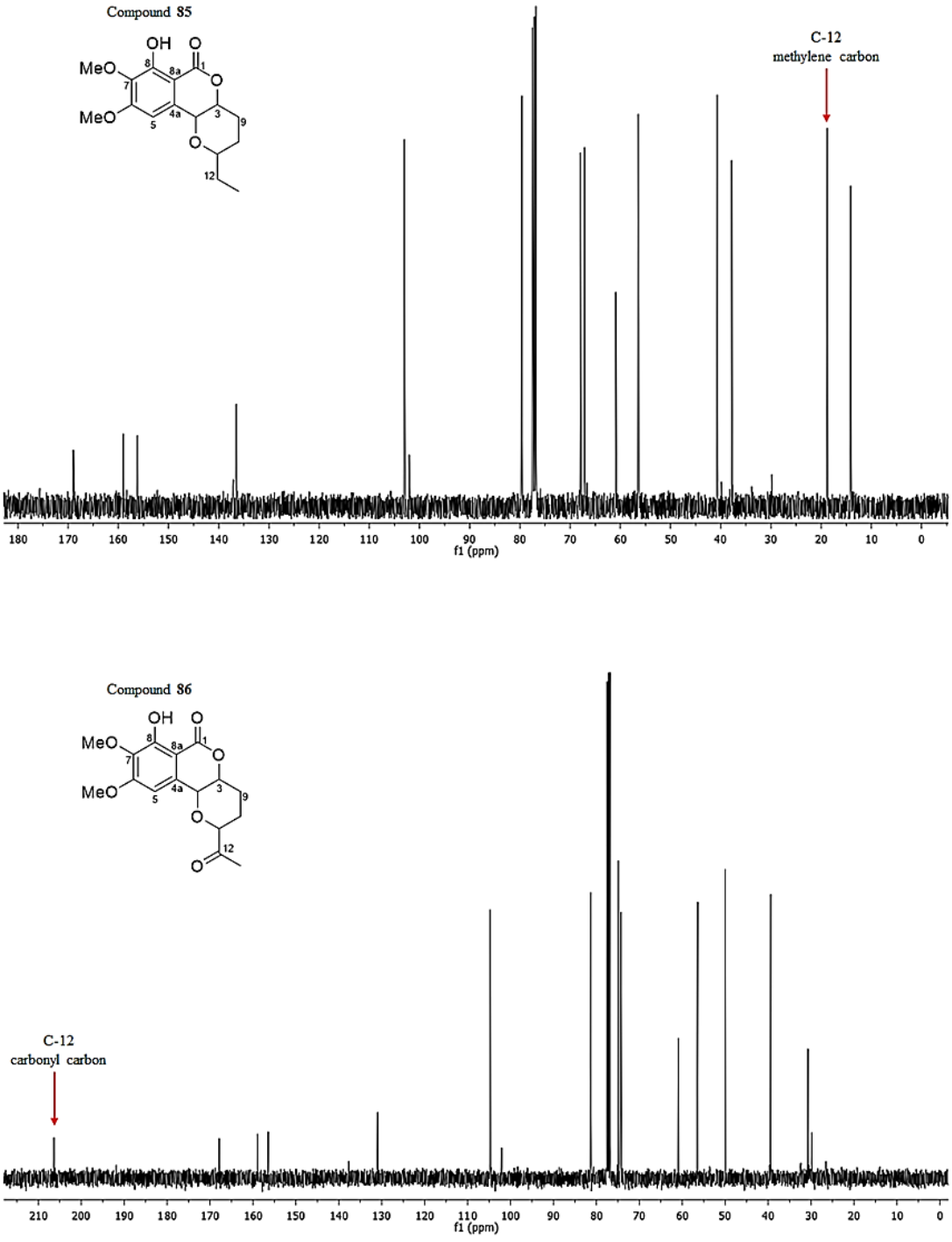

Fig. 3.42 Comparison of ^{13}C NMR spectra of compound **85** and **86** in $CDCl_3$

3.5.4.6 Structural elucidation of compound 87

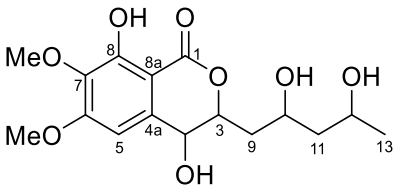

Fig. 3.43 Compound **87** (rostrarin D)

Compound **87**, obtained as a colorless oil, and its molecular formula was assigned as $C_{16}H_{22}O_8$ on the basis of 1D (**Tables 3.4** and **3.5**) and 2D NMR data. The spectroscopic data of compound **87** were similar to those of **83**, however, **87** also exhibited typical signal for a hydroxyl group at δ_H 3.98, It suggested that the CH_2-12 of **83** was replaced by the CH-OH in **87**, but the ^1H-^1H COSY correlations from H-4 to H_3-13 were remained. Moreover, two methoxyl proton groups of **87** still existed at C-6 and C-7. Therefore compound **87** was identified as rostrarin D.

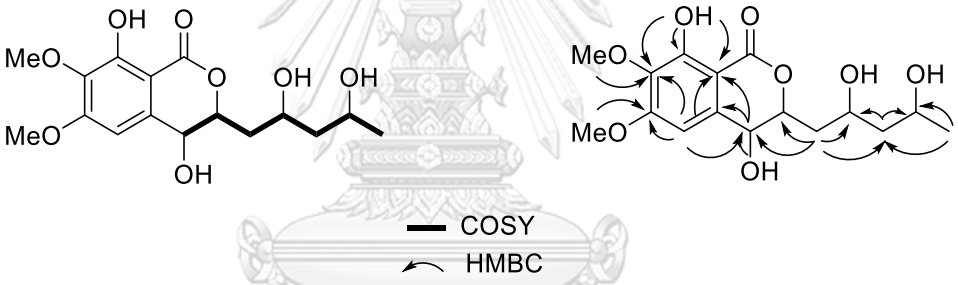

Fig. 3.44 Key COSY and HMBC correlations of compound **87**

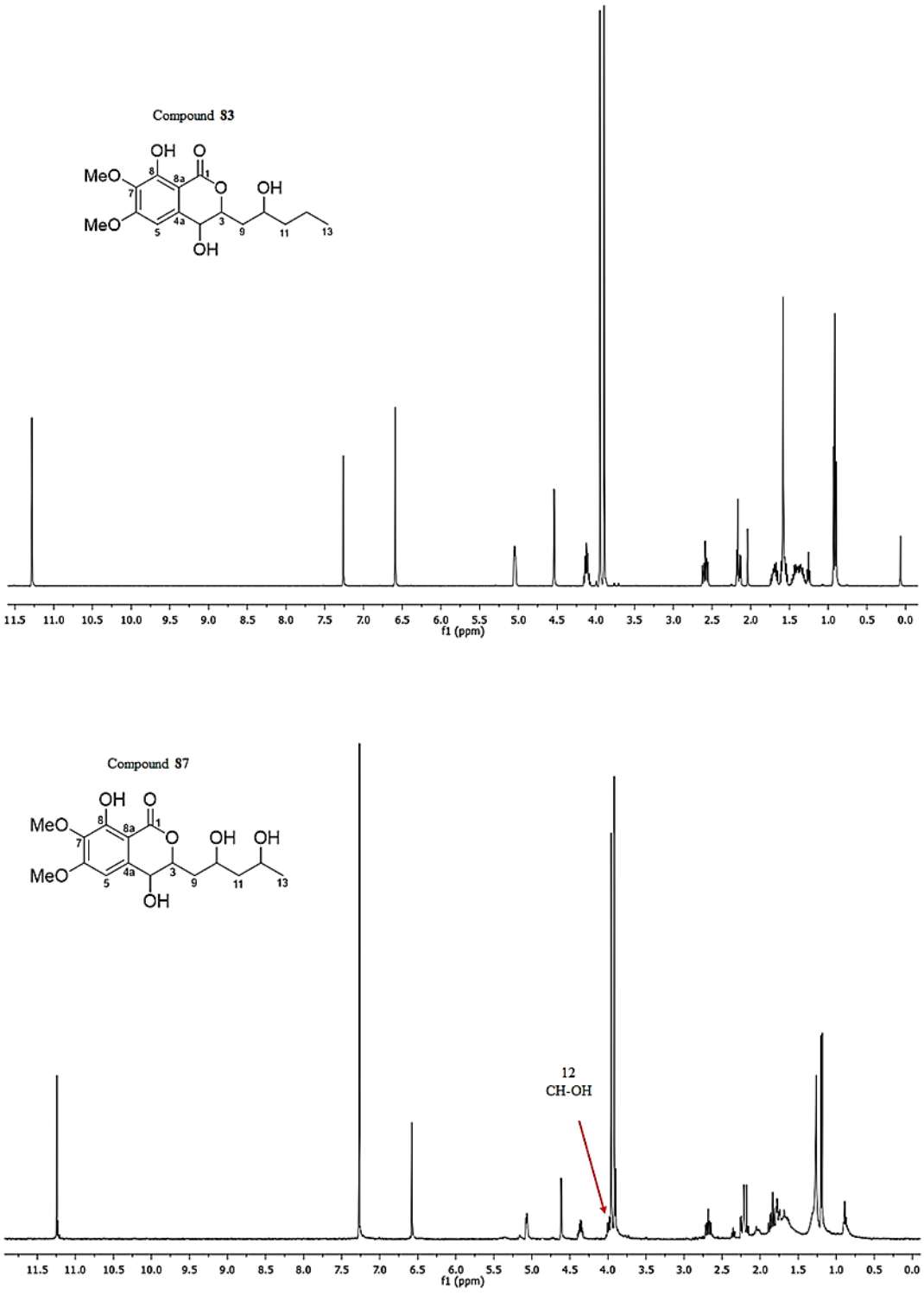

Fig. 3.45 Comparison of ^{1}H NMR spectra of compound **83** and **87** in $CDCl_3$

3.5.4.7 Structural elucidation of compound 88

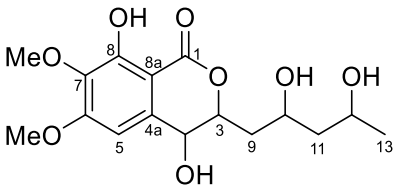

Fig. 3.46 Compound **88** (rostrarin E)

Compound **88**, obtained as a colorless oil, $[\alpha]^{20}_{D}$ -247.2 (c 0.1, MeOH), had the same molecular formula with **87**, as summarized from NMR data. Furthermore, investigation of 1D (**Tables 3.4** and **3.5**) and 2D NMR spectrum data exposed both **87** and **88** had an identical overall structure. However, the ^{13}C NMR, C-10 signal of **87** was at δ_C 78.4, and of **88** was shifted to δ_C 75.9. This suggested there was a chemical stereochemistry difference. Compound **88** was assigned to be rostrarin E.

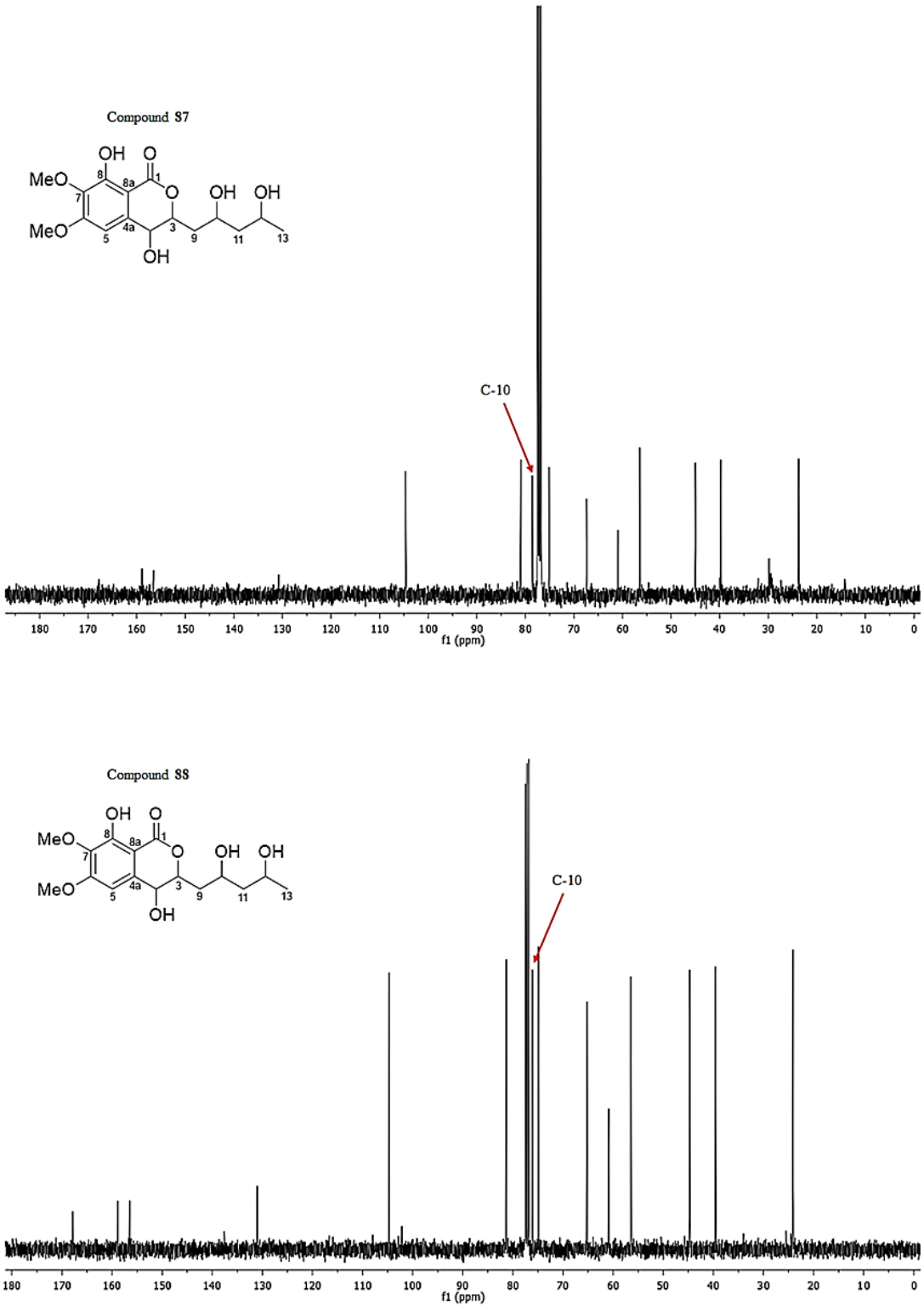

Fig. 3.47 Comparison of ^{13}C NMR spectra of compound **87** and **88** in $CDCl_3$

Table 3.4 ^{1}H NMR data of compounds **85**, **86**, **87** and **88**

position	δ_H mult, (*J* in Hz)			
	85 ($CDCl_3$)	**86** ($CDCl_3$)	**87** ($CDCl_3$)	**88** ($CDCl_3$)
1	-	-	-	-
2	-	-	-	-
3	4.74 m	4.58 s	5.06 m	5.04 m
4	4.66 d, (2.0)	4.57 s	4.61 d, (3.2)	4.54 d, (2.8)
4a	-	-	-	-
5	6.56 s	6.57 s	6.57 s	6.56 s
6	-	-	-	-
7	-	-	-	-
8	-	-	-	-
8a	-	-	-	-
9	1.87 m	2.74 m	2.20 m	2.18 m
	2.17 m	2.97 dd, (6.4, 18.0)	2.67 m	2.64 m
10	1.53 m	2.18 d, (4.8)	4.35 m	4.39 m
		2.74 m		
11	3.89 s	5.05 dd, (2.8, 5.2)	1.68 m	1.71m
			1.77 m	1.84 m
12	1.40 m	-	3.99 m	3.99 m
13	0.96 t, (8.0)	2.14 s	1.19 d, (8.0)	1.19 d, (6.0)
6-OMe	3.94 s	3.94	3.95 s	3.93 s
7-OMe	3.89 s	3.89	3.91 s	3.88 s
4-OH	-	-	4.60 m	4.56 d, (3.2)
8-OH	11.07 s	11.20 s	11.23 s	11.23 s
10-OH	-	-	4.36 m	4.39 m
12-OH	-	-	3.98 m	4.03 m

Table 3.5 ^{13}C NMR data of compounds **85**, **86**, **87** and **88**

position	δ_C ppm			
	85 ($CDCl_3$)	**86** ($CDCl_3$)	**87** ($CDCl_3$)	**88** ($CDCl_3$)
1	168.8	167.7	167.8	167.7
2	-	-	-	-
3	79.4	74.2	80.8	81.2
4	66.9	74.7	75.0	74.7
4a	136.4	130.8	130.7	130.9
5	102.8	104.6	104.5	104.5
6	158.8	158.8	158.7	158.7
7	137.0	137.5	137.9	137.5
8	156.1	156.3	156.3	156.3
8a	101.9	101.4	102.3	102.0
9	37.7	49.8	39.6	39.5
10	40.5	39.2	78.4	75.9
11	67.8	81.2	44.9	44.6
12	18.6	206.2	67.2	65.0
13	13.9	30.6	23.6	23.9
6-OMe	56.3	56.3	56.3	56.3
7-OMe	60.7	60.7	60.7	60.7

3.5.4 Biological activities of isolated compounds from endophytic fungus

The endophytic isolated compounds 1*H*-2-Benzopyran-1-one,3,4-dihydro-4,8-dihydroxy-3-[(2*R*)-2-hydroxypentyl]-6,7-dimethoxy-,(3*R*,4*R*)- (**83)** and rostrarin B (**85**) were subjected to biological activities including anti-cancer, anti-inflammatory activities, together with α-glucosidase inhibitory activity. Unfortunately, all of them did not show any significant activity (**Tables 3.6** to **3.8**). According to Li and coworkers (2016) [92], isocumarin had the strong ani-fungal activity against *Colletotrichum musae* and *Rhizoctonia solani* with IC_{50} 6.25 μg/mL, the obtained isocoumarin from this study would express other bioactivites.

Table 3.6 Cytotoxic activity of pure compounds on Hep-G2, KATO-3, MCF-7 and CaSKi cell lines

Compound	IC_{50} (μM)			
Cell line	Hep-G2	KATO-3	MCF-7	CaSKi
ravenelin (**82**)	ND	ND	ND	ND
1*H*-2-Benzopyran-1-one,3,4-dihydro-4,8-dihydroxy-3-[(2*R*)-2-hydroxypentyl]-6,7-dimethoxy-,(3*R*,4*R*)- (**83**)	I	I	I	I
rostrarin A (**84**)	ND	ND	ND	ND
rostrarin B (**85**)	I	I	I	I
rostrarin C (**86**)	ND	ND	ND	ND
rostrarin D (**87**)	ND	ND	ND	ND
rostrarin E (**88**)	ND	ND	ND	ND
Doxorubicin (positive)	0.91	0.98	0.06	0.20

I = Inactive

ND=not determined

Table 3.7 anti-inflammatory activity of pure compounds on J774.A1 cell line

Compound	IC_{50} (μM)
ravenelin (**82**)	ND
1*H*-2-Benzopyran-1-one,3,4-dihydro-4,8-dihydroxy-3-[(2*R*)-2-hydroxypentyl]-6,7-dimethoxy-,(3*R*,4*R*)- (**83**)	I
rostrarin A (**84**)	ND
rostrarin B (**85**)	I
rostrarin C (**86**)	ND
rostrarin D (**87**)	ND
rostrarin E (**88**)	ND
Indomethacin (positive)	28.4

I = Inactive

ND=not determined

Table 3.8 α-Glucosidase inhibitory activity of pure compounds

Compound	IC_{50} (μM)	
Enzyme	Sucrase	Maltase
ravenelin (**82**)	ND	ND
1*H*-2-Benzopyran-1-one,3,4-dihydro-4,8-dihydroxy-3-[(2*R*)-2-hydroxypentyl]-6,7-dimethoxy-,(3*R*,4*R*)- (**83)**	I	I
rostrarin A (**84**)	ND	ND
rostrarin B (**85**)	I	I
rostrarin C (**86**)	ND	ND
rostrarin D (**87**)	ND	ND
rostrarin E (**88**)	ND	ND
Acarbose (positive)	2.3	1.5

I = Inactive

ND=not determined

CHAPTER IV
CONCLUSION

This research was aimed to investigate bioactive compounds from the plant *Tinospora baenzigeri* Forman collecting from different areas, and from mangrove-derived endophytic fungi isolated from trees inhabiting Songkhla province for anti-cancer activities against four human cancer cell lines including hepato carcinoma (Hep-G2), gastric carcinoma (KATO-3), breast carcinoma (MCF-7) and cervix carcinoma (CaSki) cell lines; anti-inflammatory on macrophage cell (J774.A1); and α-glucosidase inhibitory activity.

A total of 18 isolated compounds of *T. baenzigeri* were obtained from 2 different areas. Eleven compounds were extracted from plant obtained from local market in Bangkok, including five new: rearranged clerodane diterpenes, namely tinobaenzins A-D (**66**-**69**) and tinobaenzin A glucoside (**70**), and one known: baenzigeroside B (**61**) rearranged clerodane diterpenes, as well as two lignans: caruilignan D (**71**), lariciresinol (**72**), one sesquiterpene: aglycone of breyniaionoside D (**73**) and two phenylpropanoid amides: *N-trans*-feruloyltyramine (**74**) and *N-trans*-coumaroyltyramine (**75**). Twelve compounds were obtained from plant collected in Bueng Kan Province, seven compounds including two new rearranged clerodane diterpenes: tinobaenzigerides A (**76**) and B (**77**), three flavonoids: apigenin (**44**), naringenin (**78**), eriodictyol (**79**), as well as phenylethanoid: tyrosol (**80**), together with a lignan lariciresinol acetate (**81**), while, five compounds counting **61**, **66**, **70** and **74**-**75** was also obtained from this area. The structure establishments of these compounds were based on spectroscopic techniques. Furthermore, structures of new compounds **66**-**69** and **76** were confirmed by single-crystal X-ray crystallography technique. Due to they comprise fully oxygenated tetrahydrofuran moiety, compounds **69** and **76** are rare rearranged clerodanes. Of the 18 compounds, 13 compounds were evaluated for biological activities. Tinobaenzin C (**68**) exhibited selectivity cytotoxic activity against KATO-3 cell lines with IC_{50} values of 27.08 μM, while other compounds did not affect to any of the tested cell lines. Only *N-trans*-feruloyltyramine (**74**) displayed the weak activity against **α**-glucosidase with an IC_{50} value of 0.34 mM for sucrase inhibition and

0.36 mM for maltase inhibition. However, all of the tested compounds were inactive on anti-inflammatory activities.

In addition, EtOAc crude extract from *Setosphaeria rostrata*, an endophytic fungus isolated from the mangrove plant *Ipomoea pes-caprae* and cultured in SDB, gave five new isocoumarins, rostrarin A-E (**84**-**88**), together with two known fungal metabolites, ravenelin (**82**) and 1*H*-2-Benzopyran-1-one,3,4-dihydro-4,8-dihydroxy-3-[(2*R*)-2-hydroxypentyl]-6,7-dimethoxy-,(3*R*,4*R*)- (**83**). The compounds **83** and **85** were subjected to biological activities. Unfortunately, all of them showed to be inactive.

REFERENCES

[1] Nautiyal, O.H. Natural products from plant, microbial and marine species. The Experiment 10(1) (2013): 611-646.

[2] Dias, D.A., Urban, S., and Roessner, U. A historical overview of natural products in drug discovery. Metabolites 2(2) (2012): 303-36.

[3] Chin, Y.-w., Balunas, M.J., Chai, H.B., and Kinghorn, D. Drug Discovery From Natural Sources. The AAPS Journal 8(2) (2006): 239-253.

[4] Lahlou, M. The success of natural products in drug discovery. Pharmacology and Pharmacy 4(3) (2013): 17-31.

[5] Kinghorn, A.D., Pan, L., Fletcher, J.N., and Chai, H. The relevance of higher plants in lead compound discovery programs. Journal of Natural Products 74(6) (2011): 1539-1555.

[6] Harvey, A. Strategies for discovering drugs from previously unexplored natural products. Drug Discovery Today 5(7) (2000): 294-300.

[7] Patrick, K.S. Chemistry of peptide synthesis By N. Leo Benoiton. Taylor & Francis, Boca Raton, FL. Journal of Medicinal Chemistry 49(8) (2006): 2667-2667.

[8] Mahidol, C., et al. Biodiversity and natural product drug discovery. Pure and Applied Chemistry 70 (1998): 2065-2072.

[9] Lorenzen, K. and Anke, T. Basidiomycetes as a source for new bioactive natural products. Current Organic Chemistry. 2(4) (1998): 329-364.

[10] Li, K.T., Zhou, J., Wei, S.J., and Cheng, X. An optimized industrial fermentation processes for acarbose production by *Actinoplanes* sp. A56. Bioresour Technol 118 (2012): 580-583.

[11] Tan, R.X. and Zou, W.X. Endophytes: a rich source of functinal metabolites. Natural Product Reports 18 (2001): 448-459.

[12] Strobel, G.A. Endophytes as sources of bioactive products. Microbes and Infection 5(6) (2003): 535-544.

[13] Mehbub, M.F., Perkins, M.V., Zhang, W., and Franco, C.M.M. New marine natural products from sponges (Porifera) of the order Dictyoceratida (2001 to 2012); a promising source for drug discovery, exploration and future prospects. Biotechnology Advances 34(5) (2016): 473-491.

[14] Faulkner, D.J. Marine natural products. Natural Product Reports 18(1) (2001): 1-49.

[15] Gunasekera, S.P., Gunasekera, M., and Longley, R.E. Discodermolide: a new bioactive polyhydroxylated lactone from the marine sponge *Discodermia dissoluta*. The Journal of Organic Chemistry 55(16) (1990): 4912-4915.

[16] Murti, Y. and Agrawal, T. Marine derived pharmaceuticals-development of natural health products from marine biodiversity. International Journal of ChemTech Research 2(4) (2010): 2198-2217.

[17] Ishitsuka, M.O., Kusumi, T., and Kakisawa, H. Antitumor xenicane and norxenicane lactones from the brown alga *Dictyota dichotoma*. The Journal of Organic Chemistry 53(21) (1988): 5010-5013.

[18] Faulkner, D.J. Marine natural products. Natural Product Reports 5(6) (1988): 613-663.

[19] Hogg, J.A. Drugs from Natural Products-Animal Sources. Advances in Chemistry 108 (1971): 14-32.
[20] Newman, D.J. and Cragg, G.M. Natural products as sources of new drugs from 1981 to 2014. Journal of Natural Products 79(3) (2016): 629-661.
[21] Nassar, Y.S., Laimud, M., Afify, M., and Shawky, M.A. Platelet aggregation inhibition by Eptifibatide versus high dose Tirofiban during primary percutaneous interventions. The Egyptian Heart Journal 66(3) (2014): 241-250.
[22] Feng, Y., et al. Bear bile: dilemma of traditional medicinal use and animal protection. Journal of Ethnobiology and Ethnomedicine 5(2) (2009): 1-9.
[23] Kinghorn, A.D. Principles of drug discovery. (2009): 13-28.
[24] McRae, J., Yang, Q., Crawford, R., and Palombo, E. Review of the methods used for isolating pharmaceutical lead compounds from traditional medicinal plants. The Environmentalist 27(1) (2007): 165-174.
[25] Tarver, T. The Review of Natural Products. Eighth edition, edited by Ara DerMarderosian and John A. Beutler. Journal of Consumer Health on the Internet 18(3) (2014): 291-292.
[26] Verpoorte, R. Exploration of nature's chemodiversity: the role of secondary metabolites as leads in drug development Drug Discovery Today 3(5) (1998): 232-238.
[27] Baimai, V. Biodiversity in Thailand. The Journal of the Royal Institute of Thailand 2 (2010): 107-118.
[28] Guan, S.-h., Sattler, I., Lin, W.-h., Guo, D.-a., and Grabley, S. *p*-Aminoacetophenonic Acids Produced by a Manggrove Endophyte: *Streptomycs*. Journal of Natural Products 68(8) (2005): 1998-2000.
[29] Ananda, K. and Sridhar, K.R. Diversity of endophytic fungi in the roots of mangrove species on the west coast of India. Canadian Journal of Microbiology 48(10) (2002): 871-878.
[30] Jones, E.G., Stanley, S.J., and Pinruan, U. Marine endophyte sources of new chemical natural products: a review. Botanica Marina 51(3) (2008): 163-170.
[31] Giri, C., et al. Status and distribution of mangrove forests of the world using earth observation satellite data. Global Ecology and Biogeography 20(1) (2011): 154-159.
[32] De Wet, H., Struwig, M., and Van Wyk, B.E. Taxonomic notes on the genera Tiliacora and Tinospora (Menispermaceae) in southern Africa. South African Journal of Botany 103 (2016): 283-294.
[33] Wang, B., et al. New nor-clerodane-type furanoditerpenoids from the rhizomes of *Tinospora capillipes*. Phytochemistry Letters 15 (2016): 225-229.
[34] Najib Nik, A.R.N., Furuta, T., Kojima, S., Takane, K., and Ali Mohd, M. Antimalarial activity of extracts of Malaysian medicinal plants. Journal of Ethnopharmacology 64(3) (1999): 249-254.
[35] Pathak, A.K., Jain, D.C., and Sharma, R.P. Chemistry and Biological Activities of the Genera Tinospora. Pharmaceutical Biology 33(4) (1995): 277-287.
[36] Huang, X.Z., et al. A novel 18-norclerodane diterpenoid from the roots of *Tinospora sagittata* var. *yunnanensis*. Molecules 15(11) (2010): 8360-8365.
[37] Maurya, R., Wazir, V., and Kapil, R. Biotherapeutic diterpene glucosides from *Tinospora* species. ChemInform 26(40) (1995).

[38] Deng, Y., Zhang, M., and Luo, H. Identification and antimicrobial activity of two alkaloids from traditional Chinese medicinal plant *Tinospora capillipes*. Industrial Crops and Products 37(1) (2012): 298-302.

[39] Ruan, C.T., Lam, S.H., Lee, S.S., and Su, M.J. Hypoglycemic action of borapetoside A from the plant *Tinospora crispa* in mice. Phytomedicine 20(8-9) (2013): 667-675.

[40] Yu, D.R., et al. Neuroprotective activity of two active chemical constituents from *Tinospora hainanensis*. Asian Pacific Journal of Tropical Medicine 10(2) (2017): 114-120.

[41] Bala, M., Pratap, K., Verma, P.K., Singh, B., and Padwad, Y. Validation of ethnomedicinal potential of *Tinospora cordifolia* for anticancer and immunomodulatory activities and quantification of bioactive molecules by HPTLC. Journal of Ethnopharmacology 175 (2015): 131-137.

[42] Kongkathip, N., Dhumma-upakorn, P., Kongkathip, B., Chawananoraset, K., Sangchomkaeo, P., and Hatthakitpanichakul, S. Study on cardiac contractility of cycloeucalenol and cycloeucalenone isolated from *Tinospora crispa*. Journal of Ethnopharmacology 83 (2002): 95-99.

[43] Chang, C.C., Ho, S.L., and Lee, S.S. Acylated glucosylflavones as alpha-glucosidase inhibitors from *Tinospora crispa* leaf. Bioorganic & Medicinal Chemistry 23(13) (2015): 3388-3396.

[44] Qin, N.-b., et al. Cytotoxic clerodane furanoditerpenoids from the root of *Tinospora sagittata*. Phytochemistry Letters 12 (2015): 173-176.

[45] Katib, S., Ruangrungsi, N., Palanuvej, C., Chareonsap, P.P., and Rungsihirunrat, K. Macroscopic-microscopic characteristics and AFLP marker for identification of *Tinospora crispa* and *Tinospora baenzigeri* endemic to Thailand. Journal of Health Research 31(2) (2017): 143-149.

[46] Hanson, J.R. Diterpenoids. Natural Product Reports 26(9) (2009): 1156-1171.

[47] Tuntiwachwuttikul, P., Boonrasri, N., Bremner, J.B., and Taylor, W.C. Rearranged clerodane diterpenes from *Tinospora baenzigeri*. Phytochemistry 52 (1999): 1335-1340.

[48] Tuntiwachwuttikul, P. and Taylor, W.C. New Rearranged Clerodane Diterpenes from *Tinospora baenzigeri*. Chemical and Pharmaceutical Bulletin 49 (2001): 854-857.

[49] Mosmann, T. Rapid colorimetric assay for cellular growth and surviral: Appication to proliferation and cytotoxicity assays. Journal of Immunological Methods 65 (1983): 55-63.

[50] Carmichael, J., DeGraff, W.G., Gazdar, A.F., Minna, J.D., and Mitchell, J.B. Evaluation of a tetrazolium-based semiautomated colorimetrie assay: assessment of chemosensitivity testing. Cancer Research 47 (1987): 936-942.

[51] Tominaga, H., et al. A water-soluble tetrazolium salt useful for colorimetric cell viability assay. Analytical Communications 36 (1999): 47-50.

[52] Guevara, I., et al. Determination of nitrite/nitrate in human biological material by the simple Griess reaction. Clinica Chimica Acta 274(2) (1998): 177-188.

[53] Thanakosai, W. and Phuwapraisirisan, P. First identification of alpha-glucosidase inhibitors from okra (*Abelmoschus esculentus*) seeds. Natural Product Communications 8(8) (2013): 1085-1088.

[54] Choudhary, M., Ismail, M., Ali, Z., Shaari, K., H Lajis, N., and Rahman, A.-u. Alkaloidal Constituents of *Tinospora crispa*. Natural Product Communications 5(11) 2010: 1747-1750.

[55] Martin, T.S., Ohtani, K., Kasai, R., and Yamasaki, K. Clerodane diterpene glucosides from *Tinospora rumphii.* Phytochemistry 40(6) (1995): 1729-1736.

[56] Ma, C.M., Nakamura, N., Min, B.S., and Hattori, M. Triterpenes and lignans from Artemisia caruifolia and their cytotoxic effects on meth-A and LLC tumor cell lines. Chemical and Pharmaceutical (Tokyo) 49(2) (2001): 183-187.

[57] Yue, Z., et al. Chemical constituents of the root of Jasminum giraldii. Molecules 18(4) (2013): 4766-4775.

[58] Morikawa, H., et al. Terpenic and phenolic glycosides from leaves of Breynia officinalis HEMSL. Chemical and Pharmaceutical (Tokyo) 52(9) (2004): 1086-90.

[59] Holzbach, J.C. and Lopes, L.M. Aristolactams and Alkamides of *Aristolochia gigantea.* Molecules 15(12) (2010): 9462-72.

[60] Jie Li, W., et al. Phenolic Compounds and Antioxidant Activities of *Liriope muscari*. Molecules 17(2) 2012.

[61] Ali A. Alwahsh, M., Khairuddean, M., and Keng Chong, W. Chemical Constituents and Antioxidant Activity of *Teucrium barbeyanum* Aschers. Records of Natural Products 9(1) (2015): 159-163.

[62] Rosalba Encarnación, D., et al. Isolation of eriodictyol identical with huazhongilexone from *Solanum hindsianum*. Acta Chemica Scandinavica 53(5) 1999: 375-377.

[63] Guzmán-López, O., Trigos, Á., Fernández, F.J., de Jesús Yañez-Morales, M., and Saucedo-Castañeda, G. Tyrosol and tryptophol produced by Ceratocystis adiposa. World Journal of Microbiology and Biotechnology 23(10) (2007): 1473-1477.

[64] Mochizuki, M., Nussenblatt, R., Kuwabara, T., and Gery, I. Effects of cyclosporine and other immunosuppressive drugs on experimental autoimmune uveoretinitis in rats. Investigative Ophthalmology and Visual Science 26(2) (1985): 226-232.

[65] Colombo, D., Cassano, N., Bellia, G., and Vena, G.A. Cyclosporine regimens in plaque psoriasis: an overview with special emphasis on dose, duration, and old and new yreatment approaches. The Scientific World Journal 2013 (2013): 1-11.

[66] Kitchin, J.E.S., Pomeranz, M.K., Pak, G., Washenik, K., and Shupack, J.L. Rediscovering mycophenolic acid: a review of its mechanism, side effects, and potential uses. Journal of the American Academy of Dermatology 37(3) (1997): 445-449.

[67] Allison, A.C. and Eugui, E.M. Mycophenolate mofetil and its mechanisms of action. Immunopharmacology 47(2-3) (2000): 85-118.

[68] Wang, Q. and Xu, L. Beauvericin, a bioactive compound produced by fungi: a short review. Molecules 17(3) (2012): 2367-77.

[69] Unlu, A., Nayir, E., Kirca, O., and Ozdogan, M. *Ganoderma Lucidum* (Reishi Mushroom) and cancer. Journal of BUON 21(4) (2016): 792-798.

[70] Strobel, G.A., Hess, W.M., Ford, E., Sidhu, R., and Yang, X. Taxol from fungal endophytes and the issue of biodiversity. Journal of Industrial Microbiology 17(5-6) (1996): 417-423.
[71] Wani, M.C., Taylor, H.L., Wall, M.E., Coggon, P., and McPhail, A.T. Plant antitumor agents. VI. Isolation and structure of taxol, a novel antileukemic and antitumor agent from Taxus brevifolia. Journal of the American Chemical Society 93(9) (1971): 2325-2327.
[72] Strobel, G. and Daisy, B. Bioprospecting for microbial endophytes and their natural products. Microbiology and Molecular Biology Reviews 67(4) (2003): 491-502.
[73] Muzzamal, H., Sarwar, R., Sajid, I., and Hasnain, S. Isolation, identification and screening of endophytic bacteria antagonistic to biofilm formers. Pakistan journal of zoology 44(1) (2012): 249-257.
[74] Kaul, S., Gupta, S., Ahmed, M., and Dhar, M.K. Endophytic fungi from medicinal plants: a treasure hunt for bioactive metabolites. Phytochemistry Reviews 11(4) (2012): 487-505.
[75] Gouda, S., Das, G., Sen, S.K., Shin, H.-S., and Patra, J.K. Endophytes: A treasure house of bioactive compounds of medicinal importance. Frontiers in Microbiology 7(1538) (2016): 1-8.
[76] Mittermeier, R.A., Myers, N., Mittermeier, C.G., and Robles, G. Hotspots: Earth's Biologically Richest and Most Endangered Terrestrial Ecoregions. CEMEX, SA, Agrupación Sierra Madre, SC, 1999.
[77] Wani, Z.A., Ashraf, N., Mohiuddin, T., and Riyaz-Ul-Hassan, S. Plant-endophyte symbiosis, an ecological perspective. Applied Microbiology and Biotechnology 99(7) (2015): 2955-2965.
[78] Khan, A.L., et al. Endophytes from medicinal plants and their potential for producing indole acetic acid, improving seed germination and mitigating oxidative stress. Journal of Zhejiang University-SCIENCE B 18(2) (2017): 125-137.
[79] Sengupta, A. and Chaudhuri, S. Arbuscular mycorrhizal relations of mangrove plant community at the Ganges river estuary in India. Mycorrhiza 12(4) (2002): 169-174.
[80] Dai, J., Krohn, K., Draeger, S., and Schulz, B. New haphthalene-chroman coupling products from the endophytic fungus, *Nodulisporium* sp. from *Erica arborea*. European Journal of Organic Chemistry 2009(10) (2009): 1564-1569.
[81] Li, J., et al. Meroterpenes and azaphilones from marine mangrove endophytic fungus *Penicillium* 303. Fitoterapia 97 (2014): 241-246.
[82] Bai, Z.-Q., et al. New meroterpenoids from the endophytic fungus *Aspergillus flavipes* AIL8 derived from the mangrove plant *Acanthus ilicifolius*. Marine Drugs 13(1) (2015): 237-248.
[83] Posten, C.H. and Cooney, C.L. Growth of microorganisms. Biotechnology 1 (1993): 111-162.
[84] Moore-Landecker, E. Fundamentals of the Fungi. Prentice Hall, 1996.
[85] Griffin, D.H. Fungal Physiology. John Wiley & Sons, 1996.
[86] Zabel, R.A. and Morrell, J.J. Wood Microbiology: Decay and Its Prevention. Academic press, 2012.

[87] Stamets, P. The Mushroom Cultivator: A Practical Guide to Growing Mushroom at Home. Chilton, JS, 1983.

[88] White, T.J., Bruns, T., Lee, S., and Taylor, J. Amplification and direct sequencing of fungal ribosomal RNA genes for phylogenetics. PCR Protocols: A Guide to Methods and Applications. Academic Press, Inc., New York, 1990.

[89] McGINNIS, M.R., Rinaldi, M.G., and Winn, R.E. Emerging agents of phaeohyphomycosis: pathogenic species of *Bipolaris* and *Exserohilum*. Journal of Clinical Microbiology 24(2) (1986): 250-259.

[90] Hill, J.G., Nakashima, T.T., and Vederas, J.C. Fungal xanthone biosynthesis. distribution of acetate-derived oxygens in ravenelin. Journal of the American Chemical Society 104(6) (1982): 1745-1748.

[91] Zhang, W., Krohn, K., Draeger, S., and Schulz, B. Bioactive isocoumarins isolated from the endophytic fungus *Microdochium bolleyi*. Journal of natural products 71(6) (2008): 1078-1081.

[92] Li, W., Xu, J., Li, F., Xu, L., and Li, C. A new antifungal isocoumarin from the endophytic fungus *Trichoderma* sp. 09 of *Myoporum bontioides* A. gray. Pharmacognosy Magazine 12(48) (2016): 259-261.

APPENDIX

APPENDIX A

1. Media

The media were sterilized by autoclaving at 121 ^{o}C, 15 lb/ in^{2} 15 min

1.1 Water agar (WA)

Agar	15 g
Distilled water up to	1 L

1.2 Potato dextrose agar (PDA)

Potato dextrose broth	240 g
Agar	15 g
Distilled water up to	1 L

1.3 Potato dextrose broth (PDB)

Potato dextrose broth	240 g
Distilled water up to	1 L

1.4 Natural potato dextrose broth (NPAB)

Potato, peeled and diced	200 g
Dextrose	20 g
Distilled water up to	1 L

Boil 200 g of peels, diced potatoes for 1 h in 1000 mL of DI water. Then filter and adjust the filtrate to 1000 mL. Add the dextrose and dissolve by steaming and sterilize by autoclaving at 121 ^{o}C for 15 min.

1.5 Sabouraud's dextrose broth (SDB)

Sabouraud's dextrose broth	30 g
Distilled water up to	1 L

1.6 Yeast extract sucrose broth (YEB)

Yeast extract	20 mL
Sucrose	150 g
Agar	15 g
Distilled water up to	1 L

APPENDIX B

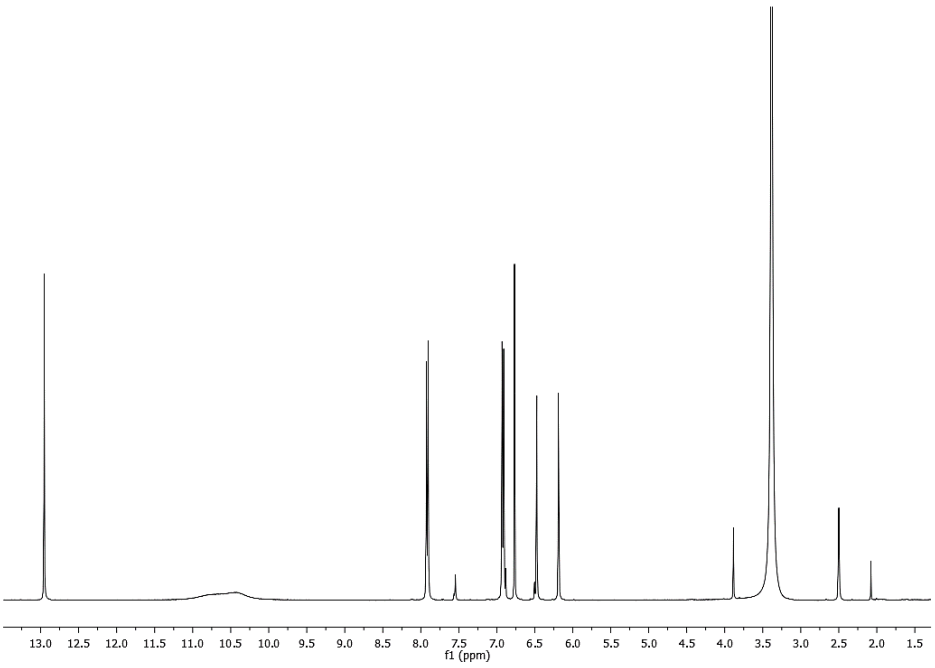

Fig. B.1 ^{1}H NMR (400 MHz, DMSO-d_6) spectrum of compound **44**

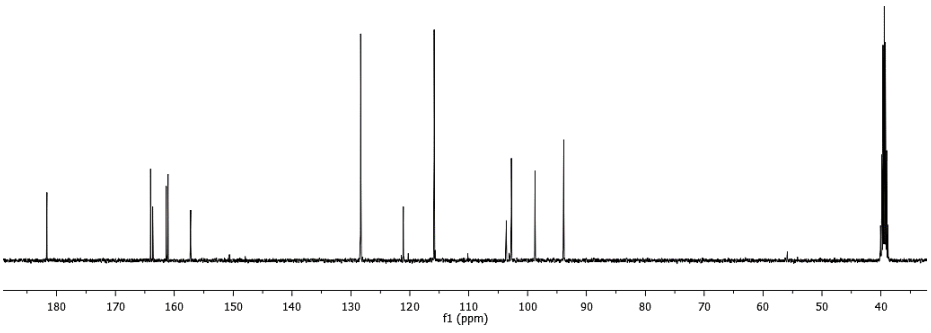

Fig. B.2 ^{13}C NMR (100 MHz, DMSO-d_6) spectrum of compound **44**

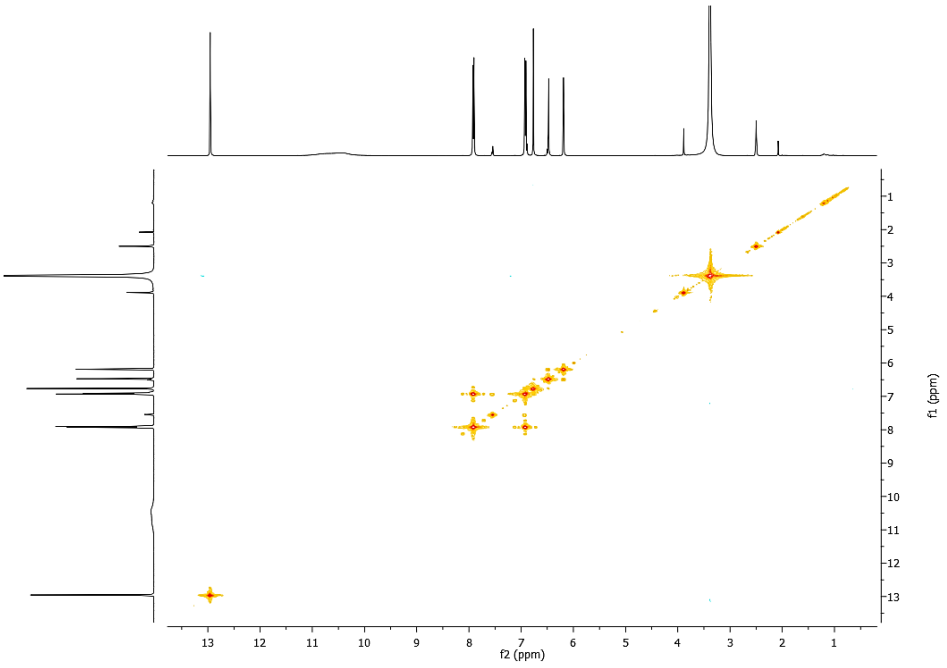

Fig. B.3 ^{1}H-^{1}H COSY spectrum (DMSO-d_6) of compound **44**

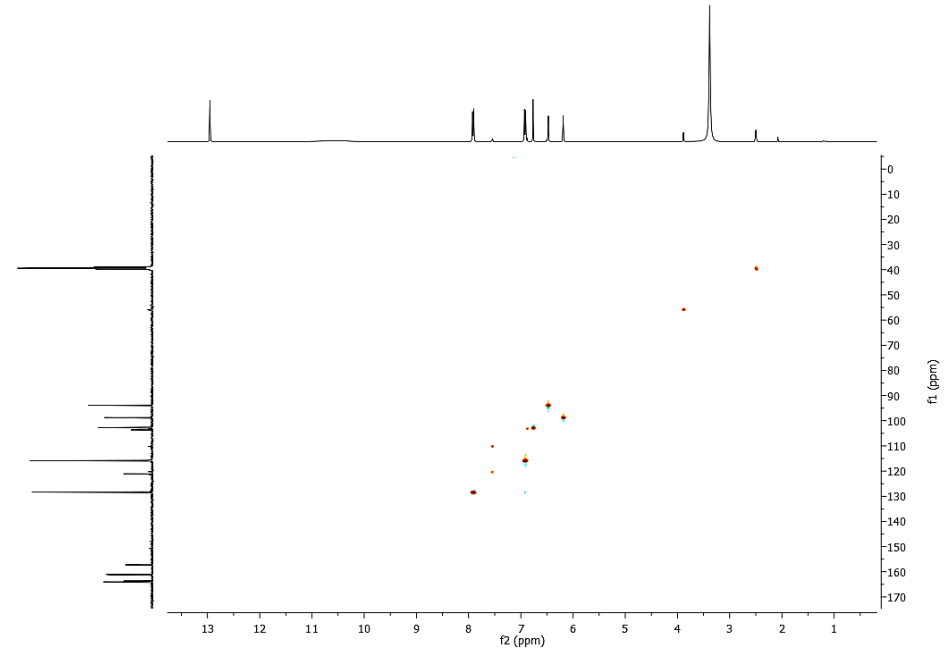

Fig. B.4 HSQC spectrum (DMSO-d_6) of compound **44**

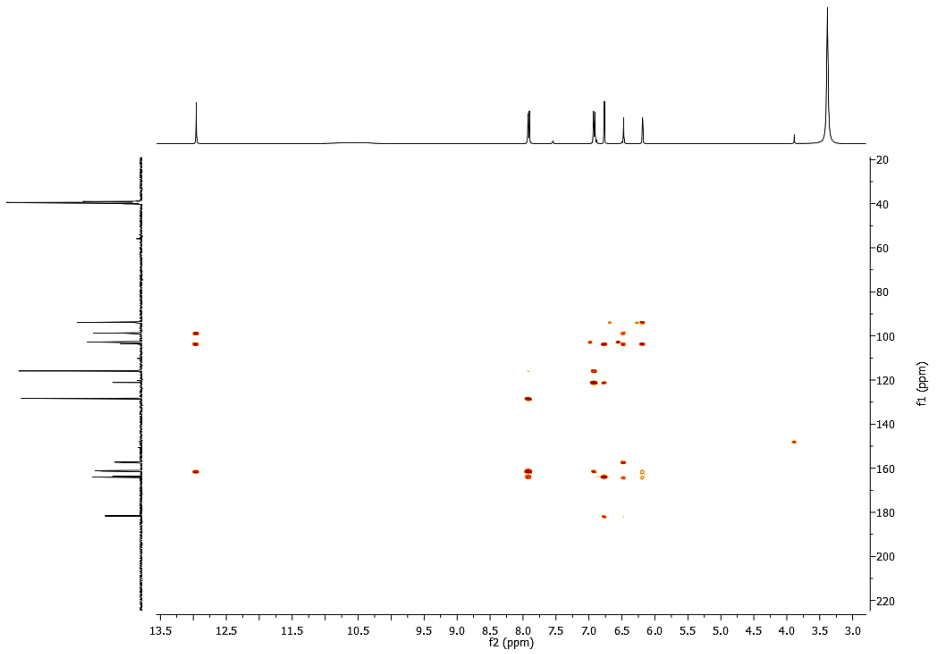

Fig. B.5 HMBC spectrum (DMSO-d_6) of compound **44**

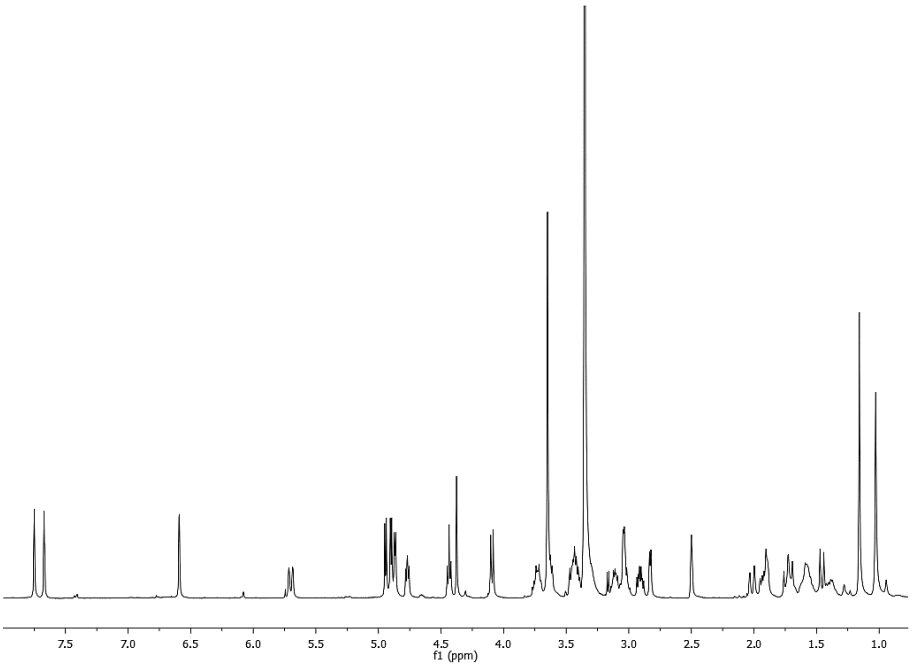

Fig. B.6 ^{1}H NMR (400 MHz, DMSO-d_6) spectrum of compound **61**

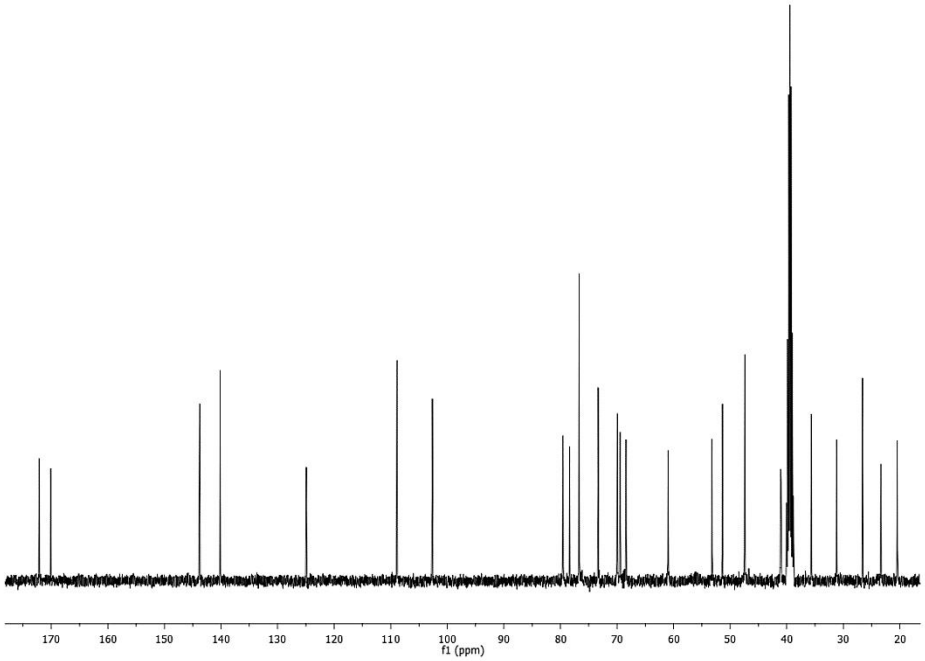

Fig. B.7 ^{13}C NMR (100 MHz, DMSO-d_6) spectrum of compound **61**

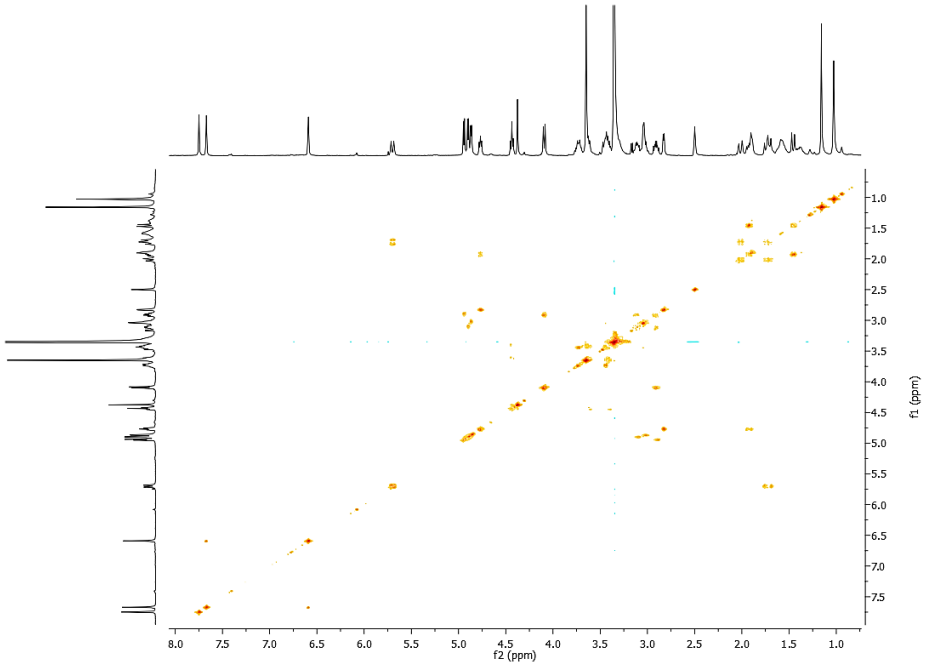

Fig. B.8 ^{1}H-^{1}H COSY spectrum (DMSO-d_6) of compound **61**

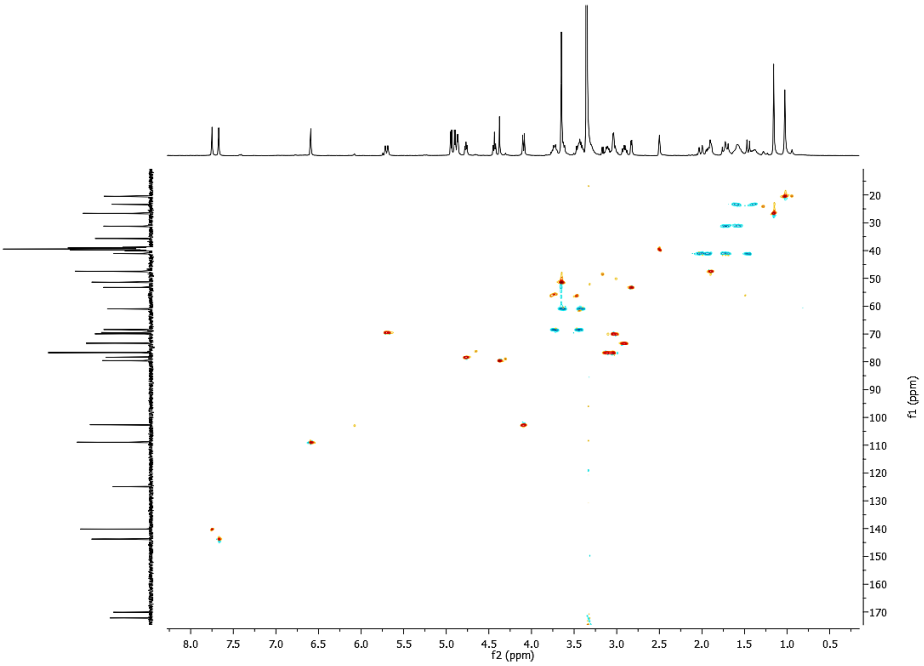

Fig. B.9 HSQC spectrum (DMSO-d_6) of compound **61**

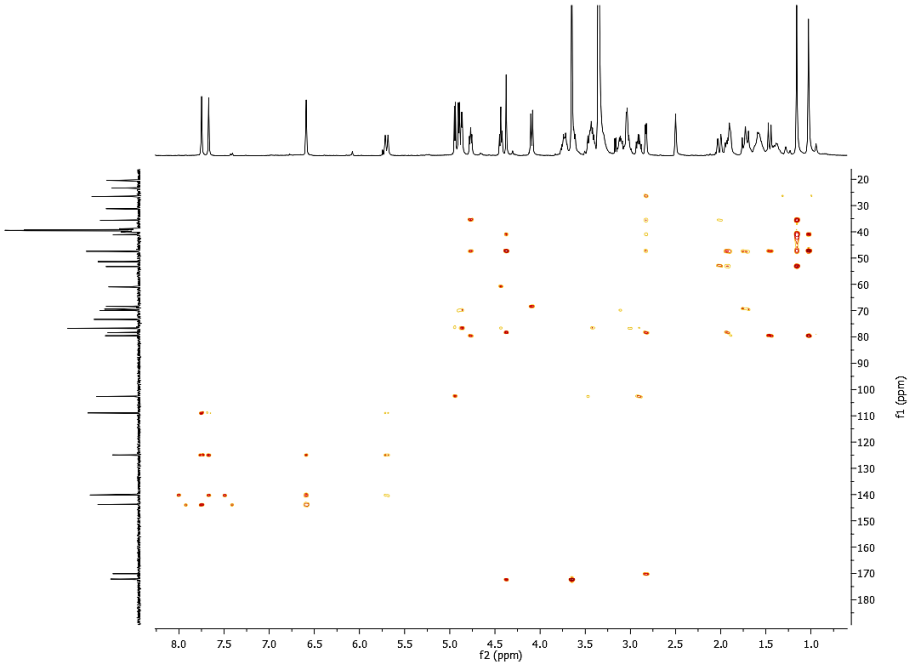

Fig. B.10 HMBC spectrum (DMSO-d_6) of compound **61**

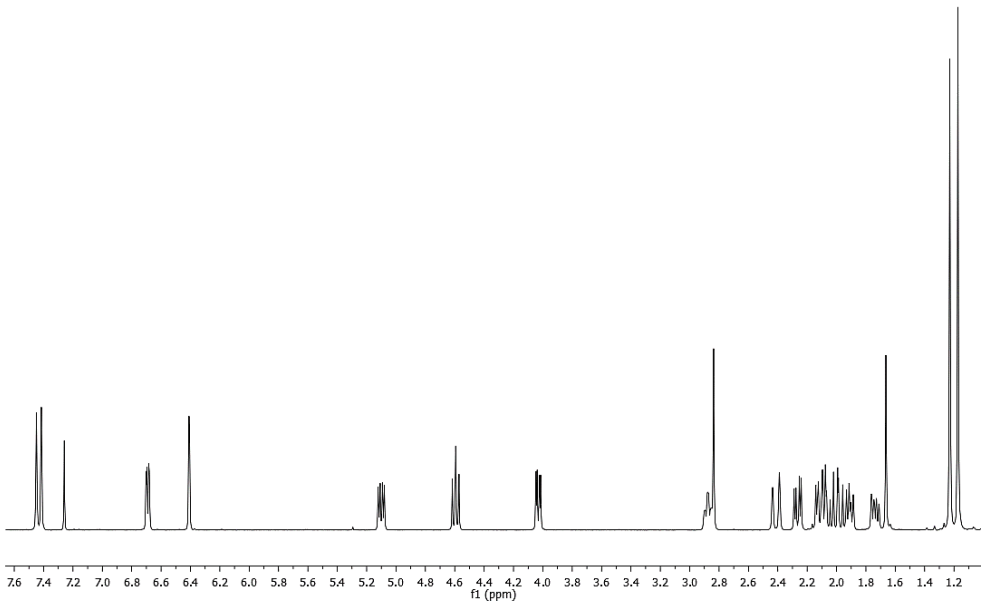

Fig. B.11 ^{1}H NMR (400 MHz, $CDCl_3$) spectrum of compound **66**

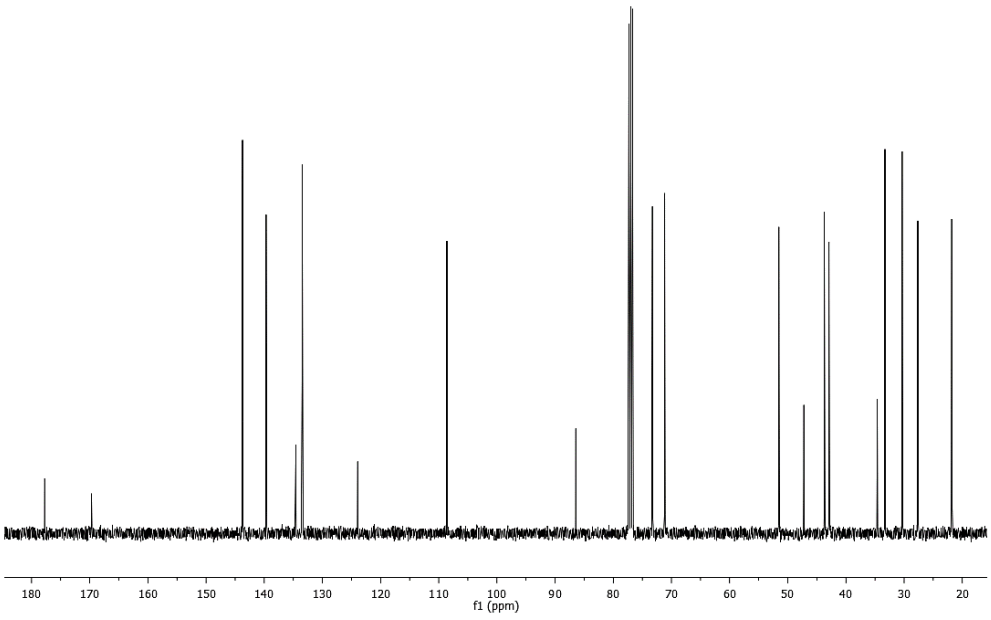

Fig. B.12 ^{13}C NMR (100 MHz, $CDCl_3$) spectrum of compound **66**

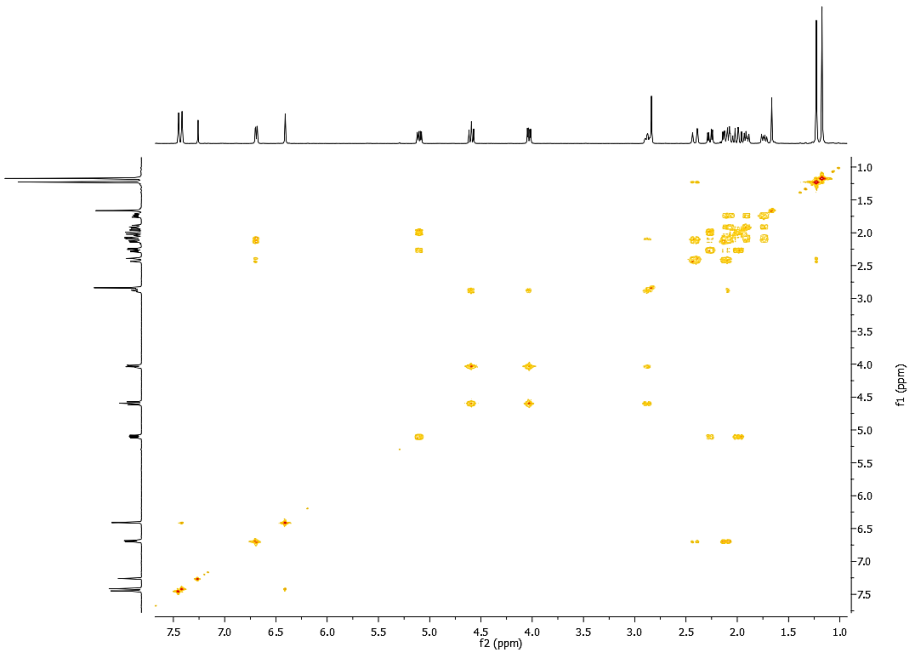

Fig. B.13 ^{1}H-^{1}H COSY spectrum ($CDCl_3$) of compound **66**

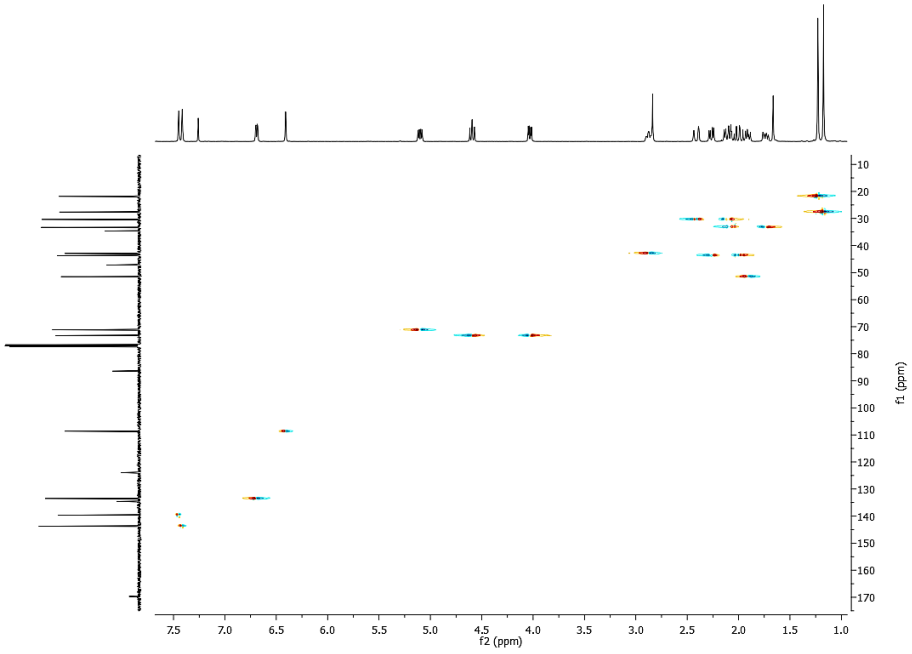

Fig. B.14 HSQC spectrum ($CDCl_3$) of compound **66**

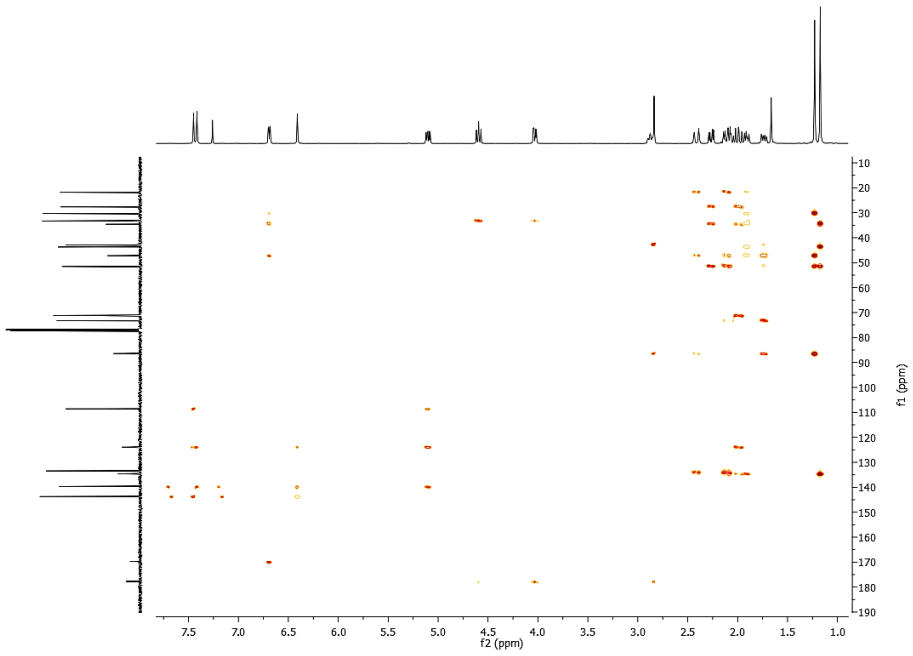

Fig. B.15 HMBC spectrum ($CDCl_3$) of compound **66**

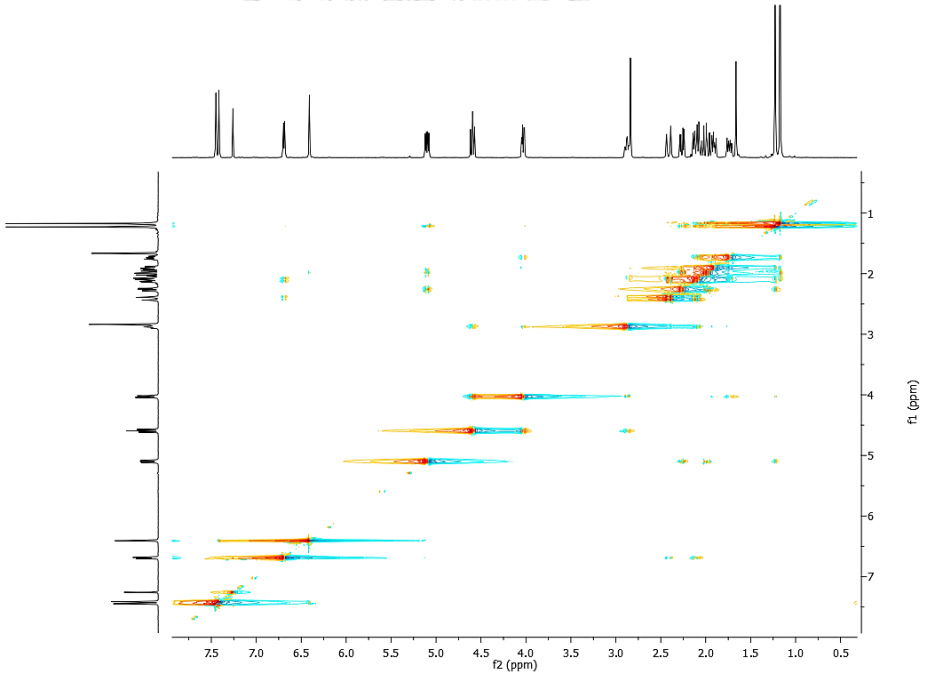

Fig. B.16 NOESY spectrum ($CDCl_3$) of compound **66**

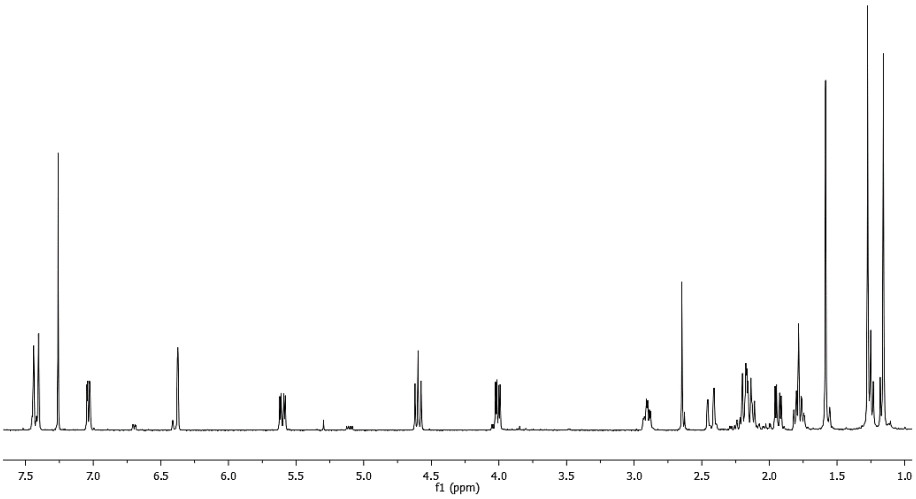

Fig. B.17 ^{1}H NMR (400 MHz, $CDCl_3$) spectrum of compound **67**

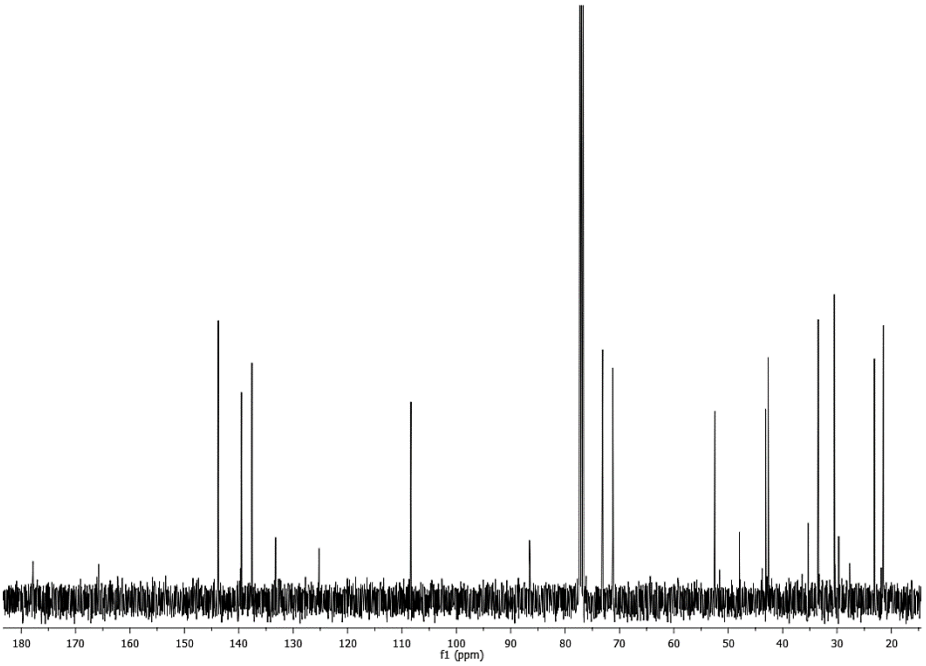

Fig. B.18 ^{13}C NMR (100 MHz, $CDCl_3$) spectrum of compound **67**

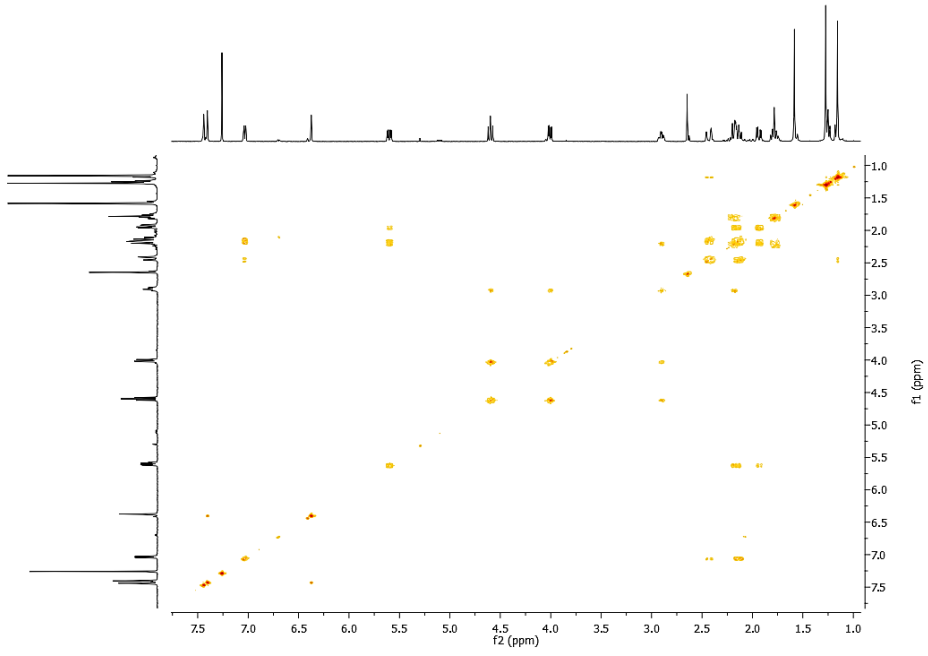

Fig. B.19 ^{1}H-^{1}H COSY spectrum ($CDCl_3$) of compound **67**

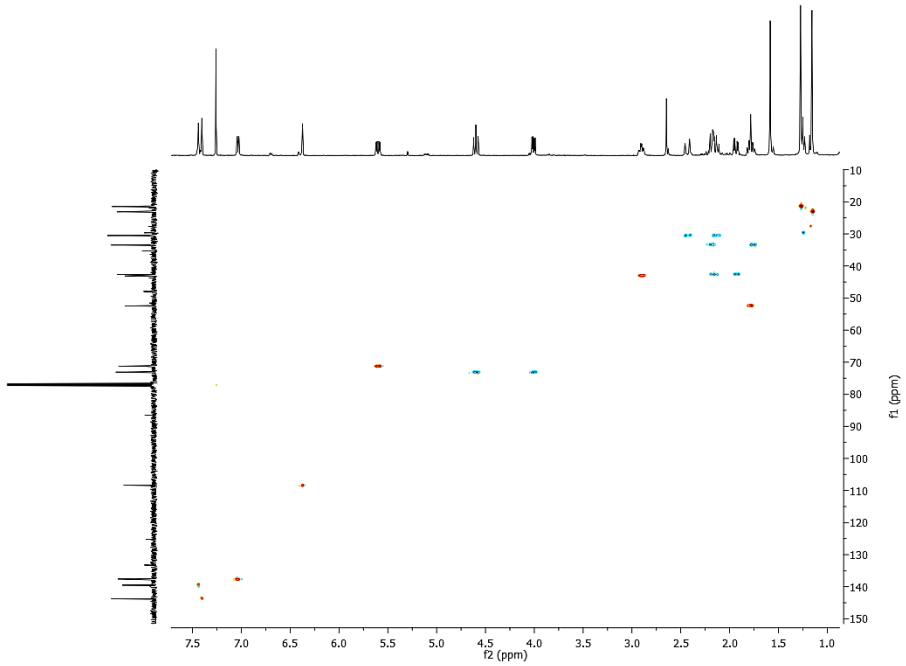

Fig. B.20 HSQC spectrum ($CDCl_3$) of compound **67**

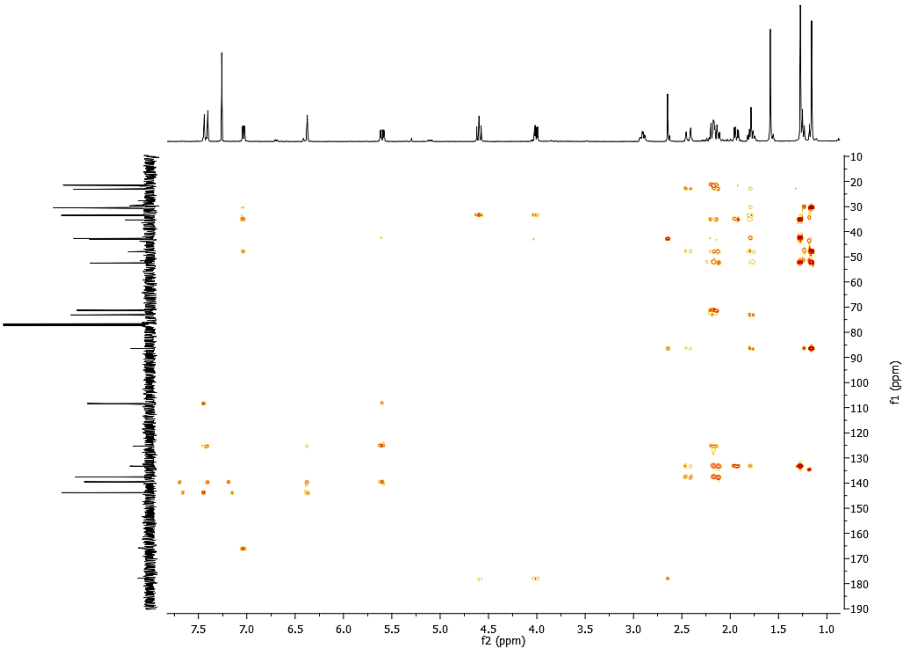

Fig. B.21 HMBC spectrum ($CDCl_3$) of compound **67**

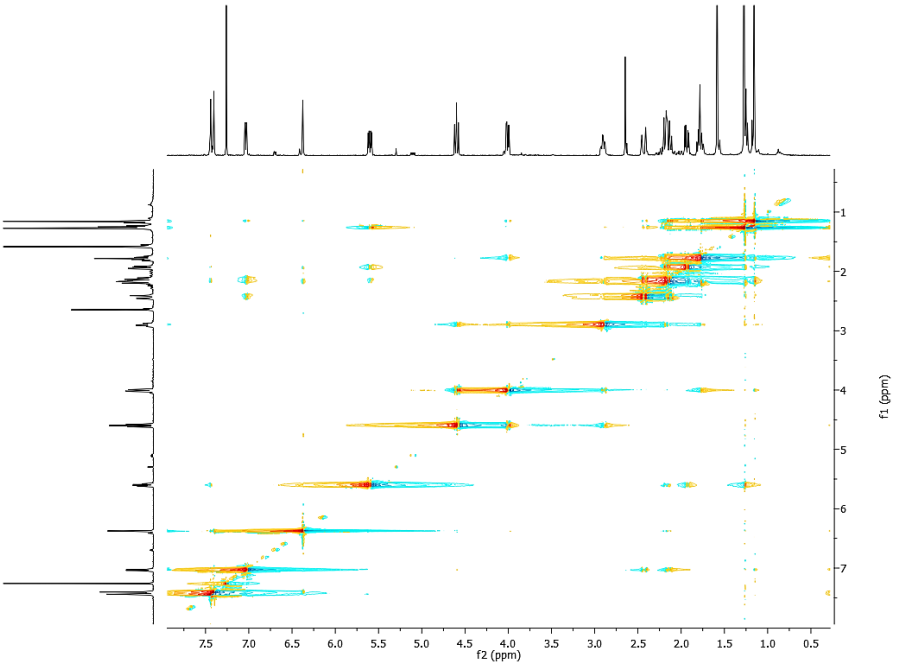

Fig. B.22 NOESY spectrum ($CDCl_3$) of compound **67**

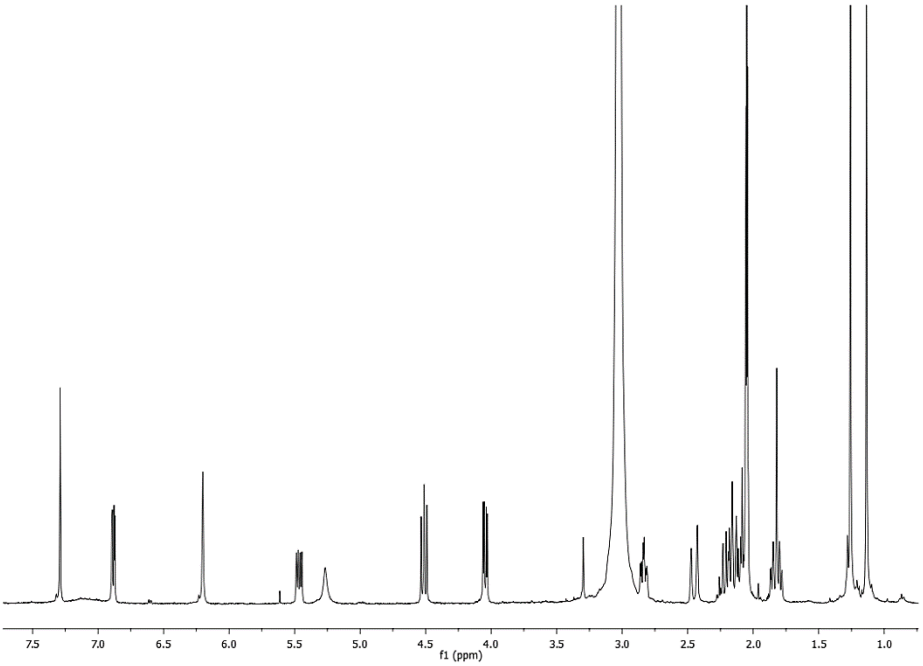

Fig. B.23 ^{1}H NMR (400 MHz, acetone-d_6) spectrum of compound **68**

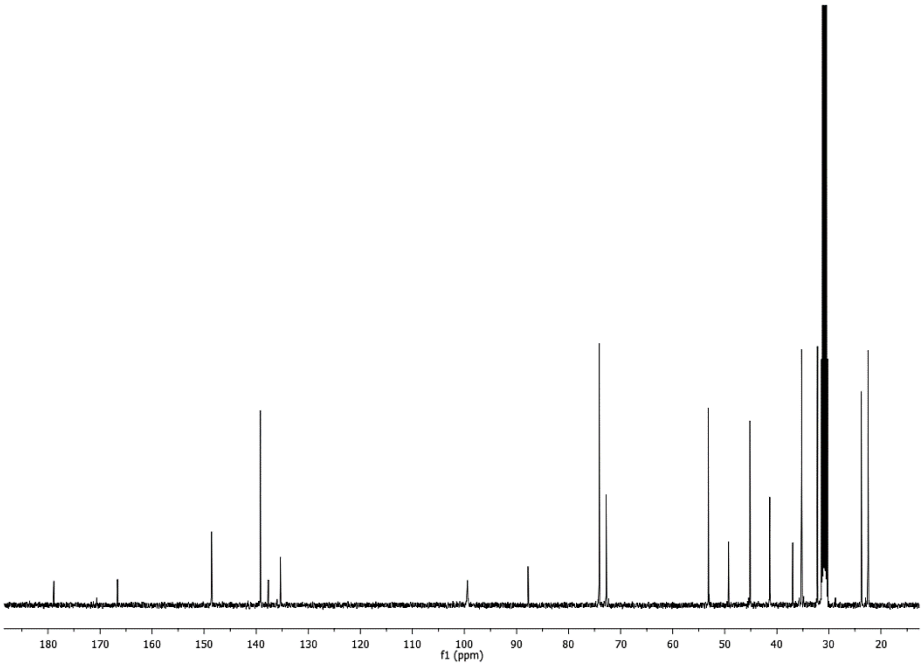

Fig. B.24 ^{13}C NMR (100 MHz, acetone-d_6) spectrum of compound **68**

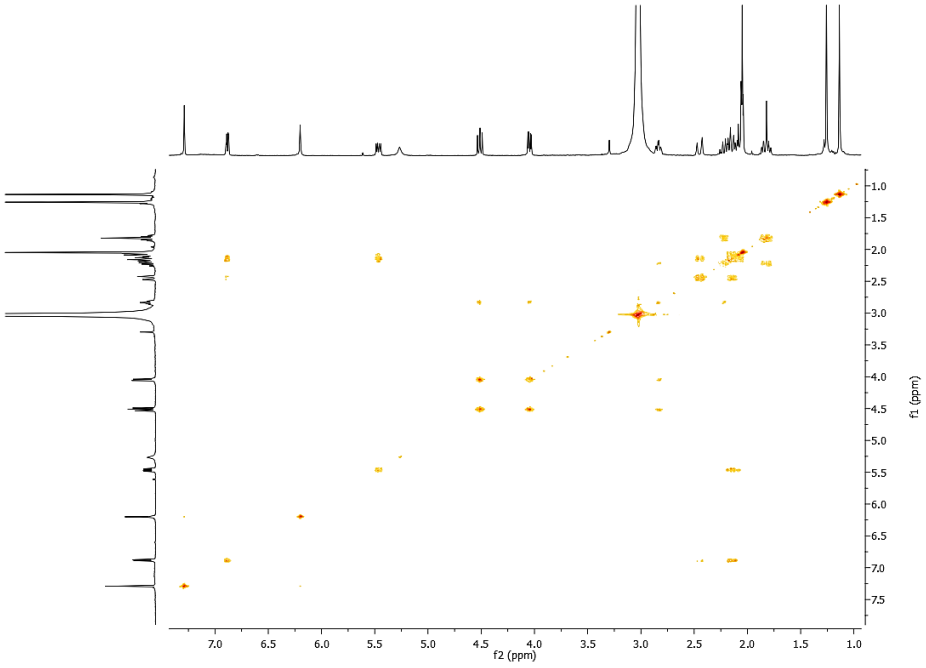

Fig. B.25 ^{1}H-^{1}H COSY spectrum (acetone-d_6) of compound **68**

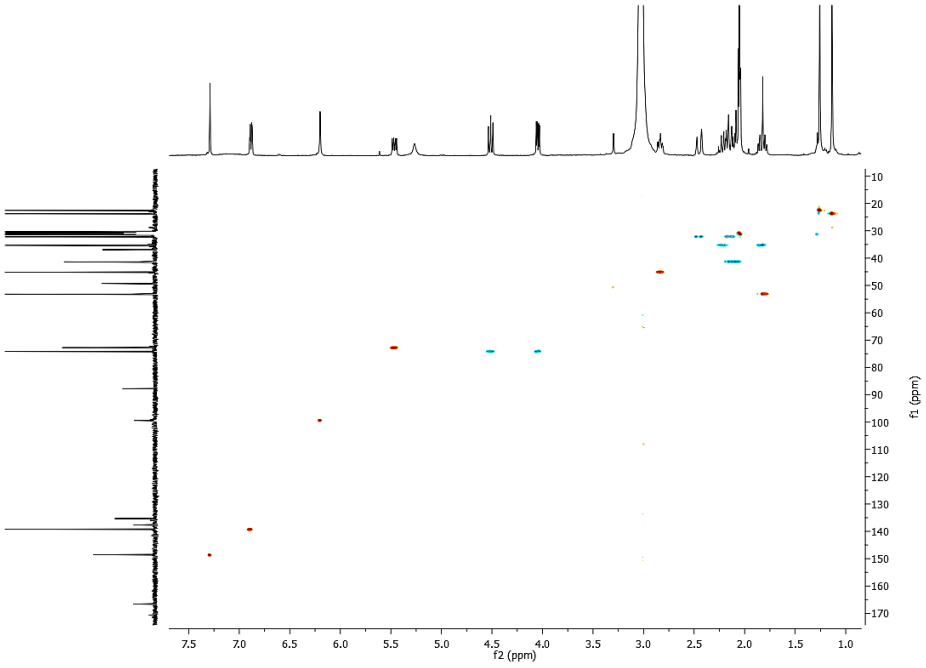

Fig. B.26 HSQC spectrum (acetone-d_6) of compound **68**

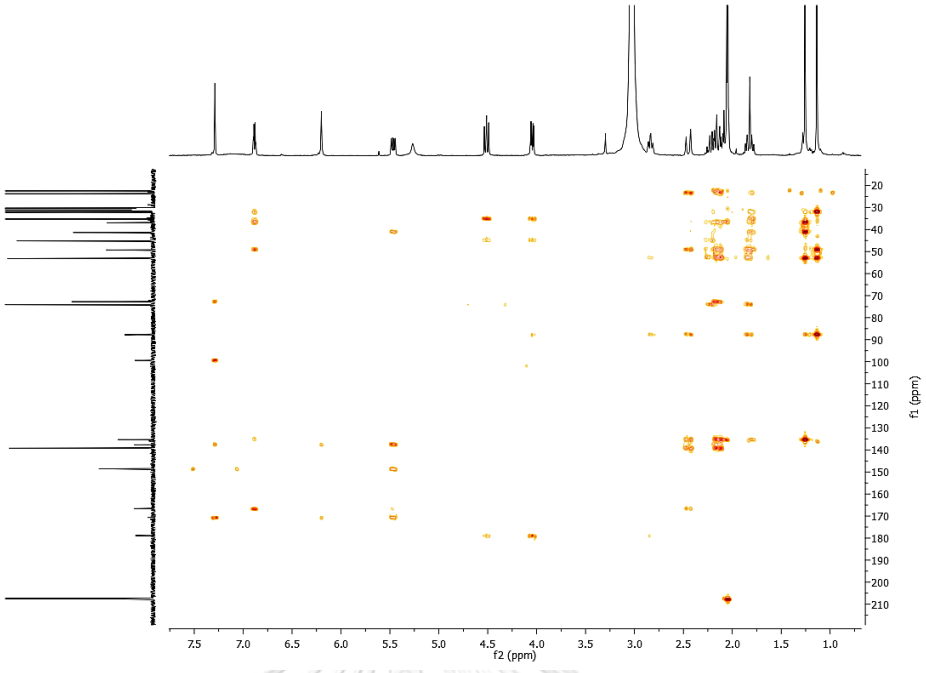

Fig. B.27 HMBC spectrum (acetone-d_6) of compound **68**

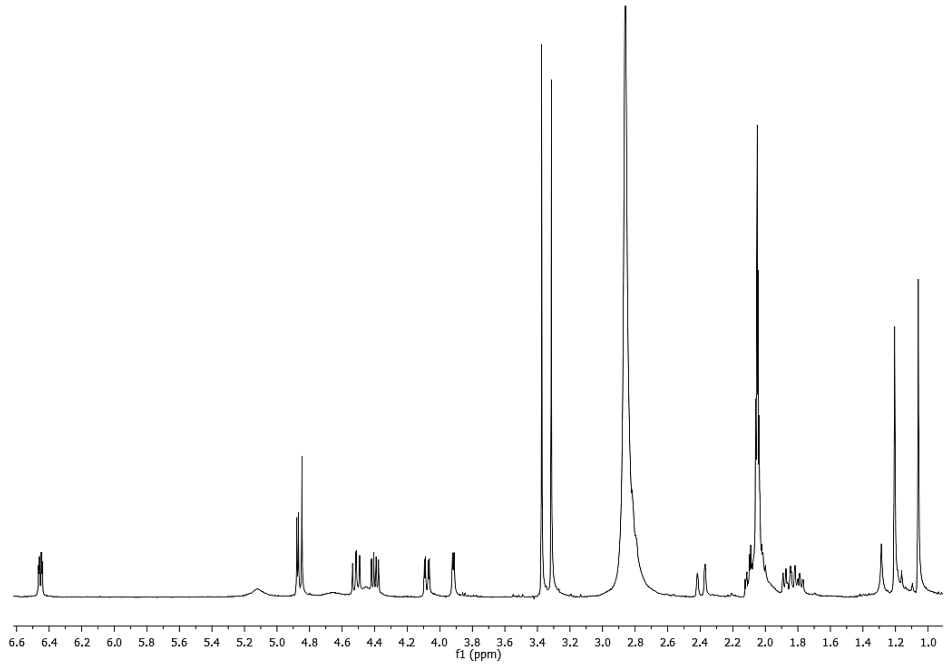

Fig. B.28 ^{1}H NMR (400 MHz, acetone-d_6) spectrum of compound **69**

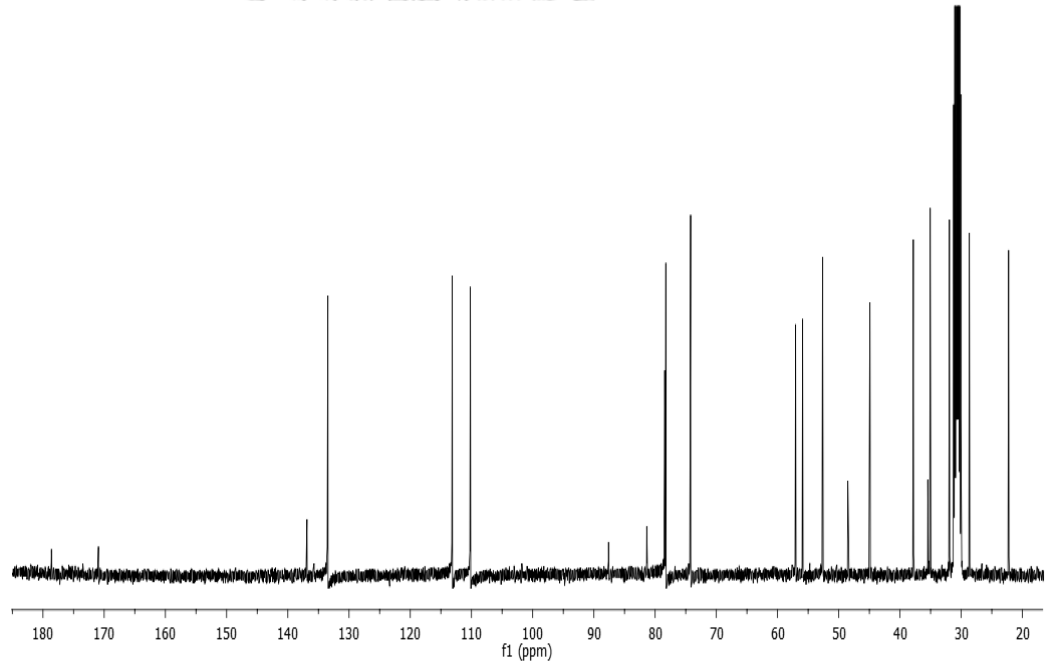

Fig. B.29 ^{13}C NMR (100 MHz, acetone-d_6) spectrum of compound **69**

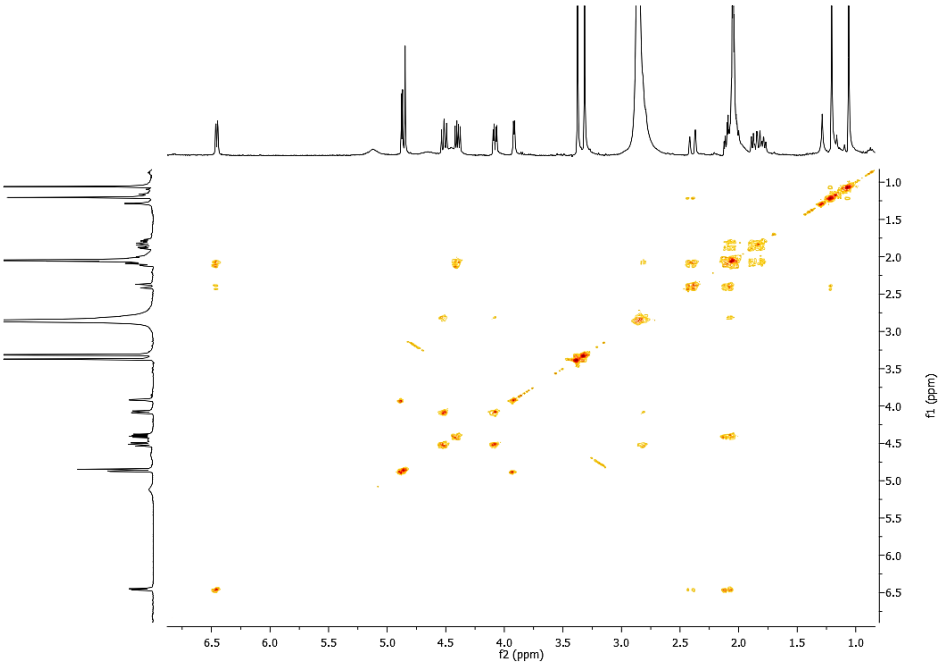

Fig. B.30 ^{1}H-^{1}H COSY spectrum (acetone-d_6) of compound **69**

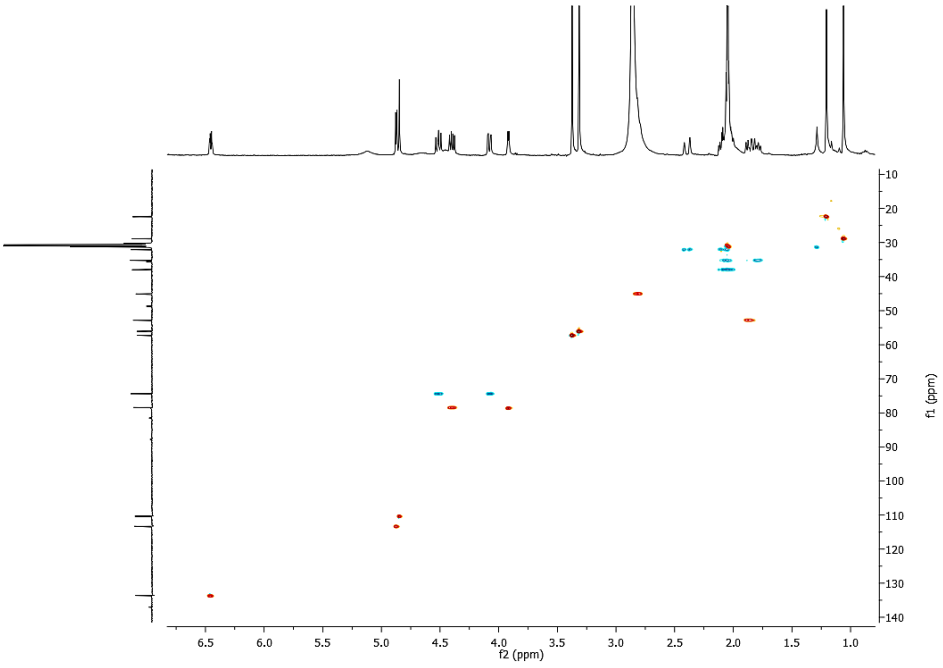

Fig. B.31 HSQC spectrum (acetone-d_6) of compound **69**

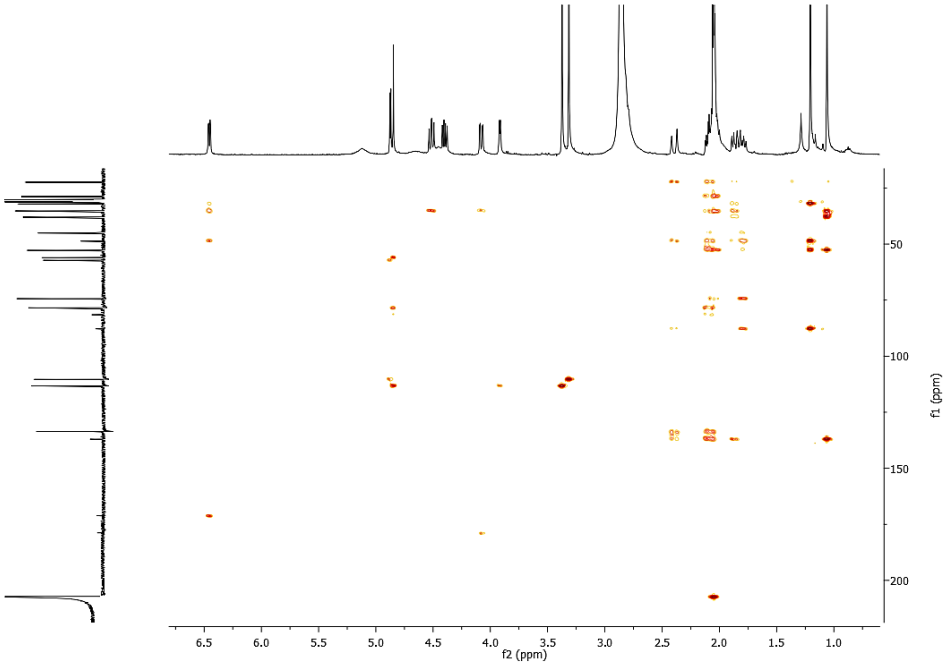

Fig. B.32 HMBC spectrum (acetone-d_6) of compound **69**

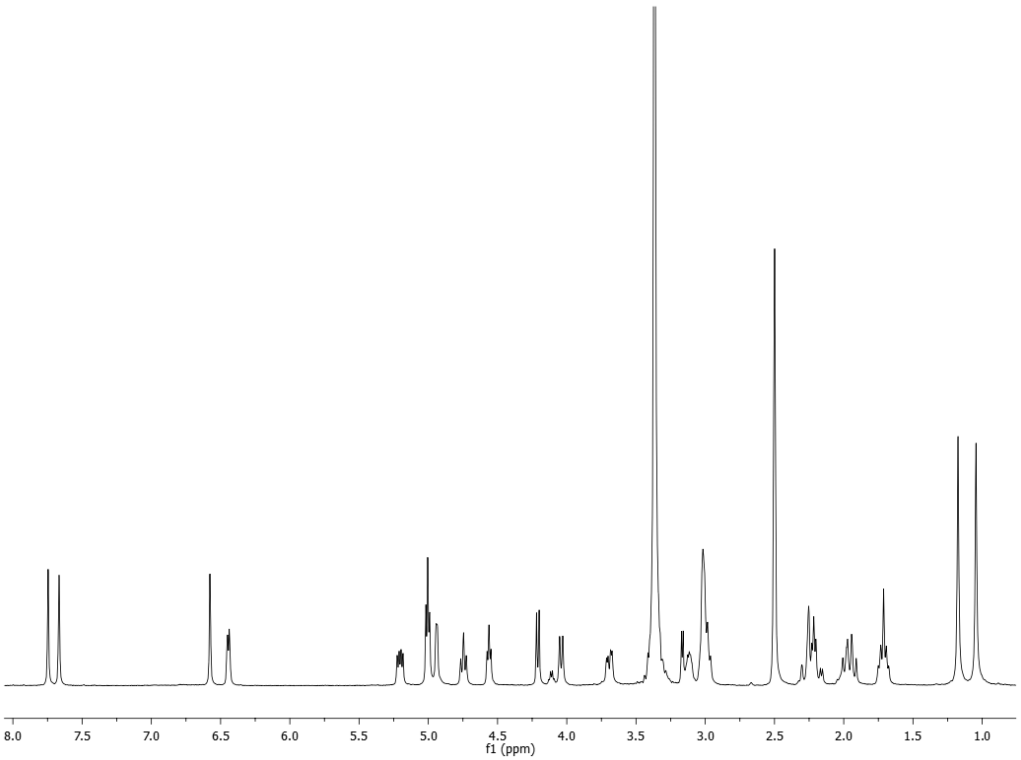

Fig. B.33 ^{1}H NMR (400 MHz, DMSO-d_6) spectrum of compound **70**

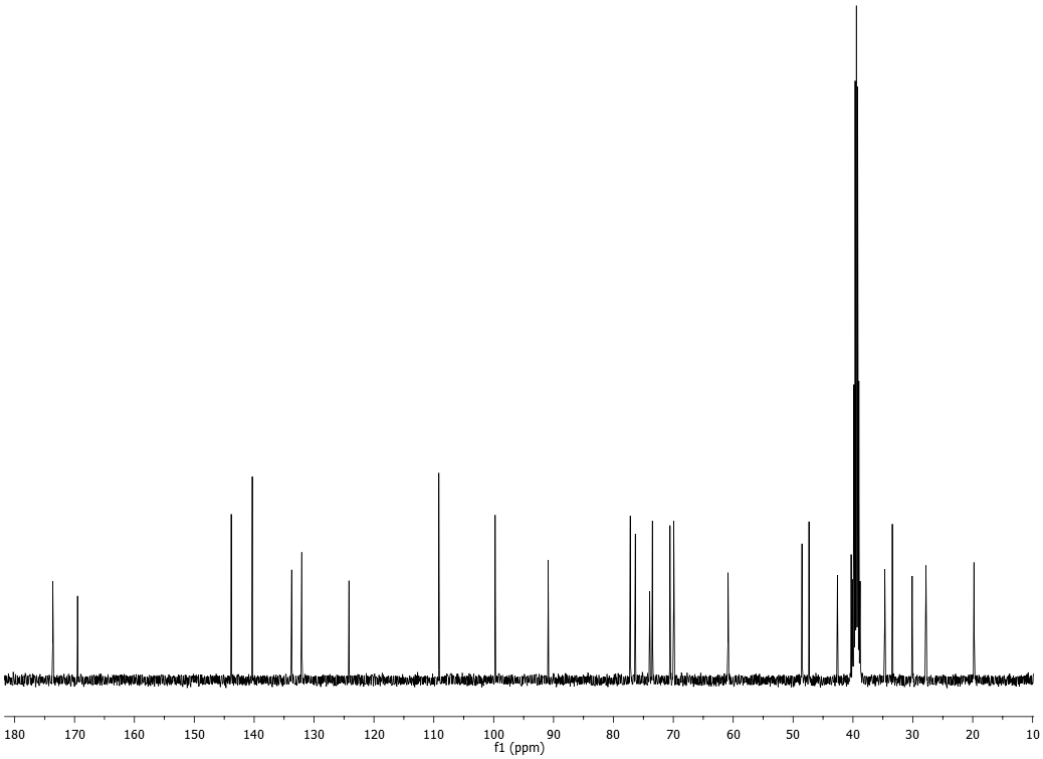

Fig. B.34 ^{13}C NMR (100 MHz, DMSO-d_6) spectrum of compound **70**

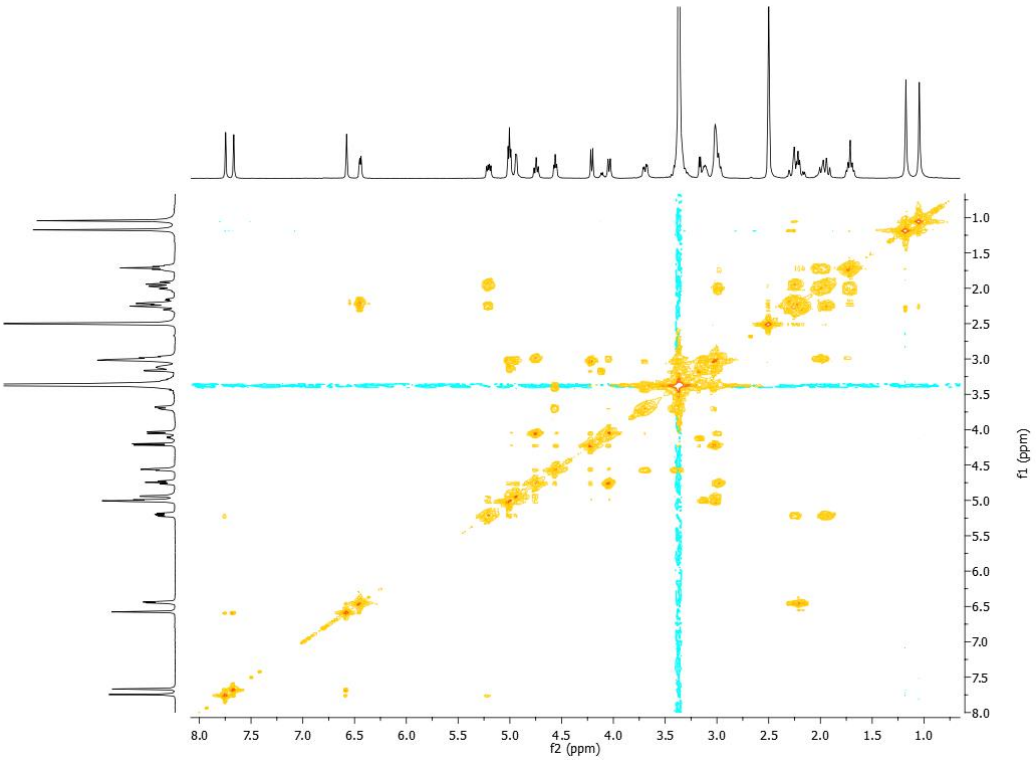

Fig. B.35 ^{1}H-^{1}H COSY spectrum (DMSO-d_6) of compound **70**

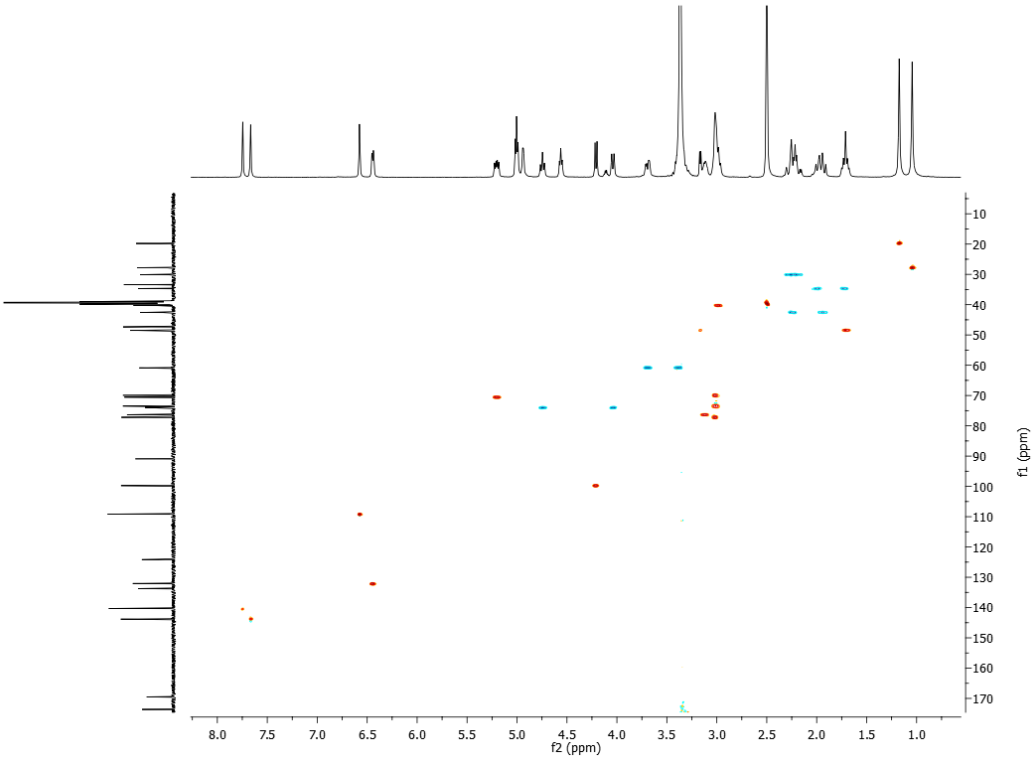

Fig. B.36 HSQC spectrum (DMSO-d_6) of compound **70**

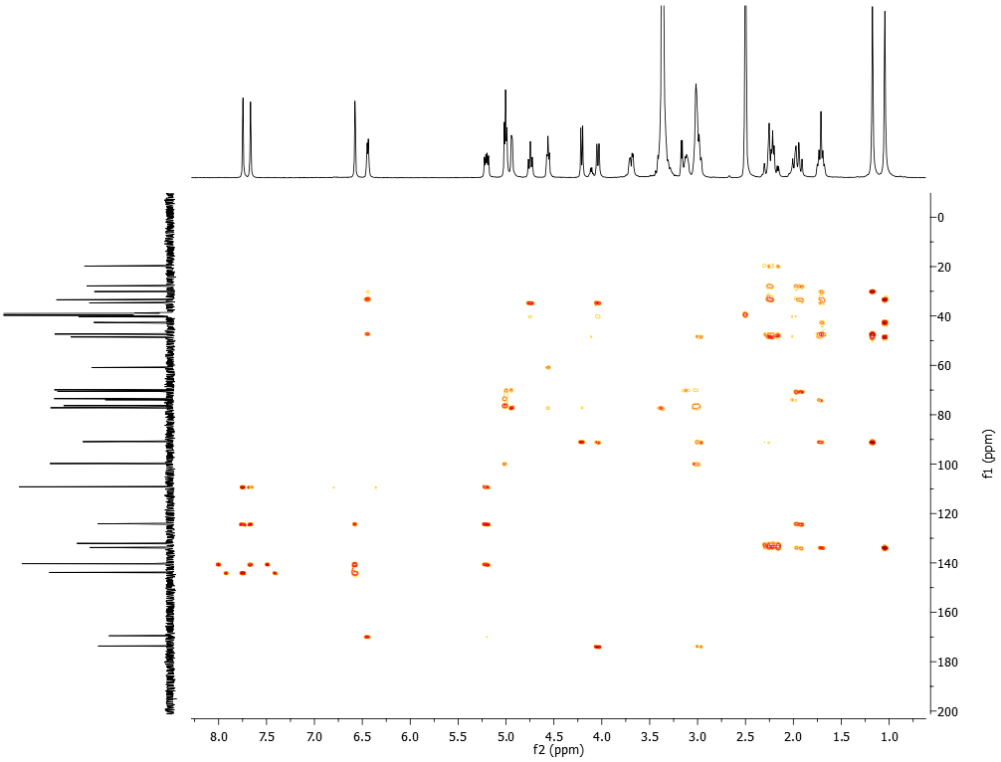

Fig. B.37 HMBC spectrum (DMSO-d_6) of compound **70**

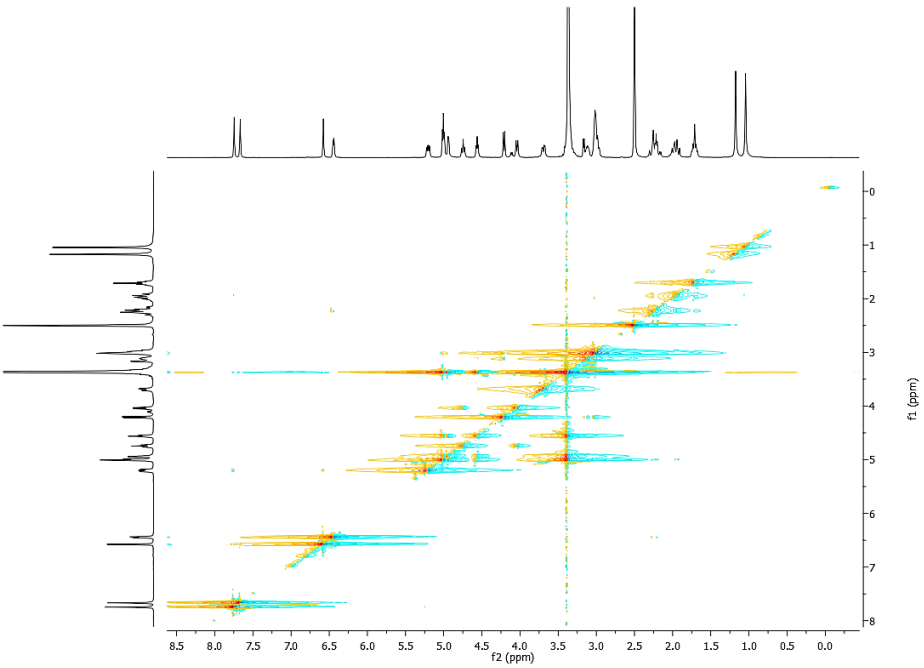

Fig. B.38 NOESY spectrum (DMSO-d_6) of compound **70**

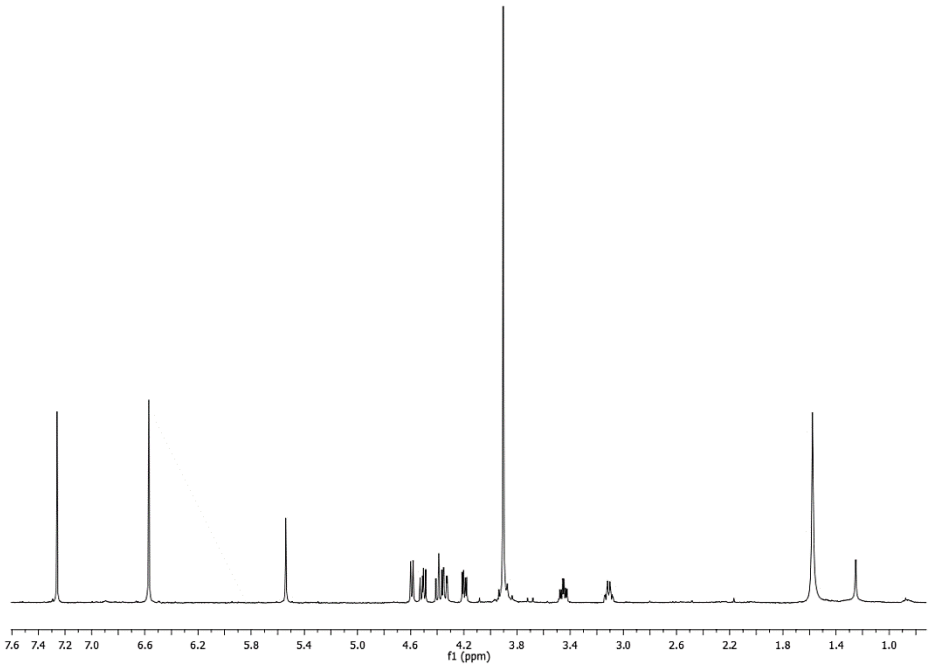

Fig. B.39 ^{1}H NMR (400 MHz, $CDCl_3$) spectrum of compound **71**

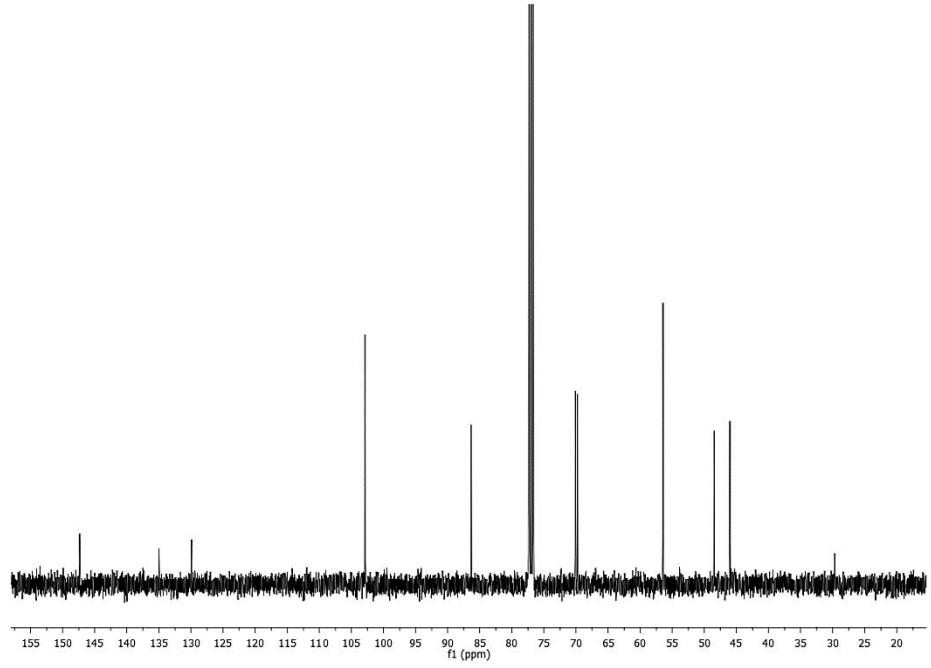

Fig. B.40 ^{13}C NMR (100 MHz, $CDCl_3$) spectrum of compound **71**

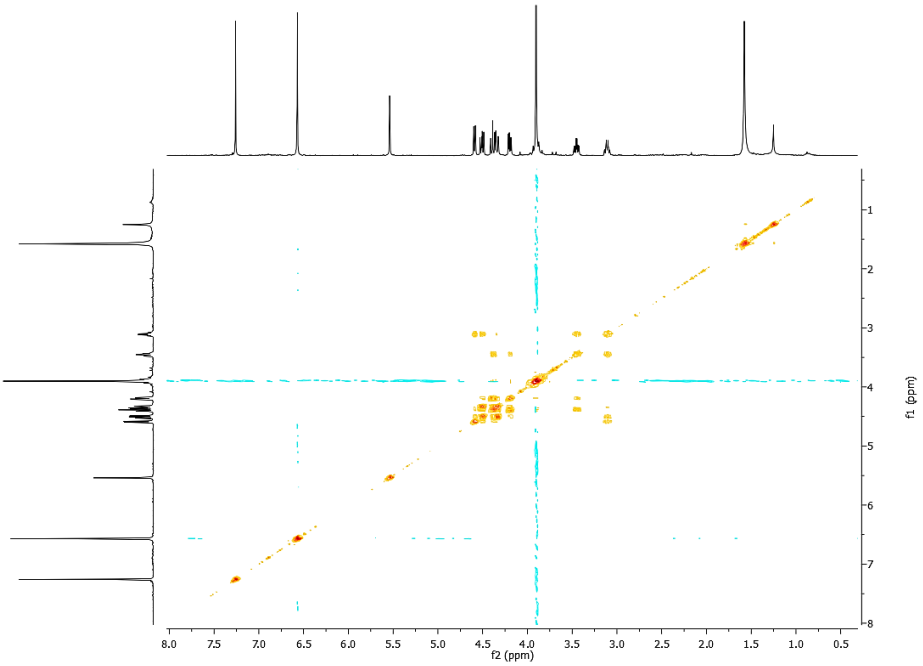

Fig. B.41 ^{1}H-^{1}H COSY spectrum ($CDCl_3$) of compound **71**

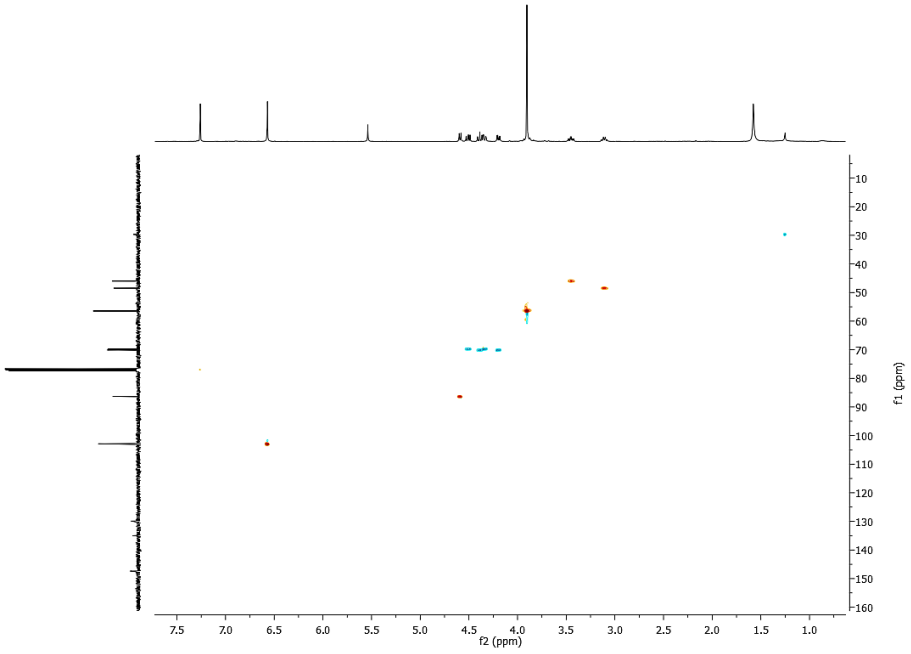

Fig. B.42 HSQC spectrum ($CDCl_3$) of compound **71**

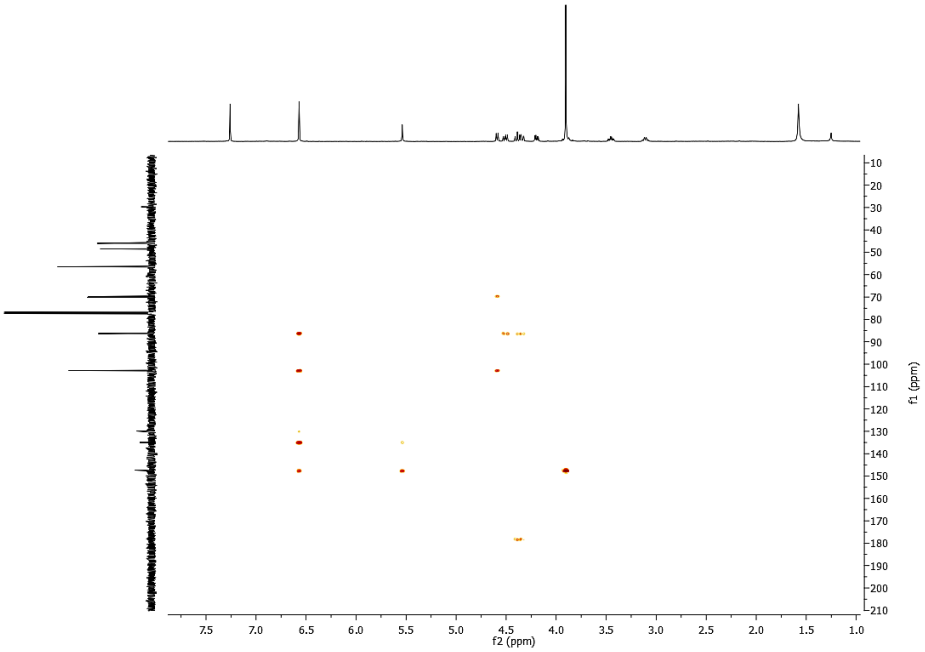

Fig. B.43 HMBC spectrum ($CDCl_3$) of compound **71**

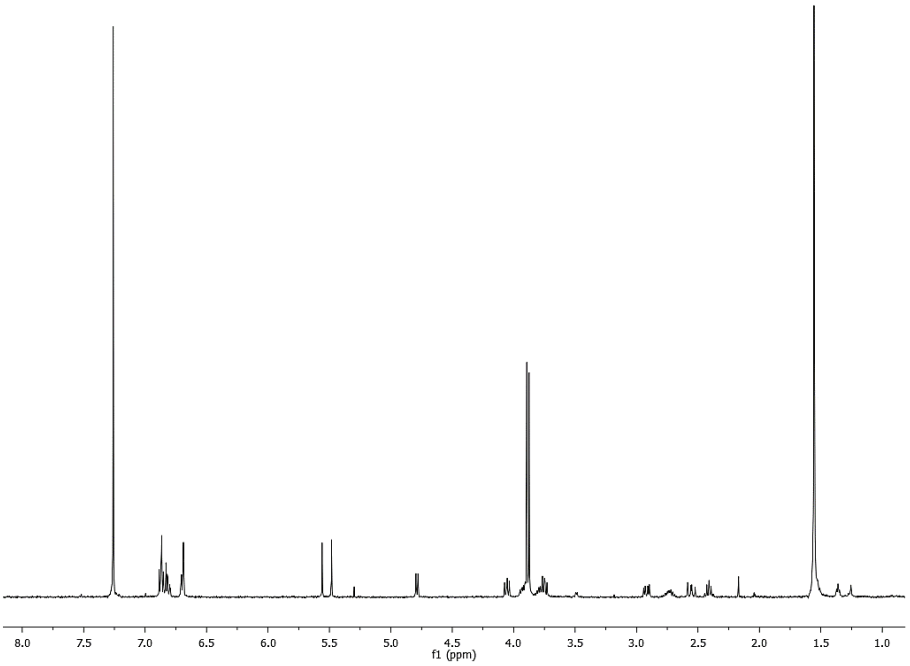

Fig. B.44 ^{1}H NMR (400 MHz, $CDCl_3$) spectrum of compound **72**

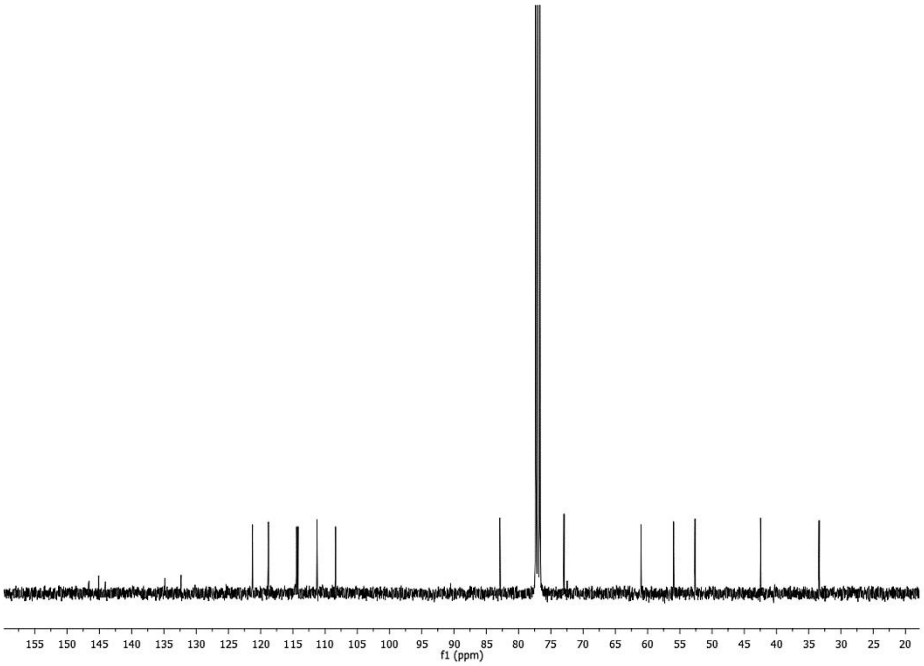

Fig. B.45 ^{13}C NMR (100 MHz, $CDCl_3$) spectrum of compound **72**

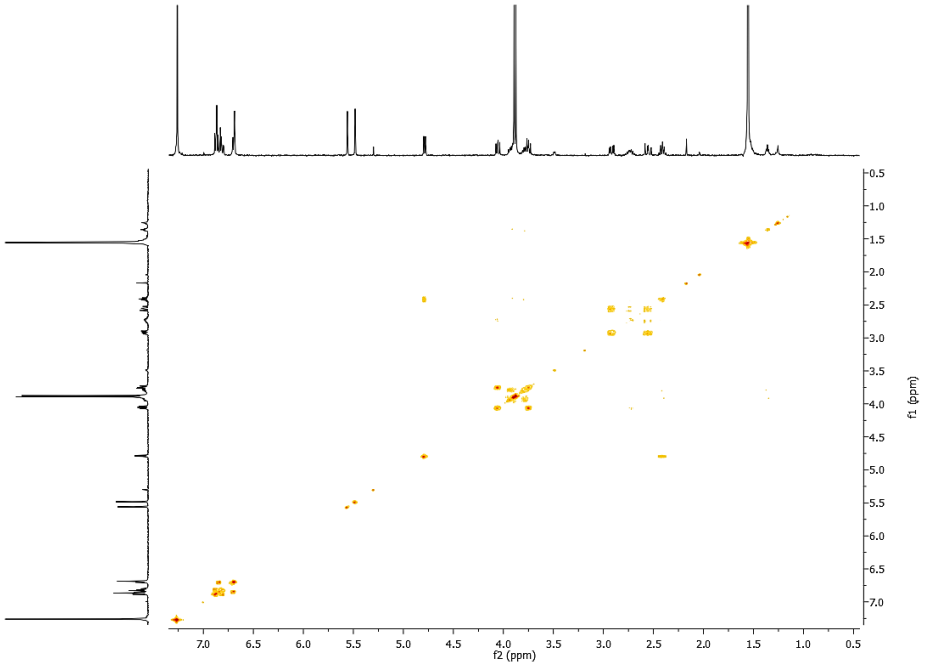

Fig. B.46 ^{1}H-^{1}H COSY spectrum ($CDCl_3$) of compound **72**

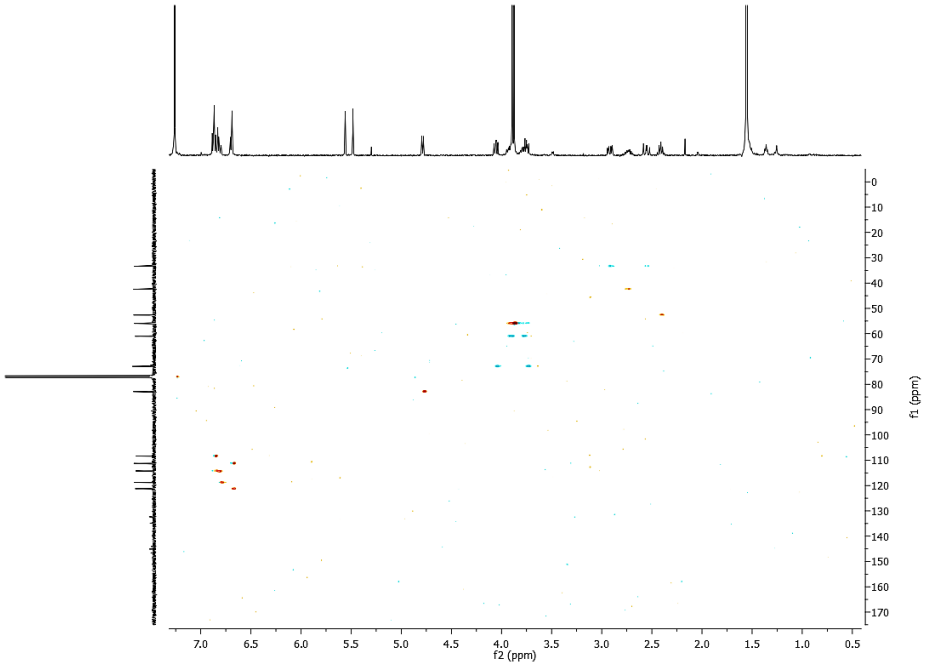

Fig. B.47 HSQC spectrum ($CDCl_3$) of compound **72**

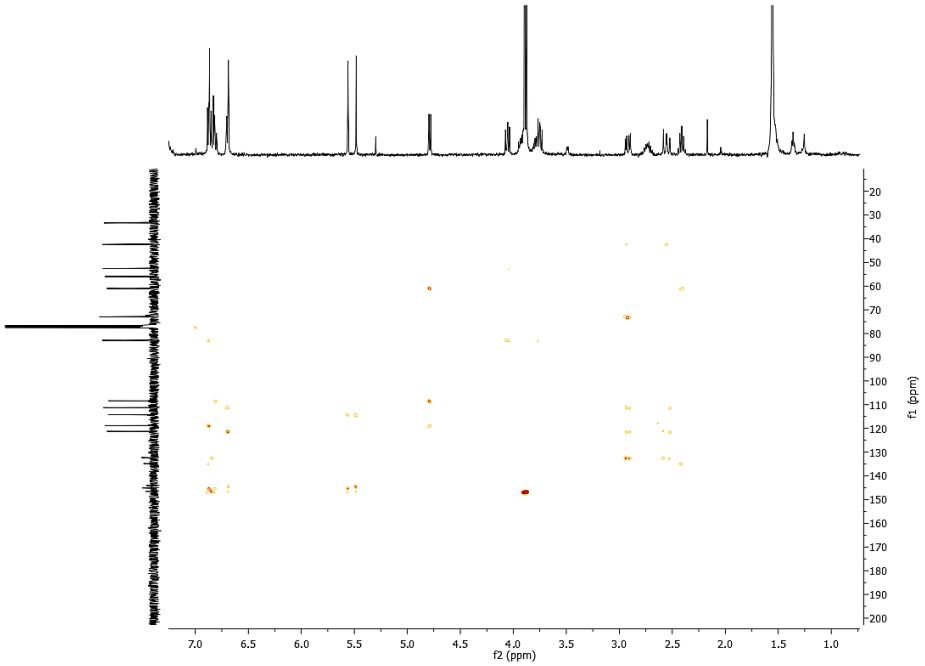

Fig. B.48 HMBC spectrum ($CDCl_3$) of compound **72**

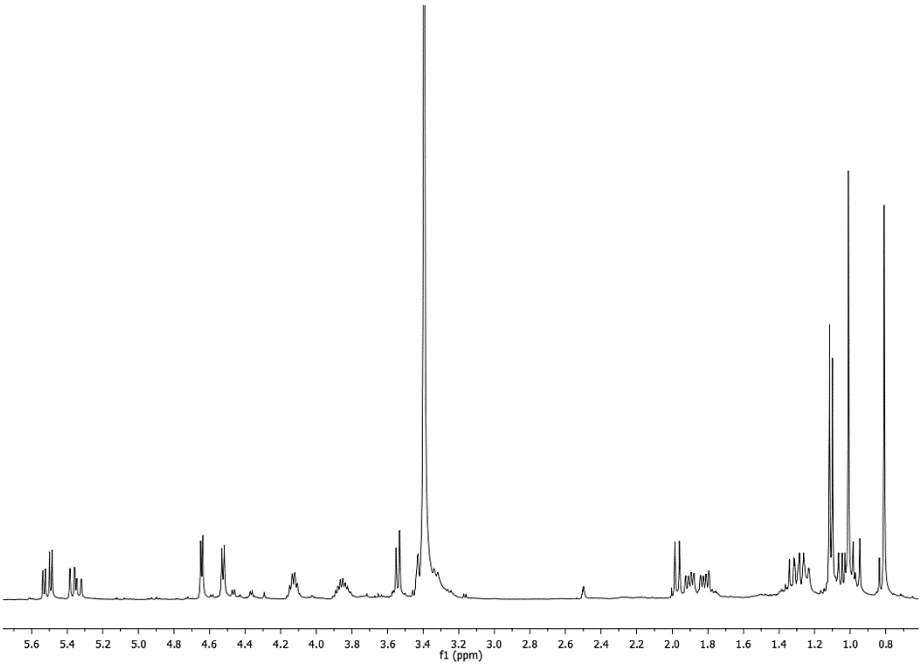

Fig. B.49 ^{1}H NMR (400 MHz, DMSO-d_6) spectrum of compound **73**

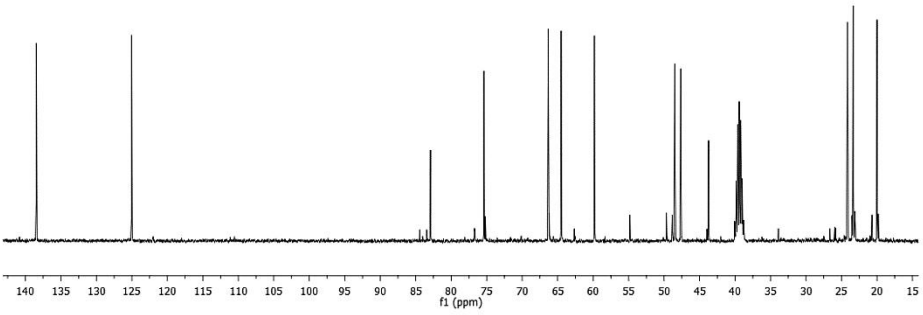

Fig. B.50 ^{13}C NMR (100 MHz, DMSO-d_6) spectrum of compound **73**

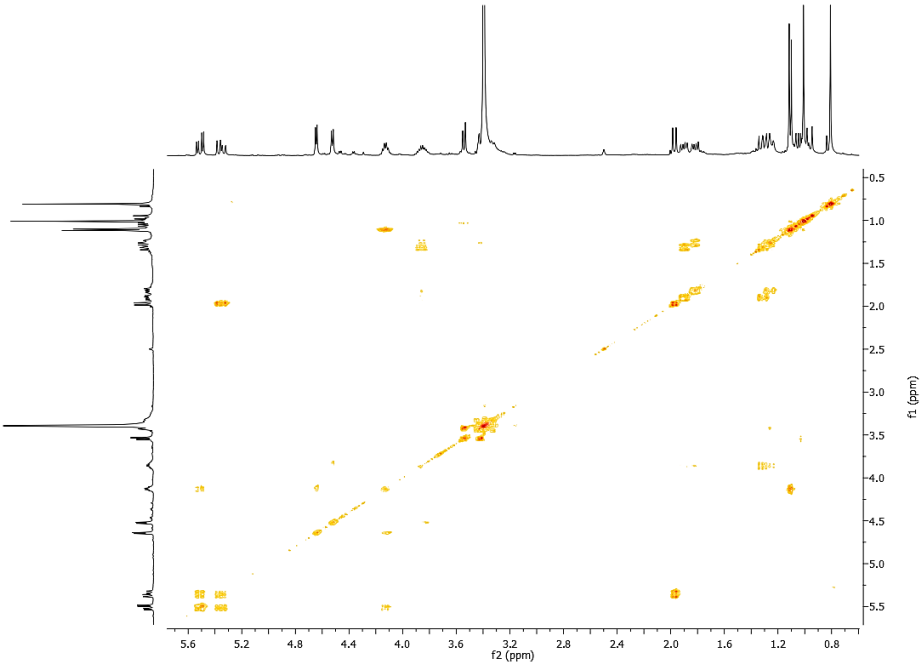

Fig. B.51 ^{1}H-^{1}H COSY spectrum (DMSO-d_6) of compound **73**

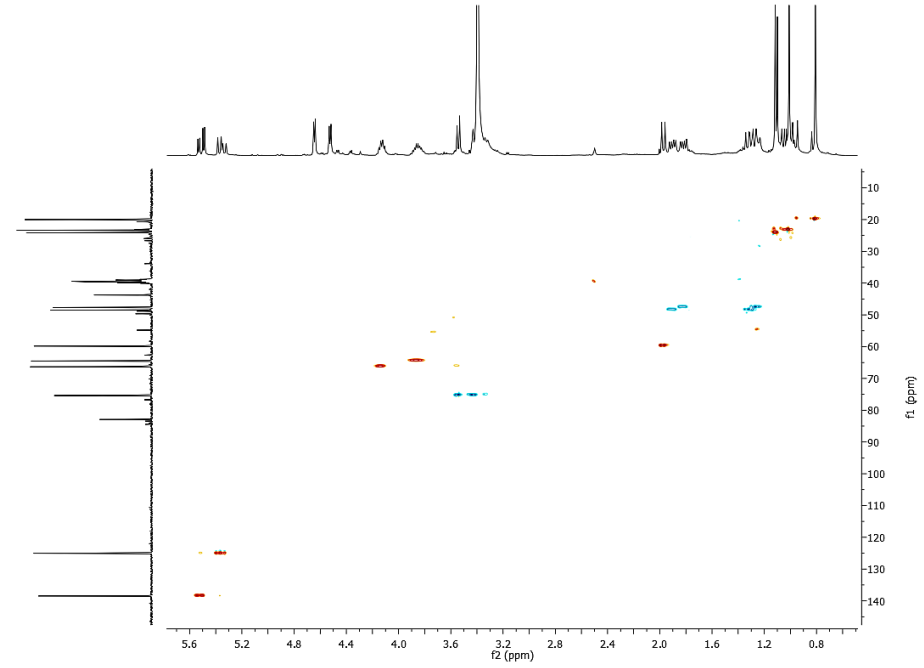

Fig. B.52 HSQC spectrum (DMSO-d_6) of compound **73**

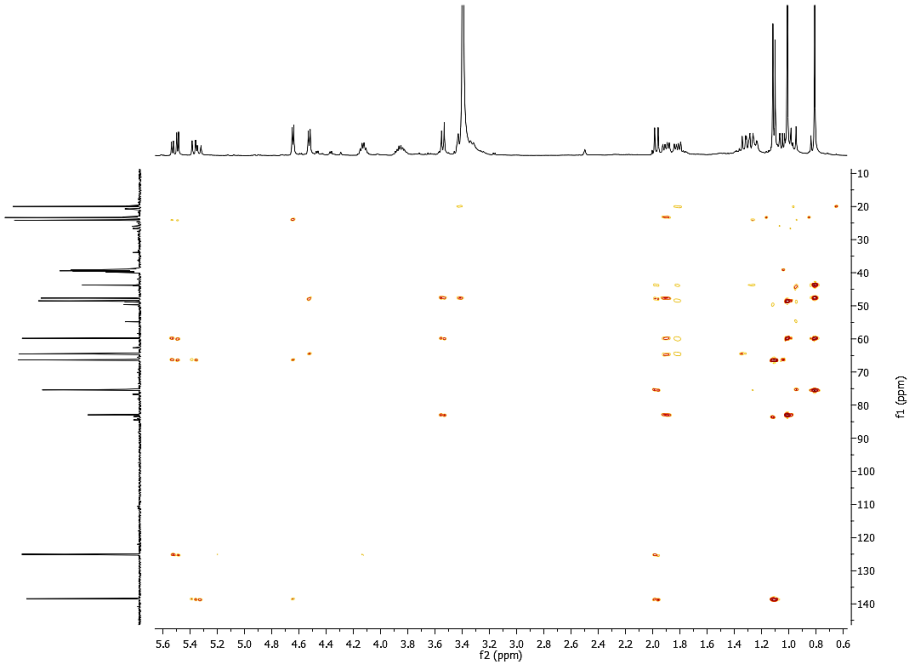

Fig. B.53 HMBC spectrum (DMSO-d_6) of compound **73**

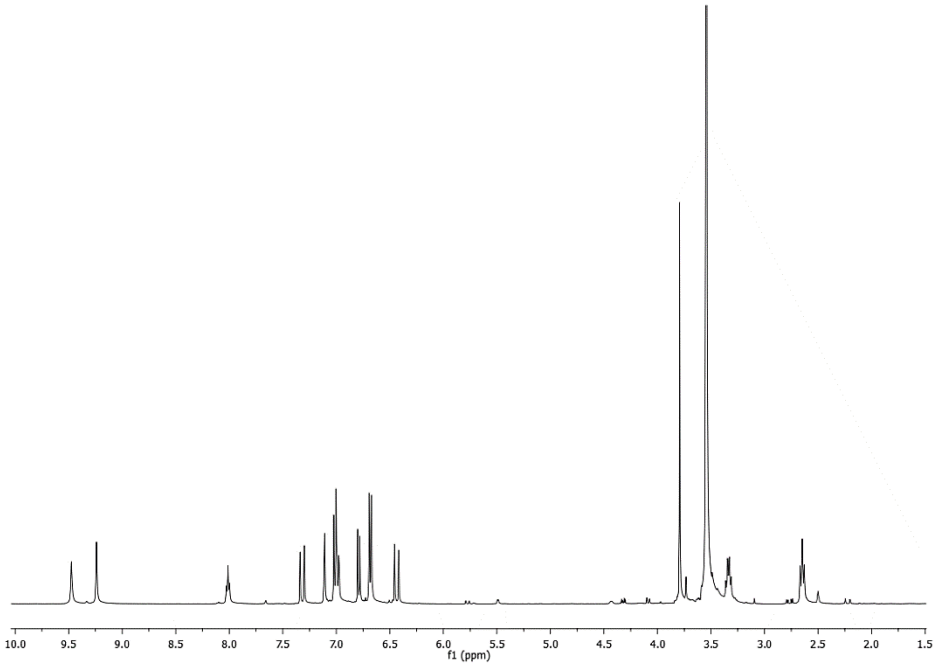

Fig. B.54 ^{1}H NMR (400 MHz, DMSO-d_6) spectrum of compound **74**

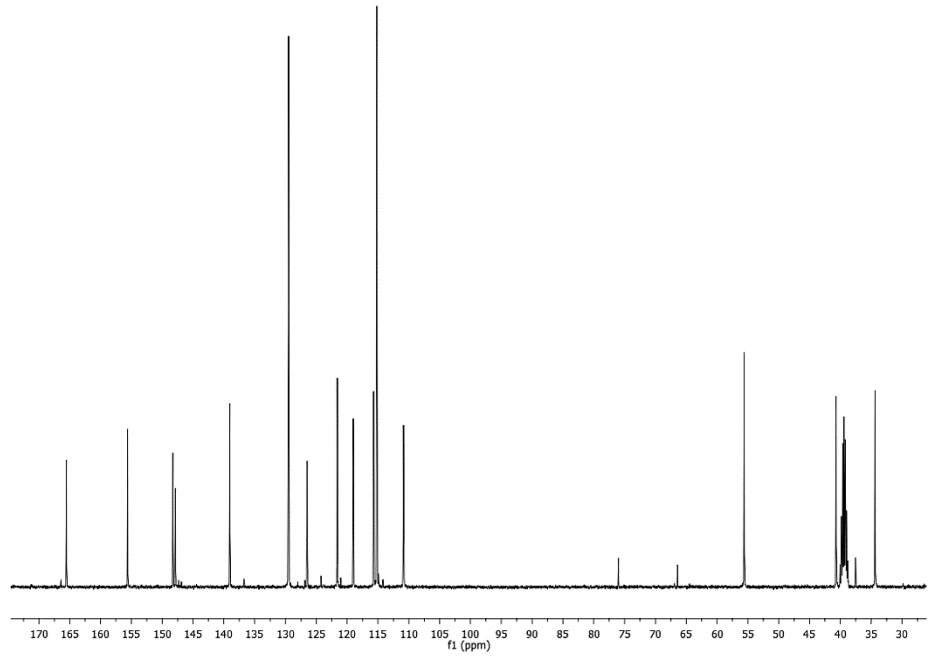

Fig. B.55 ^{13}C NMR (100 MHz, DMSO-d_6) spectrum of compound **74**

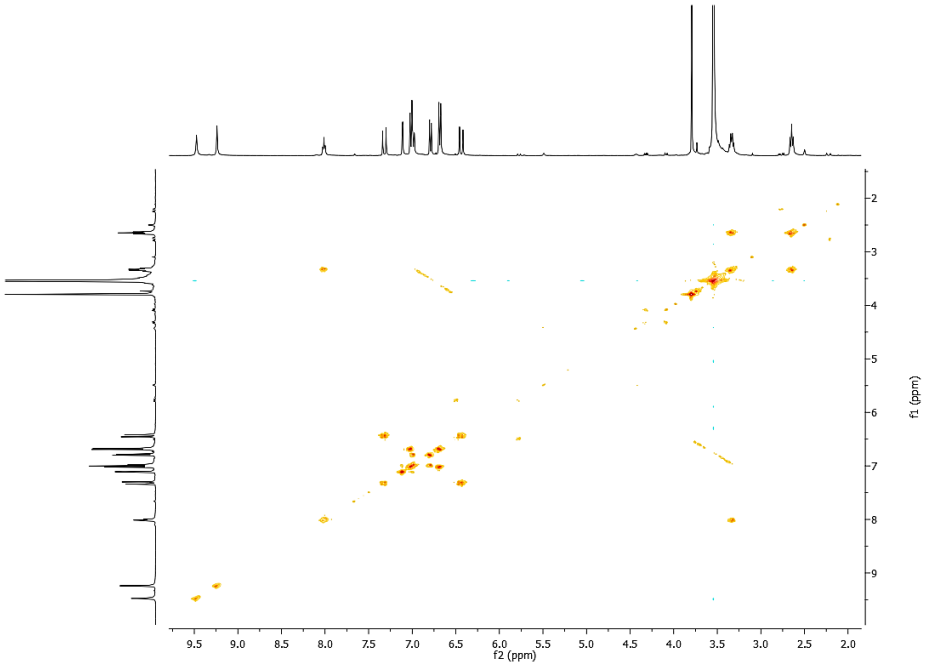

Fig. B.56 ^{1}H-^{1}H COSY spectrum (DMSO-d_6) of compound **74**

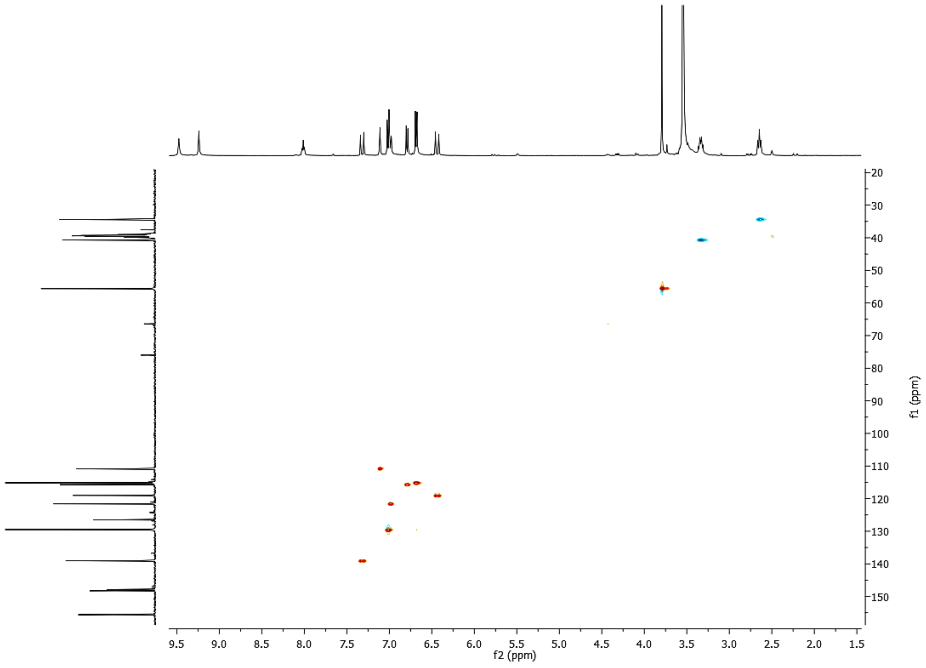

Fig. B.57 HSQC spectrum (DMSO-d_6) of compound **74**

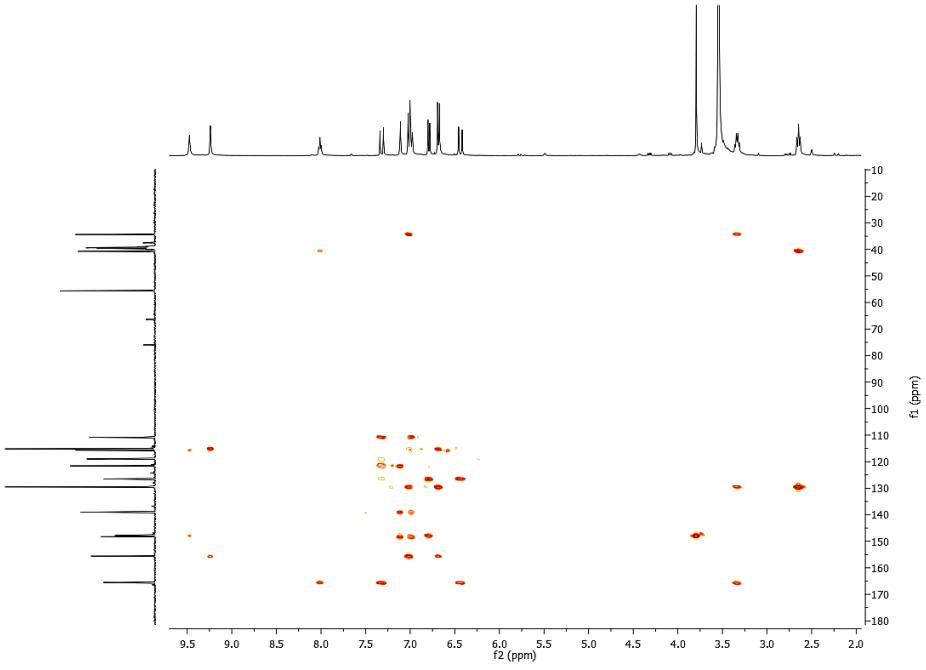

Fig. B.58 HMBC spectrum (DMSO-d_6) of compound **74**

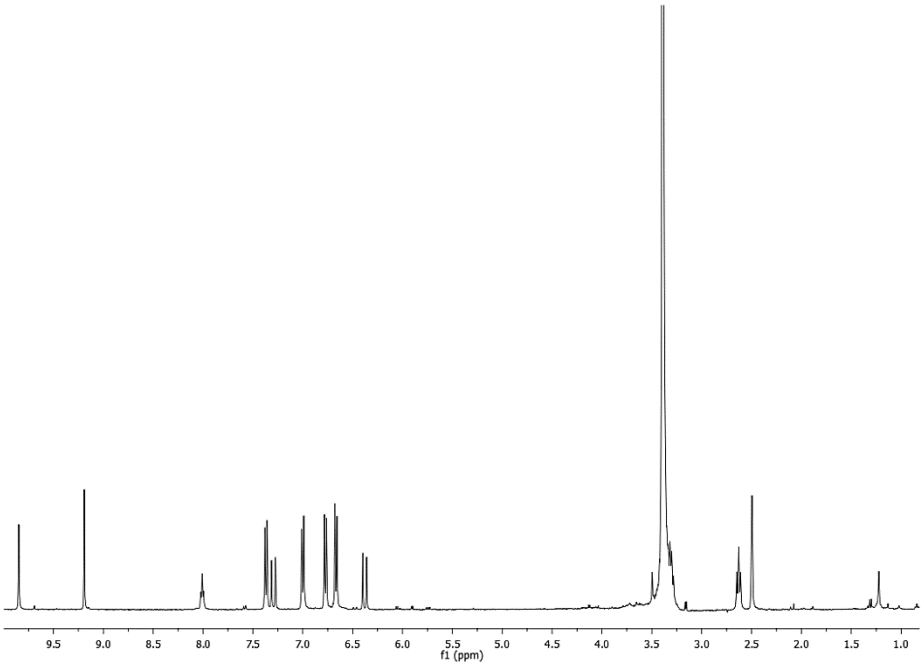

Fig. B.59 ^{1}H NMR (400 MHz, DMSO-d_6) spectrum of compound **75**

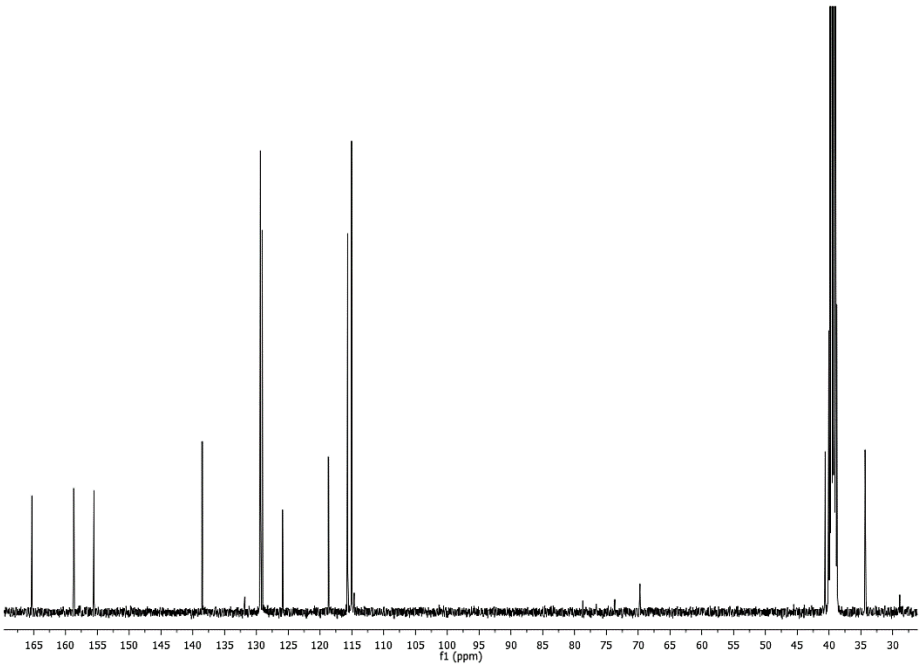

Fig. B.60 ^{13}C NMR (100 MHz, DMSO-d_6) spectrum of compound **75**

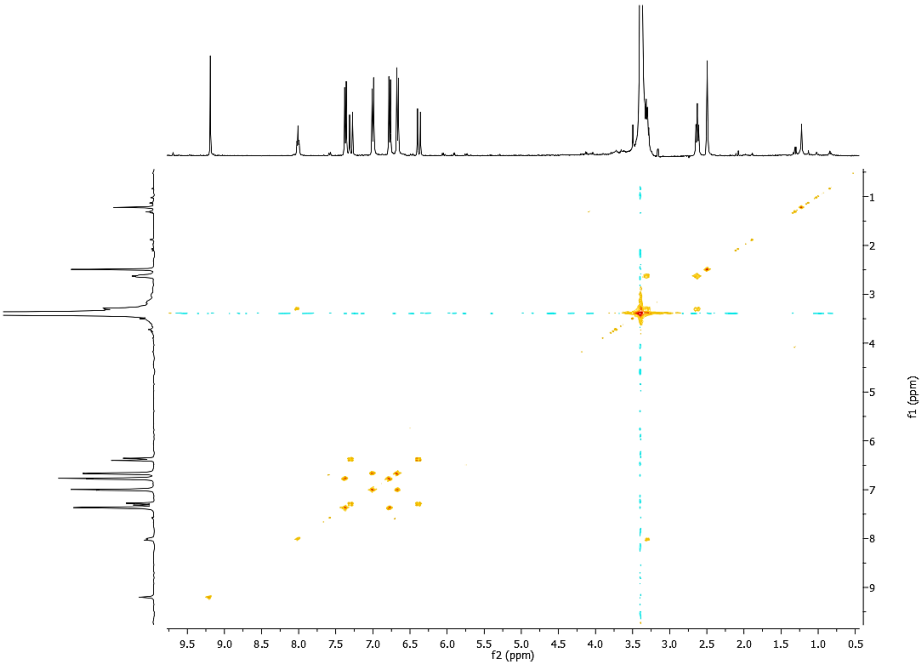

Fig. B.61 ^{1}H-^{1}H COSY spectrum (DMSO-d_6) of compound **75**

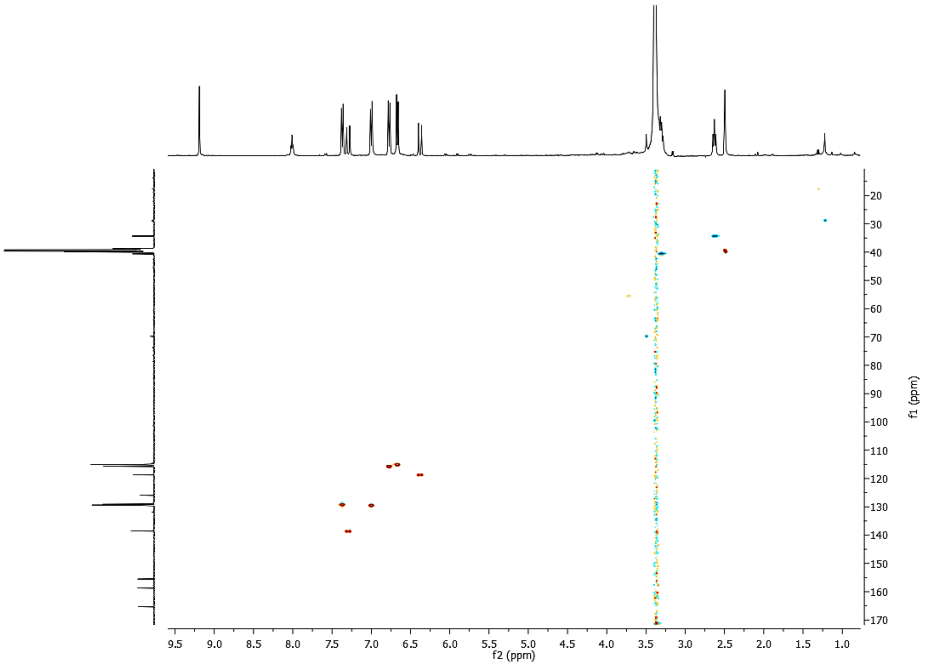

Fig. B.62 HSQC spectrum (DMSO-d_6) of compound **75**

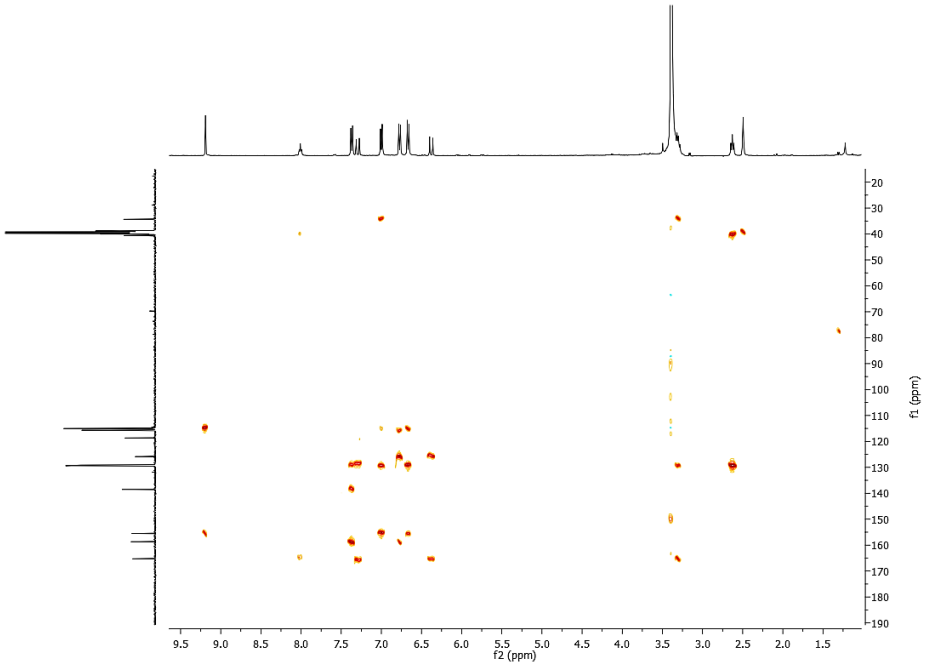

Fig. B.63 HMBC spectrum (DMSO-d_6) of compound **75**

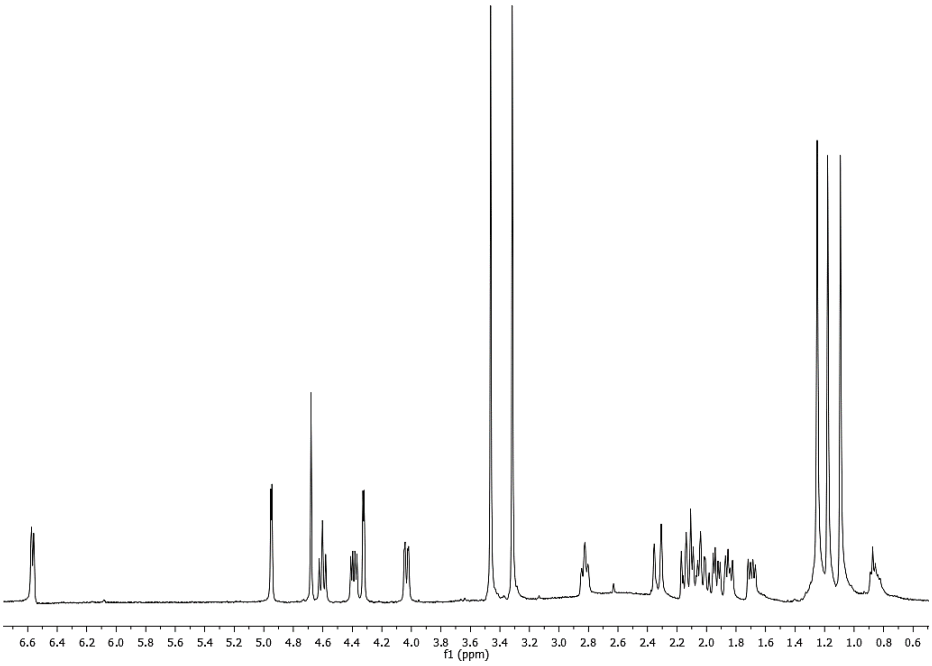

Fig. B.64 ^{1}H NMR (400 MHz, $CDCl_3$) spectrum of compound **76**

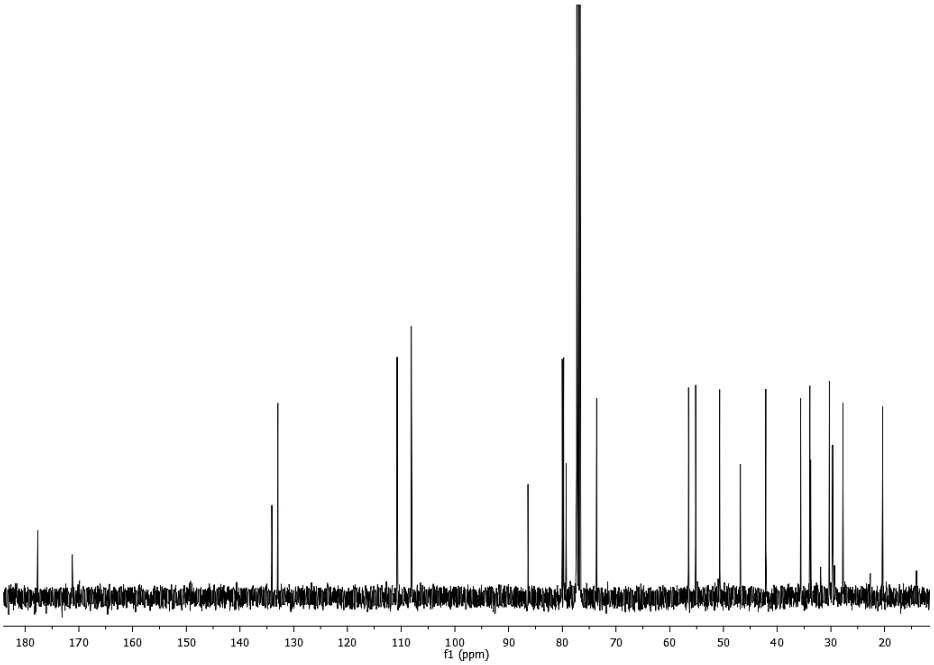

Fig. B.65 ^{13}C NMR (100 MHz, $CDCl_3$) spectrum of compound **76**

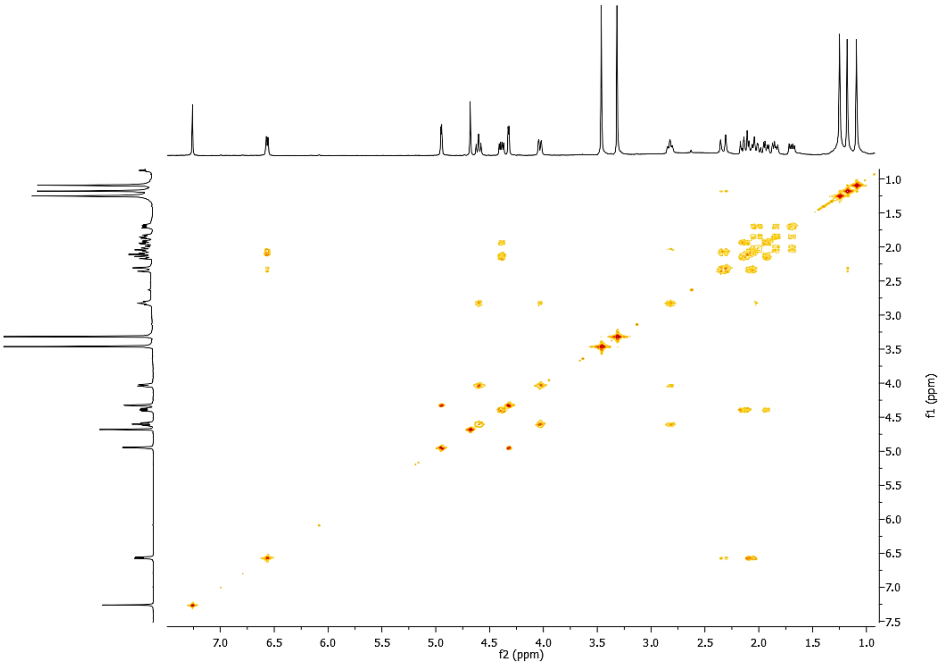

Fig. B.66 ^{1}H-^{1}H COSY spectrum ($CDCl_3$) of compound **76**

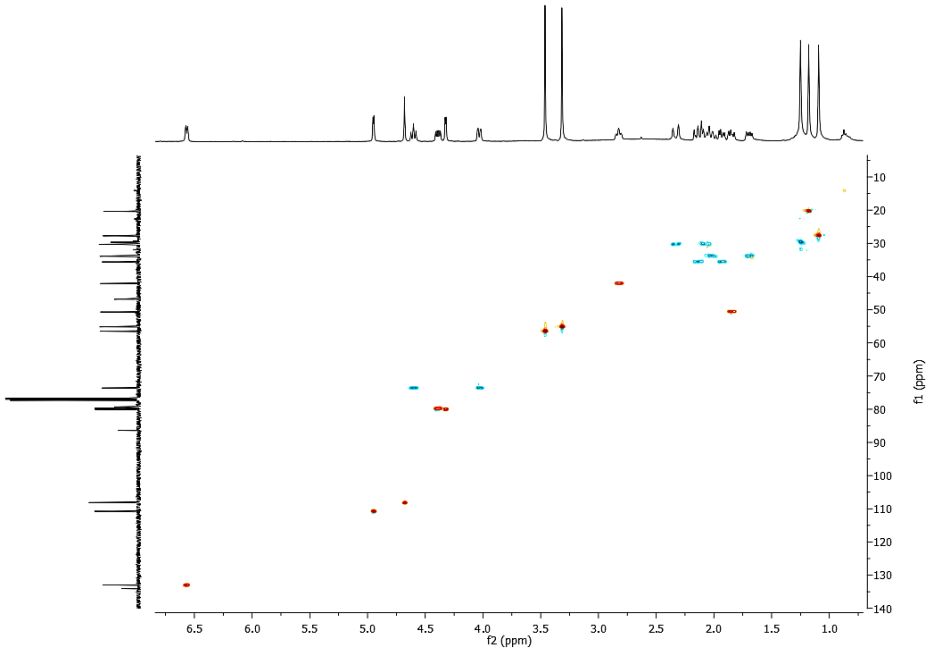

Fig. B.67 HSQC spectrum ($CDCl_3$) of compound **76**

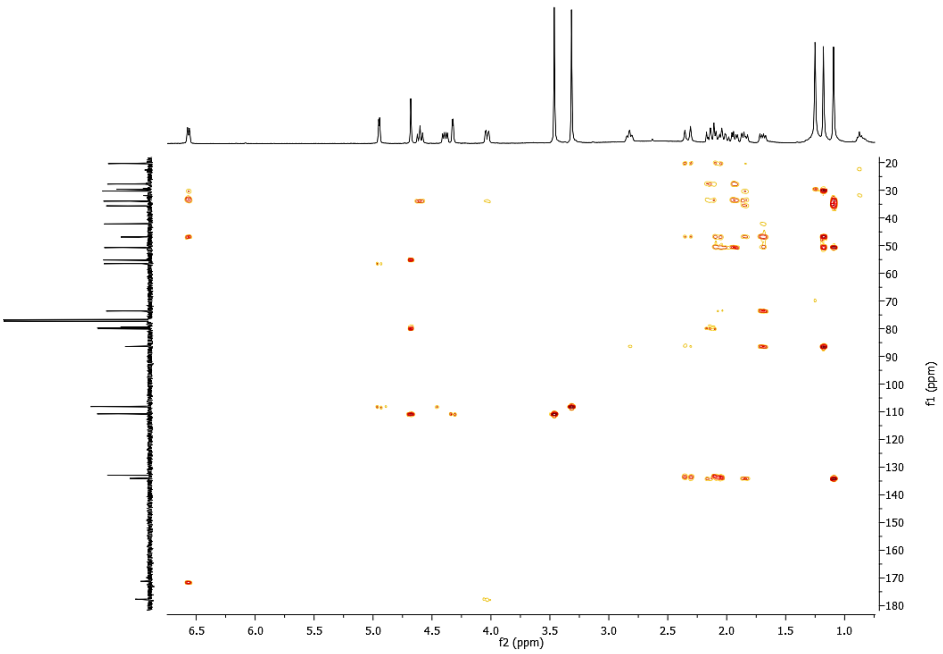

Fig. B.68 HMBC spectrum ($CDCl_3$) of compound **76**

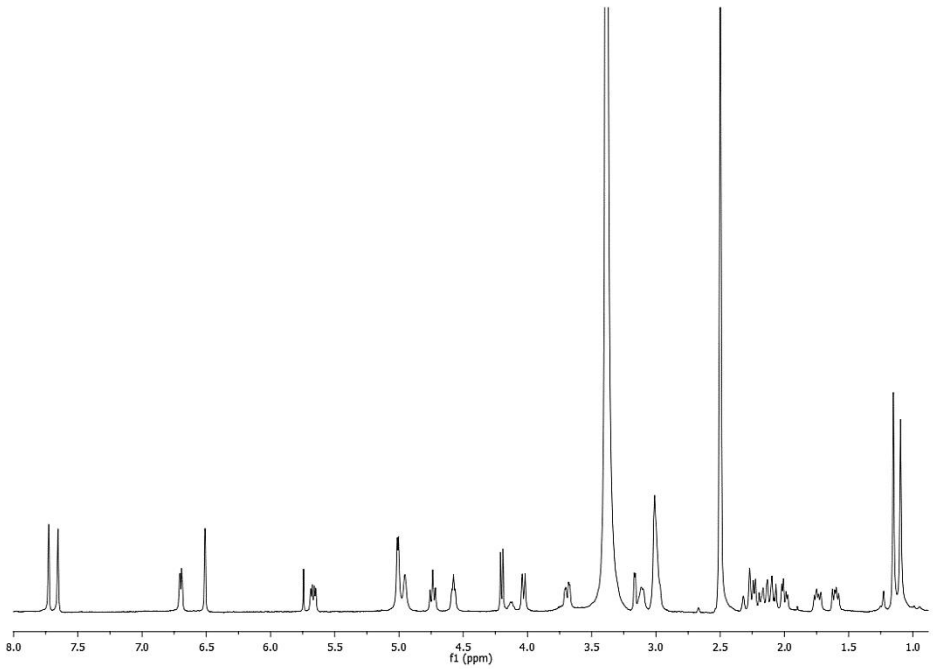

Fig. B.69 ^{1}H NMR (400 MHz, DMSO-d_6) spectrum of compound **77**

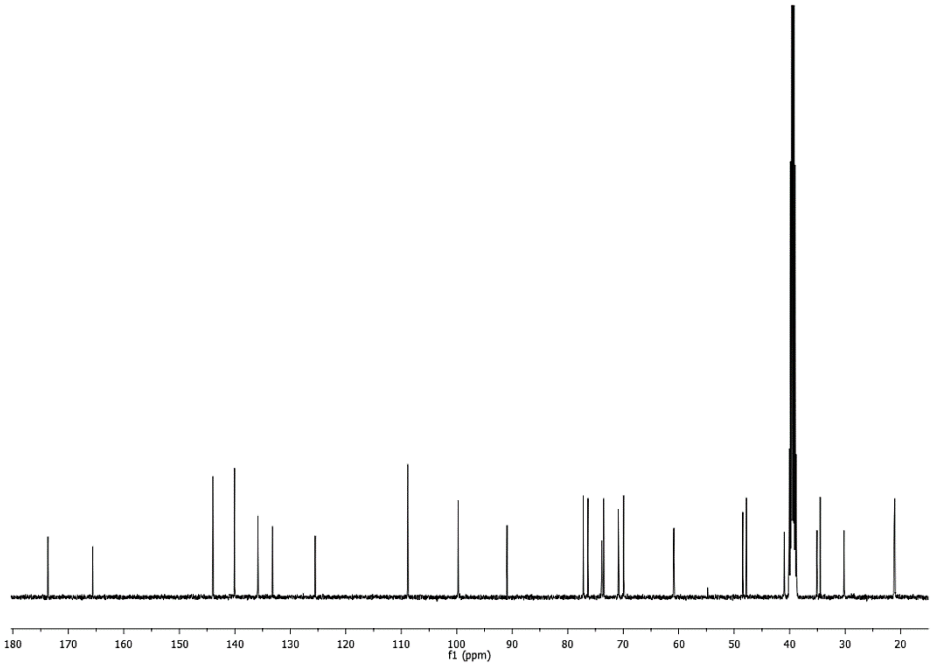

Fig. B.70 ^{13}C NMR (100 MHz, DMSO-d_6) spectrum of compound **77**

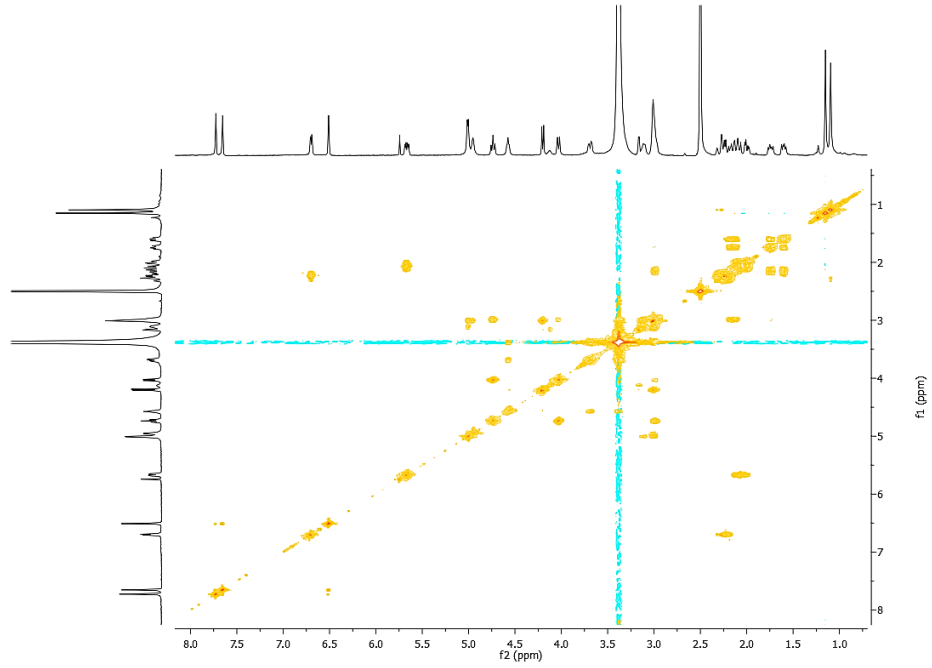

Fig. B.71 ^{1}H-^{1}H COSY spectrum (DMSO-d_6) of compound **77**

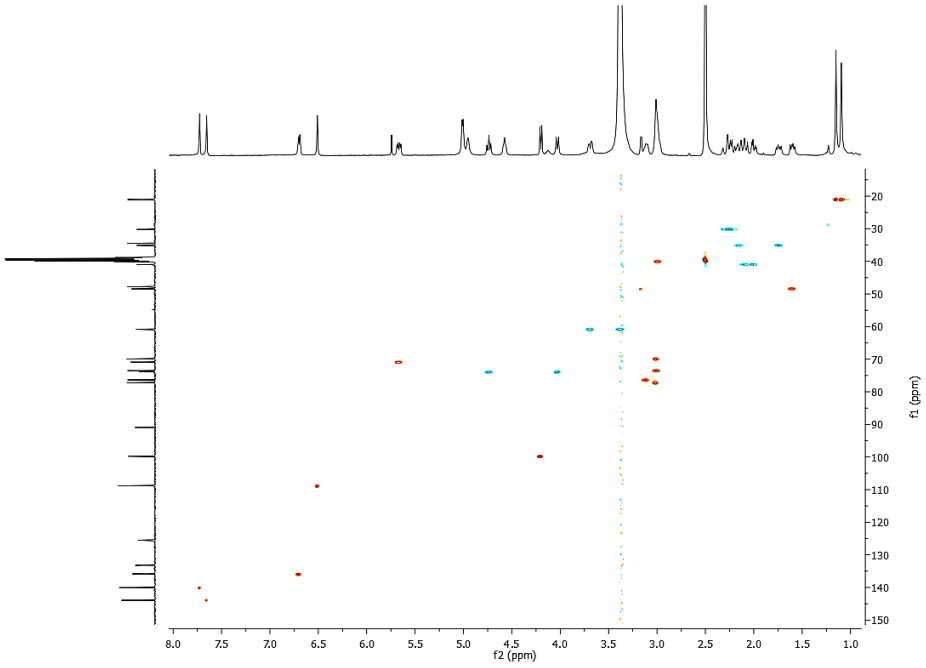

Fig. B.72 HSQC spectrum (DMSO-d_6) of compound **77**

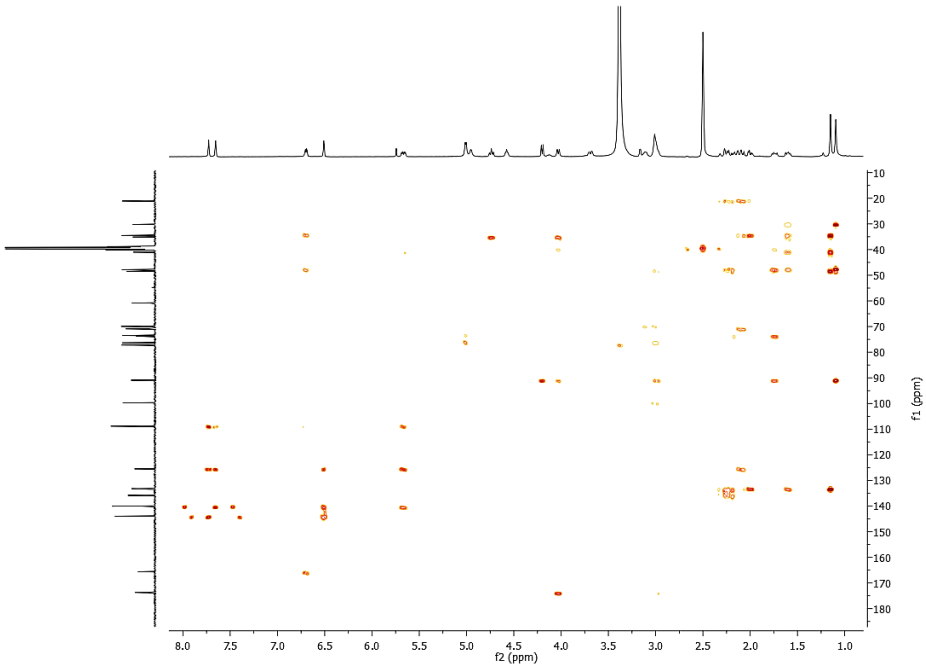

Fig. B.73 HMBC spectrum (DMSO-d_6) of compound **77**

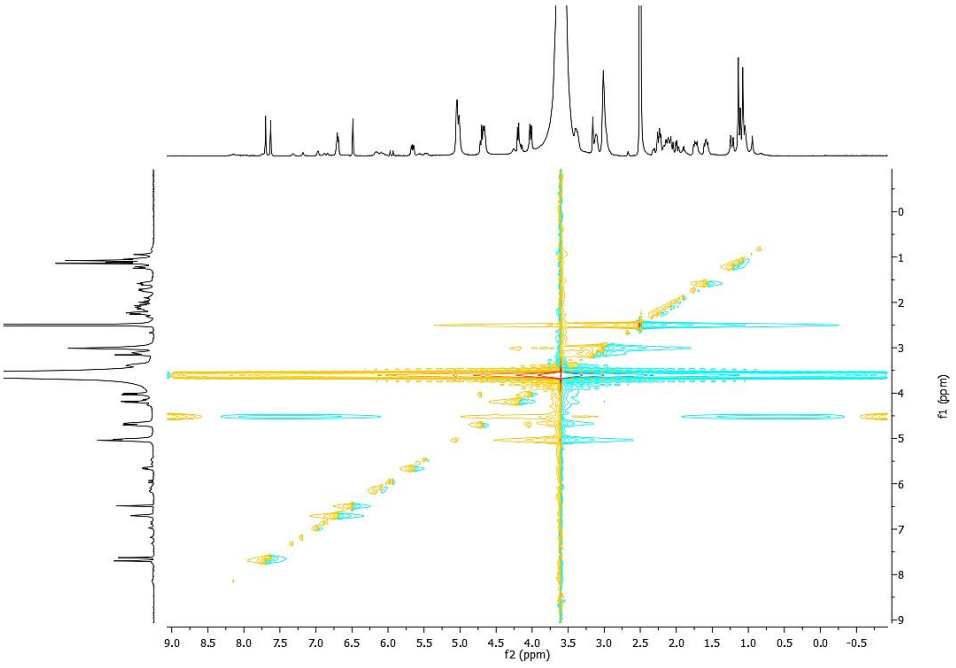

Fig. B.74 NOESY spectrum (DMSO-d_6) of compound **77**

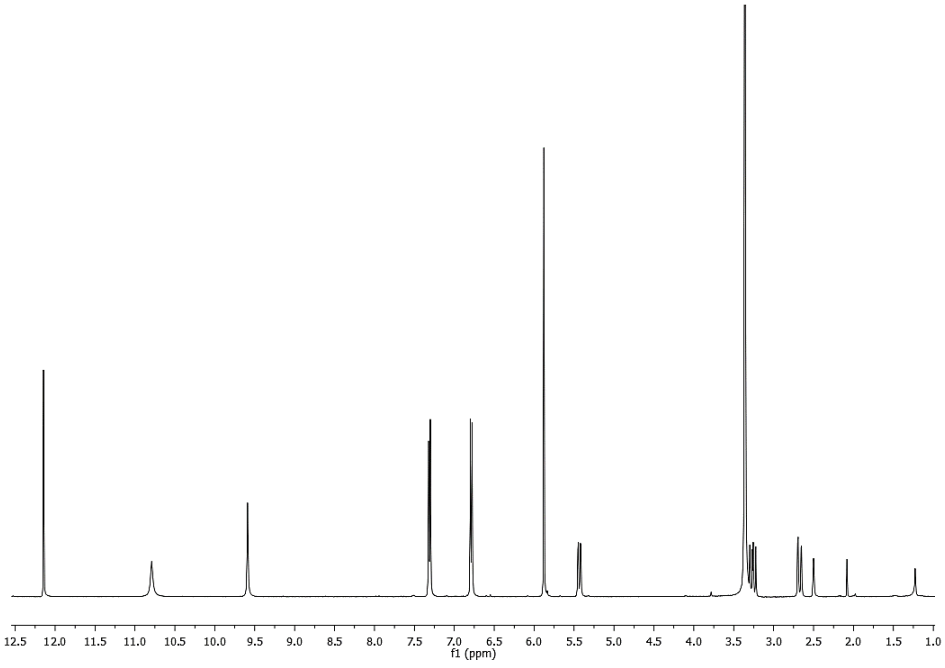

Fig. B.75 ^{1}H NMR (400 MHz, DMSO-d_6) spectrum of compound **78**

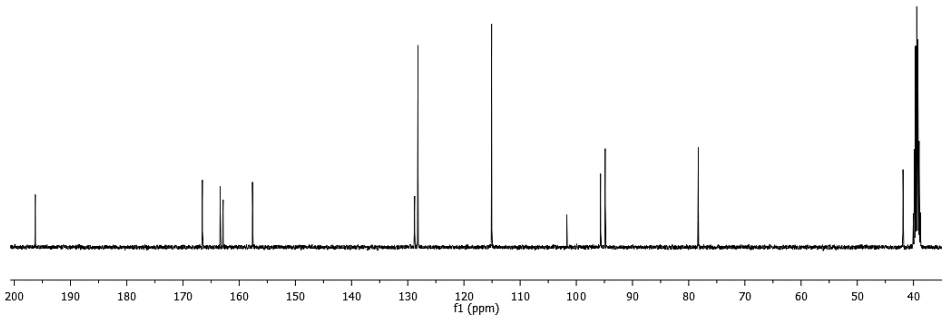

Fig. B.76 ^{13}C NMR (100 MHz, DMSO-d_6) spectrum of compound **78**

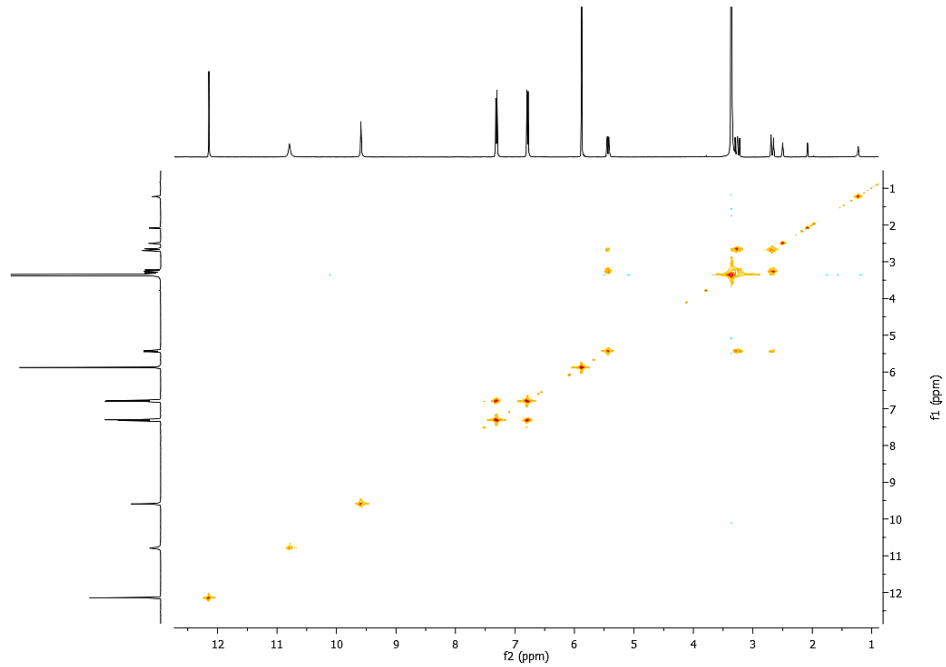

Fig. B.77 ^{1}H-^{1}H COSY spectrum (DMSO-d_6) of compound **78**

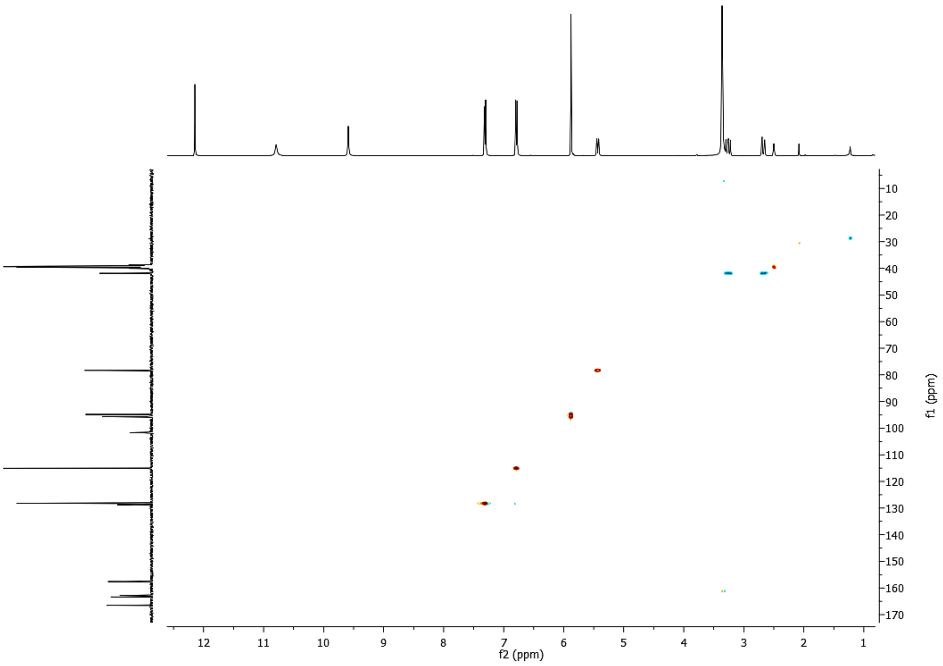

Fig. B.78 HSQC spectrum (DMSO-d_6) of compound **78**

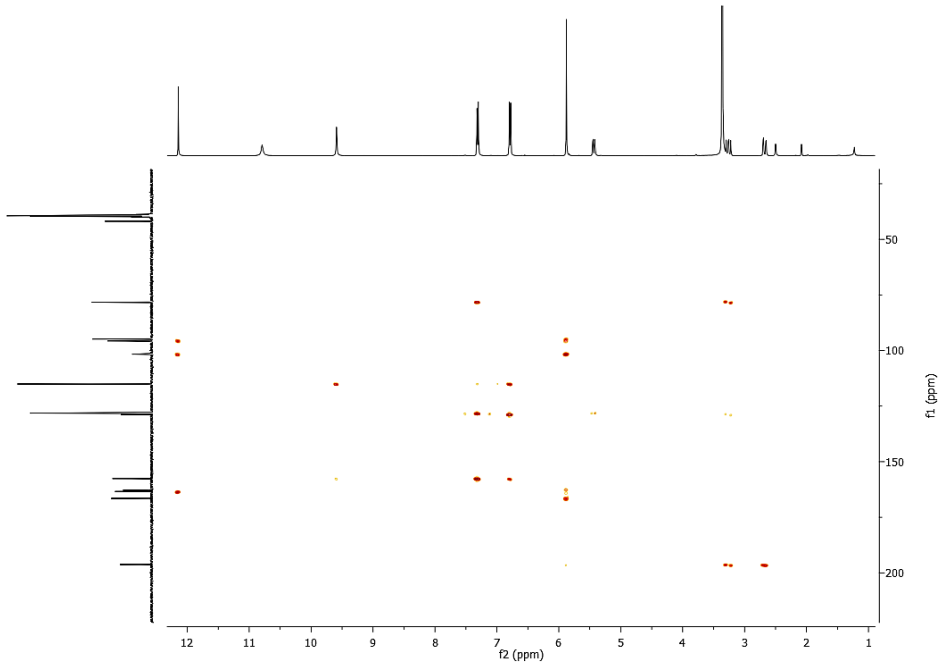

Fig. B.79 HMBC spectrum (DMSO-d_6) of compound **78**

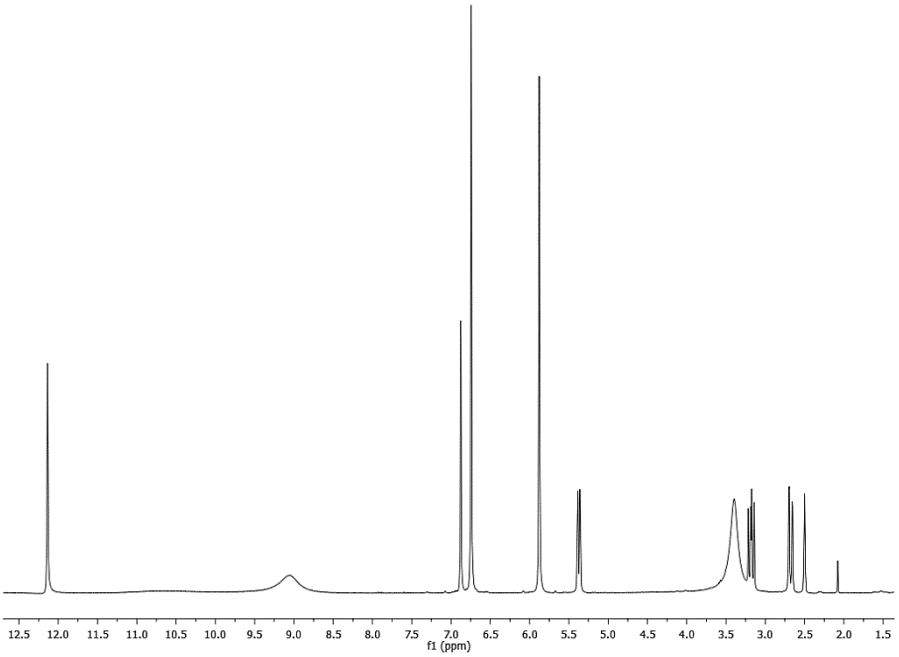

Fig. B.80 ^{1}H NMR (400 MHz, DMSO-d_6) spectrum of compound **79**

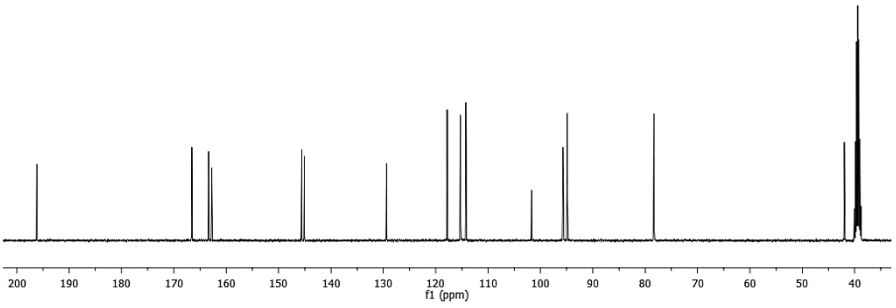

Fig. B.81 ^{13}C NMR (100 MHz, DMSO-d_6) spectrum of compound **79**

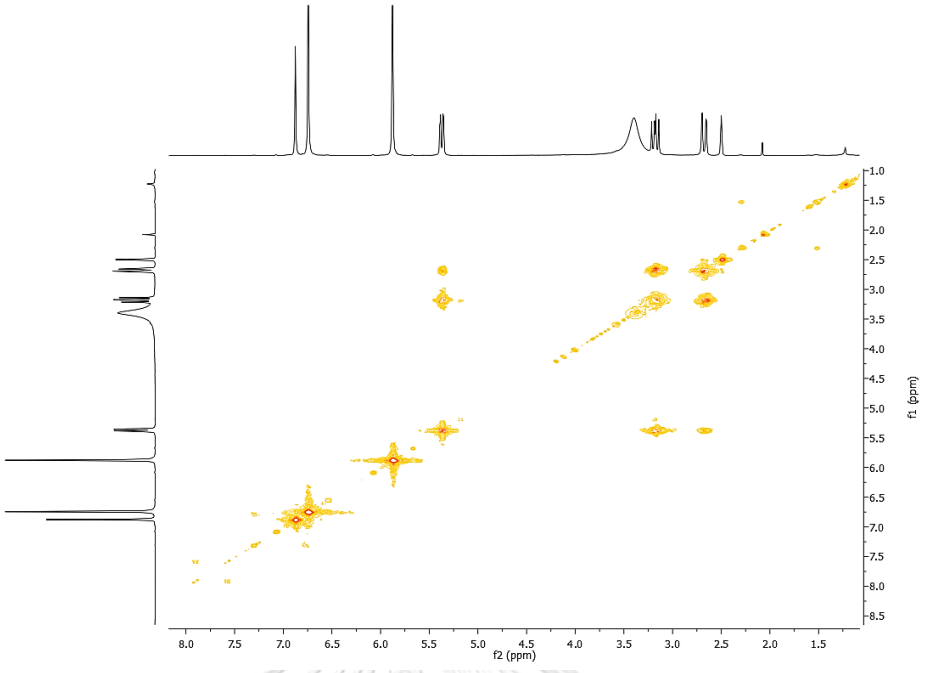

Fig. B.82 ^{1}H-^{1}H COSY spectrum (DMSO-d_6) of compound **79**

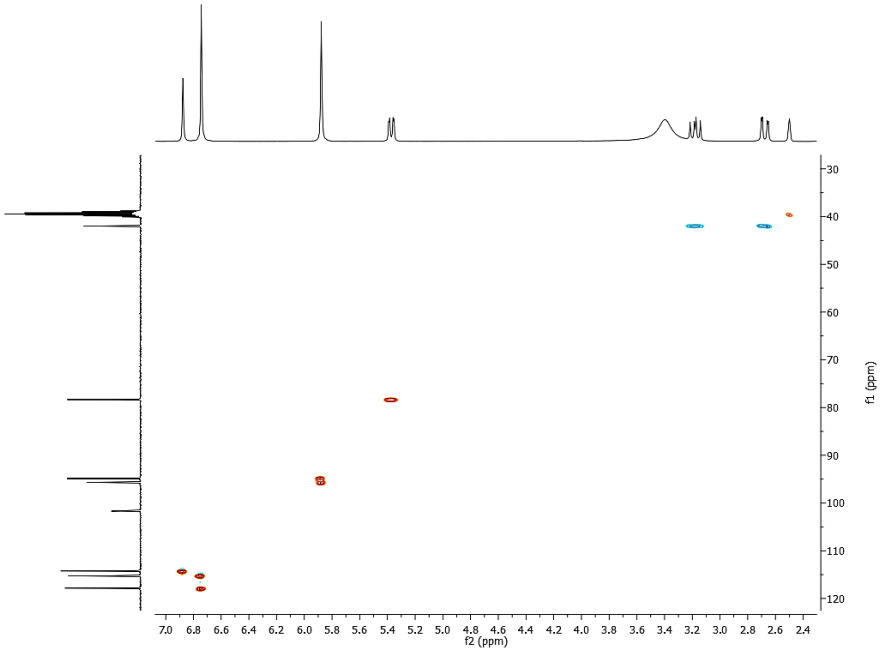

Fig. B.83 HSQC spectrum (DMSO-d_6) of compound **79**

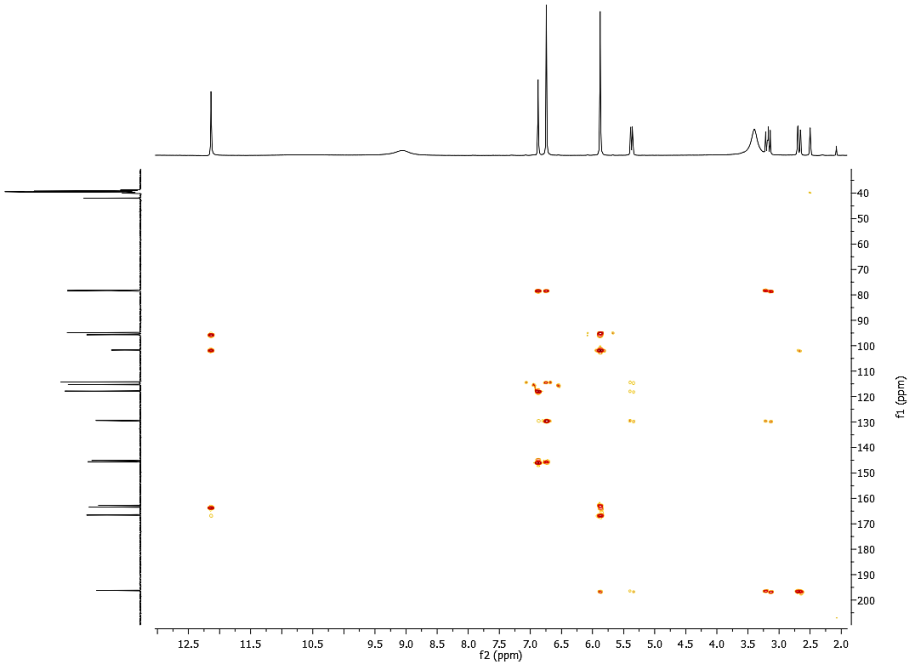

Fig. B.84 HMBC spectrum (DMSO-d_6) of compound **79**

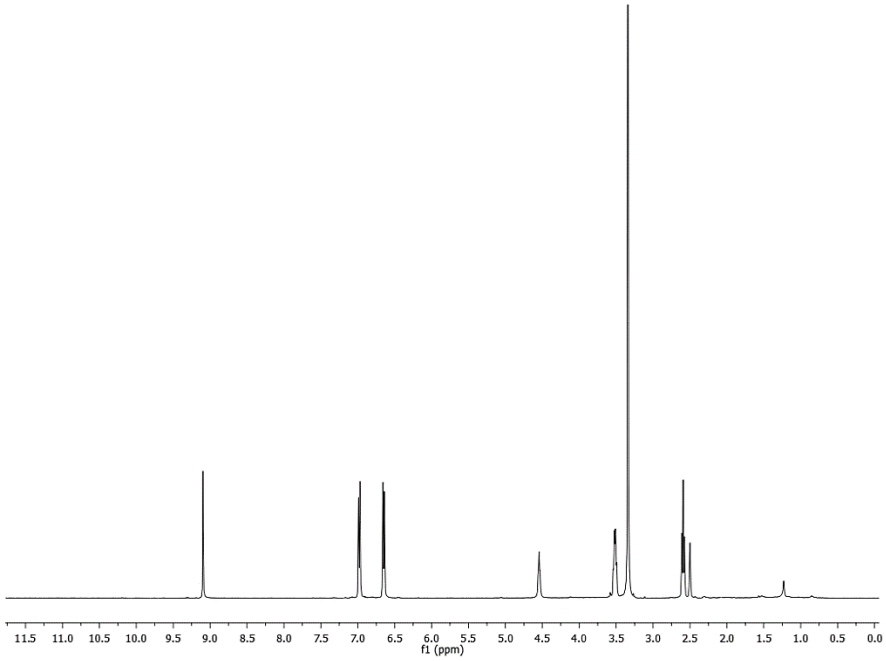

Fig. B.85 ^{1}H NMR (400 MHz, DMSO-d_6) spectrum of compound **80**

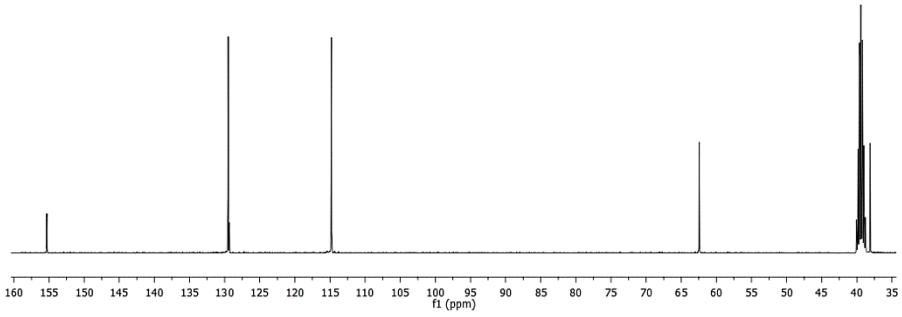

Fig. B.86 ^{13}C NMR (100 MHz, DMSO-d_6) spectrum of compound **80**

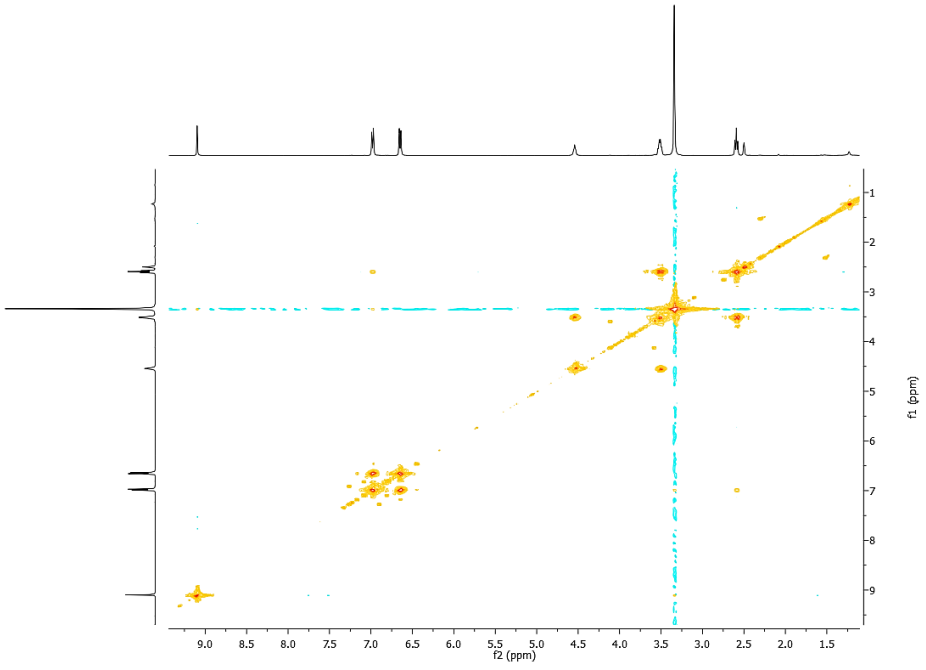

Fig. B.87 ^{1}H-^{1}H COSY spectrum (DMSO-d_6) of compound **80**

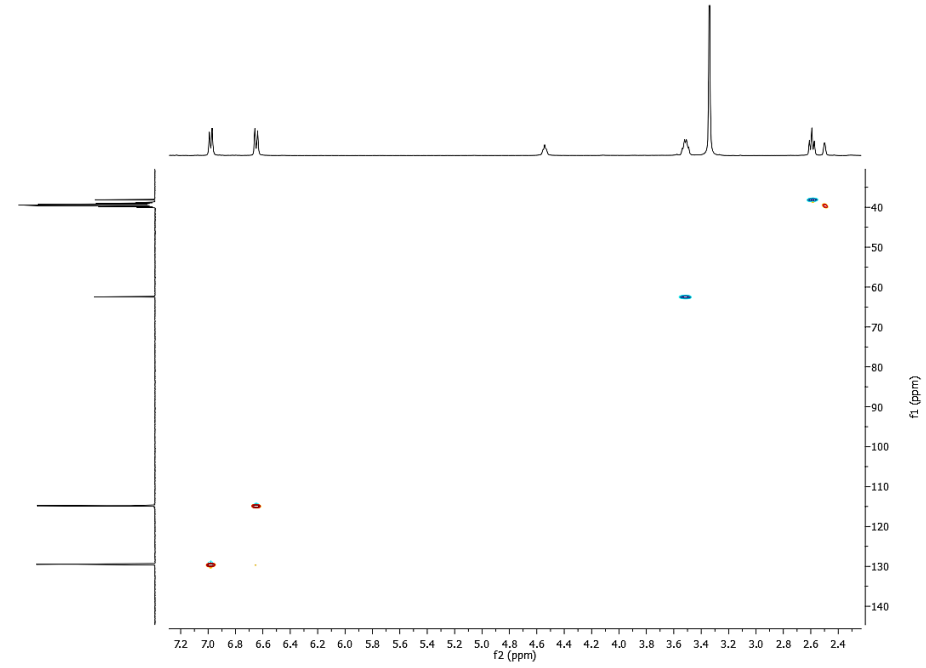

Fig. B.88 HSQC spectrum (DMSO-d_6) of compound **80**

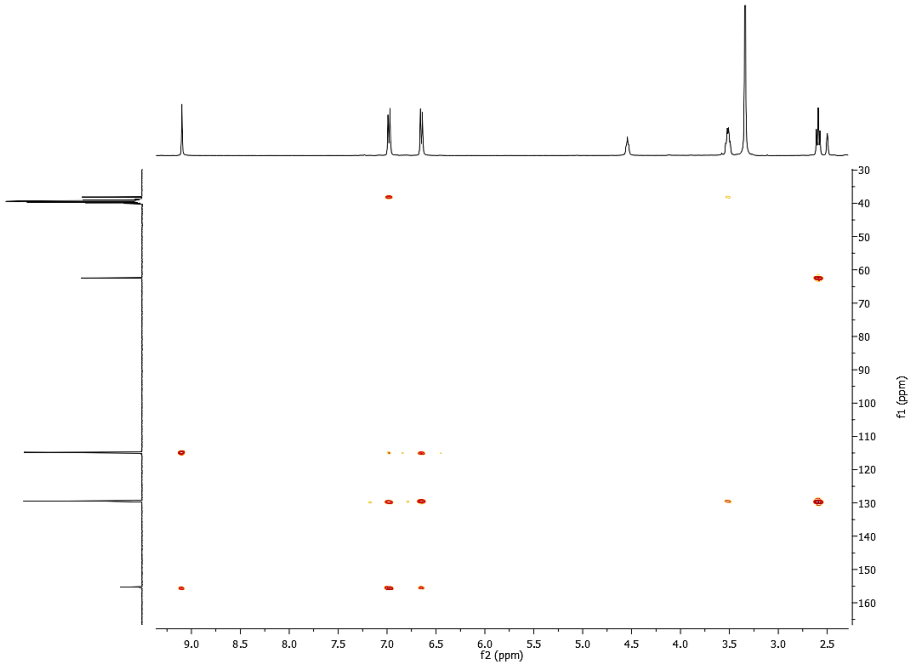

Fig. B.89 HMBC spectrum (DMSO-d_6) of compound **80**

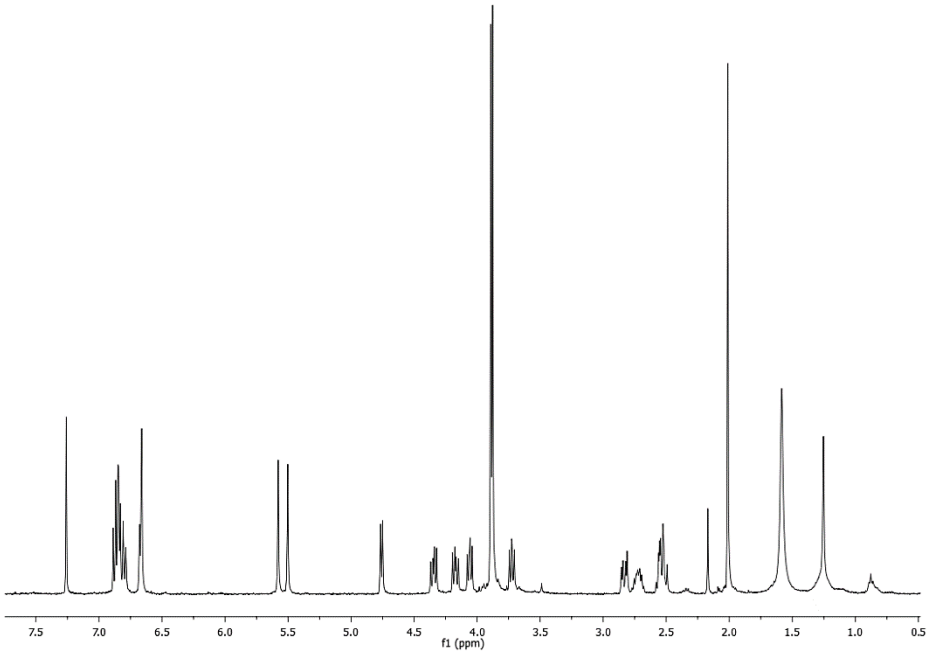

Fig. B.90 ^{1}H NMR (400 MHz, $CDCl_3$) spectrum of compound **81**

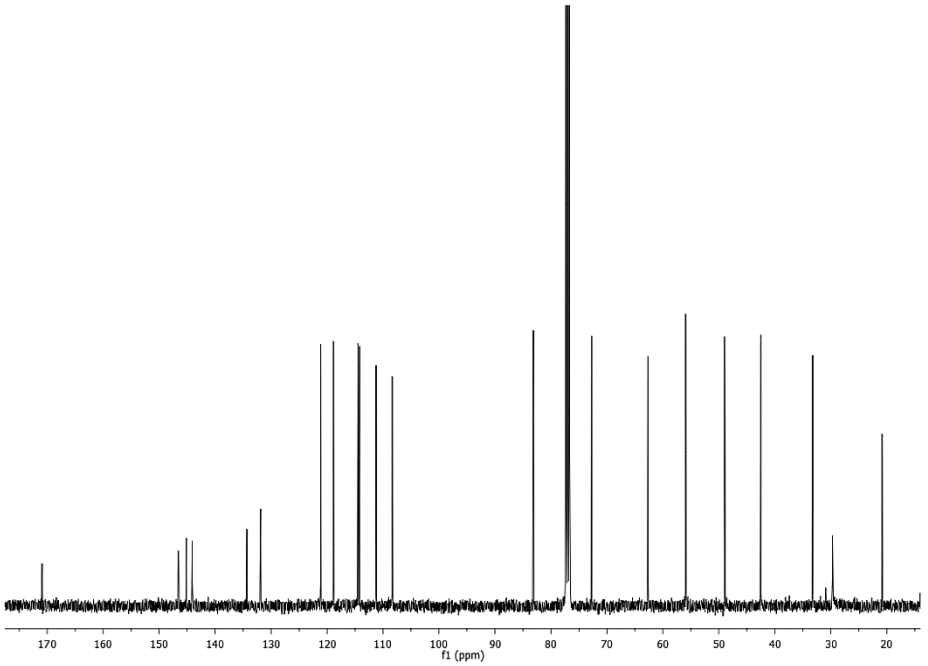

Fig. B.91 ^{13}C NMR (100 MHz, $CDCl_3$) spectrum of compound **81**

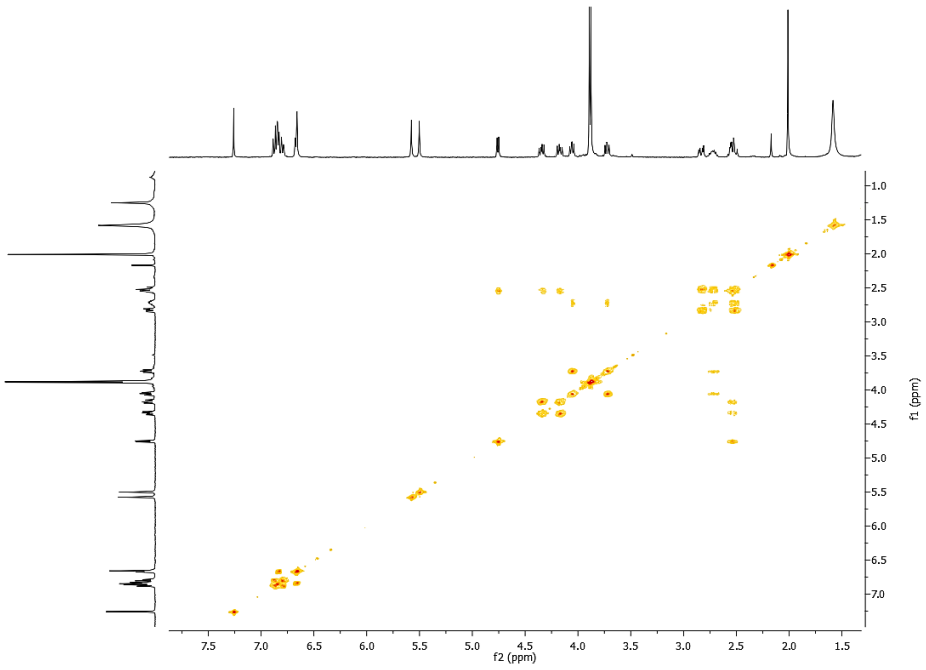

Fig. B.92 ^{1}H-^{1}H COSY spectrum ($CDCl_3$) of compound **81**

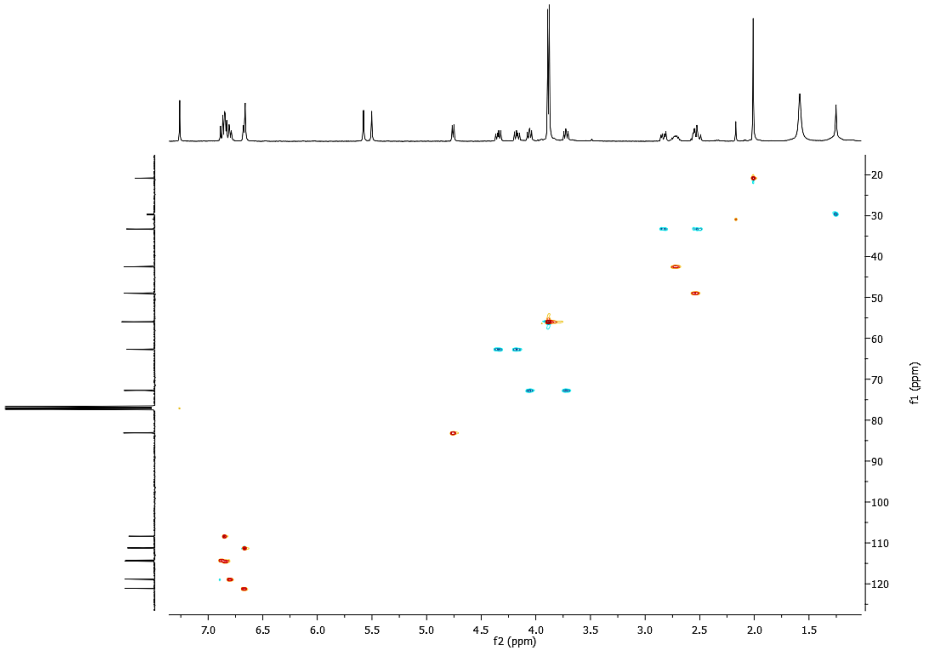

Fig. B.93 HSQC spectrum ($CDCl_3$) of compound **81**

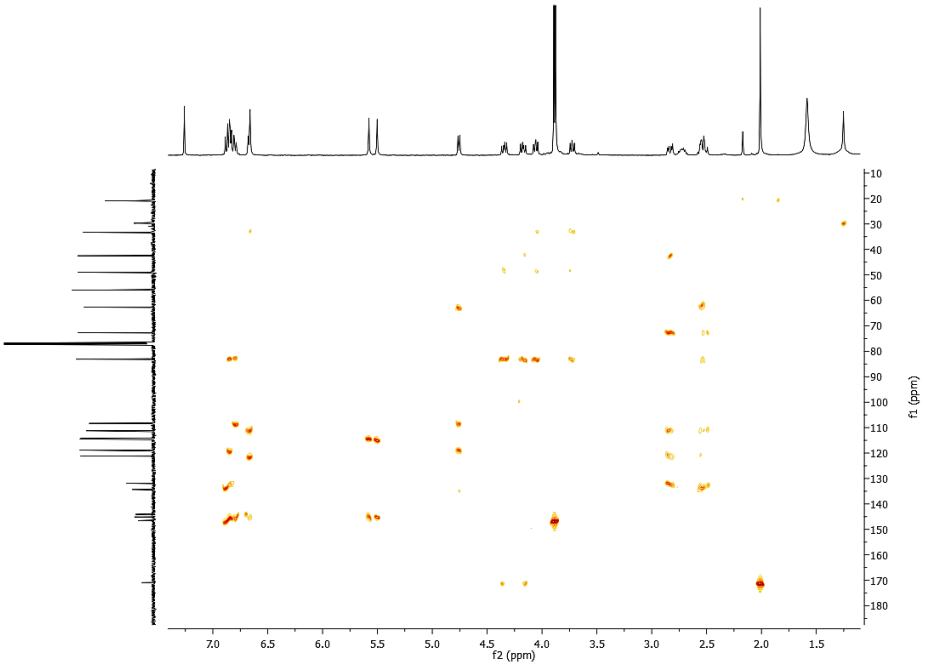

Fig. B.94 HMBC spectrum ($CDCl_3$) of compound **81**

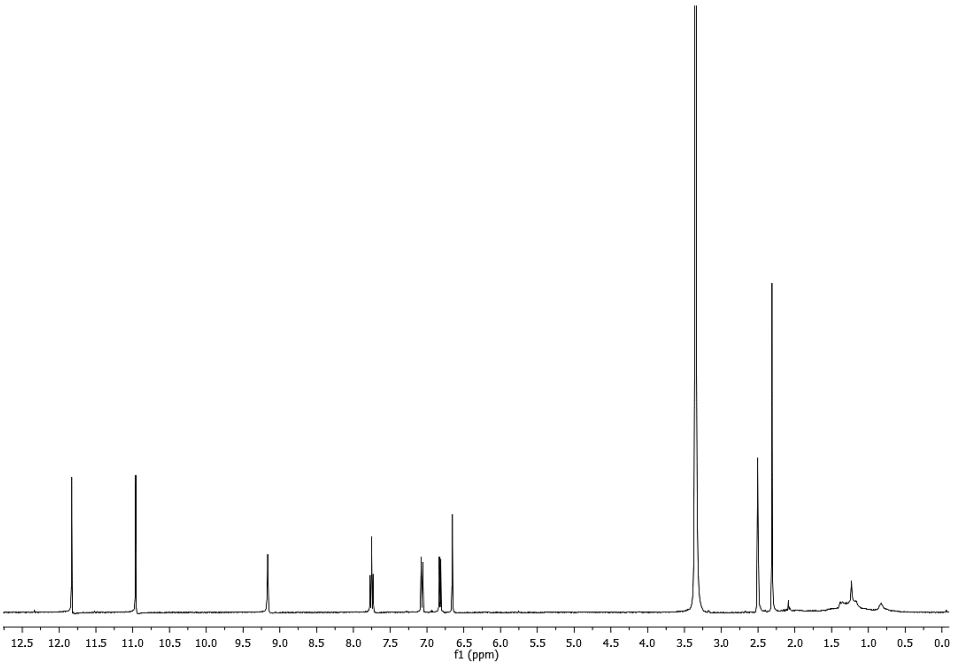

Fig. B.95 ^{1}H NMR (400 MHz, DMSO-d_6) spectrum of compound **82**

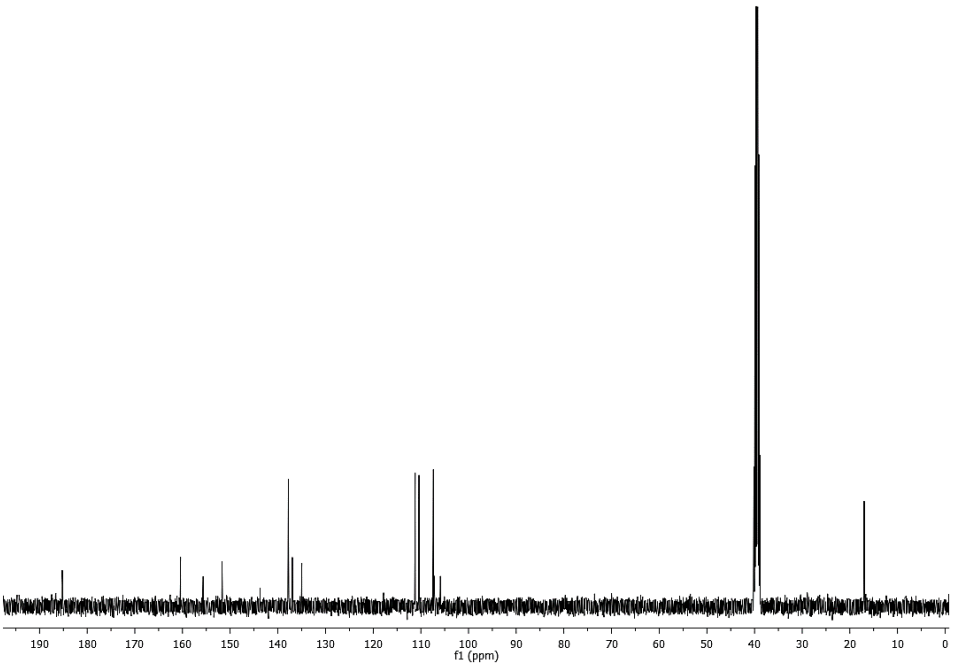

Fig. B.96 ^{13}C NMR (100 MHz, DMSO-d_6) spectrum of compound **82**

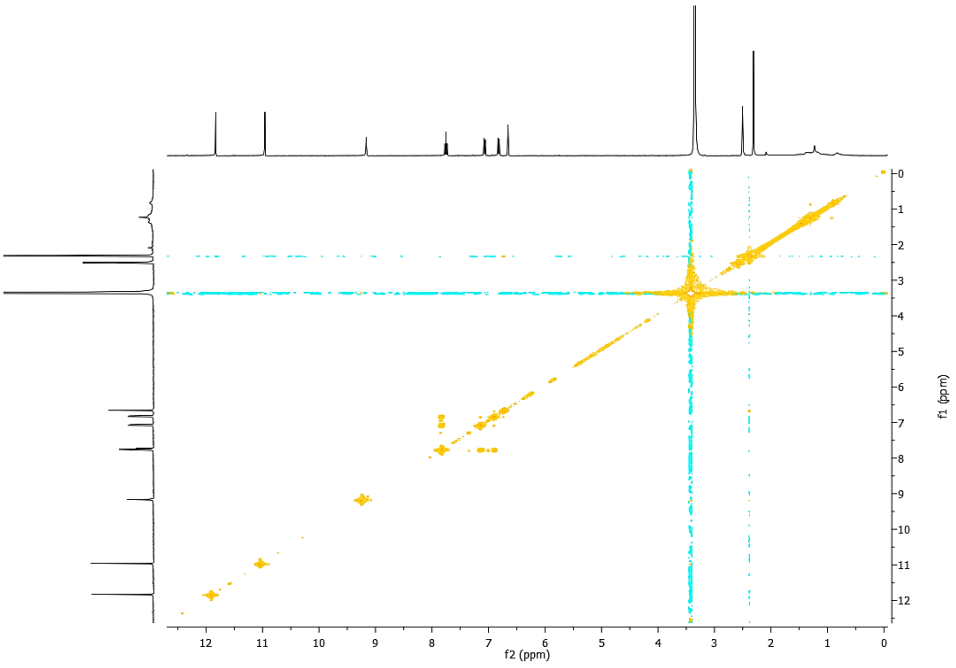

Fig. B.97 ^{1}H-^{1}H COSY spectrum (DMSO-d_6) of compound **82**

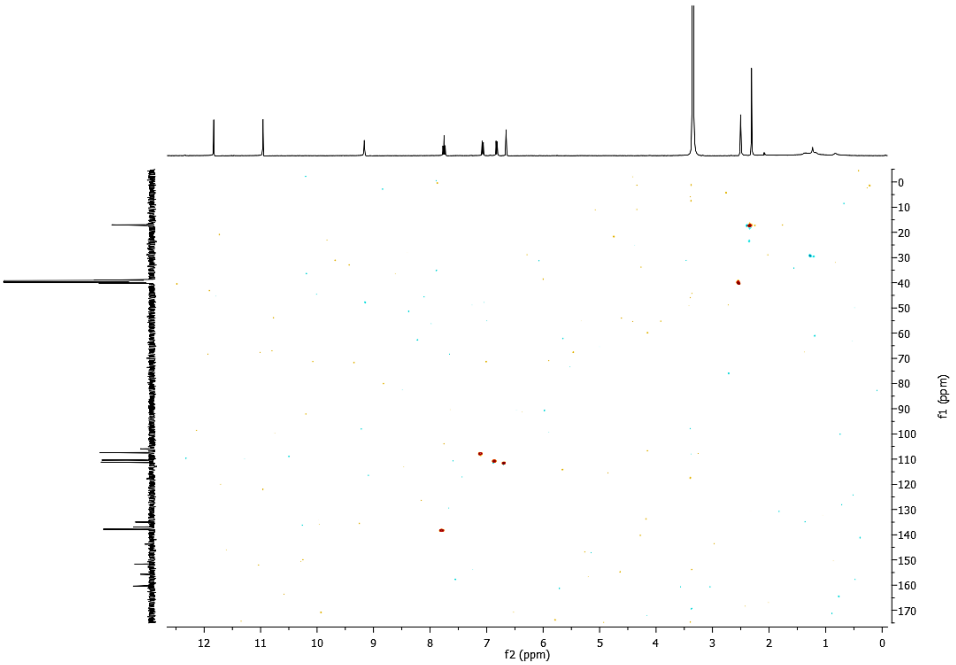

Fig. B.98 HSQC spectrum (DMSO-d_6) of compound **82**

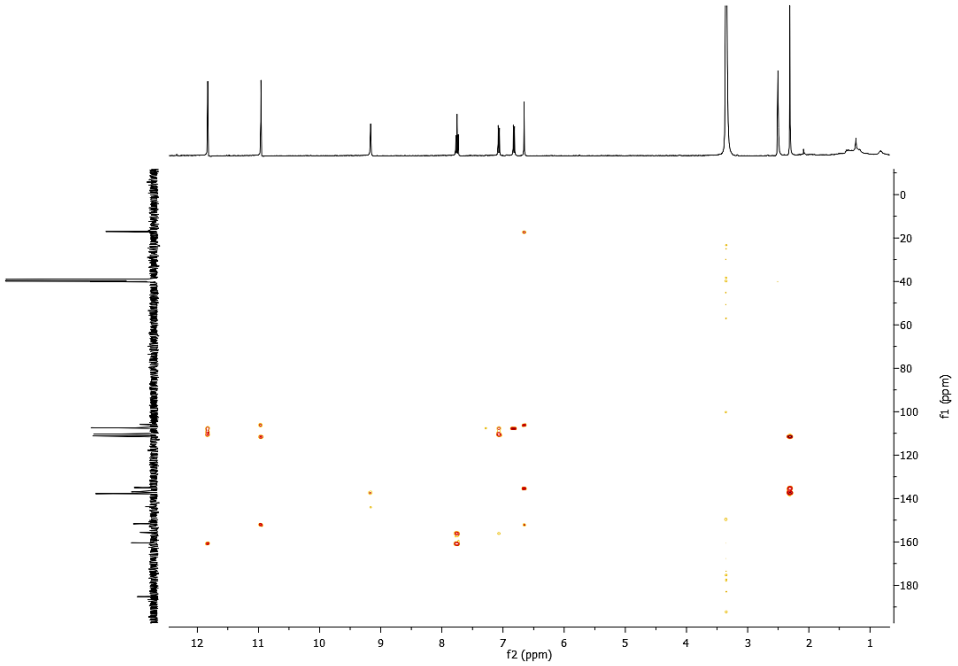

Fig. B.99 HMBC spectrum ($CDCl_3$) of compound **82**

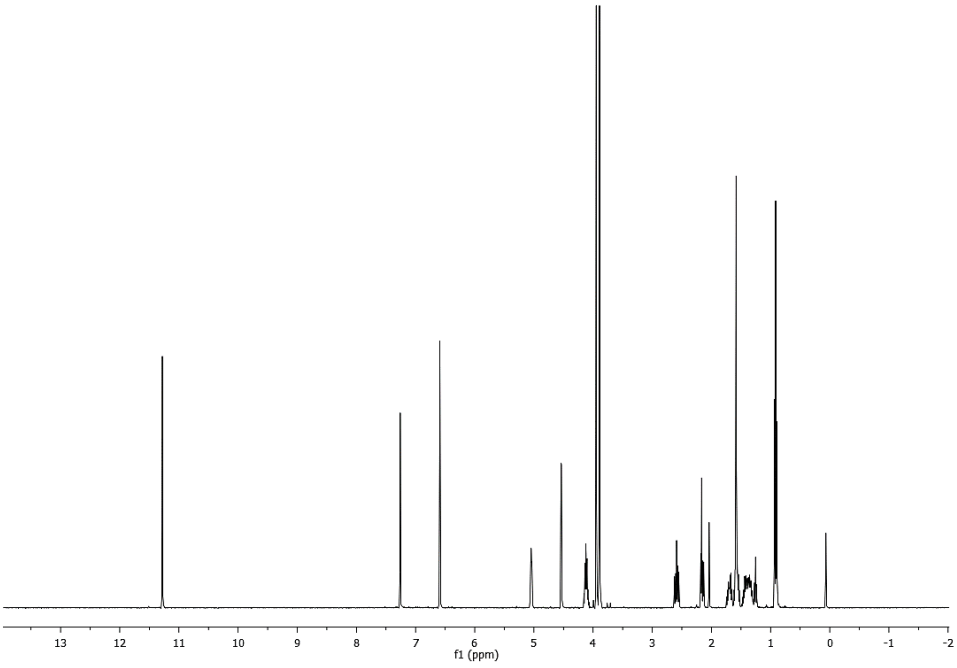

Fig. B.100 ^{1}H NMR (400 MHz, $CDCl_3$) spectrum of compound **83**

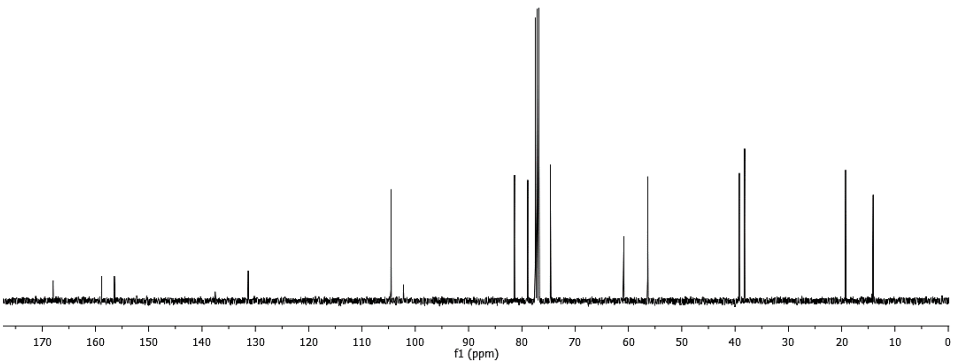

Fig. B.101 ^{13}C NMR (100 MHz, $CDCl_3$) spectrum of compound **83**

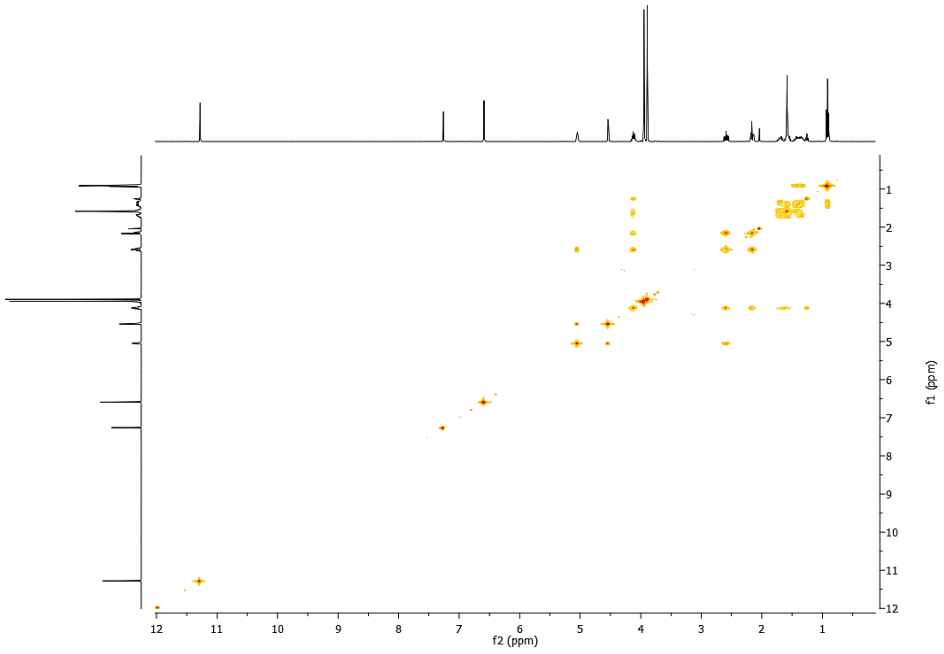

Fig. B.102 ^{1}H-^{1}H COSY spectrum ($CDCl_3$) of compound **83**

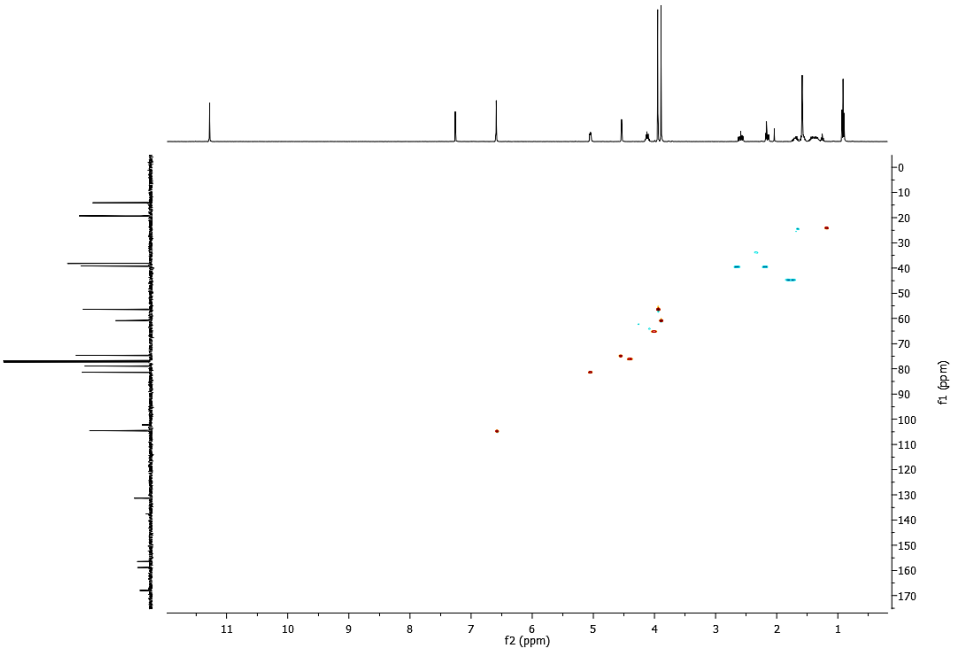

Fig. B.103 HSQC spectrum ($CDCl_3$) of compound **83**

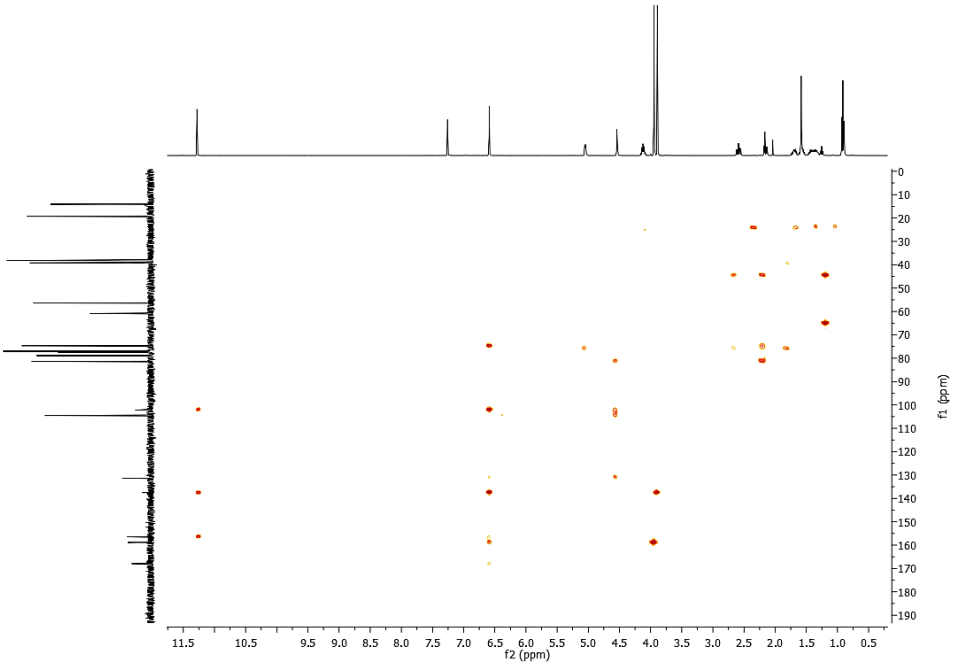

Fig. B.104 HMBC spectrum ($CDCl_3$) of compound **83**

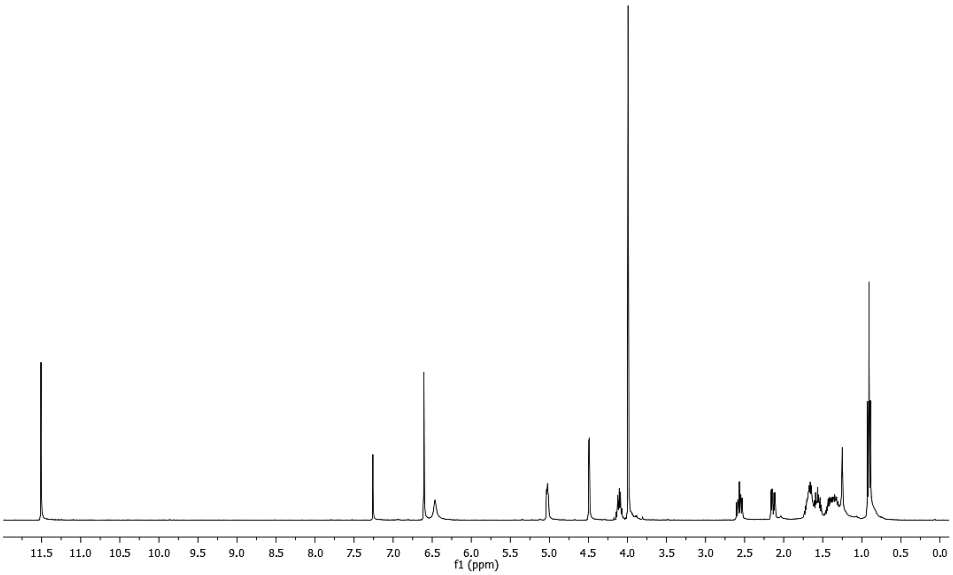

Fig. B.105 ^{1}H NMR (400 MHz, $CDCl_3$) spectrum of compound **84**

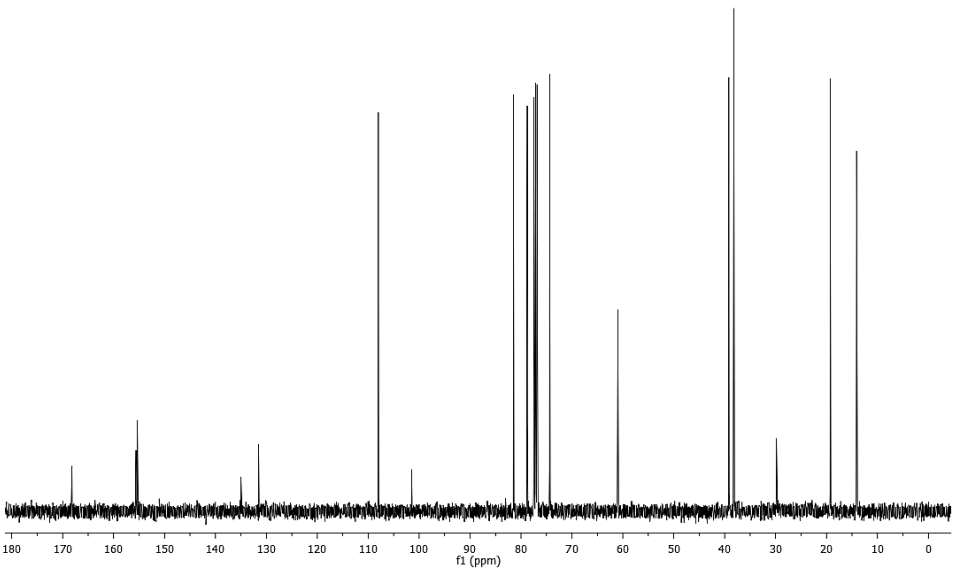

Fig. B.106 ^{13}C NMR (100 MHz, $CDCl_3$) spectrum of compound **84**

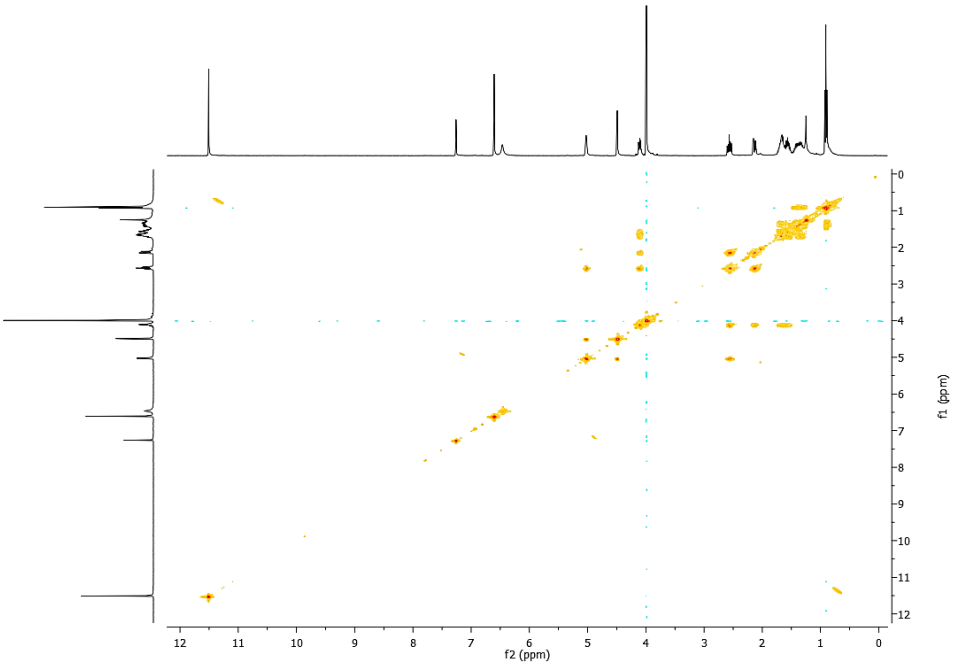

Fig. B.107 ^{1}H-^{1}H COSY spectrum ($CDCl_3$) of compound **84**

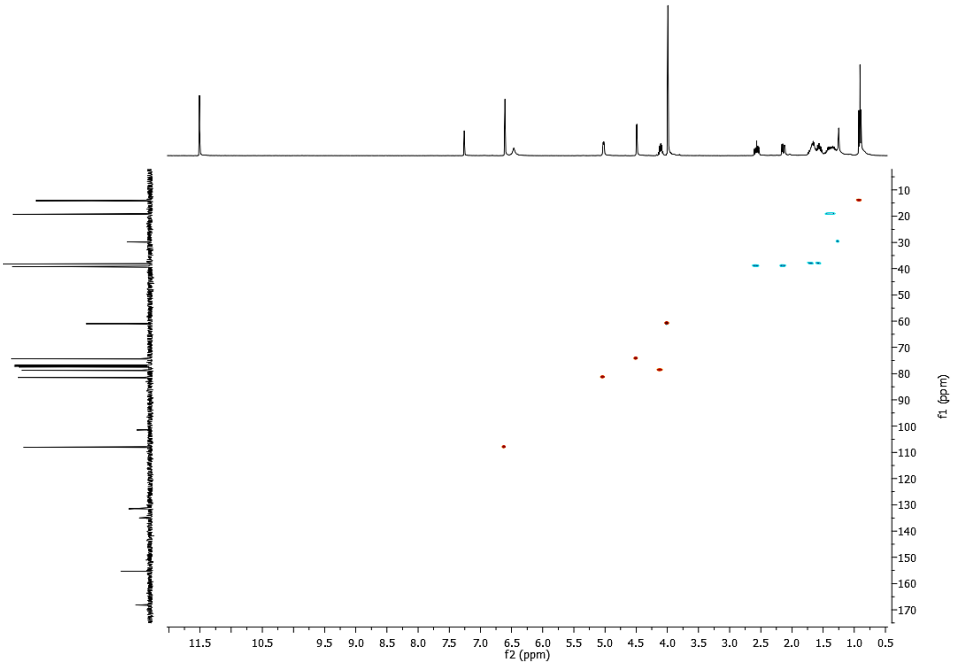

Fig. B.108 HSQC spectrum ($CDCl_3$) of compound **84**

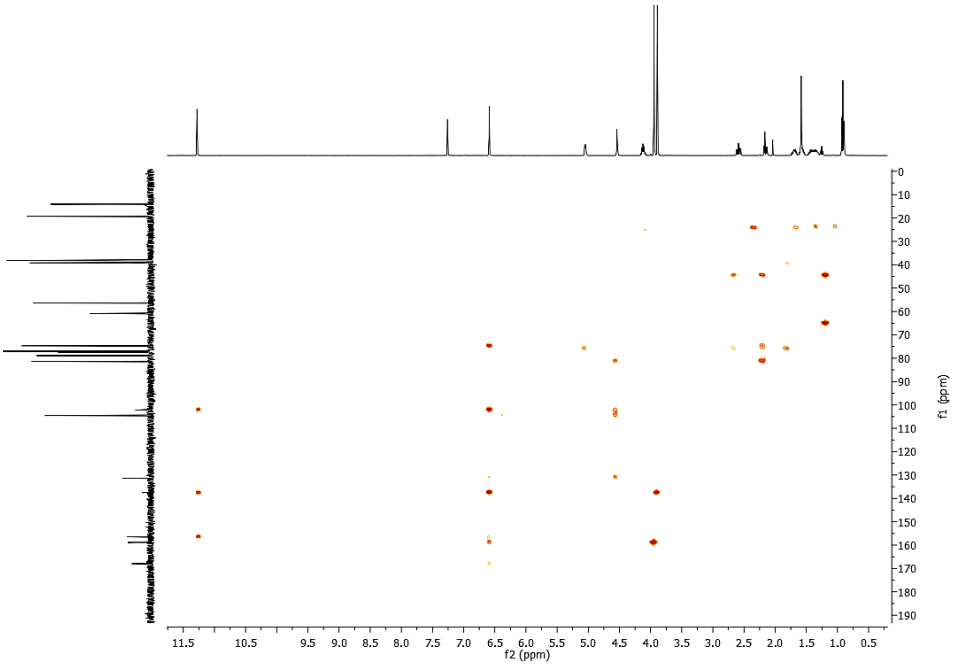

Fig. B.109 HMBC spectrum ($CDCl_3$) of compound **84**

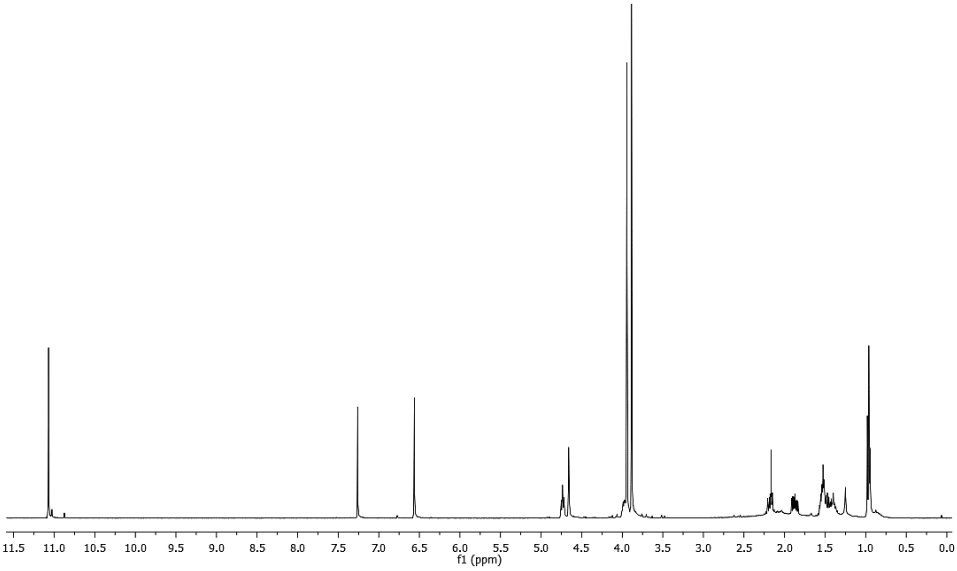

Fig. B.110 ^{1}H NMR (400 MHz, $CDCl_3$) spectrum of compound **85**

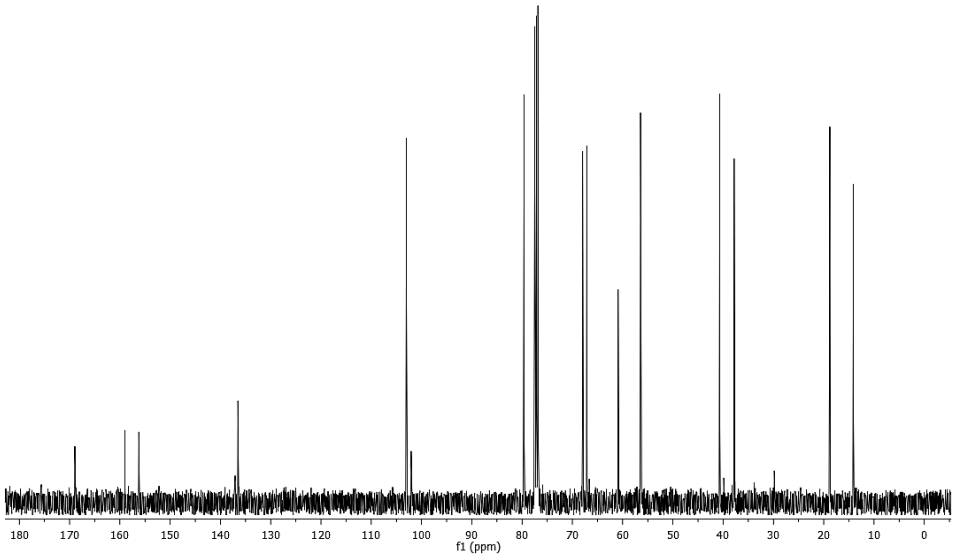

Fig. B.111 ^{13}C NMR (100 MHz, $CDCl_3$) spectrum of compound **85**

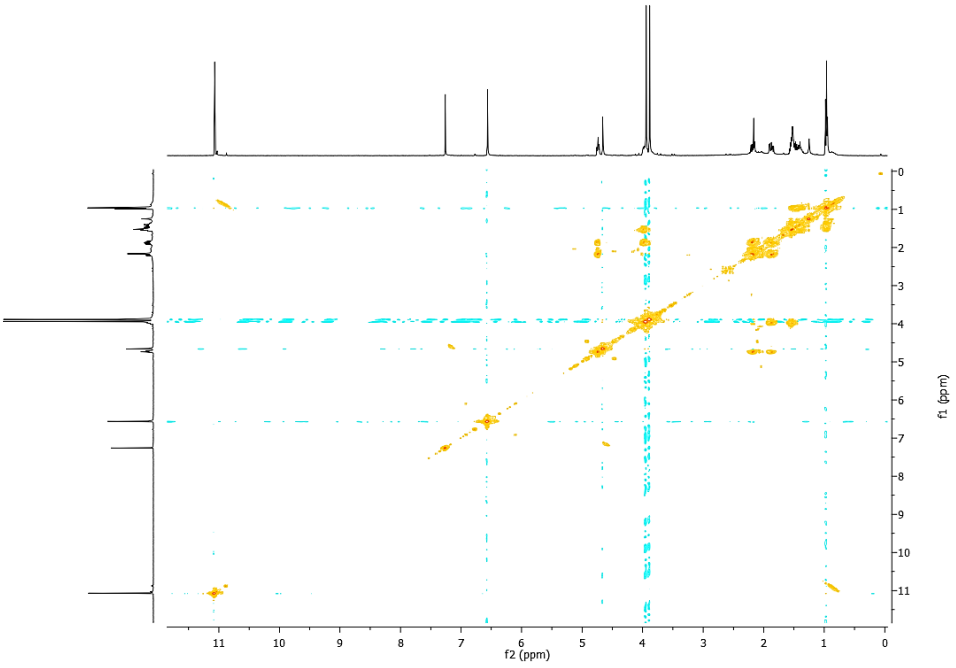

Fig. B.112 ^{1}H-^{1}H COSY spectrum ($CDCl_3$) of compound **85**

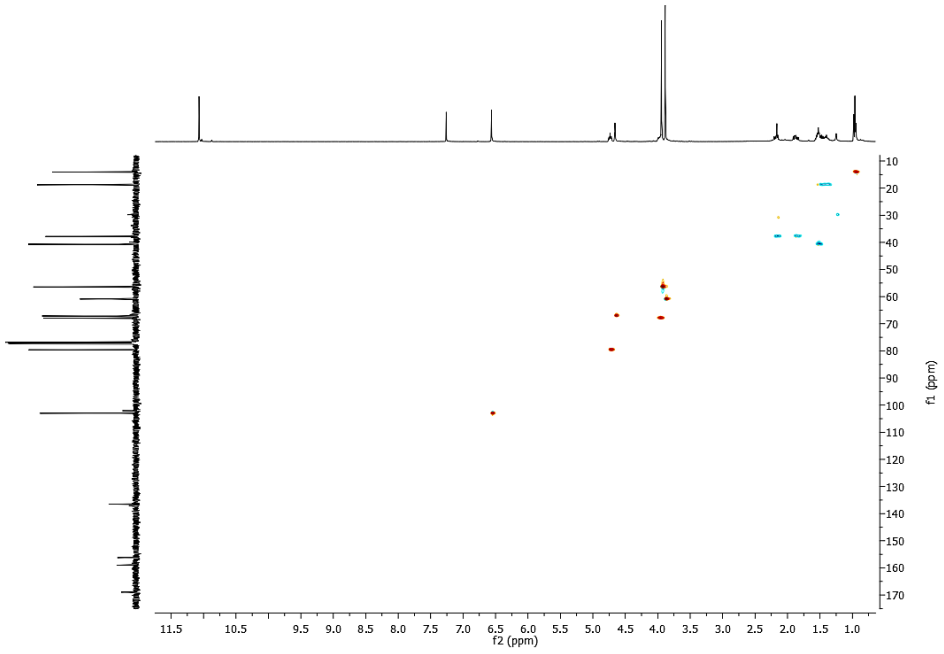

Fig. B.113 HSQC spectrum ($CDCl_3$) of compound **85**

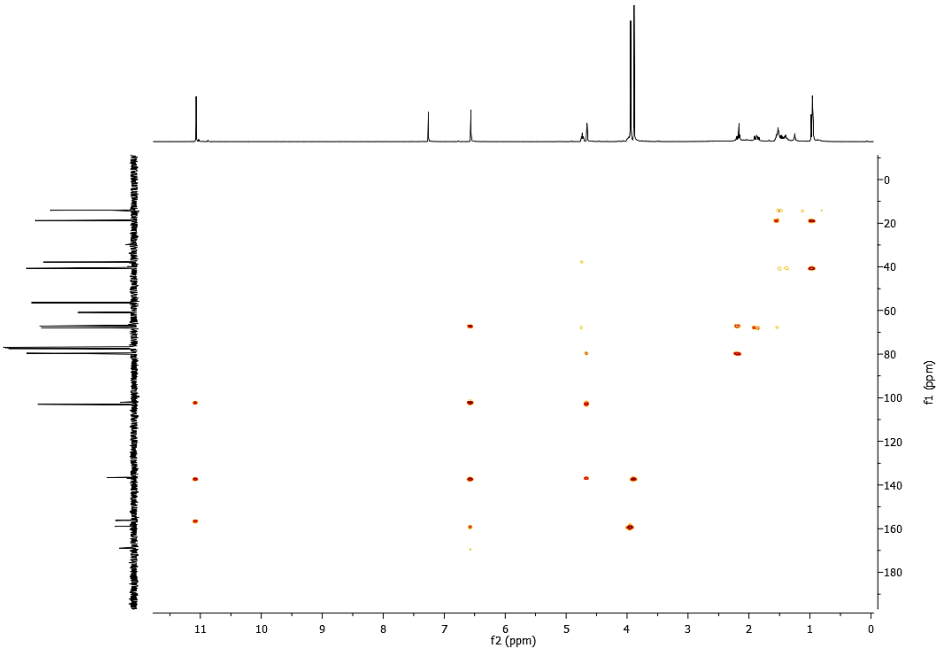

Fig. B.114 HMBC spectrum ($CDCl_3$) of compound **85**

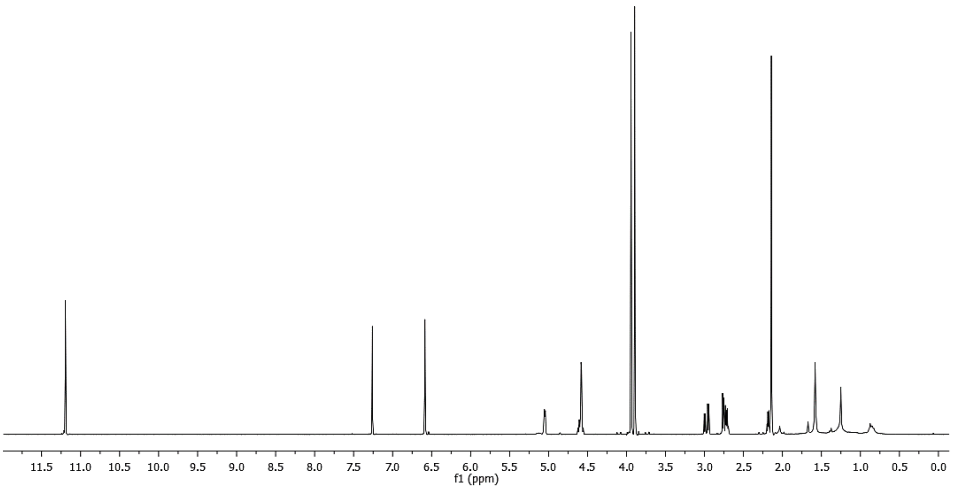

Fig. B.115 ^{1}H NMR (400 MHz, $CDCl_3$) spectrum of compound **86**

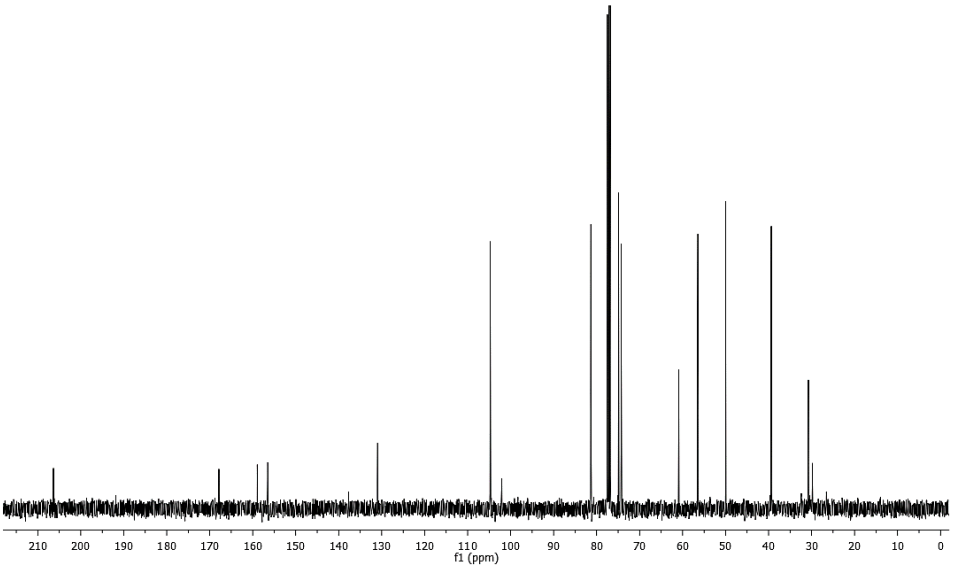

Fig. B.116 ^{13}C NMR (100 MHz, $CDCl_3$) spectrum of compound **86**

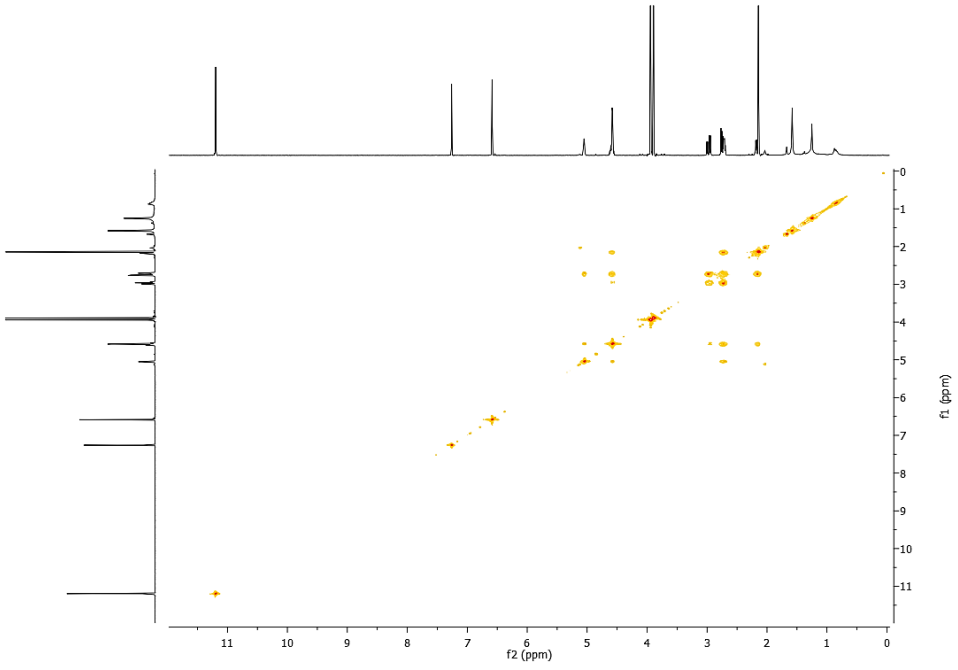

Fig. B.117 ^{1}H-^{1}H COSY spectrum ($CDCl_3$) of compound **86**

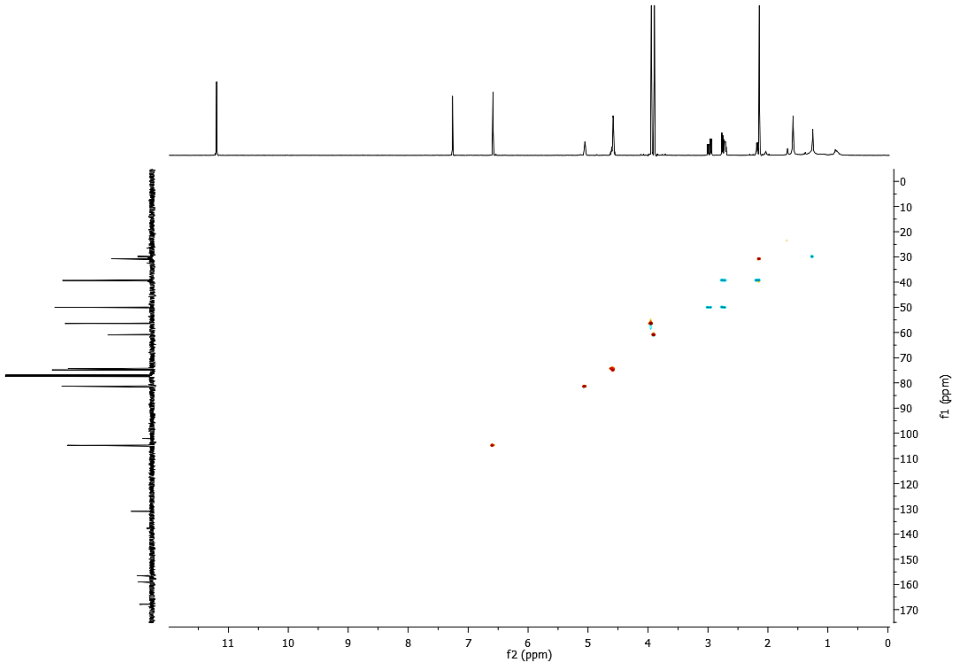

Fig. B.118 HSQC spectrum ($CDCl_3$) of compound **86**

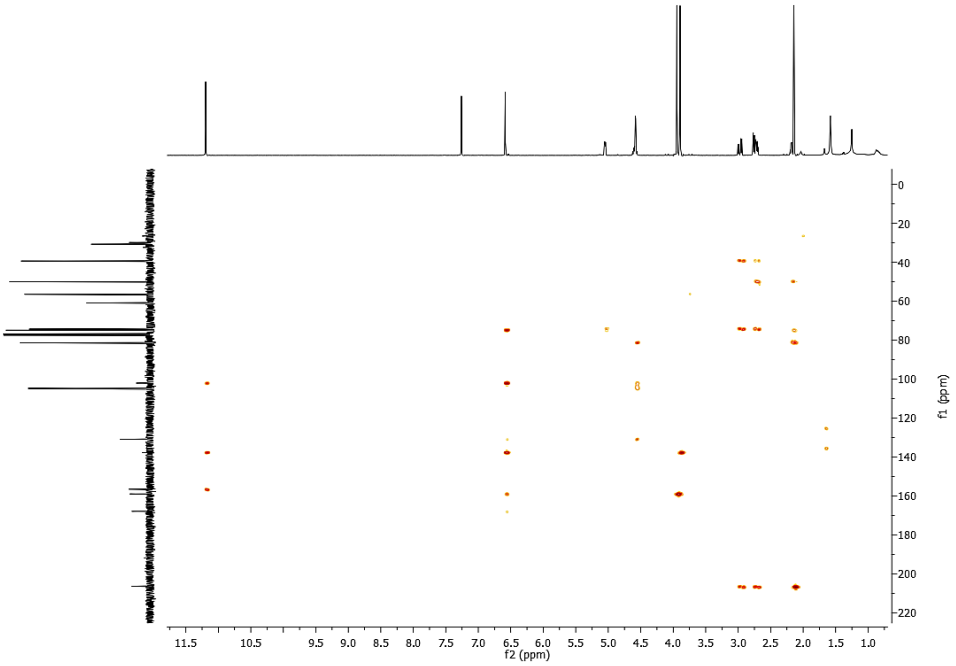

Fig. B.119 HMBC spectrum ($CDCl_3$) of compound **86**

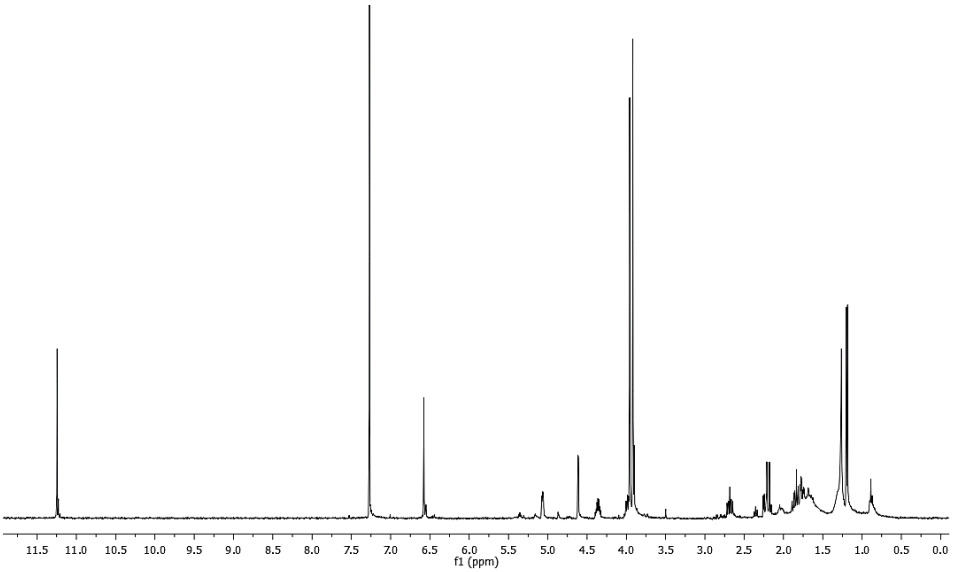

Fig. B.120 ^{1}H NMR (400 MHz, $CDCl_3$) spectrum of compound **87**

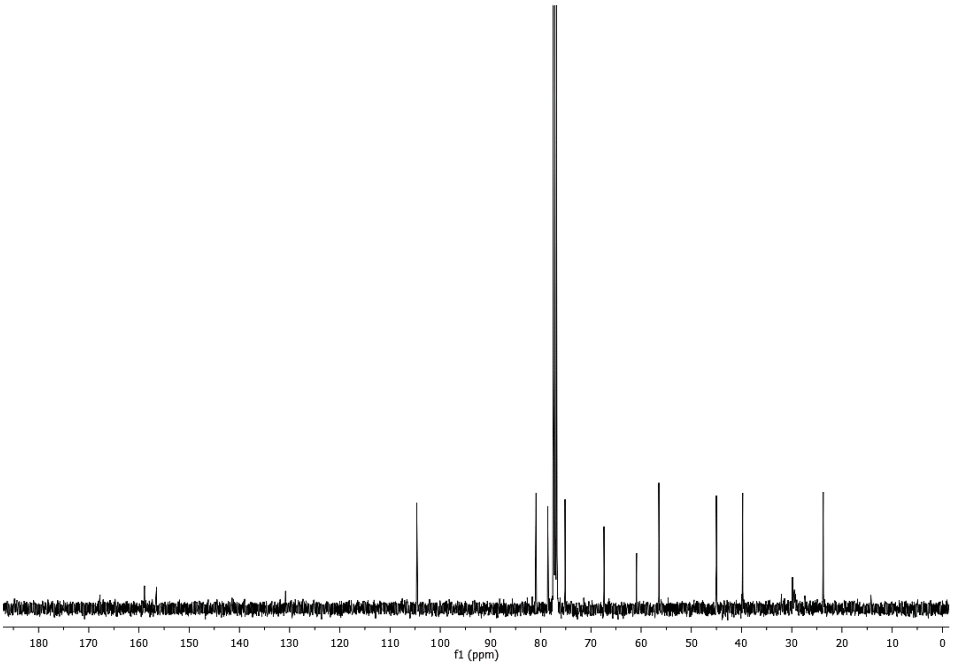

Fig. B.121 ^{13}C NMR (100 MHz, $CDCl_3$) spectrum of compound **87**

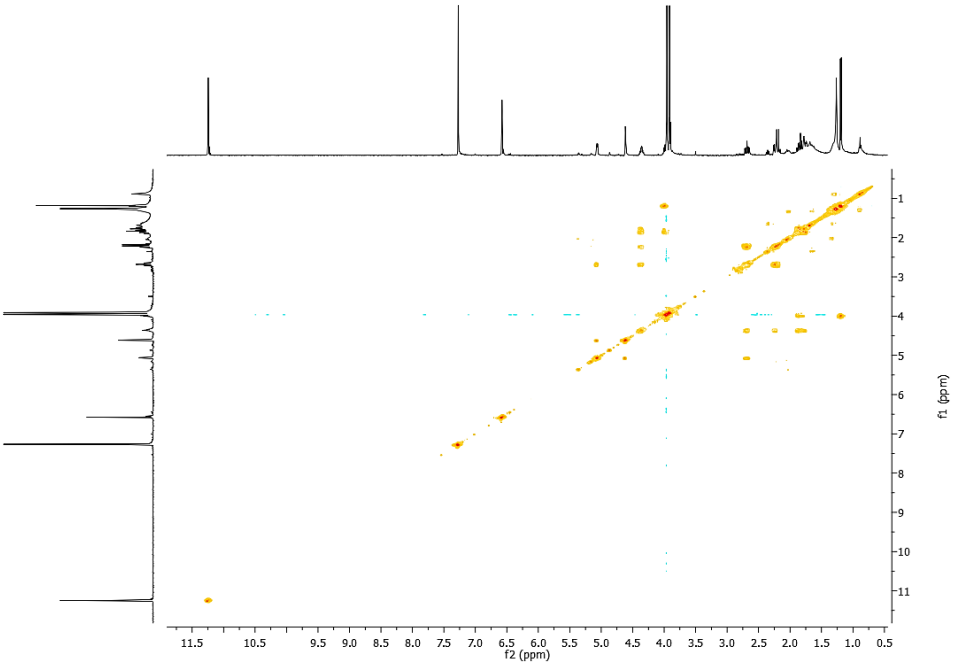

Fig. B.122 ^{1}H-^{1}H COSY spectrum ($CDCl_3$) of compound **87**

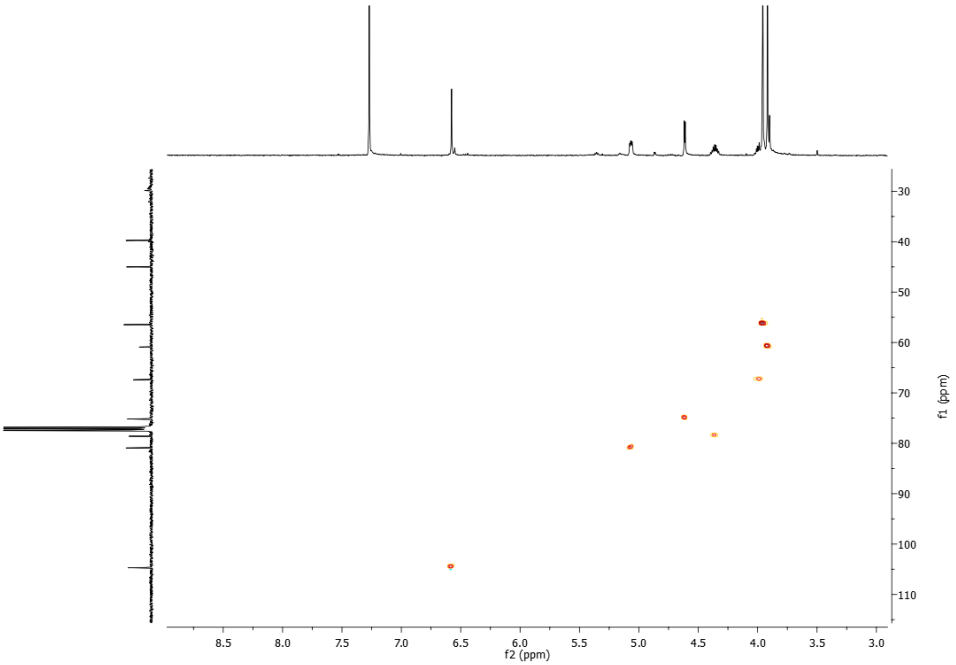

Fig. B.123 HSQC spectrum ($CDCl_3$) of compound **87**

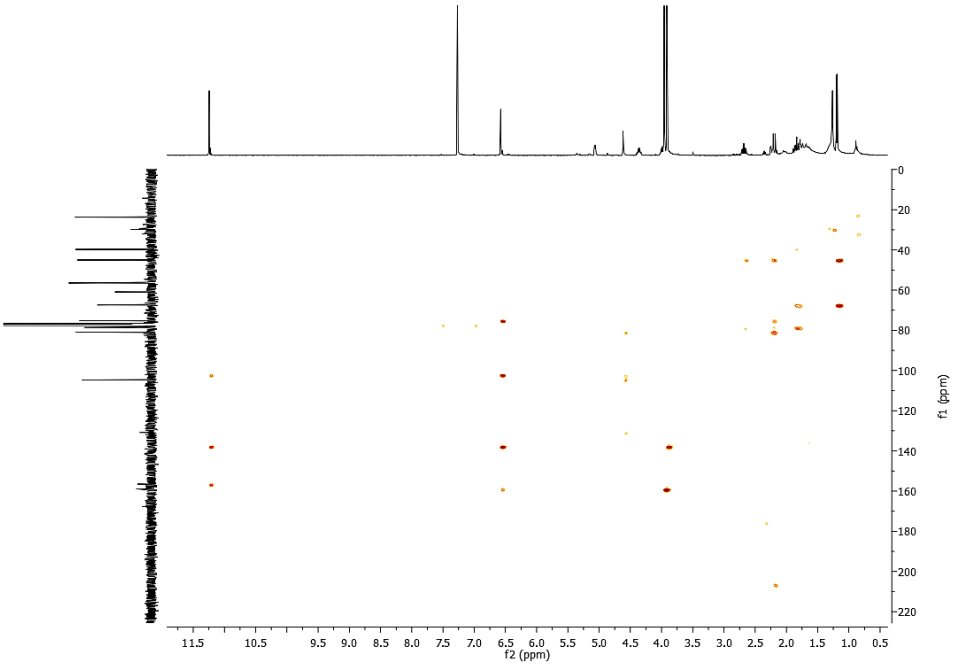

Fig. B.124 HMBC spectrum ($CDCl_3$) of compound **87**

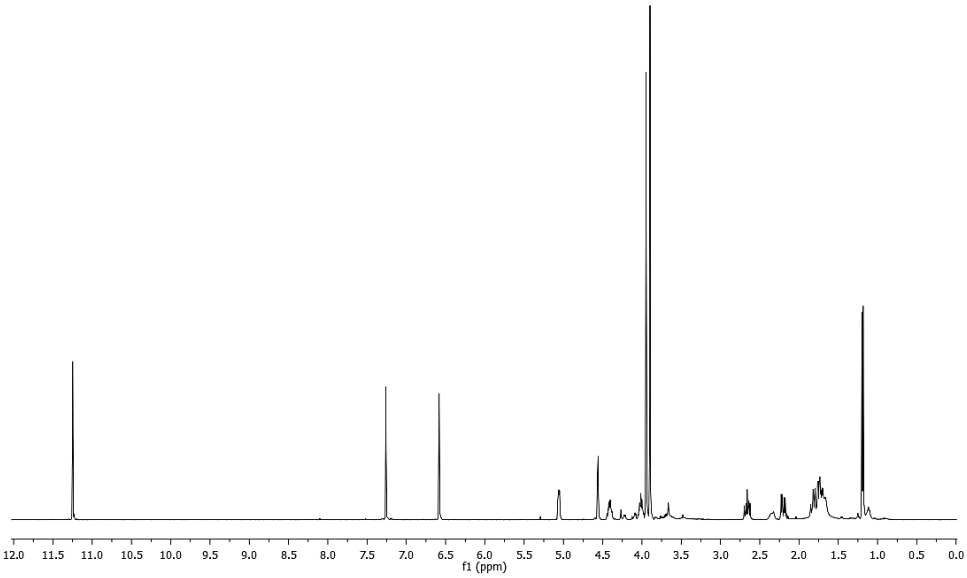

Fig. B.125 ^{1}H NMR (400 MHz, $CDCl_3$) spectrum of compound **88**

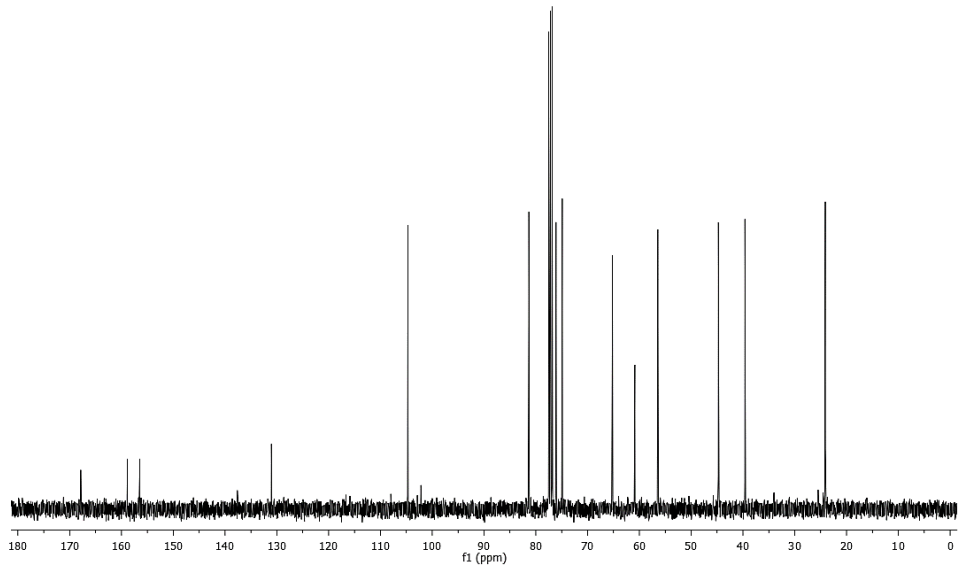

Fig. B.126 ^{13}C NMR (100 MHz, $CDCl_3$) spectrum of compound **88**

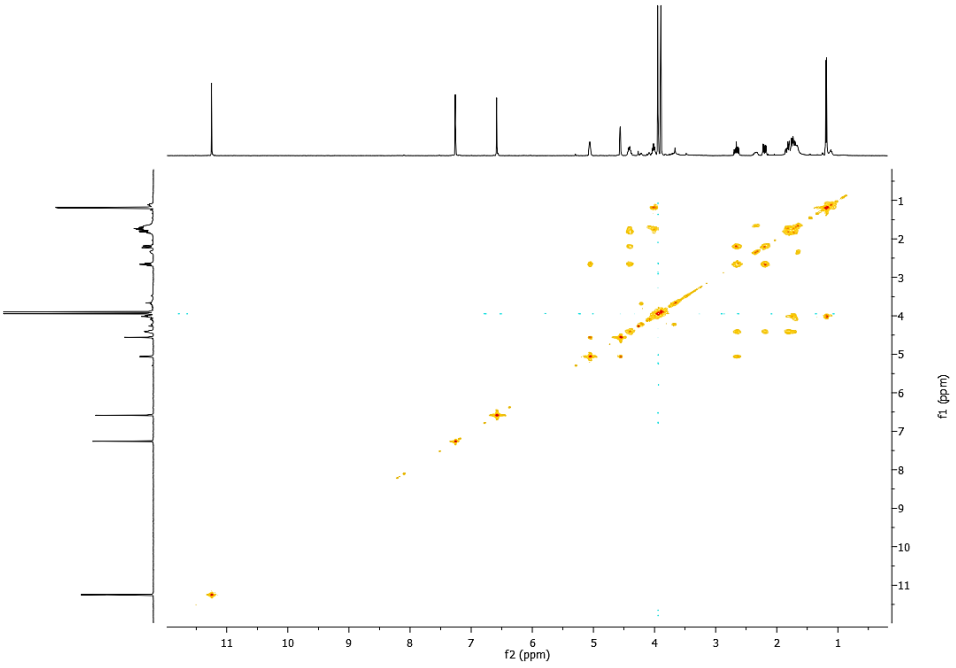

Fig. B.127 ^{1}H-^{1}H COSY spectrum ($CDCl_3$) of compound **88**

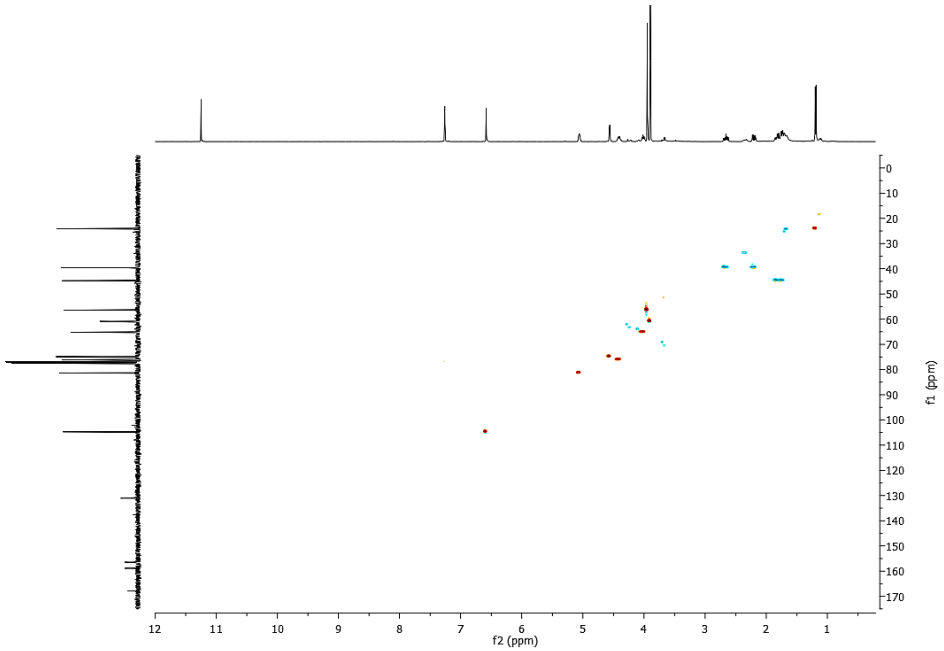

Fig. B.128 HSQC spectrum ($CDCl_3$) of compound **88**

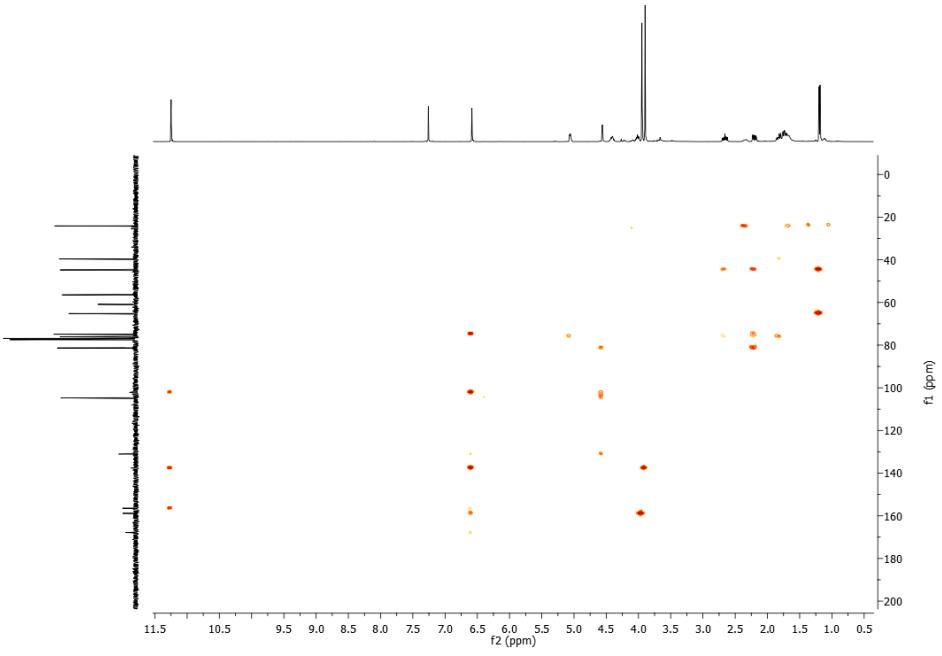

Fig. B.129 HMBC spectrum ($CDCl_3$) of compound **88**

VITA

Miss. Sujitra Hanthanong was born on September 12th, 1981 in Bangkok, Thailand. She graduated with Bachelor's Degree of Science in Biotechnology from School of Agricultural Technology, Walailuk University, in 2004. During the time she has been studing in Philosopy Degree in Biotechnology Program, Faculty of Science, Chulalongkorn University. She received the 90th Anniversary of Chulalongkorn University Fund (Rarchadaphiseksomphot) for supporting her research project.

Her present address is 214/1 Moo. 13 Tambon Tha Chai, Amphoe Si Satchanalai, Sukhothai, Thailand, 64190, Tel: +668-1532-5074.